Science Research Council
RHEL/R 191
Rutherford Laboratory Report

THE WORK OF THE RUTHERFORD LABORATORY 1969

Hobbs the Printers Ltd
Second Avenue, Millbrook, Southampton

Science Research Council

THE WORK OF THE RUTHERFORD LABORATORY IN 1969

Edited by

A P Banford and F M Telling

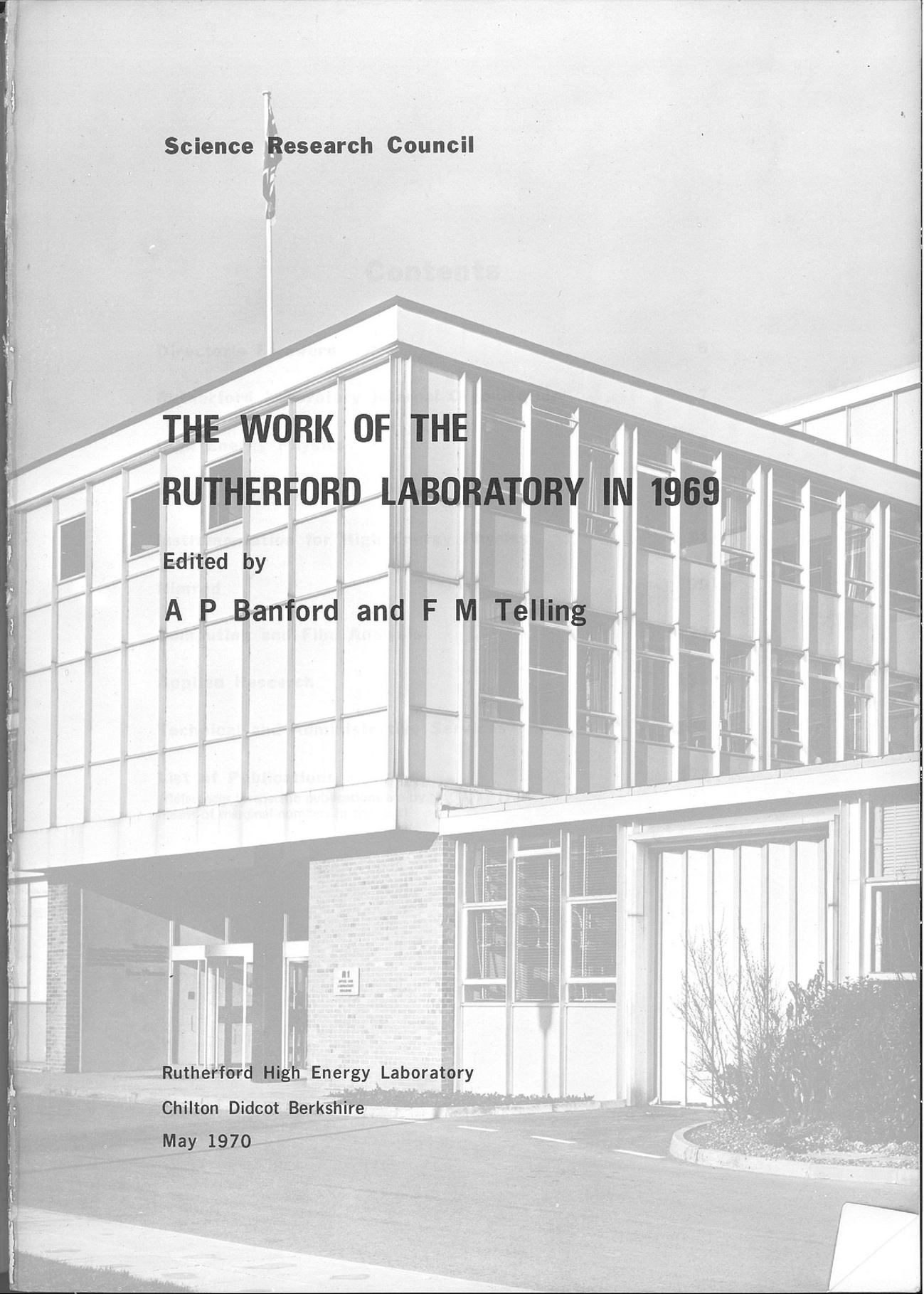

Rutherford High Energy Laboratory
Chilton Didcot Berkshire
May 1970

Contents

Director's Foreword

The year under review has been noteworthy in several respects. Utilisation of Nimrod has reached a new peak. Through continued development of beam sharing techniques and the use of the new Experimental Hall 3, on average 5·9 experiments have been run together compared with an average of 4 in 1967 and 2 in 1964. Of the 33 approved experiments on the high energy physics programme, 10 completed data-taking. We have also been successful in making more use of CERN and among the experiments now being prepared is one approved to be done on the Intersecting Storage Rings, when they first become operational at CERN in 1971.

Collaboration between CERN and the Rutherford Laboratory has led to the successful operation of our 1·5 metre chamber with an internal liquid hydrogen target surrounded by a neon-hydrogen mixture. Satisfactory tracks have been observed so that combined in the one instrument are the advantages of both the hydrogen and the heavy liquid chambers. A result of the successful development of this technique was the decision to withdraw our heavy liquid bubble chamber from further service.

Also now on the retired list is the 50 MeV proton linear accelerator, which was closed down in October after 9½ years of operation. During this period it provided over 42,000 hours of nuclear physics research time.

By the end of 1969 we had completed our report on the proposed high field bubble chamber and we are now ready to start construction of this advanced instrument. This chamber will have its 70 kilogauss magnetic field produced by a superconducting magnet. Indeed most of our applied physics activities are now devoted to the long term exploitation of superconductivity for high energy physics research. Progress is particularly encouraging and exciting.

We have decided this year to break away from the format of previous Annual Reports, which adhered strictly to the pattern of the Laboratory's internal organisation. I hope that the re-arrangement will be found to be an improvement.

G. H. Stafford.

Rutherford Laboratory Internal Organisation

HIGH ENERGY PHYSICS DIVISION.

Experimental research programme on Nimrod and the PLA. Resident counter and bubble chamber groups. Liaison with visiting teams. Nuclear electronics.

DIVISION HEAD & DEPUTY DIRECTOR: G. MANNING.

NIMROD DIVISION

Operation and development of Nimrod. Experimental area management. Design and installation of beam lines. Superconducting beam-line elements.

DIVISION HEAD: D. A. GRAY.

APPLIED PHYSICS DIVISION.

Bubble chamber operations and development. High Field Bubble Chamber project. Superconducting magnets. Polarized proton targets. Radiation protection.

DIVISION HEAD: L. C. W. HOBBIS.

COMPUTING & AUTOMATION DIVISION

Operation and development of Central Computer System. On-line applications including hardware and software for bubble and spark chamber film analysis. Theoretical High Energy Physics.

DIVISION HEAD: W. WALKINSHAW.

ENGINEERING DIVISION.

Design and manufacture of research equipment. Mechanical, Electrical and Building services. Chemical Technology. Safety services.

DIVISION HEAD & CHIEF ENGINEER: P. BOWLES.

ADMINISTRATION DIVISION.

Personnel, Finance and Accounts, Stores, Library, Transport, General and Specialised Administrative support.

DIVISION HEAD & LABORATORY SECRETARY: J. M. VALENTINE.

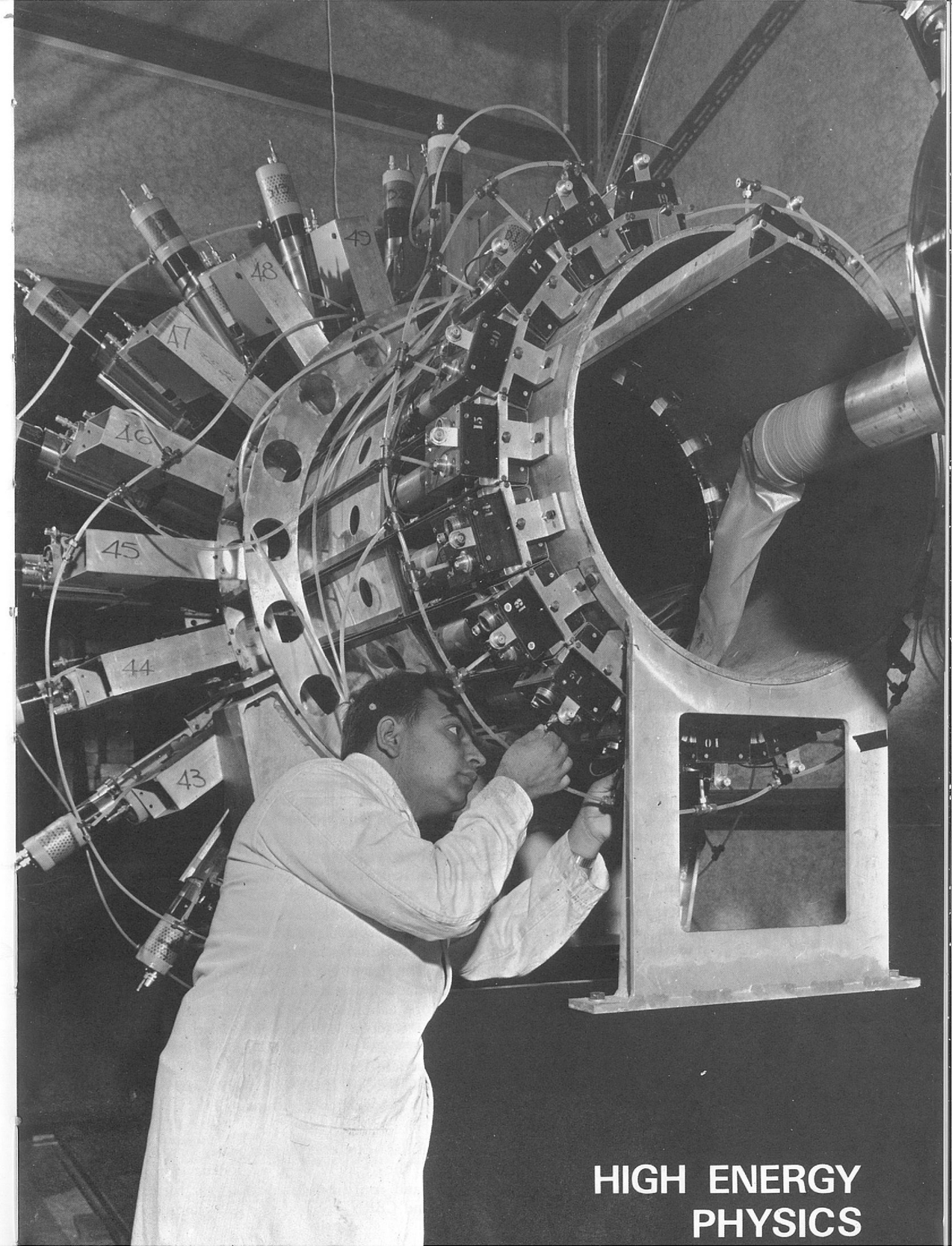

HIGH ENERGY PHYSICS

High Energy Physics

The dominant features of this last year's high energy physics activities have been the highest ever utilisation of Nimrod by experimental teams and, at the same time, an increased use of international facilities. Nimrod records report a total usage of 26,044 team-hours, and this number when divided by the actual number of hours (4,521) of 7 GeV beam achieved for high energy physics, implies an average number of teams running simultaneously of about 6. This shows a substantial improvement over last year's number of 4·8. Even greater utilisation is expected when Experimental Hall 3, commissioned during 1969, is equipped with further secondary beam lines. Data taking was completed on 7 experiments using counters and spark chambers (plus 1 at CERN) and 2 using bubble chambers. $1{\cdot}1 \times 10^6$ bubble chamber pictures were taken at Nimrod for analysis by groups both in the UK and abroad. A new development of the bubble chamber technique, a neon-hydrogen chamber with a hydrogen interaction region, was successfully tested using the 1·5m British National Chamber and opens the way for a new series of bubble chamber experiments. In parallel with the increased use of Nimrod there has been an expansion of the use of the CERN facilities in Geneva. Two teams had experiments running on CERN accelerators and other teams have been preparing for later experiments. The use of accelerators abroad by experimental teams supported financially and technically from home is already an important activity of the Laboratory and it is appropriate to discuss it at this time. Here we will be concerned only with the CERN work supported by the Rutherford Laboratory.

The CERN laboratory is situated in Switzerland only a few miles from the international airport at Geneva. Thirteen European countries participate in the work of CERN, the European Organisation for Nuclear Research, contributing to the cost of the basic programme in proportion to their net national income. Britain's share in 1969 was 21·6 per cent of the total budget of 235 million Swiss Francs and is allocated from Science Research Council funds. Over 3,000 people work on the densely packed site (figure 1) which straddles the frontier between France and Switzerland. The experimental programme is based on the use of two proton accelerators — a 600 MeV synchro-cyclotron (SC) and a 28 GeV synchroton (PS). At the latter machine, large intersecting storage rings (ISR), for experiments with colliding proton beams, are under construction. The PS experimental facilities include three bubble chambers, 81cm and 2m hydrogen and 1·2m heavy liquid. Under construction at CERN are a 3·7m hydrogen chamber and a 13 cubic metre magnet spark chamber system (the Omega project). In addition to being an outstandingly successful example of international scientific collaboration, CERN occupies a dominating position in high energy physics. Of the four basic forces in Nature, the strong, electromagnetic, weak and gravitational interactions, investigations both at CERN and the Rutherford Laboratory are directed mainly towards understanding the properties of those interactions quite unknown in the last century, the strong interaction (nuclear forces, particle collisions, etc.) and the weak interaction (beta radio-activity, particle decays, etc.). Of the two Rutherford Laboratory supported experiments at CERN in 1969, one was concerned with the strong interaction and the other with the weak interaction.

The present theory of weak interactions has been built up over many years assuming several basic rules. The observation of the decay $K_L^o \rightarrow \pi^+\pi^-$, a decay forbidden by the rules, at Brookhaven in 1964 and confirmed later that year by experiments at the Rutherford Laboratory and CERN, showed that CP symmetry was

Figure 1. The CERN site looking towards Geneva from the extension into France. The ISR project is shown in the foreground. (Photograph by courtesy of CERN)

violated in the weak interaction. CP symmetry assumes that the physical laws remain unchanged if we simultaneously change particle into antiparticle and reflect the co-ordinate systems in a mirror. Perhaps the most interesting aspect of CP is that according to firmly accepted ideas a violation of CP symmetry implies a violation of time reversal symmetry, according to which the physical laws should remain unchanged by reversing the arrow of time. The current theory of the weak interaction has enjoyed considerable success but the violation of CP symmetry is not easily fitted into the theory. Since 1964 many experiments, at the Rutherford Laboratory and elsewhere, have sought more information on the nature of CP violation. One of the puzzling features is the small magnitude (1 in 500) of the effect. Present experiments at Nimrod on what is commonly described as the "CP puzzle" are those testing CP symmetry in the decays $K^o \rightarrow \pi e \nu$ (Experiment 14) and $K_s^o \rightarrow \pi^+\pi^-\pi^o$ (Experiment 17) and also C symmetry in $\eta^o \rightarrow \pi^+\pi^-\pi^o$ (Experiment 16). Although this last decay is due to the electromagnetic interaction it has been suggested that a violation of C symmetry in the electromagnetic interaction could be a possible source for CP violation in the weak interaction. A key experiment is to measure the asymmetry in the rates for $K^+ \rightarrow \pi^+\pi^o\gamma$ and $K^- \rightarrow \pi^-\pi^o\gamma$ in order to test both for C violation in electromagnetic interactions and CP violation in the weak interaction. Several major difficulties confront the experimenter; the decay probability of $K^\pm$ into the $\pi^\pm\pi^o\gamma$ mode is 2×10^{-4}, CP violation effects are 1 in 500 and, for practical reasons, it is desirable to use energetic kaons.

In late summer 1968 a team of physicists and support staff from the Rutherford Laboratory, and the Universities of Glasgow, Liverpool, Oxford and Warwick left for CERN with 55 tons of apparatus to study $K \rightarrow \pi\pi\gamma$ decays in a 5 GeV/c kaon beam at the CERN PS (Experiment 19). The equipment included 200 scintillation counters, 20 spark chambers, an on-line computer and 4 fully equipped

modular control rooms (figure 2). The experiment was on the PS floor for about a year. During this time it was allocated 16 weeks of PS running time, of which 9 were used for data collection. Technical effort to mount and dismantle the experiment and to service and repair the equipment was provided mainly by home-based Rutherford Laboratory staff. The team returned to the Laboratory late in 1969 with 800 magnetic tapes (total length 400 miles) for analysis on the Rutherford Laboratory IBM 360/75. It is estimated that more than 3,000 $K^{\pm} \rightarrow \pi^{\pm}\pi^{o}\gamma$ events can be identified from these tapes. Although the time spent at CERN was little more than a year the overall timescale of the experiment will be of the order of the now typical 3 years (see Table 1).

Table 1

Timetable for $K^{\pm} \rightarrow \pi^{\pm}\pi^{o}\gamma$ Experiment at CERN

January–June 1967	Detailed design of experiment.
June 1967	Approved by Nimrod Experiments Selection Panel.
September 1967	Accepted on to the CERN PS Programme to be scheduled after the October 1968 shutdown.
July–September 1968	Transfer of staff to CERN; 2 members of the group moved to CERN in July followed by another 5 in August and the remainder in September.
August–September 1968	Shipment of experimental equipment to CERN and assembly in the experimental hall.
October 1968	First run on the PS. Assembly of equipment completed.
November 1968–March 1969	Setting up of experiment.
April–September 1969	Data taking interspersed with parasitic running for calibration of equipment.
September–October 1969	Final calibration runs, survey and dismantling of experiment.
November 1969	Remainder of equipment returned to Rutherford Laboratory.
September–November 1969	Return of staff to Britain. All but 3 members of group returned in September and early October, the others returning in mid-November.
November 1969–Autumn 1970	Analysis.

Another team to arrive at CERN at the same time was the Rutherford Laboratory and University of Cambridge collaboration to perform on the synchro-cyclotron a series of experiments on πp interactions at energies from 100 to 300 MeV (Experiment 10). The CERN SC produces copious beams of low energy pions and is an ideal machine for such a series of systematic measurements of high accuracy. The experiment comprises the measurement of the total cross-sections, differential elastic cross-sections and total charge exchange cross-sections at different energies

Figure 2. Modular control rooms arriving on the CERN site for $K \rightarrow \pi\ \pi\ \gamma$ experiments at the CERN PS (Experiment 19).

using scintillation counters and spark chambers. The ultimate objective is the precise measurement of the long range nuclear forces. Essentially the low energy pions from the SC are being used to probe the outer pion cloud which surrounds the proton; centrifugal barrier effects largely shield the pion from short range forces. Once the long range forces are known accurately then the data available using higher energy pions can be used with effect to probe the short range nuclear forces. Data taking has continued throughout 1969 on successive stages of the experiment. Each stage of the experiment has required apparatus changes and a team of engineers and electricians has been 'on-call' at the Rutherford Laboratory. (On one occasion they were prevented from landing at Geneva airport due to fog and were carried on to Beirut!). The final measurements in the experiment will be completed in the spring of 1970.

Another group, this time from Queen Mary College, Daresbury Laboratory, University of Liverpool, and the Rutherford Laboratory have proposed an experiment to study the antiproton-proton reactions $\bar{p}p \rightarrow \bar{p}p$, $K^{-}K^{+}$ and $\pi^{-}\pi^{+}$ at antiproton momenta between 0·6 and 2·0 GeV/c. Only at the CERN 28 GeV PS are there fluxes of antiprotons adequate for the experiment in Europe. In November the experiment was accepted on to the CERN programme. Preparation of the apparatus, final design, search for flats and suitable schooling in Geneva, etc., have started. The timescale envisaged aims at the installation of a new beam and the apparatus in the next major PS shutdown (about November 1970). The experiment uses a large acceptance spectrometer made up from wire spark chambers and a large magnet which will be made available by CERN. The major part of the group are currently data taking in a proton-proton elastic scattering experiment (Experiment 6) at Nimrod. This experiment also uses an array of wire spark chambers.

Preparations have been increasing for the first round of experiments (1971–3) on the CERN intersecting storage rings, construction of which started in 1966. First operation is expected during 1971. There is considerable excitement in the prospect of the very energetic collisions made possible by the ISR project. Why is this so? The dimensions of the objects studied in accelerator experiments have always been paradoxically different from the size of the accelerators themselves. To look at phenomena related to atoms (dimensions of 10^{-8} cm) then nuclei (10^{-12} cm) and then particles (10^{-13} cm) has called for larger and larger accelerators of higher and higher energies. When each step was made new phenomena were revealed, new concepts about matter were suggested and some intuitive ideas about asymmetry in Nature even had to be abandoned. It is expected that the next step to higher energy will provide explanations of the many puzzling effects of today. 1969 saw the first experimental results from the 76 GeV accelerator at Serpukhov (USSR). As yet no new phenomena have been observed but the measurements (on total cross-sections and particle yields) were different from expectation. Massive construction work continues in the USA on a 200 GeV accelerator. Meanwhile in Europe the 300 GeV project (without Britain) is struggling to get approval. The ISR project at CERN

makes it possible for member states of CERN to get a glimpse of a very much higher energy region. In a conventional accelerator fast protons collide with stationary protons producing secondary particles but most of the energy of the accelerated particles is used up in maintaining the secondaries more or less along the original direction of the incident particles due to the conservation of momentum. Only a small fraction of the energy of the accelerated particles is available for other purposes e.g. the production of new particles. An approximate formula for calculating this "useful energy" is:

$$\text{Useful energy} = \sqrt{\text{Twice accelerator energy}}$$

where the energies are expressed in GeV. Thus the CERN 28 GeV PS gives about 7 GeV in useful energy and the proposed 300 GeV machine 24 GeV useful energy. If however particles of the same energy can be made to collide head-on as in the ISR then all their energy is useful, since none is needed to conserve momentum. The ISR collisions, then, have a useful energy of 56 GeV, equivalent to that produced by a 1700 GeV conventional machine (figure 3). There is, however, a price to pay; ISR experiments are limited to proton-proton collisions. Two experiments involving British groups have been accepted on to the initial programme for the ISR; one group will be supported by the Daresbury Laboratory and the other by the Rutherford Laboratory. The latter group comprises physicists from the Rutherford Laboratory and the Universities of Bristol, Cambridge, Liverpool and London (University College). The experiment will measure particle yields in the angular range 20—90° placing particular emphasis on muons of large transverse momentum as a search for the intermediate vector boson, the suggested particle mediating the weak interaction. This is analogous to the photon, the exchange quantum particle of the electromagnetic interaction. The muon detector will have 12 slabs of magnetised iron 4 inches thick with scintillation trigger counters at front and rear and in one gap and spark chambers in the remaining 10 gaps. A start has been made on assembly of a 3m × 2m 'model' of a spark chamber (final size 4m × 2m). The final detector will weigh about 250 tons and will occupy about 50 cubic metres.

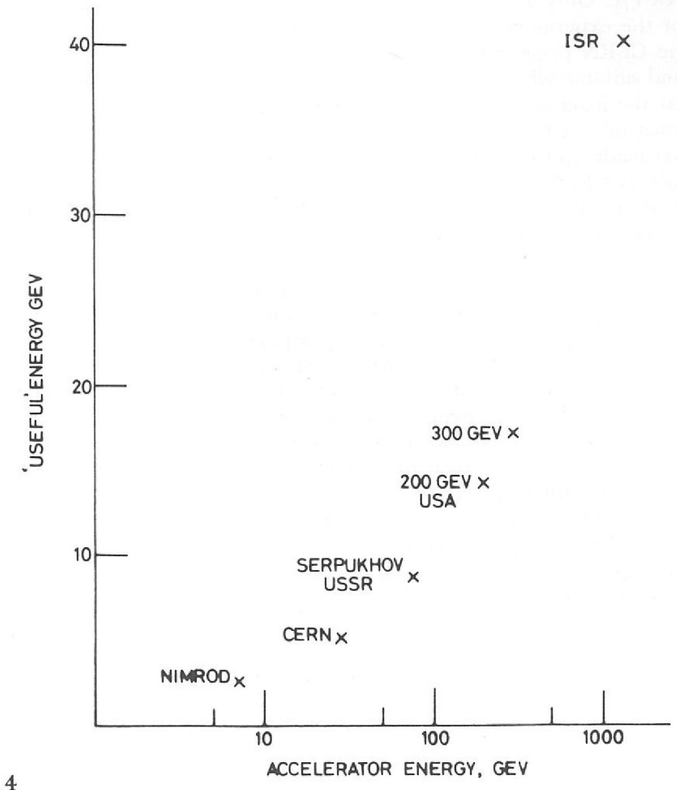

Figure 3. The relation between 'useful' energy and accelerator energy is given approximately by Useful energy = √ twice accelerator energy, where the energies are expressed in GeV.

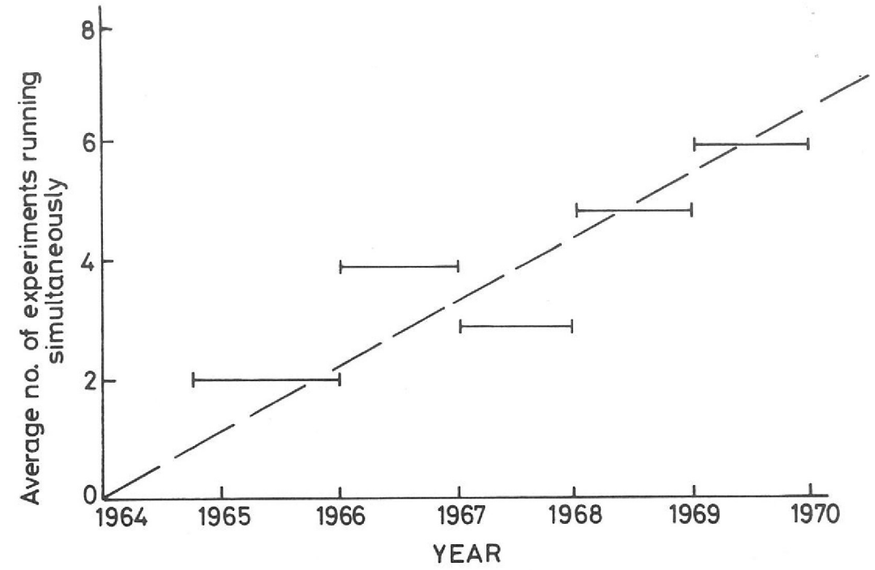

Figure 4. The average number of teams using particles from Nimrod at any given time for the years of Nimrod operation.

Many UK bubble chamber groups analyse film from both Nimrod and CERN and the experiments generally involve large collaborations from several countries. It is estimated that about 650,000 CERN pictures came to UK groups in 1969. Co-operation exists in both directions; CERN collaborated in the neon-hydrogen target work at Nimrod and film was sent from this Laboratory to many institutions abroad. Collaborations are also being set up between groups using Nimrod and groups abroad to perform spark chamber experiments using the Omega project, the large spark chamber magnet system due to start operation at CERN in early 1972.

In parallel with the growth of the Laboratory's participation in the CERN programme the use of Nimrod has been increasing steadily each year. In each three week cycle in the Nimrod schedule one day is allocated for planned maintenance, four days for machine tuning and development and the remaining 16 for high energy physics. Shutdown periods to make major changes to experiments, beam lines and machine components occur at a frequency of about one short shut-down (of about three weeks duration) and one long shutdown (of about six weeks) per year. Out of 8,760 hours in the year, 5,145 were scheduled for high energy physics and 87·9 per cent of these were actually achieved. Due to developments in target sharing in Nimrod many teams can run simultaneously. The sum of the number of Nimrod hours used by each team (team-hours) reached an all-time high of 26,044.

The average number of teams running simultaneously was 5·9 (figure 4). The average intensity was $1{\cdot}66 \times 10^{12}$ protons per pulse and more than 10^{19} protons were accelerated by Nimrod. The layout of beam lines in the Experimental Halls is shown in figure 5. Hall 3 came into use in the middle of the year with two beams lines installed in the initial phase. One beam line was removed from Hall 1, reducing the congestion there. 31 experiments are in various stages of running or analysis and are classified below as 10 strong interaction and 9 weak interaction experiments using electronic techniques (i.e. counters and spark chambers) and 12 bubble chamber experiments. The Selection Panel, a committee comprising Laboratory management and outside high energy physics experts, dealt with 12 proposals or letters of intent for future experiments; two were not approved, two CERN experiments were recommended for Laboratory support, four letters of intent received encouragement and four proposals received full approval. The CERN experiments were subsequently approved by a corresponding body at CERN. In response to the projected utilisation of Nimrod a Laboratory Committee, known as the Co-ordinating Team, have planned the installation of two or more beam lines from a second target station along the extracted proton beam X3 in Experimental Hall 3.

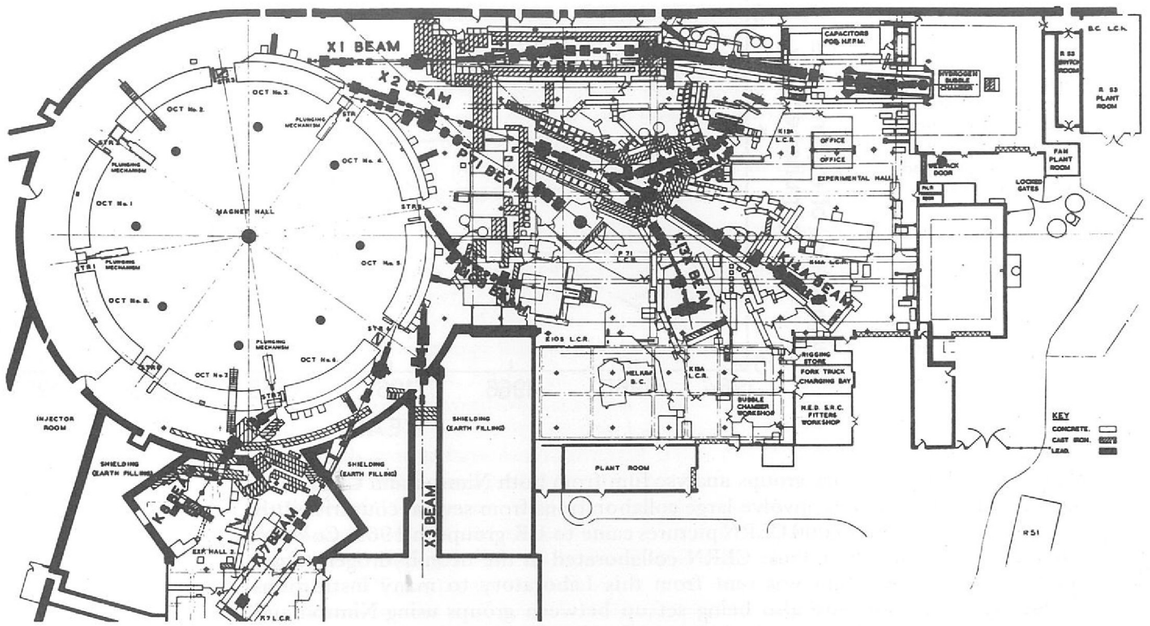

Figure 5a. Nimrod Experimental Halls 1 and 2. Layout at 31 December 1969.
(This figure is also available in pullout form at the end of the Report).

Table 2

Composition of Teams using Nimrod in 1969

	Physicists		Research Students		Support Staff*	
	Electronic Techniques	Bubble Chambers	Electronic Techniques	Bubble Chambers	Electronic Techniques	Bubble Chambers
Visitors**	59	42	40	43	11	1
Resident RL staff †	30††	9††	-	-	20	12
TOTAL	89	51	40	43	31	13

* Includes only technical assistance directly concerned with experiments and does not include engineering support.

** Staff from Universities and other groups.

† Including Rutherford Laboratory physicists at present working at CERN.

†† These numbers include 26 fixed term Research Associates and 5 staff members with joint University appointments.

Table 3

Institutions Participating in the High Energy Physics Programme.

Counter Experiments

AERE, Harwell
University of Bergen, Norway
University of Birmingham
University of Bristol
University of Cambridge
CERN, Geneva
University of Glasgow
Imperial College, London
Univeristy of Liverpool
Orsay
University of Oxford
Queen Mary College, London
Rutherford High Energy Laboratory
University of Southampton
University of Sussex
University College, London
University of Warwick
Westfield College, London

Bubble Chamber Experiments

University of Birmingham
University of Brussels, Belgium
University of Cambridge
CEN, Saclay
CERN, Geneva
College de France
Ecole Polytechnique, France
University of Edinburgh
University of Glasgow
Imperial College, London
University of Liverpool
University of Oxford
Rutherford High Energy Laboratory
University of Strasbourg, France
Tufts University, USA
University College, London
Westfield College, London

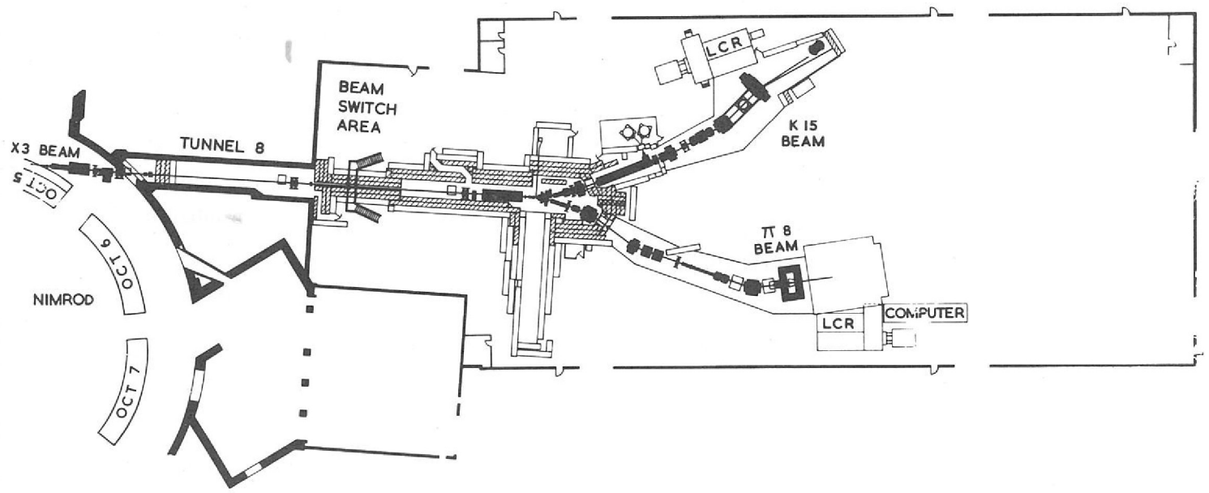

Figure 5b. Nimrod Experiment Hall 3. Layout at December 1969.
(This figure is also available in pullout form at the end of the Report).

Experiments using Electronic Techniques

STRONG INTERACTIONS

Number	Experiment	*Beam Line	Status of Expt. (at Dec. 1969)
1	Differential cross-sections measurements for π^-p elastic scattering	π5	Completed
2	Neutral states produced in K^-p interactions	K10S	Analysis
3	(a) K^+p differential cross-sections in the momentum range 0·45 – 0·90 GeV/c	K12	Analysis
	(b) K^-p differential cross-sections in the momentum range 0·45 – 0·90 GeV/c	K12	Analysis
4	(a) K^+p differential cross-sections in the momentum range 1·6 – 2·4 GeV/c	K8	Analysis
	(b) K^-p differential cross-sections in the momentum range 0·9 – 2·2 GeV/c	K8	Data taking
5	An investigation of narrow width mesons	π7	Data taking
6	Wide angle elastic pp scattering	P71	Data taking
7	Polarization effects in π^+p elastic scattering	K14A	Data taking
8	K^+p differential cross-sections in the momentum range 1 – 2 GeV/c	K15	Setting-up
9	K^+n elastic and charge exchange differential cross-sections	K12A	Installation
10	Elastic pion scattering through low energies	CERN	Data taking

* see figure 5 where applicable

The strong interaction experiments at Nimrod have been aimed at studying the properties of resonances, i.e. very short-lived particles (lifetimes or order 10^{-23} seconds). Two types of experiments can be distinguished, namely:

1. **Production experiments** in which the resonance is produced in a reaction in association with one (or more) particles and is identified by reconstruction from its decay particles. This type of experiment is more often studied using the bubble chamber technique. Often the existence of the resonance is inferred from the properties of the associated particle – *a missing mass experiment* (Experiment 5 is an example).

2. **Formation experiments** in which the incident particle and target particle coalesce briefly to form a resonance at an incident particle momentum characteristic of the mass of the resonance which immediately decays back into the initial particles – the elastic channel – or into other particles – inelastic channels. The properties of these resonances, mass, mass width, spin, parity, isotopic spin etc., are obtained by analysing their decay into two body final states. Experimentally total cross-sections, differential cross-sections and polarizations are measured and the data analysed in terms of partial wave amplitudes of different spin and parity. Most of the strong interaction experiments on Nimrod are of the formation type (Experiments 1,2,3,4,7,8 and 9). The existence of a large number of possibly overlapping resonances requires that measurements be made with high precision and at closely spaced intervals of momentum and angle.

The scattering of pions on protons can form πp baryon resonances of strangeness S = 0, and isotopic spin I = 1/2 and I = 3/2. π^+p elastic scattering is a pure I = 3/2 state and π^-p a mixture of I = 1/2 and I = 3/2 states. Very often all the available data on πp scattering is required to isolate the resonances by sophisticated computer techniques, e.g. phase-shift analyses. A substantial fraction of the world data has been produced at Nimrod. In a recent experiment (Experiment 1), analysed this year and reported at the Lund International Conference in Sweden last June, measurements were made of the differential π^-p elastic cross-sections at 30 momenta from 1·2 to 2·5 GeV/c. At each momentum, the angular distributions contained about 16,000 events. This new data was compared with the existing phase shift analysis and it was concluded that:–

a. A P13 (1860) resonance previously considered a poor candidate is now strongly supported (figure 6). (The notation is L2I, 2J (mass in MeV/c^2) where L is the usual spectroscopic symbol for orbital angular momentum, I the isotopic spin and J intrinsic spin).

b. The suggested D13 (2030) is supported by the data, and

c. There is evidence for an F17/G17 doublet with a mass near 2,000 MeV.

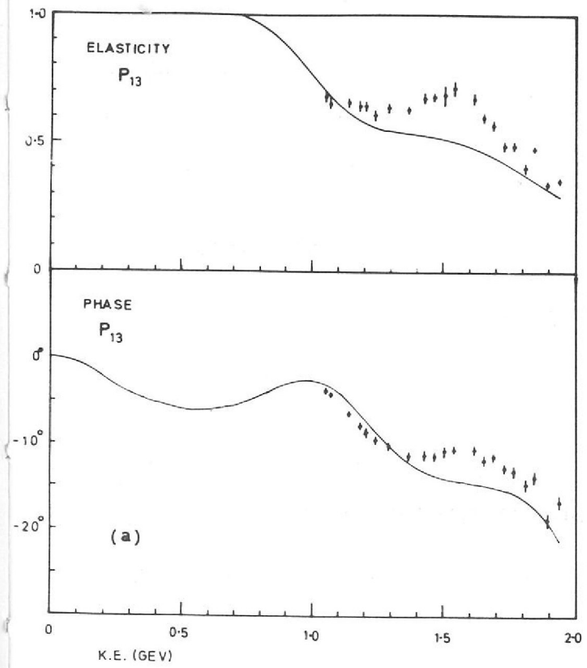

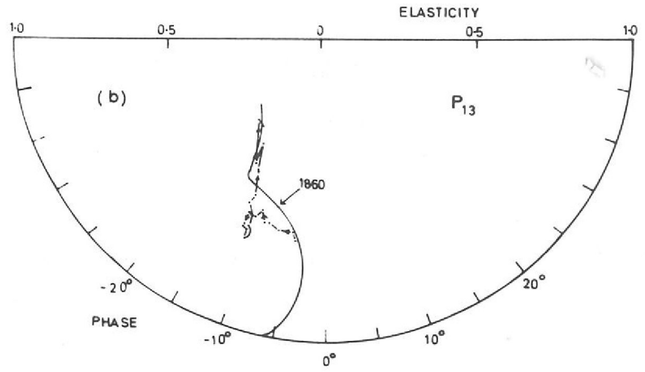

Figure 6. The P13 phase shift data from Experiment 1 compared with the latest CERN analysis (solid line). The more pronounced appearance from the data of an arc of a circle in the lowest curve is strong supporting evidence for a resonance of isotopic spin I = 1/2 and spin and parity J^P = 3/2 at a mass of 1860 MeV/c^2.

The present experimental data is unable to separate the I = 3/2 high mass resonances unambiguously. A new series of measurements (Experiment 7) has started to investigate the pion-nucleon system by measuring π^+p elastic scattering from a polarized target at approximately 70 momenta between 0·6 and 2·7 GeV/c incident π^+ momentum. This experiment complements the experiment completed in 1968 on π^-p elastic scattering from polarized protons at 50 momenta in a similar momentum range. The new LMN (double nitrate of lanthanum and magnesium) polarized target for the π^+p experiment has achieved a polarization of approximately 70 per cent and data taking has commenced.

The K^-p system can form baryon resonances of strangeness S = -1 and isotopic spin I = 0 and 1. K^-p scattering has not been so extensively studied as πp scattering due to the lower yield of K mesons from accelerators. A survey of K^-p interactions in the Saclay Hydrogen Bubble chamber at 13 K^- laboratory momenta approximately evenly spaced in the interval 1·25 and 1·85 GeV/c is nearing completion (Experiment 25). A spark chamber study of neutral states, primarily $\Lambda^o\pi^o$, $\Lambda^o\eta^o$, $\Sigma^o\pi^o$ and $\Sigma^o\eta^o$, produced in K^-p interactions in the range 0·65 to 1·25 GeV/c (Experiment 2), completed data taking in 1969, and is now being analysed. Systematic measurements on K^-p elastic scattering (Experiments 3b and 4b), using spark chambers with automatic recording on to magnetic tape through on-line computers, are now also being analysed. These two experiments between them have measured 200,000 events at a total of 46 momenta. The discovery of structure in the K^+p total cross-sections in experiments at Brookhaven and the Rutherford Laboratory in 1967 has prompted detailed measurements on elastic K^+p and K^+n scattering (Experiments 3a, 4a, 8 and 9) to establish the existence or otherwise of 'exotic' (K^+N) resonances with S = +1. Strangeness S = +1 baryons are not expected to be formed on the basis of simple quark models and so far there has been no conclusive evidence for their existence. Experiment 4a has completed data taking yielding about 4500 elastic K^+p scattering events in each of 27 momentum bins between 1·6 and 2·35 GeV/c. Analysis is nearly finished and results will be available early in 1970. In a lower momentum interval, (0·48 – 0·96 GeV/c), Experiment 3a is analysing a total of about 130,000 elastic events. The data from these experiments on both K^+p and K^-p elastic scattering represent a considerable fraction of all data in those momentum intervals and will provide valuable input for the new phase shift analyses now underway.

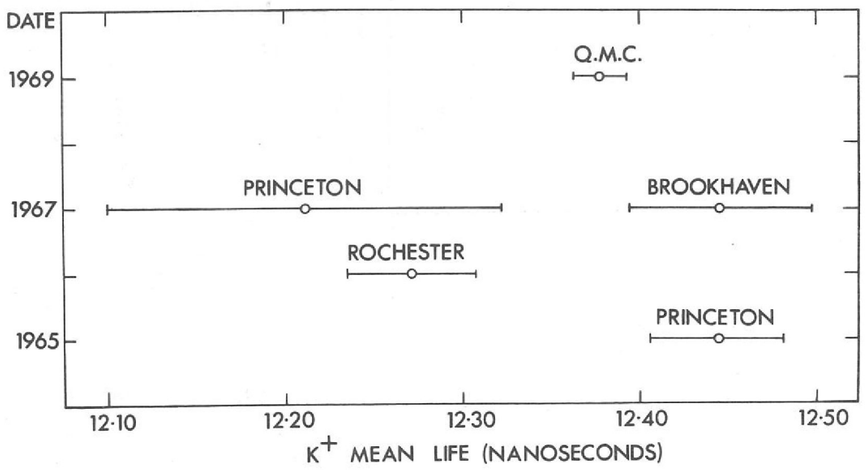

Figure 7. The value of the K^+ lifetime from Experiment 12 compared with the previous data.

Experiments using Electronic Techniques

WEAK INTERACTIONS

Number	Experiment	*Beam Line	Status of Expt. (at Dec. 1969)
11	The leptonic decay modes of the K^+ Meson	K4	Completed
12	K^+ lifetime measurement	K12	Completed
13	The β decay of the Σ^- hyperon	π4	Analysis
14	Test of the $\Delta S = \Delta Q$ rule for K^o leptonic decays	K13	Analysis
15	Test of the $\Delta I = 1/2$ rule in the decay $\Sigma^+ \rightarrow p\pi^o$	K14	Analysis
16	Search for charge asymmetry in η decay	π8	Setting-up
17	Search for the decay $K_S^o \rightarrow \pi^+\pi^-\pi^o$	K13A	Setting-up
18	Measurements of ϕ_{000}, the phase of the decay $K_L^o \rightarrow \pi^o\pi^o\pi^o$	CERN	Completed
19	Study of the decay modes $K^\pm \rightarrow \pi^\pm\pi^o\gamma$ and $K^\pm \rightarrow \pi^\pm\pi^o\pi^o$	CERN	Analysis

* *see figure 5 where applicable.*

Most of the weak interaction experiments have been concerned with various aspects of K meson decay. One experiment which completed data taking and analysis during the year was the measurement of the K^+ lifetime, the value of which had previously been in doubt (Experiment 12). The clear cut result of this experiment can be judged from figure 7. Another experiment to complete analysis was the high statistics study of the leptonic decay modes of the K^+ meson (Experiment 11). This experiment has made valuable contributions to the understanding of the form of the weak interaction in these decays. The last of a series of results has now been obtained and on completion of the experiment we review the main results:—

1. $$R = \frac{K^+ \rightarrow e^+ + \nu_e \text{ branching ratio}}{K^+ \rightarrow \mu^+ + \nu_\mu \text{ branching ratio}} = (1{\cdot}9\ ^{+0{\cdot}7}_{-0{\cdot}5}) \times 10^{-5}$$

in good agreement with the assumptions of weak interaction theory that the μ^+ and e^+ are equally coupled to strange particles and that the form of the weak interaction is (V-A) as it is in the case of non-strange particles.

2. The electron momentum spectrum in the decay $K^+ \rightarrow e^+\pi^o\nu$ (Ke3) derived from 17,000 events (figure 8), is in good agreement with the predicted pure vector coupling.

3. The Ke3 branching ratio was found to be 0·0492 ± 0·0021, a result which led to a substantial improvement and clarification in the world average value. This branching ratio strongly supports the hypothesis that $\Delta I = 3/2$ currents are absent in semi-leptonic weak interactions.

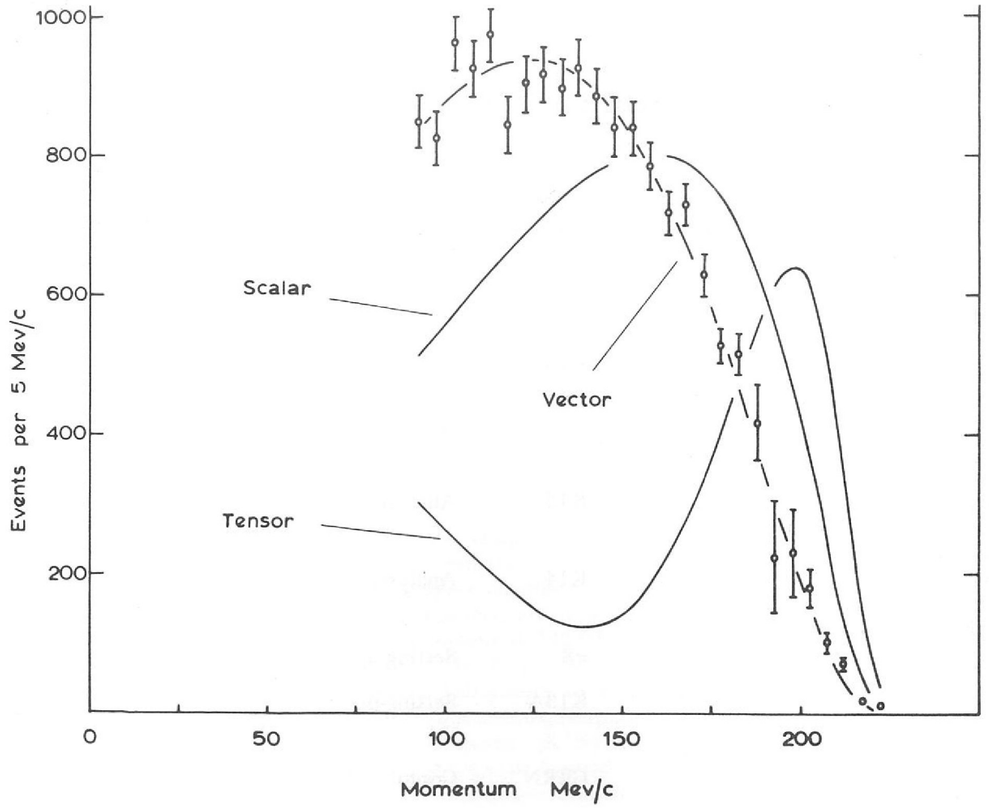

Figure 8. The final Ke3 electron momentum spectrum is compared with the predictions for pure scalar, vector and tensor couplings (Experiment 11).

4. The momentum dependence of the Ke3 form factor f_+ has been measured by studying the pi-zero energy spectrum. The result is parameterized as $\lambda^+ = 0{\cdot}045 \pm 0{\cdot}015$ and is compatible with theoretical expectations.

5. The relative branching ratio of Kμ3 ($K^+ \to \mu^+\pi^o\nu$) to Ke3 has been measured and a value of the ratio of the form factors deduced to be:—

$$\xi\,(0) = f_-(0) / f_+(0) = -\,0{\cdot}35 \pm 0{\cdot}22$$

assuming $\lambda^+ = 0{\cdot}045 \pm 0{\cdot}015$ and $\lambda^- = 0$. This result is in agreement with theoretical expectations and goes someway towards reducing the present discrepancy between values of ξ deduced from different experimental measurements.

Two Nimrod experiments on weak interactions (Experiments 14 and 15) and one at CERN (Experiment 19) completed data taking during 1969 and are expected to yield in each case more events than the present world total. Analysis is continuing and results can be expected during 1970. A new experiment in the setting-up stage in Experimental Hall 3 is the search for C-violation effects in the electromagnetic decay $\eta^o \to \pi^+\pi^-\pi^o$. To date five experiments at various laboratories with a total of about 50,000 decays have yielded conflicting results. The Nimrod experiment has been designed to produce 500,000 events of this decay.

New results on the CP violating decay $K_L^o \to \pi^o\pi^o$ have been obtained by a CERN/Orsay Rutherford Laboratory collaboration using the CERN K_L^o beam (Experiment 18). The amplitude and phase of this decay were measured to be $|\eta_{oo}| = (3{\cdot}33 \pm 0{\cdot}64) \times 10^{-3}$ and $\phi_{oo} = 51° \pm 30°$, (preliminary values subject to confirmation). Although the values are the most accurate to date the overall situation on the form of the CP violation in weak interactions is confused. Four experiments designed to study other aspects of CP violation are described below (Experiments 14, 16, 17 and 19).

The Bubble Chamber Programme

Experiment No.	Interacting System	Incident Momentum GeV/c	No. of Pictures × 10^6	Status at Dec. 1969
20	π^-p	0·45 — 0·55	0·275	Completed
21	π^+p	0·60 — 0·80	0·10	Analysis
22	π^+p	(a) 0·90 — 1·05 (b) 1·10 — 1·70	0·20 0·30	Completed Analysis
23	π^+He, pHe	1·88	0·50	Analysis
24	π^+d	4·00	0·10	Transferred to CERN
25	K^-p	1·25 — 1·85	1·4	Analysis
26	K^- heavy liquid	2·20	0·68	Analysis
27	K^-d	1·45 — 1·65	0·71	Analysis
28	K^-p	14·00	0·34 at CERN	Analysis and data taking
29	K^+p K^+d	2·10 — 2·90 2·20	0·2 0·4	Analysis Analysis
30	np	1·00 — 7·00	0·15	Analysis
31	$\bar{p}$p	1·20	0·1	Analysis
32	Test pictures and study of electron beam			
33	Test of neon-hydrogen target facility for 1·5m hydrogen chamber			

During 1969 the 1·5 metre British National Hydrogen Bubble Chamber has been largely devoted to new developments of the bubble chamber technique rather than to maximising the number of pictures taken. The philosophy adopted for the operation has been to complement the programme at CERN in the sense that the CERN 2 metre chamber has played the leading role in supplying conventional high quality film to European analysis groups whilst physicists from CERN and the UK have successfully used the 1·5 metre chamber to explore major developments in the technique. These developments should provide a unique facility for high energy physics in 1970. Nevertheless more than one million pictures in two chambers were taken during 1969.

Two developments have been considered. The first is essentially a development of the beam feeding the chamber to provide beams of short-lived hyperons, initially Λ^o's from a target just outside the chamber magnet. In January 150,000 pictures were taken as part of the development programme for this technique using fast neutrons from a target 7 metres from the chamber. This film is now being analysed (Experiment 30). A major achievement has been the operation of a sensitive

hydrogen target system within the main chamber which is filled with a neon-hydrogen mixture (figure 9). This system combines the advantages of the hydrogen bubble chamber with those of the heavy liquid chamber. This work (Experiment 33) is a collaboration between staff from CERN, Rutherford Laboratory and University College, London. The significance of this development is that the production processes, i.e. beam particle interactions, occur in pure hydrogen or deuterium (the advantage of having a simple proton or deuteron target being thereby preserved), whilst the gamma rays from the decay of neutral pions and Σ^{o} hyperons are converted in the short radiation length neon-hydrogen mixture to give measurable electron pairs. In this way events having more than one neutral secondary particle become accessible for study. This feature is clearly of great importance, particularly at high energies where many particles are produced. The technique will certainly find application both in existing chambers and, perhaps more importantly, in the new bubble chambers under construction or proposed i.e. the CERN 3·7 metre chamber and the Rutherford Laboratory High Field Bubble Chamber.

The conventional high energy physics bubble chamber programme has concentrated on two major experiments. The 1·5 metre chamber successfully operated with a deuterium filling and 400,000 pictures were taken of 2·2 GeV/c K^{+} meson interactions (Experiment 29). This is the first part of a major survey experiment to study the K^{+} nucleon interaction in the energy range 2 – 2·8 GeV/c. The data taking for this will be completed early in 1970. The 1·4 metre Heavy Liquid Bubble Chamber completed its experimental programme during the year. The study of K^{-} interactions at 2·2 GeV/c in a propane-freon mixture (Experiment 27) is now in the course of analysis. During 1969, 300,000 pictures were taken to complete the data taking for this experiment and yielding a final total of 600,000 pictures. This experiment is designed to study the properties of the Ξ^{o} hyperon, the $\Lambda^{o} - \Lambda^{o}$ interaction and the neutral decay modes of boson resonances.

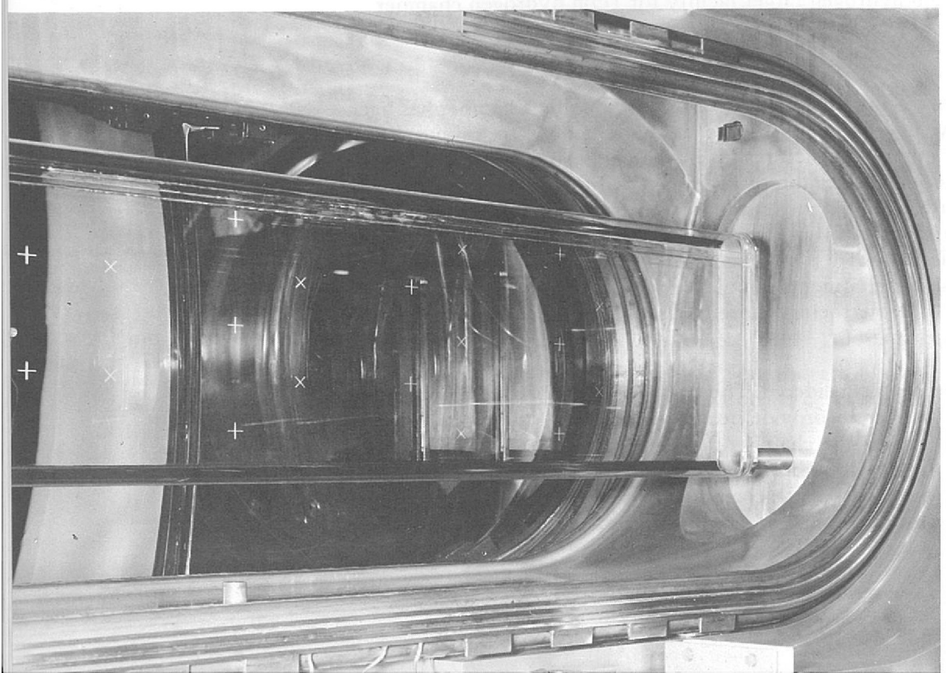

Figure 9. The neon-hydrogen target facility (Experiment 33).

During the course of a study of electrons and pions at 1·0 GeV/c undertaken to gain information on the track characteristics in the 1·5 metre hydrogen bubble chamber for the analysis of the film previously taken to study neutron induced interactions, anomalies have been observed in the content of the electron beam. Indications (Experiment 32) have been obtained of possible deviations of the bremsstrahlung and pair production spectra observed in the chamber from the form calculated from quantum electrodynamics. It is suggested that the so-called electron beam might contain particles of mass greater than that of the electron and less than that of the muon. This work, if substantiated, could clearly have very profound implications and further studies will be made during 1970.

Like most other bubble chamber groups, the Rutherford Laboratory group has been concerned with the analysis of film taken both at CERN and at Nimrod. As part of a collaboration, a study of multiparticle final states produced by 14 GeV/c K^{-} interactions (Experiment 28) in the CERN 2 metre hydrogen bubble chamber is in progress. This is the highest energy separated K^{-} beam presently available in the world and all aspects of the interactions, i.e. all final states accessible, will be studied. It is anticipated that this experiment will yield valuable data on the structure of the Q enhancement and the L meson in the $K\pi\pi$ system together with further studies of other meson and hyperon resonances and high energy production mechanisms. Analysis has also proceeded on two prong events from antiproton interactions at 1·2 GeV/c (the region of the T meson). This film is also from the CERN 2 metre chamber (Experiment 31). A further two proposals for experiments have been submitted to CERN and will take data during 1970. The first of these is a continuation of the $K^{-}p$ survey experiment to the energy region 1·0 to 1·4 GeV/c to link up with the exposure at higher energy, 1·3 to 1·8 GeV/c, performed at Nimrod. This experiment is still in the process of analysis. New results confirm the spin and parity assignments $J^{P} = 7/2+$ of the Σ (2030) and $J^{P} = 5/2+$ of the Σ (1915) (Experiment 25). The second proposal to CERN is for a large, $0{\cdot}8 \times 10^{6}$ pictures, exposure to study a 4 GeV/c π^{+} interactions in the 2 metre chamber filled with deuterium with particular interest in the splitting of the neutral A_2 meson. This was originally submitted to the Rutherford Laboratory and approved as an experiment on Nimrod. However, in the spirit of co-ordination with CERN this proposal has been taken to CERN to release time in the 1·5 metre chamber at Nimrod for further development of the neon-hydrogen target facility.

Experiment 1

UNIVERSITY OF BRISTOL
RUTHERFORD LABORATORY

Differential Cross-Section for π^-p Elastic Scattering (61, 159, 211)

Analysis of the data collected in the measurement of differential cross-sections for π^-p elastic scattering at 30 momenta in small momentum steps from 1·21 GeV/c to 2·49 GeV/c together with one measurement at 3·03 GeV/c was completed in early 1969. Details of the experimental method were given in the 1967 Annual Report (Experiment 11).

The results of the experimental measurements at the 31 momenta have been published. A total of about 500,000 elastic events were recorded giving about 16,000 events per momentum. Figures 10, 11 show differential cross-sections for π^-p at 1·30 GeV/c and 1·92 GeV/c respectively.

The new π^-p elastic scattering data were compared with cross-sections predicted by the smooth CERN phase shifts in the momentum range 1·0 to 2·0 GeV/c. Some modification of these CERN phases were found to be necessary to give acceptable agreement. The modifications necessary are indicated in the case of the P_{13} in figure 12. The smooth lines are the CERN phase shifts and the points result from the π^-p differential cross-section data of this experiment.

The results of this analysis have provided further evidence for certain N*½ nucleon resonances in the mass range 1800–2200 MeV/c^2. At the Lund Conference and in a recent publication the following conclusions were reached:

1. A P13 (1860) resonance is strongly supported.
2. The P13 (2030) is supported, but at a lower mass.
3. There is evidence for an F17/G17 doublet with a mass near 2000 MeV/c^2.
4. The possibility of structure at higher energies in the P33 and D35 waves emphasizes the need for systematic differential cross-section and polarization data both for π^+p elastic scattering and π^-p charge exchange particularly at momenta above 1·5 GeV/c.

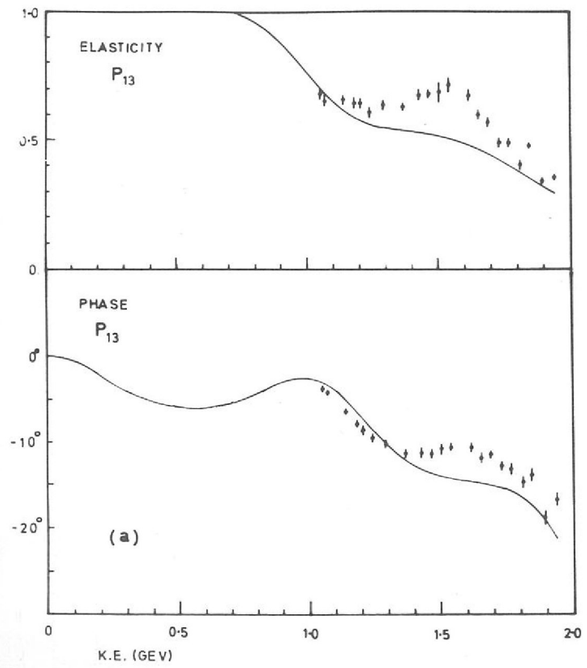

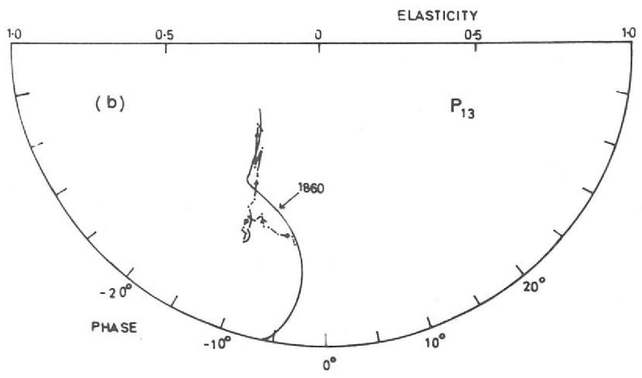

Figure 12. The P13 phase shift data from Experiment 1 compared with the latest CERN analysis (solid line). The more pronounced appearance from the data of an arc of a circle in the lowest curve is strong supporting evidence for a resonance of isotopic spin I = 1/2 and spin and parity $J^P = 3/2$ at a mass of 1860 MeV/c^2.

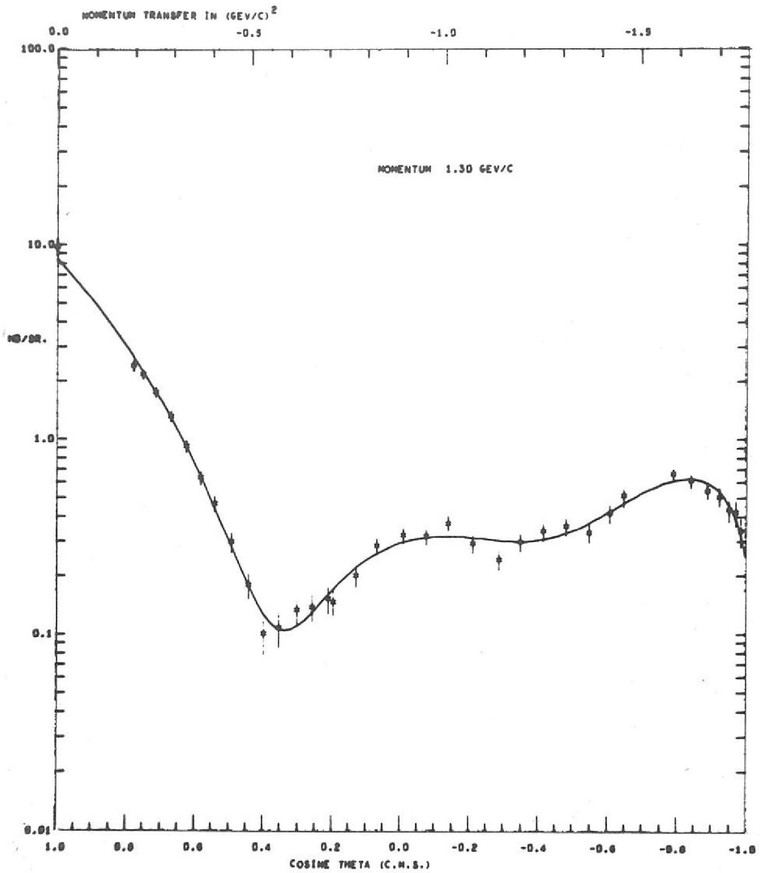

Figure 10. π^-p Differential cross-sections measured at 1·30 GeV/c. (Experiment 1).

Figure 11. π^-p Differential cross-sections measured at 1·92 GeV/c. (Experiment 1).

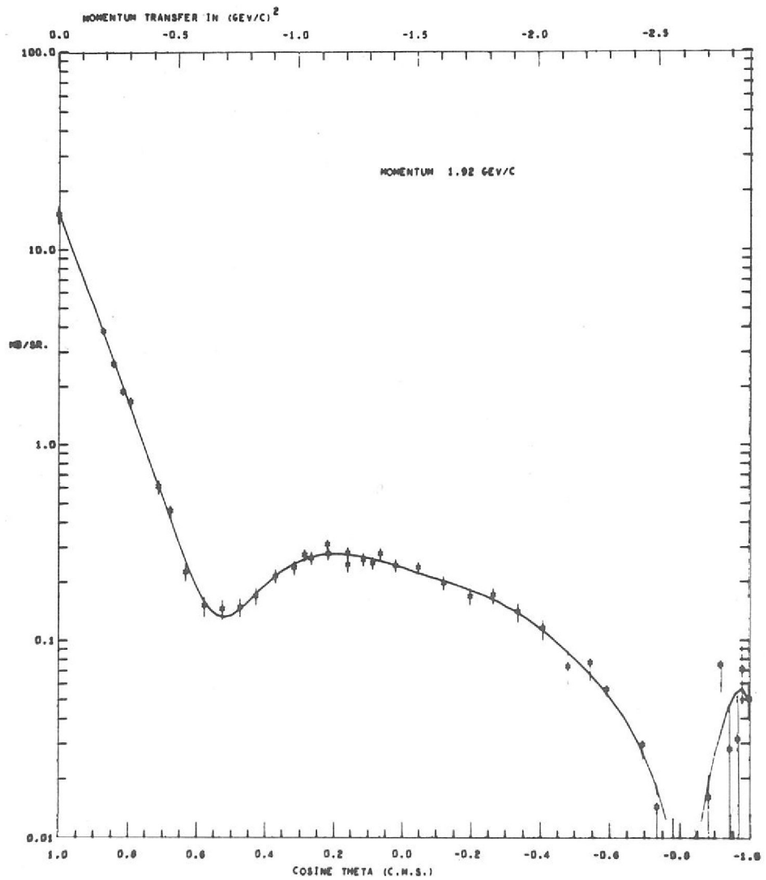

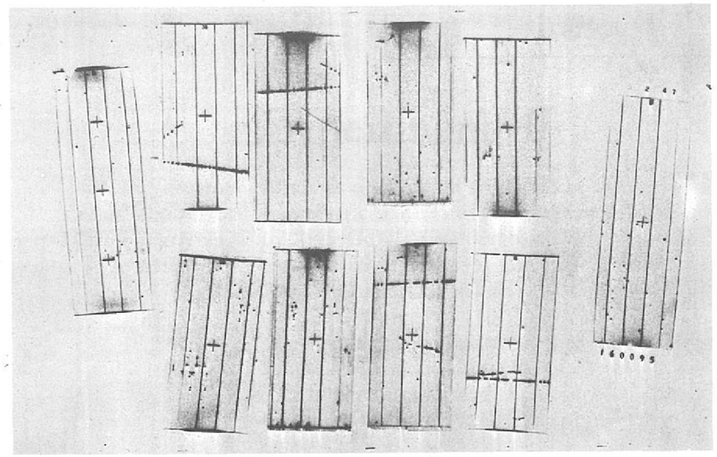

Figure 13. Spark chamber photograph from Experiment 2. This event has been fitted to the reaction $K^- + p \rightarrow \Lambda^\circ + \pi^\circ$.

Experiment 2

UNIVERSITY OF OXFORD

Neutral States Produced in K^-p Interactions

This experiment is a study of neutral states, primarily $\Lambda^\circ\pi^\circ$, $\Lambda^\circ\eta^\circ$, $\Sigma^\circ\pi^\circ$ and $\Sigma^\circ\eta^\circ$, produced in K^-p interactions. A partial wave analysis of these reactions will allow a separation of some of the many excited hyperon states formed by the K^-p system.

Two data runs have now been completed, yielding 300,000 photographs, covering 15 momentum points every 20 MeV/c from 700 to 1000 MeV/c. Wire chamber particle co-ordinates are also recorded on magnetic tape for each event. About 1 frame in 6 contains a useful event, and the scanning and measuring of these events is proceeding at the present time.

Computer programs have been written for the geometric reconstruction, kinematic fitting, weighting and angular distribution fitting, and below we give an example of the fit obtained to a $\Lambda\pi^\circ$ event, with a comparison of fitted particle energies, and energies measured on the film using particle ranges and spark counting of gamma-ray showers.

Event No. 160095. $K^- + p \rightarrow \Lambda^\circ + \pi^\circ$ (shown in figure 13)

K momentum	Pion momentum	Proton momentum	$\gamma 1$	$\gamma 2$
Fitted 731 MeV/c	114 ± 4	921 ± 13	276 ± 12 Fit	51 ± 9 Fit
	104 ± 10 from range	> 590 from range	295 ± 70 spark count	51 ± 12 spark count

Experiment 3

UNIVERSITY OF BIRMINGHAM
RUTHERFORD LABORATORY

$K^\pm p$ Differential Cross-Sections

Elastic differential cross-sections are being measured for K^-p and K^+p scattering in the laboratory angle range 5° to 180°. The K^-p data are at 14 momenta between 650 and 960 MeV/c; the K^+p data are at 13 momenta between 480 and 960 MeV/c. The aim of the experiment is to provide a set of data with improved statistical accuracy and small momentum steps. Phase shift analysis of the K^-p data should help to clarify the present confusion in the Y* spectrum in this mass range (1630–1780 MeV). One of the interests of the K^+p data is in information on possible 'exotic' resonances (Z*) which are not expected to exist in the simple quark model.

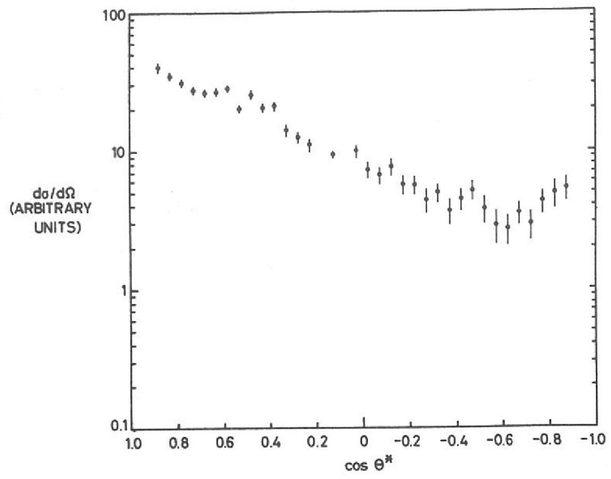

Figure 14. Differential cross-sections for K^+p elastic scattering at 1·437 GeV/c (Experiment 4).

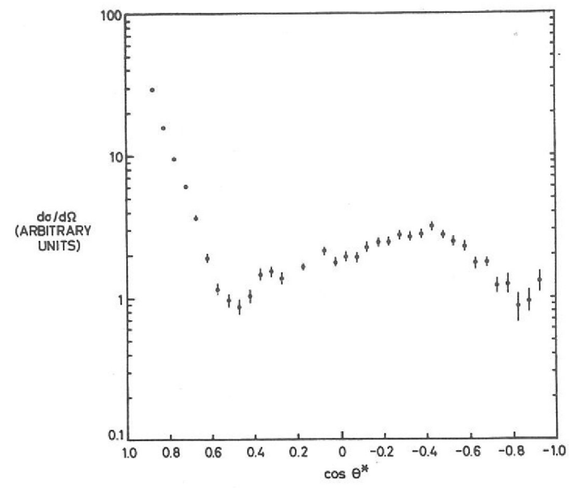

Figure 15. Differential cross-sections for π^+p elastic scattering at 1·715 GeV/c (Experiment 4).

Arrays of scintillation counters and sonic spark chambers in a separated K-meson beam, (derived from X2), were used to study firstly K^+p and secondly K^-p elastic differential cross-sections. The only substantial change in the apparatus since the previous report was the installation of a septum magnet as the first element of the secondary beam line. This reduced the production angle of the beam from 15° to 8°, which doubled the beam intensity. Data taking was completed by December 1969. For intermediate angles the scattered K and recoil proton were both detected in separate systems, one each side of the target. For forward and backward scattering this was not possible so either a K or a proton was detected and momentum analysed with a magnetic spectrometer. The spectrometer geometry involved a rather loose trigger so that the data includes μ's and π's from K decay. These can be separated kinematically over much of the angular range but a region of confusion does exist. The relatively poor signal to noise ratio means that systematic effects have to be well understood. The correlation data is much cleaner; the analysis has already reached an advanced stage and should be completed in the near future.

Experiment 4

UNIVERSITY COLLEGE, LONDON
RUTHERFORD LABORATORY

$K^\pm p$ Differential Cross-Sections (202, 204, 206)

The data-taking phase of this group of experiments, in which it is aimed at obtaining differential cross-sections for K^+p and K^-p elastic scattering over a wide range of momenta with the aid of a computer-controlled wire spark chamber system, is now nearing completion. Figure 14 shows the results of a K^+p measurement at 1437 MeV/c. During the course of testing the equipment, a substantial amount of data on π^-p and π^+p scatters were obtained, the latter at one momentum only (figure 15). The table summarises the numbers (rounded) of elastic scatters at present extracted from the raw data.

Process	Momentum Range	No. of momenta	No. of events
π^+p	1·715 GeV/c	1	60,000
π^-p	1·0–1·4 GeV/c	14	100,000
K^+p	1·4–2·3 GeV/c	28	150,000
K^-p	1·0–1·4 GeV/c	13	30,000
K^-p	1·7–2·4 GeV/c	19	30,000

All the data is still subject to small corrections which are currently being investigated and applied. Nevertheless preliminary phase shift analyses are being carried out on the π^-p and K^+p data. The latter at present show no positive evidence for the suspected Z_1 (2170) resonance. The former appear to give results compatible with the CERN phases for all except four of the partial waves, which show a systematic deviation. There is at present no evidence that any of the new resonances of the CERN analysis will be washed out by our data, although it is likely that a final complete phase shift analysis will result in a modification of some of the resonance parameters.

A provisional Legendre polynomial analysis of the high momentum K^-p data is suggestive of the spin and parity assignments $9/2^-$ and $9/2^+$ respectively for the $Y_1^*(2250)$ and $Y_1^*(2350)$, although it is clear that more data will be required to make firm statements about these parameters.

Experiment 5

IMPERIAL COLLEGE, LONDON
UNIVERSITY OF SOUTHAMPTON

An Investigation of Narrow Mesons Produced in π^-p Interactions

This experiment is an attempt to search for and study narrow mesons in π^-p collisions over a mass range from about 500 to 2000 MeV/c^2. The equipment consists essentially of a precisely controlled and variable pion beam, a hydrogen target, 6 neutron counters near the forward direction and, surrounding the target, an arrangement of counters differentially sensitive to both charged particles and photons. It is therefore of the 'missing-mass' class of experiments. The emphasis so far has been on working very close to the reaction threshold and on studying the variation in the yield of neutrons and protons as the beam momentum is varied.

Data has now been collected at a statistical level suitable for a reasonable study of threshold effects at momentum intervals of 0·5% from 700 MeV/c to 4 GeV/c. Some data has also been accumulated at fixed momenta a few hundred MeV/c above the thresholds for the A_2 and R_3.

By comparison with experiments incorporating spark chambers, relatively little rejection of spurious events is possible once the run data has been obtained. Thus much effort has been directed towards making the electronic selection relatively clean. For the same reason, most of the analysis to date has been concerned with system performance.

That the basic idea of the experiment is sound can be seen from a study of ω (eg figure 16), η and dipion production, and backward elastic and charge exchange scattering at low momentum, all of which show very clearly. These processes are invaluable in giving a detailed picture of the response of the equipment, both to neutrons and protons, and also to various modes of decay.

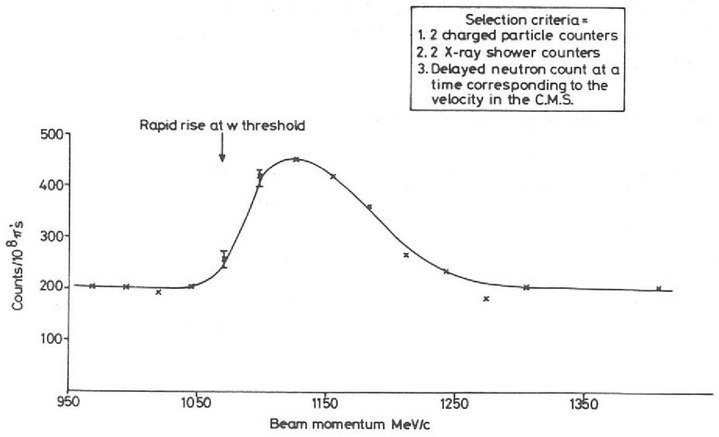

Figure 16. Measured yield curve of events satisfying an electronic criterion designed to pick out the most prolific decay of the ω (783). (Experiment 5).

Experiment 6

AERE, HARWELL
UNIVERSITY OF BERGEN,
QUEEN MARY COLLEGE, LONDON
RUTHERFORD LABORATORY

Wide Angle Elastic Proton-Proton Scattering

The aim of this experiment is to measure differential cross-sections for p-p elastic scattering from 1·4–4 GeV/c and 40°–90° centre of mass angle.

Figure 17 is a schematic diagram of the apparatus showing the two picket fences of counters for detecting scattered protons. After a suitable trigger from the counter logic the event geometry is recorded using an array of core-readout wire spark chambers. Data is written by an on-line PDP8 onto 7-track magnetic tape. The PDP8 is also used to generate a CRT display and to compile a series of histograms used to monitor apparatus performance. Analysis will be off-line on the Rutherford Laboratory IBM 360/75.

By December 1969 data had been taken at eleven momenta from 1·4–3·0 GeV/c and will be completed to 4·0 GeV/c early in 1970. Analysis has now begun, and it is hoped that preliminary results will appear in the near future.

Figure 17. Schematic diagram of the apparatus used in the measurements of wide angle proton-proton scattering (Experiment 6).

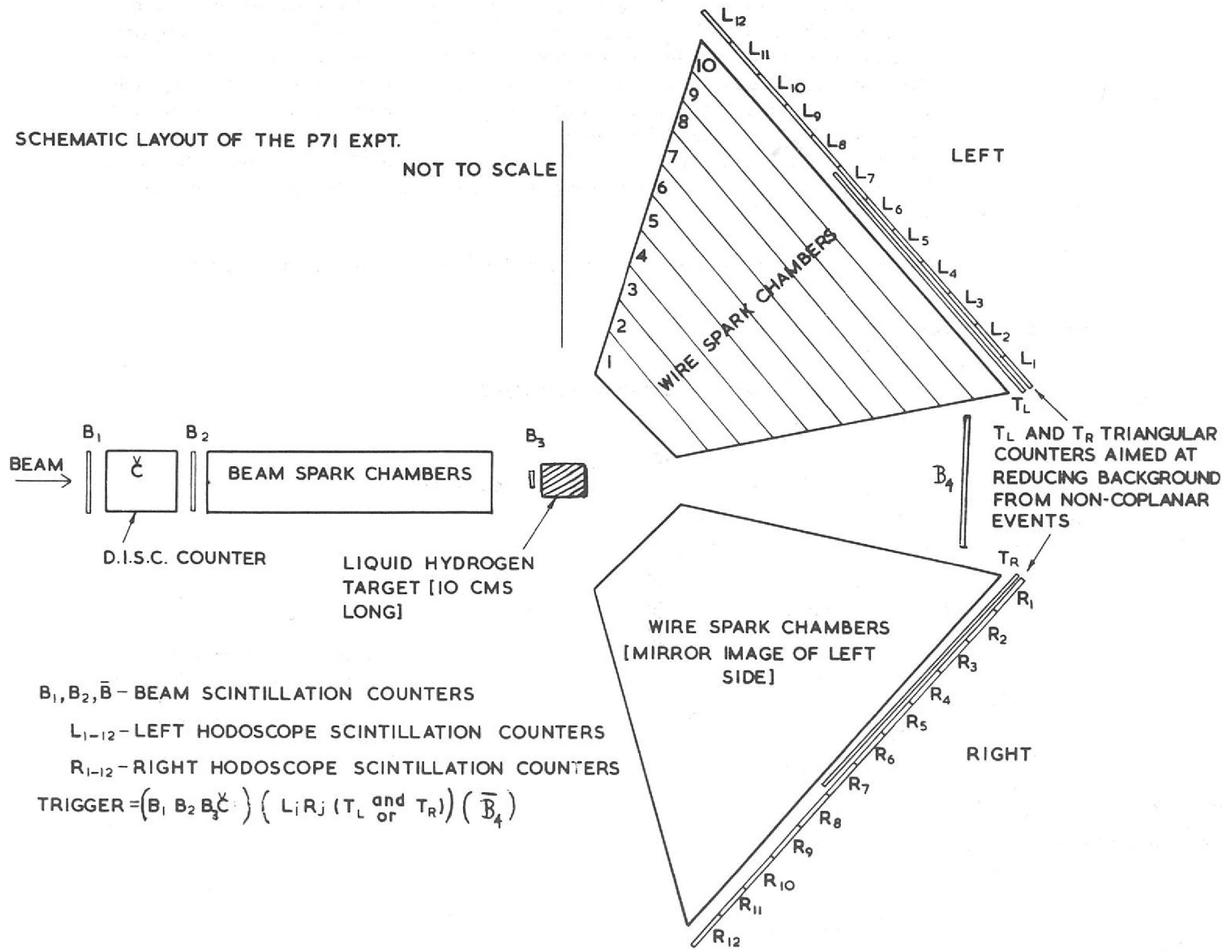

Experiment 7

UNIVERSITY OF OXFORD
UNIVERSITY OF WARWICK
RUTHERFORD LABORATORY

Polarization Effects in π^+p Elastic Scattering

The present experiment is a continuation of the work on πp scattering described in the Annual Reports of 1966 (Experiment 10) and 1967 (Experiment 7). The asymmetry in the scattering of π^- mesons by polarized protons was measured at 50 different momenta from 0·643 to 2·14 GeV/c. Data was obtained at values of cos θ ranging from approximately +0·9 to - 0·95 in the c.m. system at each incident pion momentum. The results have been expressed in the form of an expansion in terms of first associated Legendre polynomial series and compared with the predictions of recent phase shift solutions. It is concluded that although these analyses give satisfactory predictions of the general features of the results, no one solution gives complete agreement with the data above about 1·0 GeV/c.

It is planned to continue the investigation of the pion nucleon system by measuring π^+p elastic scattering from a polarized target at approximately 70 momenta between 600 MeV/c and 2700 MeV/c incident π^+ momentum. The π^-p system is a combination of I = ½ and I = 3/2 states. The acquisitions of polarization data on π^+p elastic scattering, which is a pure I = 3/2 system, will facilitate a full I-spin phase shift analysis.

The experimental layout is shown in figure 18. Electrons in the beam are vetoed by a gas Cerenkov counter. Pions are separated from protons at low momenta by a separator and by time of flight. At higher momenta a DISC Cerenkov counter is required. The new LMN polarized target has achieved a polarization of approximately 70%, which can be measured by an NMR system to an accuracy of ± 4%. The counter hodoscope consists of vertical counters to determine scattering angle, horizontal counters to enable elastic (coplanar) events to be separated from inelastic background, and Cerenkov counters to separate pions from protons in those regions where they are not clearly distinguishable by kinematics. It is hoped to extract differential cross-sections from the data if the background is not too high.

Setting up has been completed and a small amount of data has been taken.

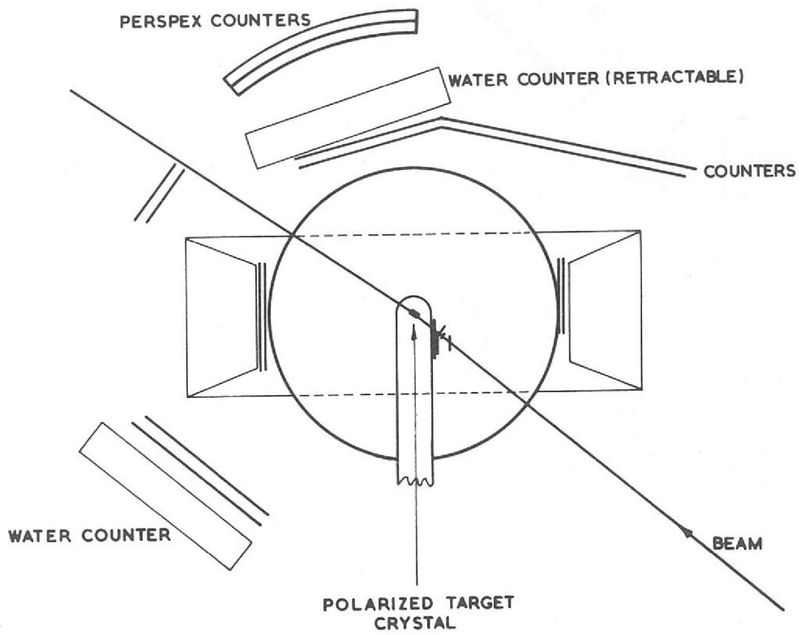

Figure 18. Plan view of the apparatus used in Experiment 7 (Polarization Effects in π^+p Elastic Scattering).

Experiment 8

UNIVERSITY OF BRISTOL
RUTHERFORD LABORATORY

Differential Cross-Sections for K^+p Elastic Scattering

With the discovery of structure in the positive kaon-proton total cross-sections in experiments at Brookhaven and this Laboratory (see Experiment 2, 1967 Annual Report), experiments designed to establish the existence or otherwise of resonances in the positive kaon-nucleon system have become important. Phase shift analysis using elastic differential cross-sections and polarization data for the pion-nucleon system has been effectively used in establishing a number of resonance states in this system. Already these methods of analysis are being extended to available positive kaon-proton data such as the polarization effects already measured at CERN and Argonne. This experiment is designed to measure accurate differential cross-sections for K^+p elastic scattering over the angular range of about 7° to 180° in the centre-of-mass at closely spaced momenta from 0·9 GeV/c to at least 1·6 GeV/c. It is planned to add this data to the polarization measurements for a phase shift analysis.

Positive kaons produced from an external target receiving protons from Nimrod in Experimental Hall 3 are focussed onto a 30 cm hydrogen target. Scattered protons and kaons are detected in spark chambers. These chambers use acoustic microphones developed in this laboratory for the accurate particle location necessary for selecting elastic events. A spectrometer magnet together with spark chambers is being used to determine the momenta of forward going scattered particles (either protons or kaons). The positional information derived from the microphones is fed in digital form directly into the core store of an Argus 400 computer. Use of this computer on-line for recording and monitoring data will permit a high rate of data collection for later analysis on the IBM 360/75.

Towards the end of 1969 some beam from Nimrod has been used in the testing of spark chambers, a differential Cerenkov counter and a number of scintillators. The spark chamber testing has been helped considerably by the on-line use of the computer.

During the December-January shut-down the hydrogen target and spectrometer magnet are being installed and the experiment should begin taking beam for setting up in the first cycle of 1970.

Experiment 9

BIRMINGHAM UNIVERSITY
RUTHERFORD LABORATORY

K^+ n Elastic and Charge Exchange Cross-Sections

Early in 1970, a Kn scattering experiment, will be set up to run at the same momenta as the Kp experiment (Experiment 3), for which data taking is complete. Installation is at present in progress. The channels to be studied are

$K^+ + n \rightarrow K^+ + n$ (I = 0 and 1)
$K^+ + n \rightarrow K^o + p$ (I = 0 and 1) S = +1
c.f. $K^+ + p \rightarrow K^+ + p$ (pure I = 1)

and $K^- + n \rightarrow K^- + n$ (pure I = 1)
c.f. $K^- + p \rightarrow K^- + p$ (I = 0 and 1) S = - 1

The reason for interest in these new channels is the extra information given regarding the isospin content of the K-N scattering amplitudes. Currently existing data is of poor quality statistically, except at a few isolated momenta through the range concerned. It is intended to obtain about 10^4 events for each channel, at each momentum.

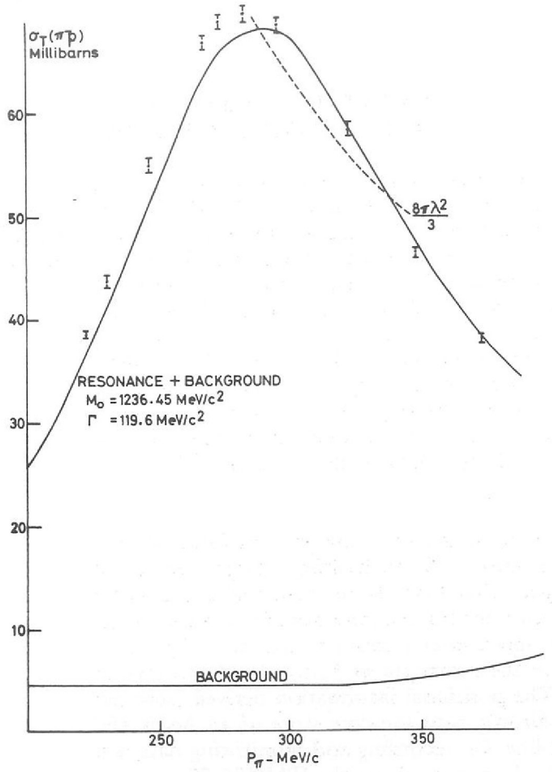

Figure 19. Results of the π^-p total cross-section measurements in Experiment 10. The solid curve is the best fit to earlier data with a resonance mass of 1236·45 MeV/c^2 and a width of 119·6 MeV/c. The dotted line shows the unitarity limit for the resonant phase shift. The "background" at the bottom of the figure represents the contribution of non-resonant waves.

Technically, the equipment is largely similar to that used for Experiment 3. Sonic spark chambers are appropriate, since data taking rates are high (ruling out optical chambers), accidental backgrounds are low, and only one charged particle is present for legitimate events (making wire spark chambers unnecessary). The largest chambers to be used are 3 × 2m^2 in area. Some of the spark chambers are run in high field regions (inside the spectrometer magnet). Tests on such sonic chambers carried out towards the end of the previous experiment indicate that this presents no major problems. The beam is identical to that used previously.

Experiment 10

UNIVERSITY OF CAMBRIDGE
RUTHERFORD LABORATORY

Elastic Pion Scattering Through Low Energies

310 MeV is traditionally the boundary between low and medium energy πp scattering. At this energy, the complete scattering amplitude has been determined with high accuracy by groups working with the Berkeley cyclotron. Above it are inelasticity, synchrotrons, and complicated phase shift analyses. Below it is an untidy tangle of early experiments, some good, some bad, but most indifferent by present standards, and done at scattered (and frequently ill-defined) energies, where University groups happened to be able to run their cyclotrons. The scattering is almost purely elastic, and, as Hamilton and co-workers showed in an analysis of the early data, is very clearly described using dispersion theory. Crossing symmetry restricts the states entering the theory to the nucleon, ρ and σ singularities, plus well-known dispersion integrals. Putting this in more physical terms, the centrifugal barrier largely shields the pion from short-range forces, and scattering in this low energy region is a sensitive probe of the outer pion cloud which surrounds the proton. These long-range interactions play a role wherever pions interact with nucleons or other pions; and this in practical terms is a large part of high energy physics.

Experimentally, the region from 100 to 300 MeV is attractive because of the dominating N*(1238) resonance at 195 MeV. The small non-resonant partial waves can be measured accurately from their interference with the resonant P33 wave. The aim of the experiment is to take advantage of this favourable situation, and determine the coupling constants of the π, ρ and σ to the nucleon with the maximum accuracy attainable before Coulomb effects, which violate charge independence, set a limit.

The π^- measurements have been carried out in a branch of the variable energy π^- beam set up at the CERN SC. Results on the total cross-sections are shown in figure 19. The solid curve is the best fit to earlier data, with a resonance mass 1236·45 MeV/c^2 and a width of 119·6 MeV/c^2. The dotted line shows the unitarity limit for the resonant phase shift. The "background" at the bottom of the figure is the contribution of non-resonant waves.

These results are preliminary, in the sense that small ($\lesssim$ 1 per cent) corrections remain to be made, which depend on the data from the angular distribution, not yet fully evaluated. The final accuracy will be about ± 0·5 per cent. In figure 20 the experimentally determined P13 phase shift is plotted against laboratory π^- momentum. The full line is an empirical fit. The dotted line shows earlier results, from a CERN phase shift analysis.

Measurements of the angular distribution for elastic scattering have been made with three techniques. In the angular region where protons emerge from the liquid hydrogen target, conventional πp coincidence techniques quickly and simply give an accuracy of ± 1 per cent. In a second measurement, the counters were supplemented by spark chambers to investigate unwanted backgrounds in detail. Finally a magnetic spectrometer and 5 double-gap spark chambers were used to identify the pion over the part of the angular range where recoil protons stopped in the target.

π^+ measurements have been made in the same beam from 80 to 145 MeV. The remaining measurements on higher energy π^+ will be made in a different beam derived from the external proton beam.

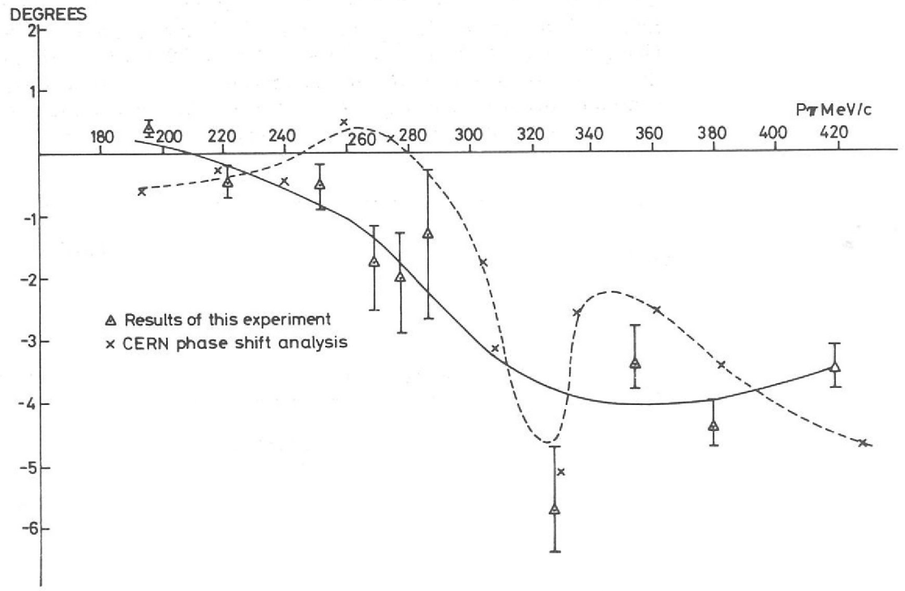

Figure 20. The experimentally determined P13 phase shift (Experiment 10) is shown plotted against laboratory π^- momentum. The full line is an empirical fit. The dotted line shows earlier results from a phase shift analysis.

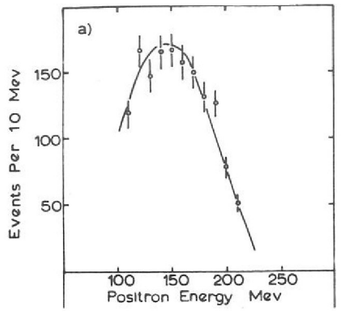

Figure 21(a). Ke3 positron energy spectrum distorted by Bremsstrahlung losses in the beryllium chamber.

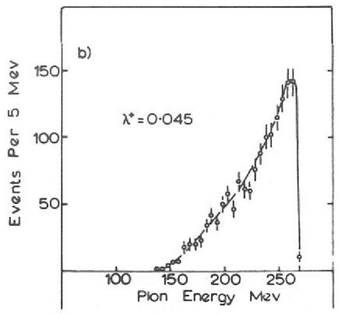

Figure 21(b). Ke3 π^o energy spectrum with experimental distortions. The fitted curves in (a) and (b) are for vector coupling with $\lambda^+ = 0{\cdot}045$.

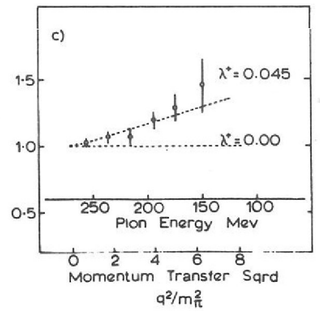

Figure 21(c). Momentum dependence of the form factor f_+ as a function of q^2.

Experiment 11

UNIVERSITY OF OXFORD

The Leptonic Decay Modes of the K^+ Meson (89, 188)

This experimental study of the decay modes $K^+ \to e^+\pi^o\nu$, $\mu^+\pi^o\nu$ has been already described in previous Annual Reports. The analysis of the data has now been completed. The experiment is concerned with the following measurements:

1. The positron momentum spectrum in the Ke3 mode;
2. The branching ratio for the Ke3 mode;
3. The relative branching ratio of the Kμ3 and Ke3 modes;
4. The π^o energy spectrum in the Ke3 mode.

The first three sections of the analysis have been described in the previous reports. The final section involved studying the Dalitz plot distribution of a subset of the data where both the e^+ and π^o were detected. The results are shown in figure 21 with the positron (a) and π^o (b) energy spectra.

Assuming vector coupling in Kℓ3 decay, the momentum dependence of the form factor f_+ may be deduced from the π^o energy spectrum and is shown in figure 21 (c). Thus for $f_+(q^2) = f_+(0)\ (1 + \lambda^+ q^2/m_a{}^2)$, $\lambda^+ = 0{\cdot}045 \pm 0{\cdot}015$ including radiative corrections. Using the value of λ^+ and assuming $\lambda^- = 0$, the Kμ3 data (section 3) gives $\xi(0) = f_-(0)/f_+(0) = -\ 0{\cdot}35 \pm 0{\cdot}22$, for the ratio of the form factors in Kℓ3 decay. These results are compatible with theoretical expectations and go someway towards reducing the discrepancy between values of ξ deduced from branching ratio and polarization methods.

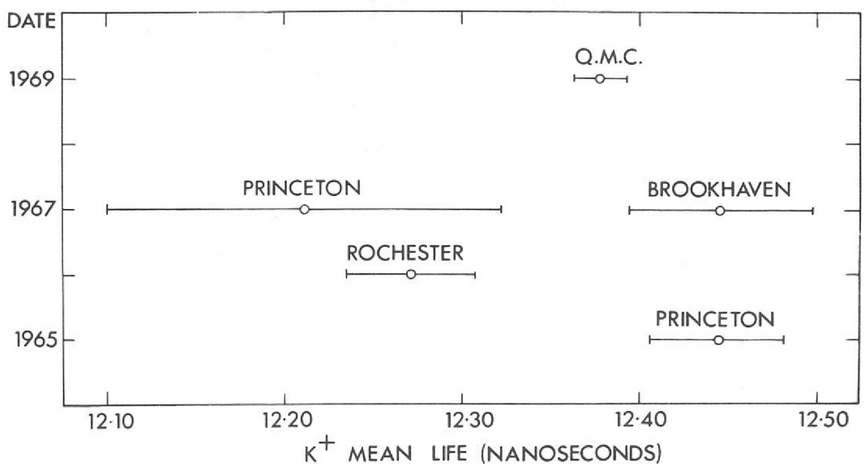

Figure 22. The value of the K^+ lifetime from Experiment 12 compared with the previous data.

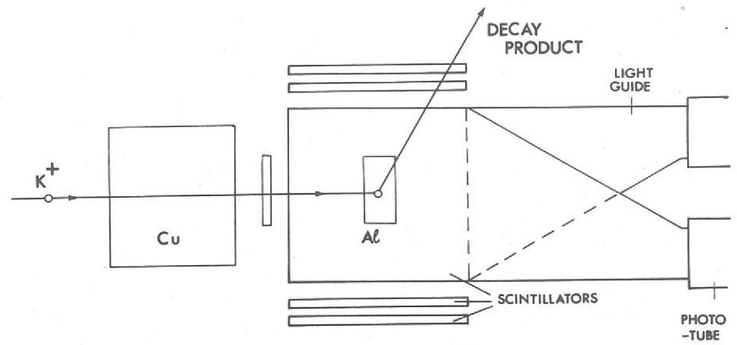

Figure 23. Schematic diagram of the apparatus used in Experiment 12.

Experiment 12

QUEEN MARY COLLEGE, LONDON

K^+ Lifetime Measurement (141)

This experiment, which was completed during 1969, measured the mean lifetime of the K^+ meson to an accuracy of nearly 1 part in 1,000 and hence resolved the discrepancy of about 4·5 standard deviations between the previous 2 best measurements (figure 22). In this experiment, 800 MeV/c K^+ mesons in an electrostatically enriched beam were selected by a DISC Cerenkov counter. The kaons were then slowed down in a copper degrader and finally brought to rest in an aluminium block surrounded on four sides by pairs of scintillation counters which detected decay products (figure 23). A signal from the entering kaon was used as a start pulse in a time to amplitude converter (TAC) and a signal from a decay product as a stop pulse.

The resultant pulse height from the TAC was fed into a multichannel pulse height analyser which stored a time spectrum from 0 to 100 ns (figure 24). The spectrum was read onto paper tape at convenient intervals for computer analysis.

The electronics was calibrated and its linearity checked using a temperature controlled crystal oscillator. About 3×10^6 kaon decays were analysed. The result was a mean lifetime of $12{\cdot}380 \pm 0{\cdot}016$ ns. The major part of the error is due to systematic effects in the time calibration and linearity of the electronics, but it includes also a statistical standard deviation of $\pm\ 0{\cdot}0045$ ns. The time spectrum over 6 mean life times showed no deviation from a pure exponential at the 0·1 per cent level. A full account of the experiment and analysis is being prepared for publication.

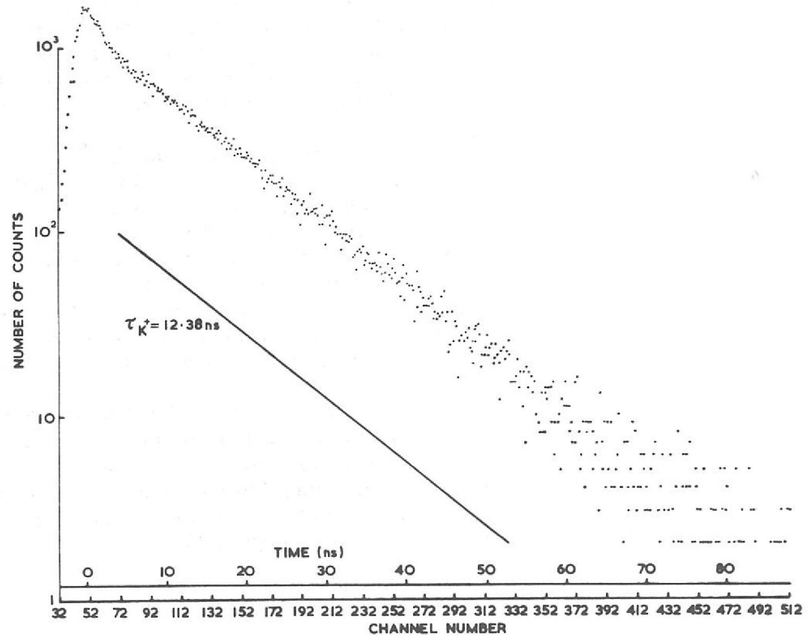

Figure 24. Typical time of flight spectrum from Experiment 12.

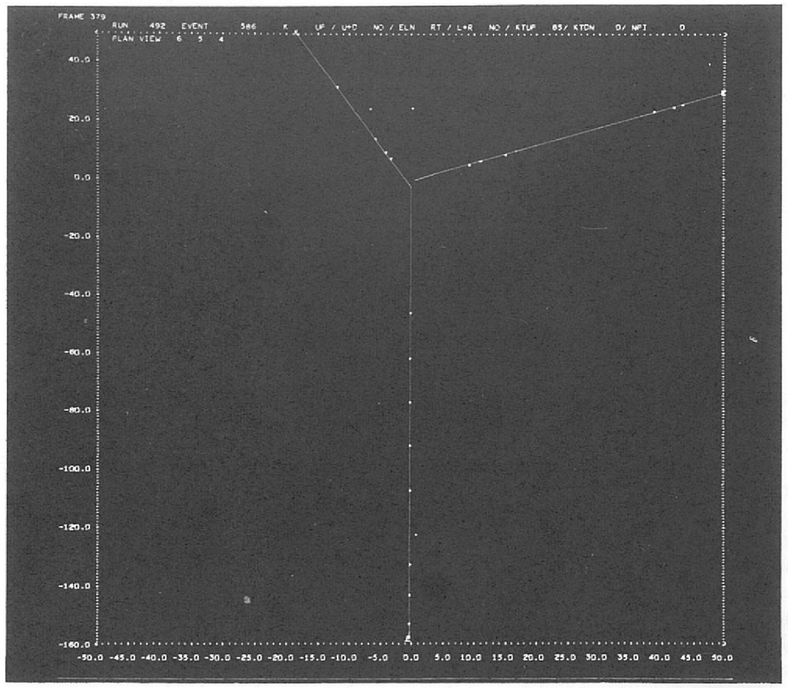

Figure 25. Computer reconstruction of an event from Experiment 13 (β-decay of the Σ^- hyperon). The vertical track is the incident pion which interacts in liquid hydrogen to produce a K^+ and a Σ^-. The K^+ which decayed after 37 nano-seconds is shown to the left and the Σ^- which is not drawn, beta decayed after travelling 2·5 cms to give an electron which is shown to the right.

Experiment 13

QUEEN MARY COLLEGE, LONDON
AERE, HARWELL
RUTHERFORD LABORATORY

The β Decay of the Σ^- Hyperon (1, 32)

The electron asymmetry parameter is measured for the beta decay of polarized sigmas, $\Sigma^- \rightarrow n e^- \bar{\nu}$, which were produced with a mean polarization of - 0·3 ± 0·08 by the reaction $\pi^- p \rightarrow \Sigma^- K^+$, by observing the angular distribution of the electron directions, defined by the unit vector $\hat{e}$ in the sigma rest frame, about the sigma polarization vector $\bar{P}_\Sigma$. This is given by $I(\alpha,\cos\theta) \propto (1 + \alpha P_\Sigma \cos\theta)$, where $\cos\theta = \bar{P}_\Sigma . \hat{e}$ and $\bar{P}_\Sigma$ is positive in the direction $\bar{\pi} \times \bar{\Sigma} / |\bar{\pi} \times \bar{\Sigma}|$. This measurement is made to determine the form of the weak interaction responsible for the decay and to test the prediction of Cabibbo theory that it is V + 0·3A.

The data from this experiment is now being analysed. The main problem is that of identification of some of the 100 beta decay events expected in the 110,000 triggers, which were recorded on magnetic tape in the form of digitizations produced by wire spark chambers. So far about 11 events have been found in that ten per cent of the triggers in which the K^+ lived longer than 9 nano-seconds.

The methods of finding these events involves a program which reconstructs the incident π^-, the K^+ and the e^- tracks. If it finds these three tracks only, it fits them to the two vertex topology of sigma production and decay. 239 events were found which satisfied these criteria and they were plotted on 35 mm film. Criteria defining the sigma production and decay vertices were obtained by scanning film of two prong and normal decay triggers respectively, for events in which the physical process sought had been correctly reconstructed. The 11 beta decay events were found by scanning the film for events which satisfied these criteria and in which the electron track was not part of a Dalitz pair of a γ-ray shower.

A typical event is shown in figure 25. The vertical track is the incident pion which interacts in liquid hydrogen to produce a K^+ and a Σ^-. The K^+, which decayed after 37 nano-seconds, is shown to the left and the Σ^-, which is not drawn, beta decayed after travelling 2·5 cm to give an electron which is shown to the right. The lifetime distribution of these sigmas is consistent with the measured sigma lifetime and is shown in figure 26.

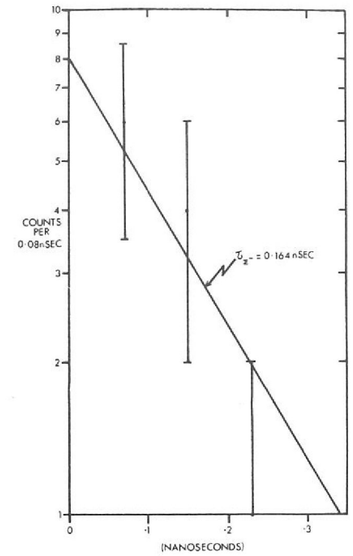

Figure 26. Measured life-time distribution of Σ's in Experiment 13.

A maximum likelihood fit has been done to the distribution of $\cos\theta$ for these 11 events and figure 27 shows the logarithm of the likelihood function plotted against the asymmetry parameter. We find $\alpha = + 0{\cdot}4 \pm 1{\cdot}2$. The matrix element $\langle n|\gamma\mu(g_V - g_A\gamma_5)|\Sigma^-\rangle$ defines the sign of g_A/g_V which is related to α by the expression:

$$\alpha \simeq - \, 2(g_A/g_V)(1 + (g_A/g_V))/(1 + 3(g_A/g_V)^2)$$

Figure 28 shows the logarithm of the likelihood function plotted against g_A/g_V using this relationship. We find $g_A/g_V = -0{\cdot}3 \, {}^{+\,0.4}_{-\,4.2}$.

There are three published results from bubble chambers, two of which give a mean value for $|g_A/g_V|$ of $0{\cdot}30 \, {}^{+\,\cdot16}_{-\,\cdot13}$ and the third is $g_A/g_V = + \cdot16 \, {}^{+\,\cdot19}_{-\,\cdot18}$. These results are consistent with the predictions of Cabibbo theory within the errors.

Now that the mechanism for obtaining the result from this experiment has been established, it is hoped to increase its statistical significance. Attempts are being made to retrieve those events where the K^+ lived less than 9 nano-seconds and those in which the incident pion track chosen does not match up with the K^+, to form a good production vertex, because of the confusion caused by the high beam intensity at which the data was taken. This will give about four times as many events.

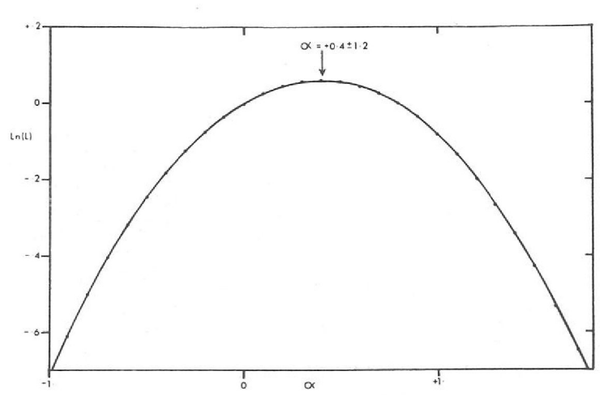

LOGARITHM OF LIKELIHOOD FUNCTION AGAINST α

Figure 27. Maximum likelihood fit for the electron angular distribution from the events recorded in Experiment 13.

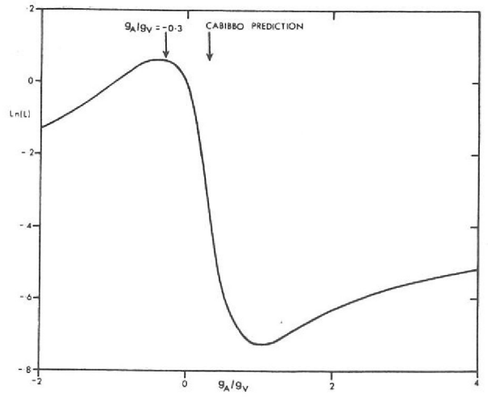

LOGARITHM OF LIKELIHOOD FUNCTION AGAINST g_A/g_V

Figure 28. The graph shows the logarithm of the maximum likelihood function (figure 27, Experiment 13) plotted against g_A/g_V.

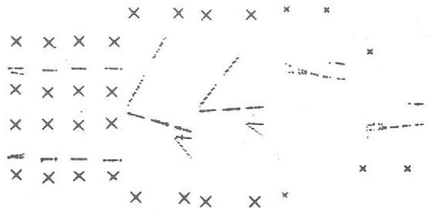

Figure 29(a). An event taken directly from a film exposed in the ΔS=ΔQ experiment (no. 14).

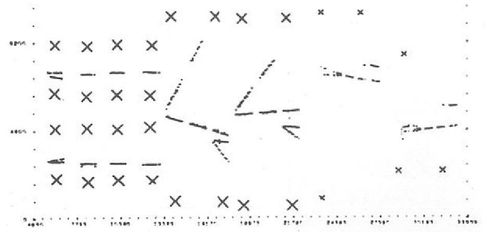

Figure 29(b). Shows the same event after the film has been measured on Cyclops (a flying-spot digitizer) and the resulting co-ordinates displayed on a graph plotter.

Experiment 14

UNIVERSITY OF CAMBRIDGE
RUTHERFORD LABORATORY

Test of the $\Delta S = \Delta Q$ Rule for K^o Leptonic Decays (138)

This experiment to test the $\Delta S = \Delta Q$ rule and CP-conservation in the decay $K^o \to \pi\, e\, \nu$ has been described in the 1968 Annual Report (Experiment 7). Data taking was completed in June 1969 and the analysis is now well under way. Neutral kaons were produced from the reaction $\pi^- p \to \Lambda^o K^o$, and events were recorded using optical spark chambers. A total of 580,000 pictures were taken of which 140,000 were of the more common decay mode $K^o \to \pi^+\pi^-$ for calibration purposes.

The film is being measured both on hand measuring machines and automatically using the CYCLOPS flying-spot digitizer. The latter method gives greater accuracy, but it seems necessary at the moment to provide guidance for the track finding routines. This has been done successfully both using the hand measurements as rough digitizings and with the aid of an interactive CRT display. Figure 29 shows an automatically measured event re-displayed on a graph plotter, with the original photograph for comparison.

To date 30 per cent of the film taken has been analysed in detail, and this contains approximately 3,000 Ke3 events with the electron sign determined. Each of these events is being kinematically fitted and re-examined by a physicist.

It is hoped to obtain a preliminary value for the ratio $x = \frac{\Delta S = -\Delta Q \text{ amplitude}}{\Delta S = +\Delta Q \text{ amplitude}}$ from this initial sample early in 1970, and to publish a final result based on about 10,000 Ke3 decays by the end of the year.

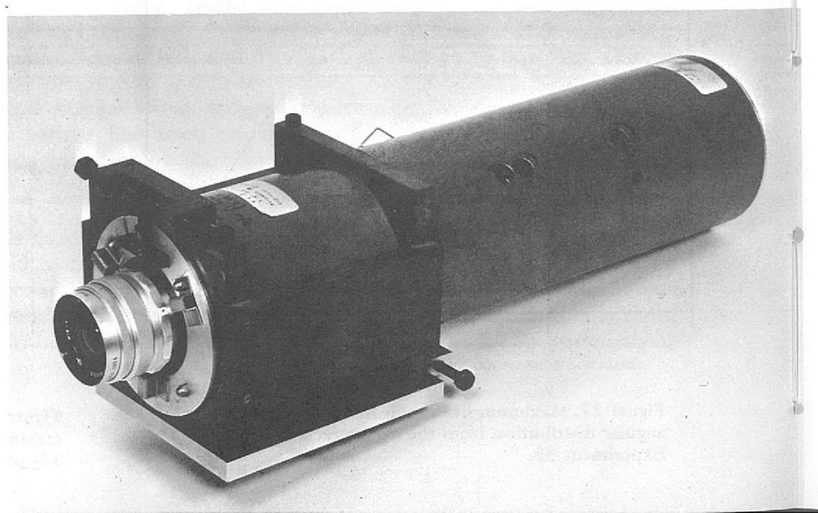

Figure 30. One of the vidicon cameras used to view spark chambers in Experiment 15.

Experiment 15

WESTFIELD COLLEGE, LONDON
UNIVERSITY OF SUSSEX
RUTHERFORD LABORATORY

Test of the $\Delta I = 1/2$ Rule in the Decay $\Sigma^+ \to p\pi^o$ (136)

The present theory of weak interactions allows non-leptonic strangeness changing transitions with a change in isotopic spin ΔI of 1/2, 3/2 or 5/2. There is strong experimental evidence for a $\Delta I = 1/2$ selection rule. The decay rates and asymmetry parameters of the non-leptonic sigma hyperon decays are sensitive tests of the $\Delta I = 1/2$ rule. The asymmetry parameters in the decay $\Sigma^+ \to p\pi^o$ can be determined by measuring the polarization of the decay proton with respect to the Σ polarization direction.

A separated beam of π^+ mesons of momentum 1110 MeV/c incident upon liquid hydrogen was used to produce polarized sigmas by the reaction $\pi^+ p \to \Sigma^+ K^+$. Thin foil spark chambers measured the direction of the K^+ and the decay proton from $\Sigma^+ \to p\pi^o$ and the polarization and range of the proton were measured in an aluminium plate spark chamber. The chambers were viewed by an array of 8 vidicon cameras (figure 30). The spark positions were immediately digitized and recorded directly on magnetic tape. Data taking has been completed with over one million triggers recorded using 300 magnetic tapes. An analysis of the operation of the vidicon system has now been completed. The digitizing of a full vidicon scan line is 4096 counts. From an analysis of proton tracks from p-p elastic scattering test data a spatial accuracy of about ± 0·2mm was achieved over a scan length of 69 cm i.e. *resolution* (FWHM) is somewhat worse than two parts in 4,000. Two spark images closer together than about one per cent of the scan cannot be separated due to the finite size of the vidicon's electron beam spot i.e. *resolving power* is about 40 parts in 4,000. The relation between real space positions and digitizer count is linear to within about ± 0·5%. A fifth order polynomial fit is required to reproduce the positions of lines on a ruled fiducial plate to an accuracy of 0·2mm. One scan is used for each spark chamber gap and four sparks per line can be digitized. In the system used in this experiment there was an overall dead-time of about 50 ms. The nonleptonic Σ decays are conventionally parameterized in terms of their decay rates and the three parameters

$$\alpha = \frac{2\mathrm{Re}\,(S^*P)}{S^2 + P^2}, \quad \beta = \frac{2\mathrm{Im}(S^*P)}{S^2 + P^2}, \quad \gamma = \frac{S^2 - P^2}{S^2 + P^2}$$

where S and P are respectively the S- and P- wave decay amplitudes. Since γ is nearly -1, the Σ^+ polarization is readily observable through the up-down asymmetry given by the familiar decay distribution

$$I = 1 + \alpha \bar{P}_\Sigma \cdot \bar{q}$$

where $\bar{q}$ is a unit vector along the momentum of the decay proton in $\Sigma^+ \to p\pi^o$ and $\bar{P}_\Sigma$ is the polarization of the Σ^+ from the production reaction $\pi^+ p \to \Sigma^+ K^+$. The polarization of the proton is given by

$$(1 + \alpha \bar{P}_\Sigma \cdot \bar{q})\, \bar{P}_p = (\alpha + \bar{P}_\Sigma \cdot \bar{q})\, \bar{q} + \beta(\bar{P}_\Sigma \times \bar{q}) + \gamma \bar{q} \times (\bar{P}_\Sigma \times \bar{q})$$

Initially the analysis of the data is concentrated on the determination of $\alpha . P_\Sigma(\theta)$ from the decay angular distribution where θ is the sigma production angle. The latest value of $|\alpha \bar{P}|$, where $\bar{P}$ is the mean Σ polarization, is 0·67 indicating that the large sigma polarization required for a measurement of the β and γ parameters is present.

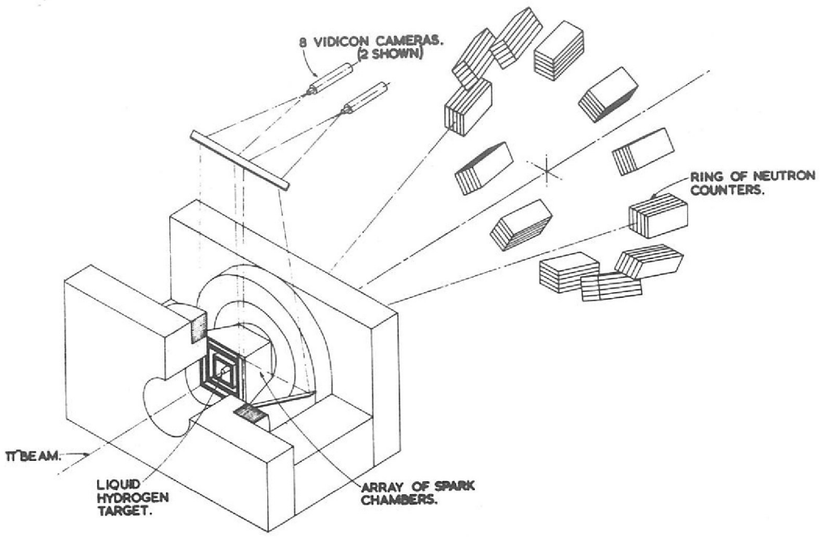

Figure 31. A diagram of the apparatus used in the search for charge asymmetry in η decay (Experiment 16).

Experiment 16

WESTFIELD COLLEGE, LONDON
UNIVERSITY OF SUSSEX
RUTHERFORD LABORATORY

Search for Charge Asymmetry in η Decay (136)

The purpose of this experiment is to test for an asymmetry in the decay $\eta^o \rightarrow \pi^+\pi^-\pi^o$, which would imply that C symmetry is violated in the electromagnetic interaction. A violation of C means that a set of anti-particles do not obey the same physical laws as the equivalent set of particles (i.e. different physics in an anti-world to that in our world). This work follows naturally from previous experiments by the Laboratory on CP violation in $K_L^o \rightarrow \pi^+\pi^-$ and in $K_L^o \rightarrow \pi^o\pi^o$, both being weak interactions.

There is already evidence for a charge asymmetry in the $\eta \rightarrow 3\pi$ decay, but the present measured asymmetry

$$A = \frac{N^+ - N^-}{N^+ + N^-} = 1{\cdot}5 \text{ per cent} \pm 0{\cdot}5 \text{ per cent where } \begin{matrix} N^+ = N\,(E^+ > E^-) \\ N^- = N\,(E^- > E^+) \end{matrix}$$

has only three standard deviation significance, and therefore requires confirmation. In the new Nimrod experiment at present being set up, it is hoped to increase the number of measured events to some 400,000 compared with 36,000 in the previous most accurate experiment.

A diagram of the apparatus is shown in figure 31. The η^o mesons to be studied are produced in the process $\pi^- p \rightarrow \eta^o n$ and are selected from unwanted background processes by measuring the time-of-flight of the neutron in the ring of 60 neutron detectors. Detailed descriptions of the neutron counters, the spark chambers and the magnet will be found in the Instrumentation section (pages 82–97).

In figure 32 a measured time-of-flight spectrum is shown. The various particles produced show up as peaks in the time spectrum, and the required η^os are seen as a strong peak. Neutrons, detected in the "η^o peak" cause the spark chambers in the experiment to trigger. The spark chambers within the large magnet (surrounding the hydrogen target) detect the π^+ and π^- from the η^o decay and measure their momenta. The number of times the π^+ is more energetic than the π^- is denoted by N^+ and the opposite situation by N^- and thus each event is analysed to see if it contributes to N^+ or N^-. It is expected that one million events will be recorded in the spark chambers by the on-line vidicon system, and that of these some 400,000 will lie within the fiducial volume and meet the kinematic requirements of the $\eta \rightarrow 3\pi$ decay. It is hoped to start data taking in the spring of 1970.

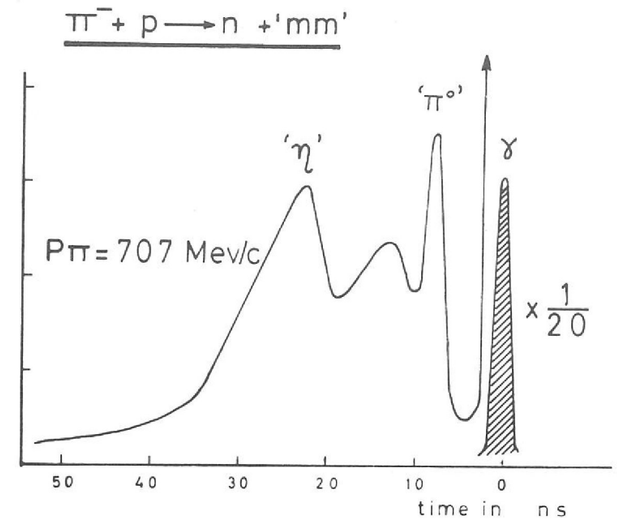

Figure 32. Measured time of flight spectra from Experiment 16. The various particles produced show up as peaks in the time spectra and the required η's are seen as a strong peak.

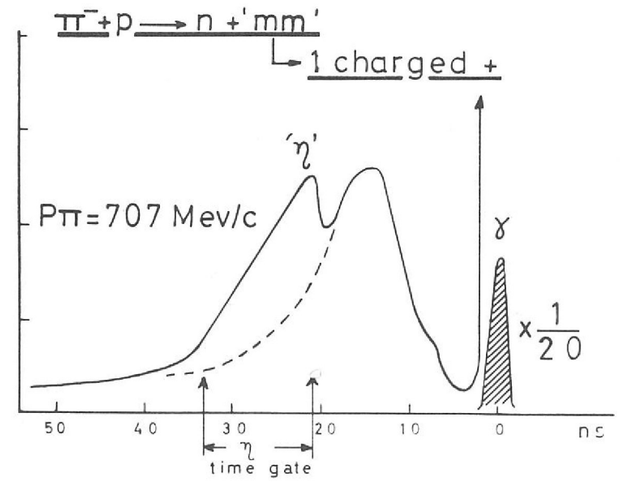

Experiment 17

UNIVERSITY OF CAMBRIDGE
RUTHERFORD LABORATORY

Test for CP Violating Amplitude in $K^o \rightarrow 3\pi$

K^o decays are known to have a small CP violating component. This effect first observed in $K_L^o \rightarrow 2\pi$ has been substantiated and observed also in $K_L \rightarrow \pi e \nu$ and $K_L \rightarrow \pi\mu\nu$. However the source of the violation is still unknown. It may be a universal small effect ($\sim 10^{-3}$ in amplitude) or have its roots in one of a number of particular processes which themselves strongly violate CP but act only to a small extent in the decays observed.

This experiment will measure the time dependence of $K^o \rightarrow \pi^+\pi^-\pi^o$ with 7,000 events up to 20 K^o short lifetimes. Any interference between K_L and K_S to 3π must involve a CP violating amplitude which will be measured with a standard deviation $\lesssim$ 10 per cent of the allowed $K_L \rightarrow 3\pi$. The present experimental limit of the amplitude ratio is about unity.

Neutral kaons of positive strangeness are produced by the reaction $\pi^- p \rightarrow \Lambda^o K^o$. An optical spark chamber spectrometer measures the momenta of $\sim$ 1035 MeV/c incident π^- on a polythene/scintillator target. The Λ and K decay inside a 40 inch gap magnet which contains 14 optical spark gaps such that the momenta can be measured to $\sim$ 5 per cent, sufficient to kinematically separate the wanted K decay from the others. A counter array demands 4 charged particles after a neutral state determined by a veto counter just after the target. The apparatus is

shown in the figure 33. The π^- beam and the target are similar to those used in the previous experiment in the K13 position ($\Delta S = \Delta Q$ experiment). Trigger rates have been measured and some film taken with 6 gaps in the decay region. The trigger rates are higher than expected mainly due to γ conversions but are at an acceptable level which would result in a total number of pictures of $\sim$ 600,000 in about 100 days data taking. Final installation will be completed during the shutdown and data taking should commence in about March after a final period of setting-up in February.

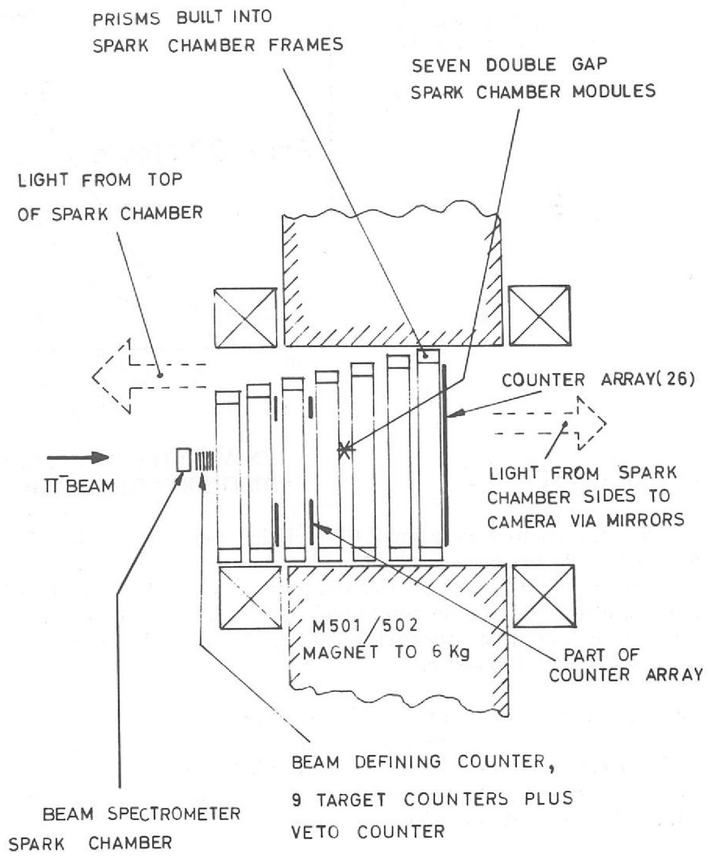

Figure 33. Diagram of the apparatus used in Experiment 17 ($K^\circ \to 3\pi$).

Experiment 18

CERN,
ORSAY
RUTHERFORD LABORATORY

Measurement of ϕ_{oo}, the Phase of the Decay $K_L^\circ \to \pi^\circ\pi^\circ$ (134)

The analysis of the first experiment proposed by this collaboration (a measurement of the phase ϕ_{oo} of η_{oo}) has been completed. The final results are

$$\phi_{oo} = 51^\circ \pm 30^\circ$$
$$|\eta_{oo}| = (3{\cdot}33 \pm 0{\cdot}64) \times 10^{-3}$$

The second experiment to obtain a 10 per cent measurement of $|\eta_{oo}|$ is now in the analysis stage. A total of 360,000 photographs were taken, approximately 50 per cent of these had a 20 cm copper regenerator in the beam and 50 per cent had no regenerator. The films with no regenerator give directly a measure of $|\eta_{oo}|$ and these together with the regenerator film should give a more precise measure of ϕ_{oo} than that obtained with the first experiment (see above).

The analysis should be completed by mid 1970. The scanning is virtually finished and this has all been done at the Rutherford Laboratory by a team of 14 part-time scanners. The films are measured at CERN or Orsay.

It is hoped to obtain a new upper limit for $|\eta_{ooo}|$, where

$$|\eta_{ooo}| = \frac{\text{amplitude } (K_S^\circ \to 3\pi^\circ)}{\text{amplitude } (K_L^\circ \to 3\pi^\circ)}$$

from the film of the second experiment.

The present limit is $|\eta_{ooo}| \leqslant 10$ and this data should give an order of magnitude improvement on this limit.

Finally a total of 240,000 photographs were taken to obtain the decay rates of K_S° and K_L° to 2γ. These rates can possibly exhibit CP violation.

The analysis of these last two experiments will not be complete until early 1971.

Experiment 19

UNIVERSITY OF GLASGOW
UNIVERSITY OF LIVERPOOL
UNIVERSITY OF OXFORD
UNIVERSITY OF WARWICK
RUTHERFORD LABORATORY

A Study of the Decay Modes $K^\pm \to \pi^\pm\pi^\circ\gamma$ and $K^\pm \to \pi^\pm\pi^\circ\pi^\circ$

The aims of this experiment are:

(i) To measure the charge asymmetry in the rates for $K^\pm \to \pi^\pm\pi^\circ\gamma$ in order to test for C non-invariance in electromagnetic interactions and CP non-invariance in the weak interaction and to measure for this mode the electric and magnetic dipole structure amplitudes and the interference between the electric dipole amplitude and the inner bremsstrahlung.

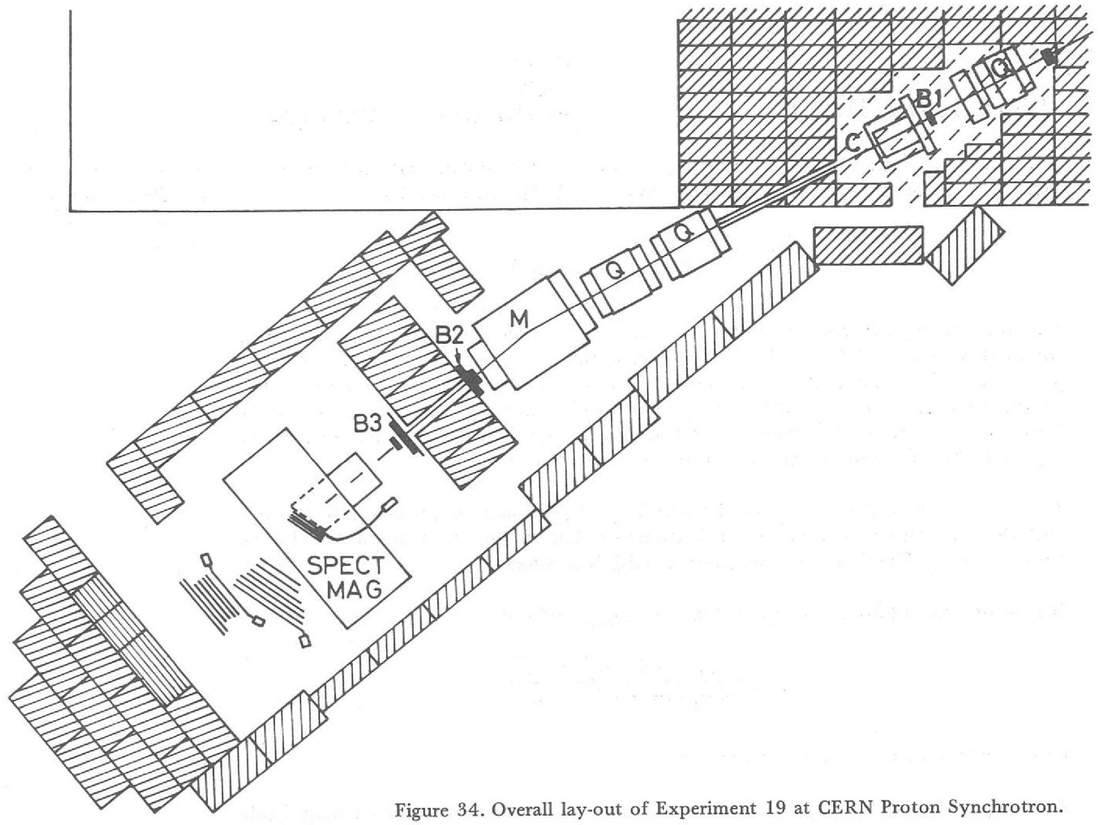

Figure 34. Overall lay-out of Experiment 19 at CERN Proton Synchrotron.

(ii) To measure the charge asymmetry in the rates for $K^{\pm} \rightarrow \pi^{\pm}\pi^{o}\pi^{o}$ in order to test for $\Delta I = 5/2, 7/2$ CP non-invariant terms in the non-leptonic interaction.

The data taking phase of the experiment is now complete and all equipment has been dismantled and returned to the Rutherford Laboratory. Analysis of the experiment which was started at CERN on the CDC 6600 has been transferred to the IBM 360/75.

The experiment was carried out in a 5 GeV/c unseparated kaon beam at the CERN PS. The overall layout of the experiment is shown in figure 34. A differential gas Cherenkov counter C identified the kaons in the beam, and a system of counter hodoscopes and wire spark chambers at B_1, B_2 and B_3 defined their momenta and directions. The vector momentum of the charged pion, produced when a kaon decayed into either of the two desired final states, was measured by 12 sonic spark chambers at S_1 and S_2 in conjunction with a large spectrometer magnet. As shown in figure 35 six of these chambers were placed within the gap of the spectrometer magnet.

The final state γ-rays (including those from the neutral pion) were detected by a 1 metre square counter hodoscope. This enabled the outgoing directions of the γ-rays to be defined to within $\pm$ 0·5° in the laboratory system.

Information from the counters and spark chambers was fed into a DDP 516 computer for preliminary analysis and also recorded on magnetic tape for detailed analysis later.

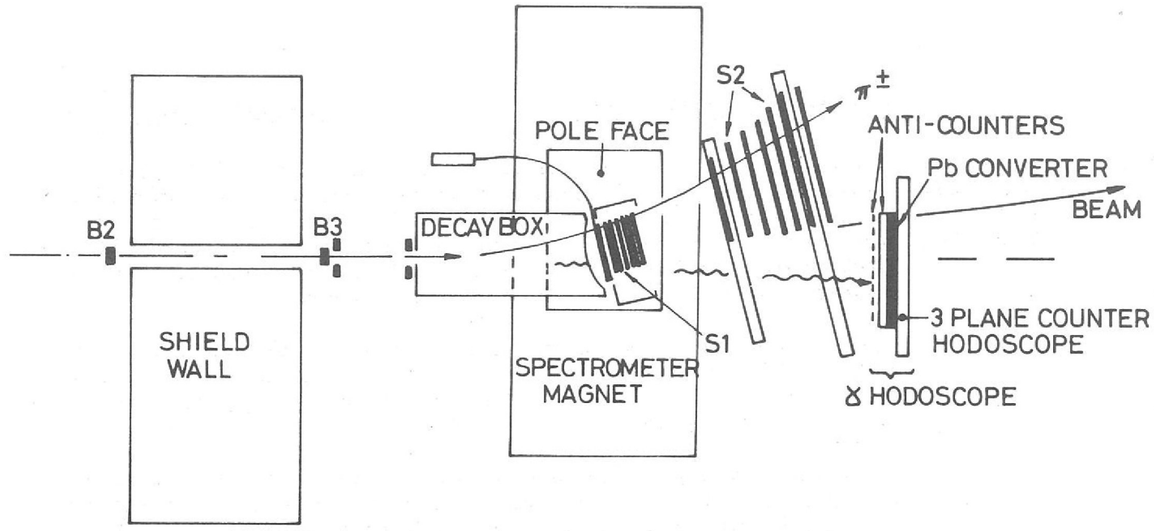

Figure 35. Diagram of the experimental apparatus used in Experiment 19.

Experiment 20

UNIVERSITY OF OXFORD

275,000 pictures were taken in the Saclay 80 cm bubble chamber at Nimrod in 1966-1967, covering the momentum range 450 to 550 MeV/c. The analysis of these is now complete and the results ready for publication. A further 300,000 pictures were taken at Saturne (Saclay) in 1968-1969, which will extend the momentum range to 400 to 740 MeV/c.

π^-p Reactions at Low Incident π^- Momenta (162, 205)

The principal interest is in the inelastic reactions $\pi^-p \rightarrow \pi^+\pi^-n$ and $\pi^-p \rightarrow \pi^-\pi^o p$. The Dalitz plot for $\pi^+\pi^-n$ (figure 36) shows some Δ^- production and a strong enhancement of events at high $\pi^+\pi^-$ mass. This anomaly can be explained in terms of the production of an interacting spin zero isospin zero $\pi\pi$ system. The $\pi\pi$ phase shifts in this mass range are still unknown. There is no need to invoke a low-mass σ -meson and a narrow ϵ^o resonance is preferred to a broad one. Figure 37 shows a fit to the $(\pi^+\pi^-$ mass$)^2$ spectrum at 505 MeV/c. This experiment has also measured directly the partial wave structure of the inelastic reactions, which will give improved πN elastic phase analyses.

Figure 36. Dalitz plot for the reaction $\pi^-p \rightarrow \pi^+\pi^-n$ at 552 MeV/c. (Experiment 20).

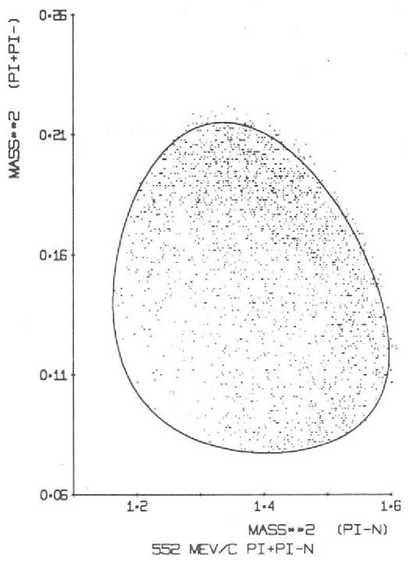

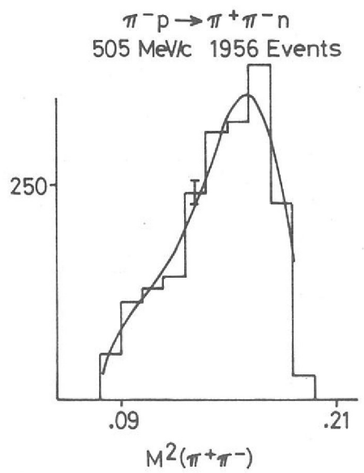

Figure 37. The graph shows a fit to the measured $\pi^+\pi^-$(mass)^2 spectrum from the reaction $\pi^-p \rightarrow \pi^+\pi^-n$ at 505 MeV/c (Experiment 20).

Experiment 21

UNIVERSITY OF OXFORD

π^+p Interactions between 0·6 and 0·8 GeV/c (15, 152, 154, 189)

Measurement of all 100,000 pictures, taken at momenta of 0·6, 0·65, 0·7, 0·75 and 0·8 GeV/c in the Saclay 80 cm hydrogen bubble chamber, is now complete. The inelastic final states $\pi^+\pi^0$ p and $\pi^+\pi^+$n have been subjected to a partial wave analysis and acceptable fits achieved at all momenta. The details of this analysis will be published shortly in Nuclear Physics B, and as a Rutherford Laboratory Preprint. Figure 38 shows data for the $\pi^+\pi^0$ p final state at 0·8 GeV/c.

Values have been obtained for the inelasticity in the incident waves S31, P31, P33, D33, D35 and F35 (figure 39). The values differ in some details from those deduced from elastic phase shift analyses, but are in generally good agreement with a similar analysis of independent data made by a Saclay group.

At present an investigation into possible systematic errors in the elastic scattering data is being made. It is hoped that it will be possible to publish the elastic scattering data within the next year, thus completing the experiment.

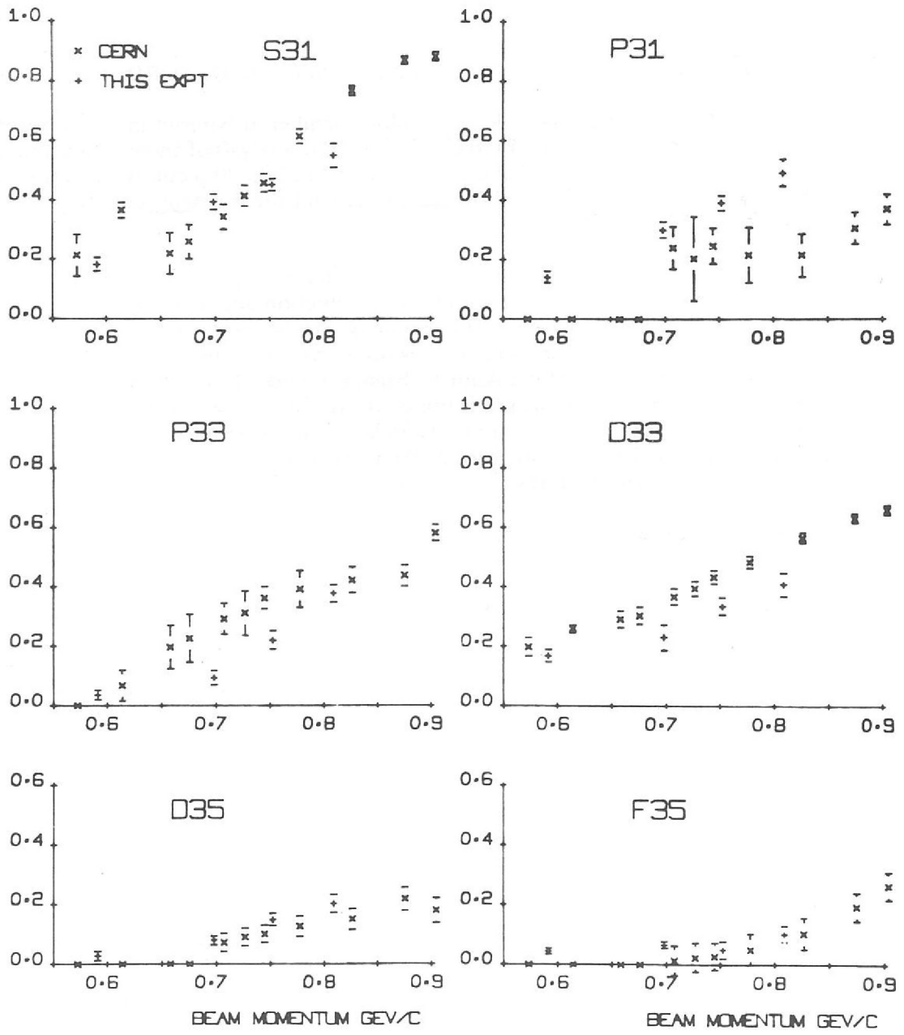

Figure 39. A comparison of the values of $\sqrt{(1-\eta^2)}$ obtained from the results of Experiment 21 and the values obtained from an earlier phase shift analysis.

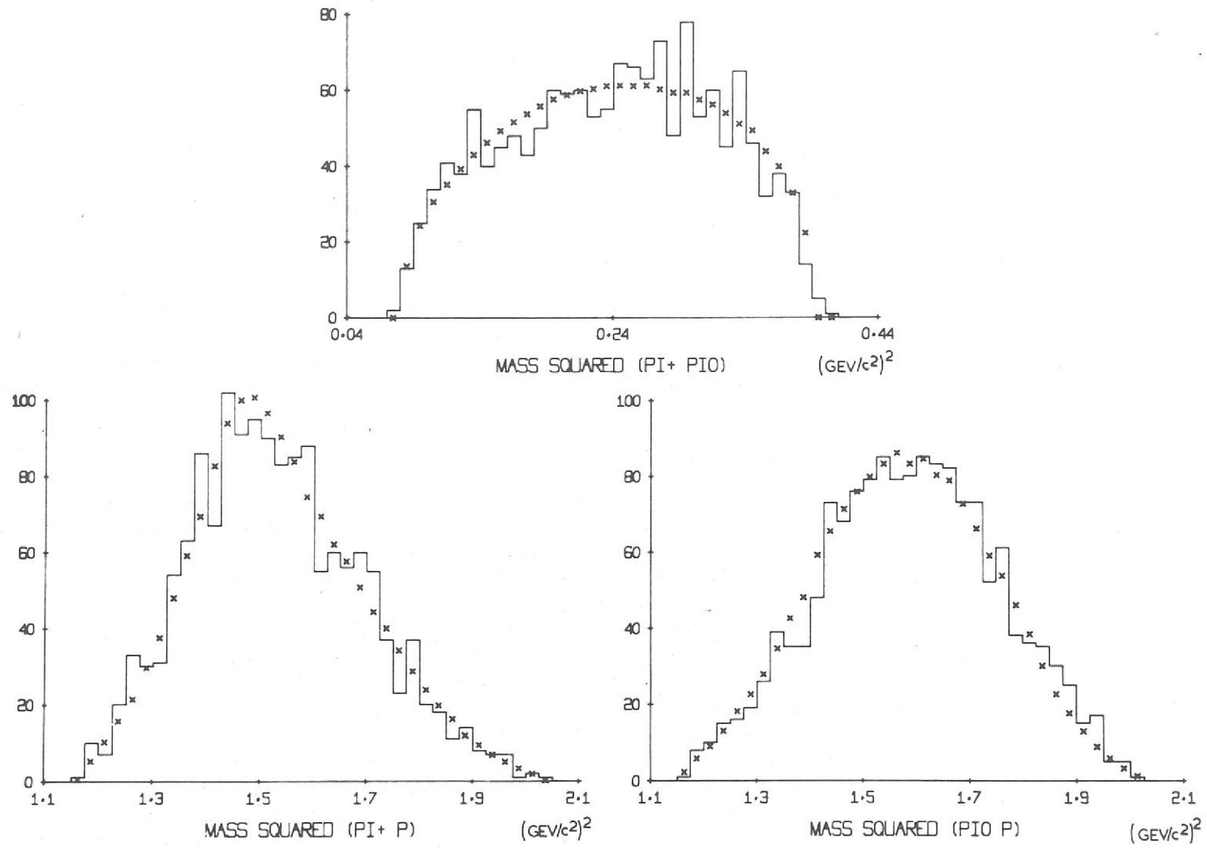

Figure 38. The projections of the Dalitz plot for the final state $\pi^+\pi^0$ p on the three mass squared axes for the 0·8 GeV/c data determined in Experiment 21. The points are the values obtained from one of the phase shift solutions proposed by the team.

Experiment 22

IMPERIAL COLLEGE, LONDON
WESTFIELD COLLEGE, LONDON

π^+p Interactions in the range 0·9 – 1·7 GeV/c (148, 158)

(i) 0·90 – 1·05 GeV/c

Film from the Saclay 80 cm chamber at 0·90, 0·95, 1·00 and 1·05 GeV/c has been completely analysed and has yielded approximately 55,000 fitted events.

Elastic Scattering

The elastic differential cross sections, based on about 5,000 events at each of the incident momenta, are in fairly good agreement with recent counter measurements for most centre-of-mass scattering angles. The only serious disagreement occurs close to 180° where the differential cross-sections obtained from the present bubble chamber experiment are very nearly 50% lower than previously reported values. When this discrepancy was first noticed checks were made to ensure that backward elastic events were not being overlooked or discarded at some stage of the analysis. In particular, the scanning, fitting and event classification procedures were investigated in detail and showed no evidence for the preferential mishandling of these events.

Until recently, phase shift analyses of pion nucleon scattering have relied almost exclusively on differential cross-section and polarization measurements made using counter techniques. The differential cross-section measurements now being made using bubble chamber and spark chamber methods should be less susceptible to systematic errors and will probably make further evaluations of partial-wave amplitudes worthwhile.

We have attempted to determine whether small changes to the CERN (Lovelace et al.) phases and inelasticities could be made in such a way as to provide adequate fits to our 180° differential cross sections. Several fits, using CERN results as starting values, have been made, including fits constrained to remain in reasonable agreement with these results. There is suggestive evidence that appreciable modifications of one or two waves may be necessary to achieve satisfactory fits. To obtain unique and reliable solutions for the I = ½ pion nucleon amplitude in this way would require the additional constraint imposed by accurate π^+p polarization measurements. Until these are available it does not appear useful to pursue the present fitting techniques any further. A paper on the elastic scattering results has been written and will shortly be submitted for publication.

Single Pion Production

The 30,000 single pion production events are being used to study the inelastic decay modes of the I = ½ pion nucleon resonances observed in the elastic channel. As a first step in the analysis of this data the Dalitz plot distributions have been fitted using the isobar model in the formulation of Deler and Valladas.

The pion nucleon effective mass distributions in both single pion production channels show strong production of the Δ(1236). Several methods have been used to obtain an estimate of the amount of $\pi\Delta$ production, all of which indicate that this process accounts for at least 75% of the single pion events. Preliminary fits have been made assuming only $\pi\Delta$ production together with an incoherent phase-space background. These are in much better agreement with the results published recently by the Saclay group than with the original DS3 dominated model of Olsson and Yodh. Statistically the fits are not very satisfactory, however, and at present the fitting programs are being modified to allow inclusion of ρN and $\pi N^*_{1/2}$ production as an alternative form of interfering background. The moment fitting technique suggested by the Saclay group is also being adopted.

(ii) 1·10 – 1·70 GeV/c

Film at eight momenta between 1·10 and 1·70 GeV/c obtained from the British National Chamber is being used to extend the analysis described above to the region of the higher mass N* resonances. Film at 1·2 and 1·3 GeV/c has been predigitized and will shortly be measured on the Imperial College HPD.

Experiment 23

UNIVERSITY OF OXFORD

π^+ and p Interactions at 1·88 GeV/c in Helium (212)

Scanning and measuring of the 300,000 pictures taken in the helium bubble chamber exposed to π^+ and the 200,000 pictures taken with protons is complete. Analysis of the π reaction $\pi^+ He^4 \rightarrow \pi^+\pi^-\pi^+He^4$ is essentially complete. There are 130 events in this final state, and there is nothing in the data which requires $\pi^+\pi^-\pi^+$ resonant behaviour: a simple one pion exchange model seems adequate to reproduce most features. Geometrical reconstruction and kinematic fitting of the proton events is nearly complete; there are about 100 events in the final state p $\pi^+\pi^-He^4$.

The data shows a narrow peak in the $\pi^+\pi^-$p mass distribution; it is not yet clear whether this is the N*(1400) produced coherently or whether the kinematics of N*(1236) production alone can account for this phenomenon.

Experiment 24

UNIVERSITY OF BIRMINGHAM
RUTHERFORD LABORATORY

Study of 4 GeV/c π^+ Interactions in Deuterium

This experiment was originally proposed for running at the Rutherford Laboratory but has since been submitted to CERN to release time at Nimrod for the development of the target facility. The proposal is now for 800,000 pictures to be taken in the CERN 2 metre chamber. The principal aim of the experiment is to study with high resolution and statistics the neutral bosons produced in reactions of the kind $\pi^+D \rightarrow ppB^o$; of particular interest will be the splitting of the neutral A_2 meson. The experiment will of course benefit considerably from the precision and speed of measurement now available on the Rutherford Laboratory HPD system and should yield about 40 events per microbarn cross-section. A number of pictures were taken at Nimrod during early 1969; however, in view of the move to the CERN chamber together with difficulties experienced during this run with the operating conditions in the 1·5 metre chamber, it is unlikely that this film will be useful for physics.

Experiment 25

CEN, SACLAY
COLLEGE DE FRANCE
UNIVERSITY OF STRASBOURG
RUTHERFORD LABORATORY

A Study of K^-p Interactions in the range 1·25 to 1·85 GeV/c (140, 155)

K^-p interactions, at 13 incident K^- laboratory momenta approximately evenly spaced in the interval 1·25 to 1·85 GeV/c are being studied. The pictures were taken at Nimrod using the Saclay hydrogen bubble chamber.

The K^-p system can form baryon resonances of strangeness −1 and isotopic spin 0 or 1. The properties of these resonances, e.g. mass, width, spin, parity, isotopic spin, are obtained from analysing their decay into two-body final states. Experimentally, total cross-sections, differential cross-sections and polarization are measured, and the data are then analysed in terms of partial wave amplitudes of different spin and parity.

The various final state topologies in this experiment are at different stages of analysis. The common topologies are:

(a) Zero-prong events with one or two visible neutral decays; in particular the channels $\Lambda^o\pi^o$, $\Sigma^o\pi^o$.

(b) Two-prong events. These yield, for example, the two-body states K^-p (elastic), $Y^*\pi$, K^*p, K^*n.

(c) Two-prong events with a visible neutral decay. These yield intermediate 2-body states such as $Y^*\pi$, K^*p (which decay into $\Lambda^o\pi^+\pi^-$, $\Sigma^o\pi^+\pi^-$, $K^o p\pi^-$ etc.)

(d) Two-prong events with a charged decay. The analysis of these channels was reported last year and has been published.

The reaction $K^-p \rightarrow \pi^o\Lambda$

Analysis of the reaction $K^-p \rightarrow \pi^o\Lambda$ has recently been completed. The $\pi^o\Lambda$ final state has an isotopic spin of 1, hence this reaction allows one to make a study of the formation and decay of baryon resonances with strangeness −1 and isotopic spin 1.

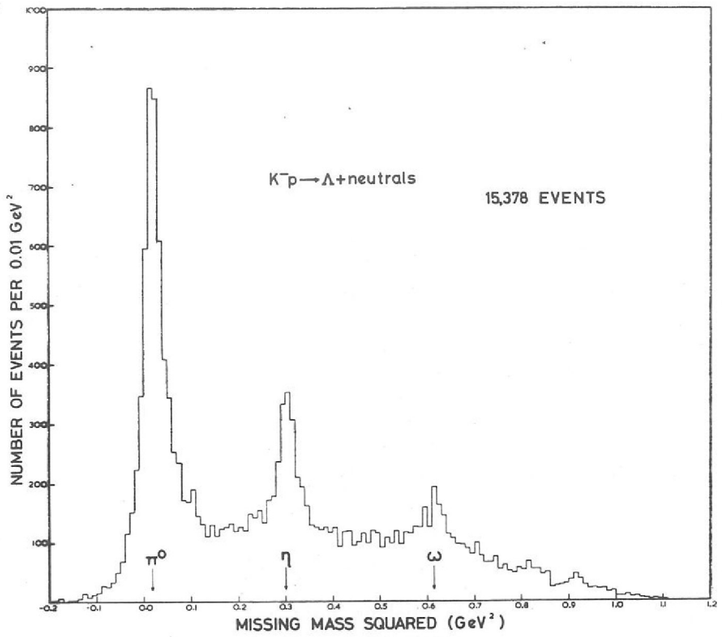

Figure 40. Distribution of missing mass squared to the Λ in the reaction $K^-p \rightarrow \Lambda$ + neutrals for all incident momenta combined (Experiment 25).

This channel is observed in the events with a topology of zero-prong with a visible neutral decay, i.e. a disappearing beam track with a Λ or K^o decay associated. Approximately 26,500 events of this topology were measured to yield a sample of 15,378 events where the Λ decay hypothesis was selected by kinematic and ionisation constraints. Figure 40 shows the spectrum of the missing mass squared associated with the Λ for these events. The peaks in the distribution correspond to events where the Λ is produced together with a π^o, η or ω particle which then decays into neutral particles (not detected in a bubble chamber); in addition the distribution contains events of the type $\Sigma^o\pi^o$, $\Lambda^o\pi^o\pi^o$, etc. A final sample of 4,805 $\Lambda\pi^o$ events with a possible contamination of 4 per cent $\Sigma^o\pi^o$ events was obtained.

Cross-sections at the thirteen momenta were determined by normalising to the number of τ decays ($K^- \rightarrow \pi^+\pi^-\pi^-$). These are shown plotted in figure 41, with the previous measurements in this region.

At each momentum the differential cross-section and polarization distribution have been expressed as sums of Legendre and associated Legendre polynomials respectively, using the method of moments.

A partial wave analysis of this data has resulted in a measurement of the parameters of the dominant resonance in this region, the Σ(2030) with spin and parity 7/2+. These are: Mass = 2030 ± 10 MeV, Width = $165 \pm {}^{30}_{15}$ MeV, and $\sqrt{xx'} = 0{\cdot}2 \pm 0{\cdot}02$ where x and x′ are the elastic and πΛ branching fractions.

Evidence supporting the existence of another resonance, the Σ(1915), with spin and parity 5/2+ was also obtained. In addition, there was an indication of a possible resonance with spin 3/2, however this will require another experiment with higher statistics to clarify the situation.

A partial wave analysis has been carried out on a compilation of the data from the present experiment together with that previously published. The P3 resonance at M≈2070 is confirmed and evidence found for two further states: P1(1920) and D3(1940). All these new states can be accommodated in SU(3) groups containing known N* resonances.

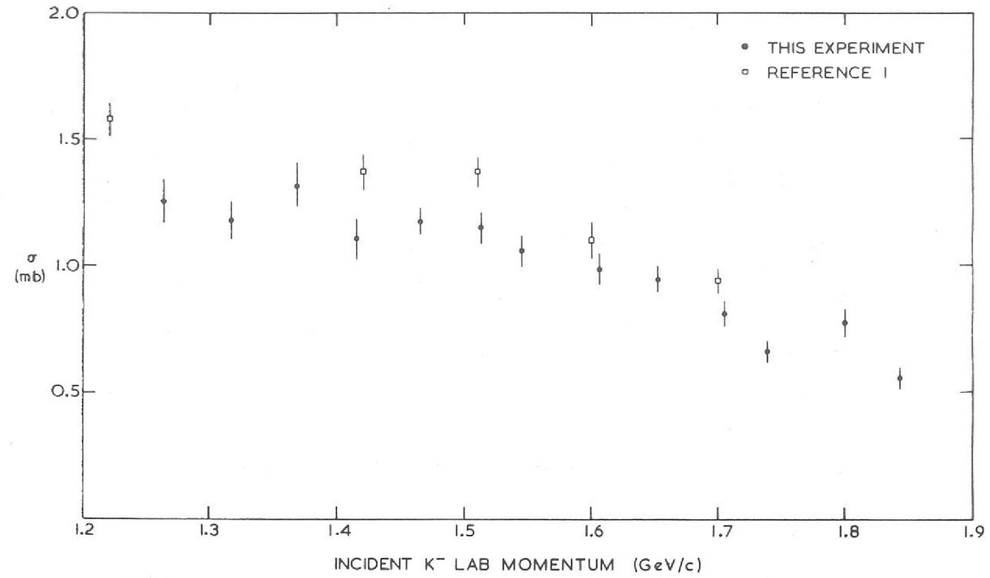

Figure 41. Cross-section for the reaction $K^-p \rightarrow \Lambda^o\pi^o$. The solid circles show the results from Experiment 25. The squares are the results from previous measurements in this region.

The reaction $K^-p \rightarrow \Sigma\pi$

Partial wave analysis of this channel is well advanced. The reactions $\Sigma^+\pi^-$ and $\Sigma^-\pi^+$ show very different angular distributions readily explicable in terms of t-channel effects. It is hoped that by simultaneously treating the data to conventional s-channel partial wave analysis useful information will be obtained on s and t-channel duality.

2-prong events

Data on approximately 60,000 2-prong events have been analysed in collaboration with the Strasbourg University Bubble Chamber Group. The events may be divided into two types:

(i) The elastic reaction $K^-p \rightarrow K^-p$

Approximately 2,000 events of this type have been obtained at each beam setting (26,000 events in all). The differential cross-sections can therefore be measured with a precision considerably greater than in previously published work. The angular distributions are quantitatively described by fitting to a Legendre polynomial expansion.

$$\frac{d\sigma}{d\Omega} = \lambda^2 \sum_{n=0}^{N} A_n P_n (\cos\theta)$$

where N is the maximum order required to fit the data. In this experiment N = 7 is required, indicating the formation of J = 7/2 resonances in this energy region.

Using the values of the A_n coefficients from all the momentum points, together with the corresponding data from the charge exchange reaction $K^-p \rightarrow \overline{K}^o n$ (also measured in this experiment), and polarization data from counter experiments, a partial wave analysis of the elastic channel is under way which, it is hoped, will reveal the presence of new Y* resonances together with their spin and parity quantum numbers.

(ii) Inelastic events

The remainder of the events are examples of inelastic collisions, mostly involving single pion production in the reactions: $K^-p \to K^-p\pi^o$, $K^o p\pi^-$ or $K^-n\pi^+$.

The two body mass plots for the first reactions at 1·739 GeV/c are displayed in figure 42, clearly showing a strong K* (890) in the Kπ combination together with some Y* (1520) in the K^-p combination. The other two reactions are dominated by K* (890) production with no sign of any other strong resonance production.

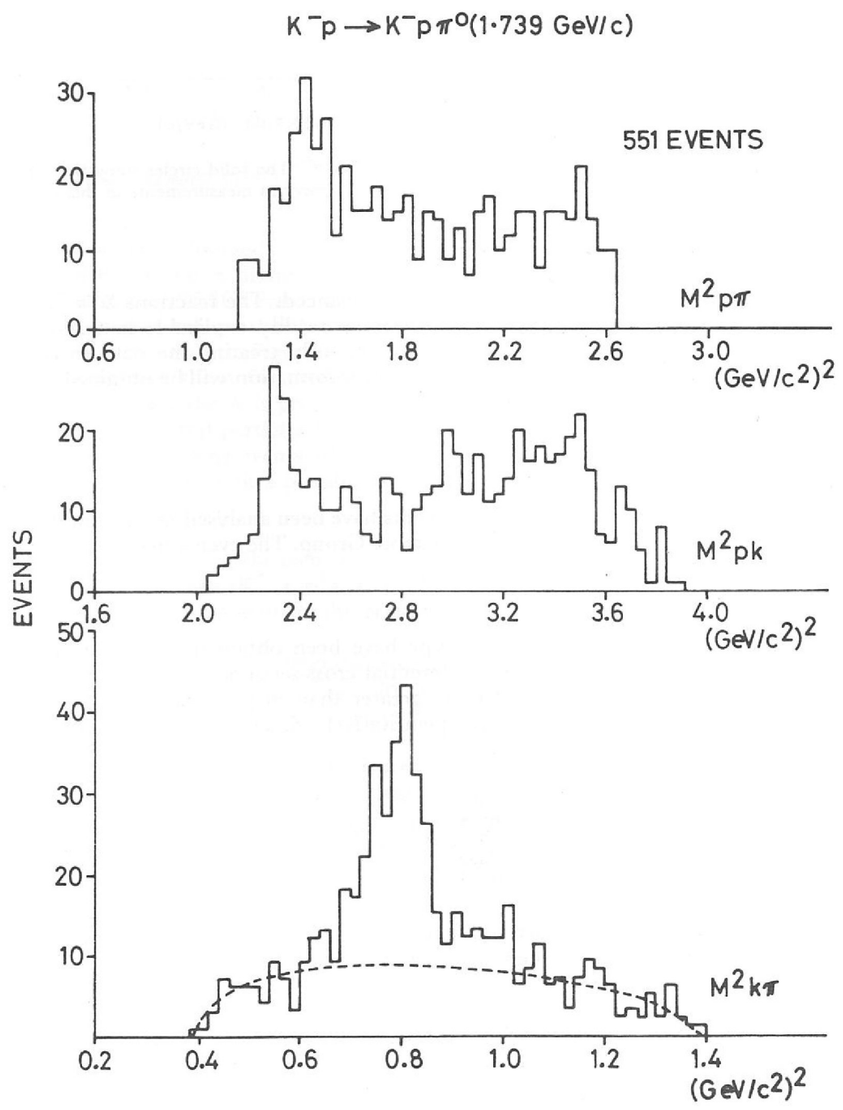

Figure 42. Two body mass plots for the reaction $K^-p \to K^-p\pi^o$ at 1·739 GeV/c (Experiment 25).

Again by studying the variation in the properties of the pseudo two-body reactions K*p and Y*π as a function of total energy it is hoped to be able to draw conclusions on the intermediate formation of Y* resonances observed in different decay modes.

Two prong events with a visible neutral decay

The principal reactions studied in this topology are: $K^-p \to \Lambda^o\pi^+\pi^-$ (a), $\Lambda^o\pi^+\pi^-\pi^o$ (b), $\Sigma^o\pi^+\pi^-$ (c) and $\overline{K}^o p\pi^-$ (d). Cross-sections for these processes at all momenta covered by the survey are given in Table 4.

Table 4

Momentum GeV/c	$\Lambda^o\pi^+\pi^-$ σ (mb)	$\Lambda^o\pi^+\pi^-\pi^o$ σ (mb)	$\Sigma^o\pi^+\pi^-$ σ (mb)	$\overline{K}^o p\pi^-$ σ (mb)
1·26	3·05 ± 0·53	0·97 ± 0·23	0·73 ± 0·19	1·46 ± 0·39
1·32	2·62 ± 0·35	1·36 ± 0·22	0·73 ± 0·14	1·56 ± 0·30
1·37	2·40 ± 0·32	1·79 ± 0·25	0·62 ± 0·12	1·95 ± 0·33
1·42	2·63 ± 0·35	1·72 ± 0·26	0·70 ± 0·14	1·78 ± 0·33
1·46	2·63 ± 0·20	2·07 ± 0·17	0·78 ± 0·08	1·99 ± 0·20
1·51	2·56 ± 0·26	2·43 ± 0·25	0·79 ± 0·11	1·76 ± 0·25
1·55	2·67 ± 0·22	2·41 ± 0·20	0·64 ± 0·08	2·34 ± 0·24
1·61	1·98 ± 0·25	2·19 ± 0·27	0·66 ± 0·12	2·02 ± 0·31
1·65	2·33 ± 0·17	2·36 ± 0·17	0·71 ± 0·07	2·47 ± 0·21
1·70	2·23 ± 0·22	2·23 ± 0·22	0·65 ± 0·09	2·19 ± 0·27
1·74	2·37 ± 0·22	2·52 ± 0·23	0·71 ± 0·09	2·54 ± 0·28
1·80	1·87 ± 0·24	2·27 ± 0·27	0·80 ± 0·13	2·54 ± 0·36
1·84	2·18 ± 0·27	2·26 ± 0·27	0·63 ± 0·11	2·01 ± 0·30

There are also contributions from the final states $\overline{K}^o p\pi^-\pi^o$, $\overline{K}^o\pi^+\pi^-n$. Analyses of the four main channels is in progress.

The reaction (a) i.e. $\Lambda^o\pi^+\pi^-$ final state is dominated by Σ (1385) production which accounts for about 50 per cent of the events. There is also a significant, (5 – 10 per cent) amount of ρ^o production. A partial wave analysis of the $\Sigma(1385)\,\pi$ channel will be attempted.

Reaction (b) shows the following contributions from resonance production, averaged over all momenta. $K^-p \to \Lambda\omega^o$, 62 per cent; $K^-p \to \Lambda^o\eta^o$, 2 per cent; $K^-p \to \Sigma(1385)\,\pi\pi$, 17 per cent and $K^-p \to$ Y* (1520) $\pi\pi$, 1 per cent. A partial wave analysis of the $\Lambda\omega^o$ channel is in progress.

The $\Sigma^o\pi^+\pi^-$ channel, reaction (c), shows the presence of both $\Sigma(1385)$ and $\Sigma(1660)$ each accounting for about 15 per cent of the events.

Reaction (d), $\overline{K}^o p\pi^-$, is dominated by production of the K* (890). A partial wave analysis of the K*p final state is in progress and will of course include the data on the same final state coming from the 2-prong topology without a seen K^o.

Experiment 26

UNIVERSITY COLLEGE, LONDON
TUFTS UNIVERSITY, USA
UNIVERSITY OF BRUSSELS
CERN

2·2 GeV/c K^- Exposure in the 1·4m Heavy Liquid Bubble Chamber

Over 600,000 pictures were taken, approximately half of them in 1969. The main aims of the experiment are:

(i) to find the lifetime of the Ξ^o by a method which uses the γ rays from the Ξ^o decay π^o to fix the decay point.

(ii) to study the $\Lambda^o - \Lambda^o$ interaction and the properties of the Ξ^- and Ξ^* resonances.

(iii) to search for X^o and ϕ^o neutral decays and radiative Y* decays.

The first experiment involves two complete scans of the film in order to eliminate possible bias on the Ξ^o lifetime due to scanning loss of these complex events. More than half of the film has been scanned twice by now, and the scan should be completed by Spring 1970. As a by-product of this scan we are finding events with a K^+ and two Λ hyperons. These will be used to study the invariant mass distribution of the $\Lambda\Lambda$ state (see figure 43) Ξ^- and Ξ^* properties will also be studied.

A separate investigatory scan has begun for two prong and zero prong events with a Λ and γ-rays. The immediate motive of this scan is to search for radiative Y* decays, but it will also help us to estimate the number of η' and ϕ events in our film with a view to possible further studies on decays of these particles.

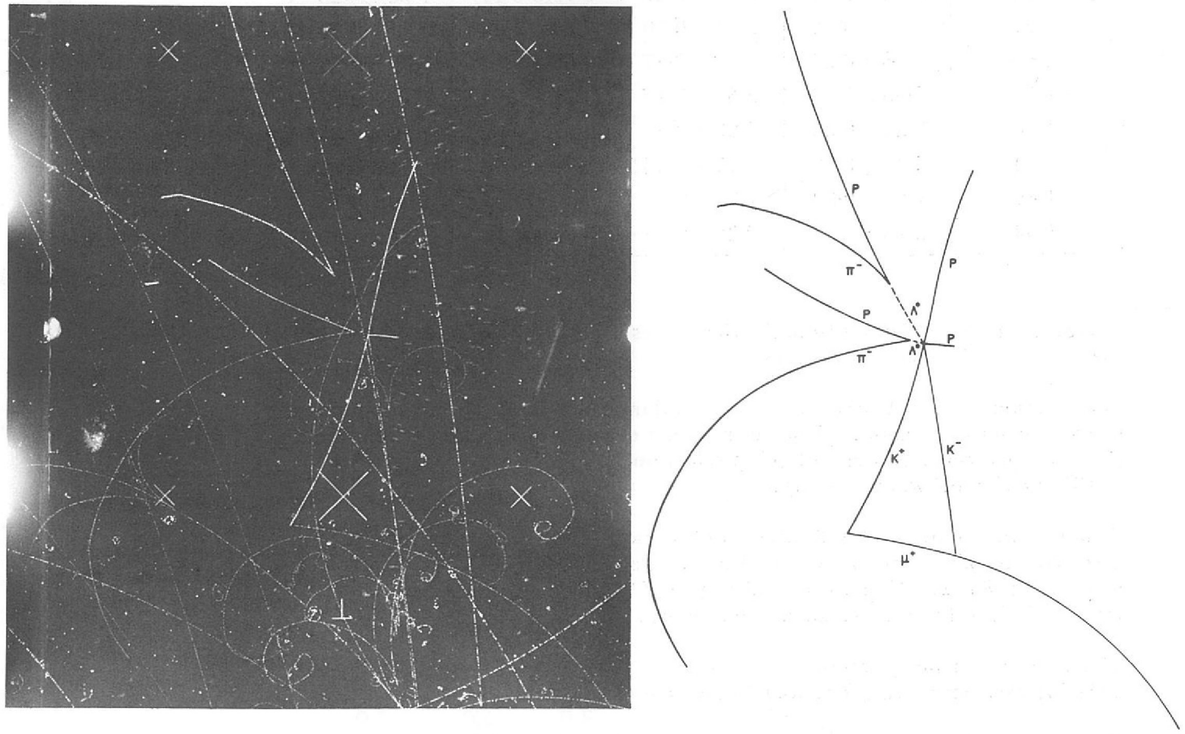

Figure 43. K^- + nucleus → $K^+\Lambda\Lambda pp$ + invisible recoils. This event (recorded in Experiment 27) was caused by a series of interactions inside a complex nucleus. A Ξ^- hyperon was probably formed but it interacted with a proton before it could escape from the nucleus. The $\Lambda\Lambda$ pairs formed in such events give a unique opportunity to study the $\Lambda\Lambda$ interactions.

Experiment 27

UNIVERSITY OF BIRMINGHAM
UNIVERSITY OF EDINBURGH
UNIVERSITY OF GLASGOW
IMPERIAL COLLEGE, LONDON

K^-d Interactions in the range 1·45 to 1·65 GeV/c (90, 192, 197)

Approximately 700,000 pictures were taken using K^- mesons at 1·45 and 1·65 GeV/c in the Saclay Bubble Chamber filled with deuterium.

Particular attention has been paid to the reaction $K^- n \rightarrow \Lambda^o \pi^-$ and a partial wave analysis has been performed. This analysis confirms the values for mass, width and $\sqrt{x_e x_r}$ for the Σ (2030) and also gives values of these parameters for the $\Sigma(1910)$. The $\Sigma(1910)$ is not very strong in the data but its inclusion always improves the probability for a fit. A very marked change in the $P_{3/2}$ amplitude is observed near 2080 MeV; the data can in fact be well fitted if a resonance is included in this wave.

Channels of the type $K^- n \rightarrow Y^*\pi$ are currently being analysed in a search for $Y^*\pi$ decay modes of the $\Sigma(1910)$, $\Sigma(2030)$ and $\Sigma(2080)$. Preliminary results show a strong decay of the $\Sigma(2030)$ to $\Sigma(1385) + \pi$ and work is in progress on final states involving the $\Lambda(1520)$.

Experiment 28

RUTHERFORD LABORATORY
CEN, SACLAY
ECOLE POLYTECHNIQUE, PARIS

14 GeV/c K^- Interactions

During the first half of 1969, an experiment to study high energy K^- proton interactions was initiated in collaboration with physicists of the Ecole Polytechnique (Paris) and the Commissariat a l'Energie Atomique (Saclay). The CERN 2m chamber was exposed to a 14 GeV/c K^- beam; a total of 340,000 pictures were taken which will yield a total of approximately 300,000 events. At the end of the year, the RHEL portion of the film was three-quarters scanned and HPD measurement had begun. Physics analysis of the data from the three laboratories is expected to begin during the third quarter of 1970.

Experiment 29

IMPERIAL COLLEGE, LONDON
WESTFIELD COLLEGE, LONDON
CEN, SACLAY

K^+p and K^+d Interactions in the range 2·0–2·8 GeV/c (14, 153, 156, 157)

In this survey experiment 40,000 pictures have been taken at each of the momenta 2·1, 2·3, 2·5, 2·7 and 2·9 GeV/c in hydrogen and 400,000 pictures have been taken in deuterium at 2·2 GeV/c. The hydrogen film was shared between the three collaborating groups for analysis. Scanning, predigitizing for HPD and a first measurement of the film has been completed at all momenta. A second pass to improve the rather low success rate is well advanced. It is expected that the analysis will be completed early in 1970.

A preliminary analysis of the three channels $K^+p \rightarrow K^+p$, $KN\pi$ and $KN\pi\pi$ was presented to the 1969 Lund Conference. A paper on the elastic data has also been published.

More detailed studies of the production and decay of Δ (1236) and K* (890) in the quasi-two body channels are being carried out, together with a Veneziano fitting of the differential cross-sections.

Experiment 30

UNIVERSITY OF CAMBRIDGE

Strange particle production

n-p Interactions from 1 to 7·5 GeV/c

In January 1968 about 40,000 test pictures were taken of neutrons in the 1·5m hydrogen bubble chamber. The neutrons were produced by focussing a scattered-out 7·5 GeV/c proton beam on to a target about 5m from the chamber, and sweeping all charged particles out of the beam emerging from the target. About 21,500 of the pictures were scanned for events involving strange particle decays, yielding about 1400 potential events. The analysis of these is now complete and the results of this are:—

(i) the cross-sections for the most common channels are:

Final state	No. of events	Cross-section (in μb)		
		2·6–4·0 GeV/c	4·0–5·5 GeV/c	5·5–7·5 GeV/c
$\Lambda^\circ pK^\circ$	21	109 ± 41	45 ± 23	73 ± 23
$\Lambda^\circ nK^\circ\pi^+$	20	11 ± 11	148 ± 41	129 ± 27
$\Sigma^- pK^+$	48	56 ± 14	58 ± 12	26 ± 7
$\Sigma^+ nK^+\pi^-$	22	zero	42 ± 3	32 ± 9
$\Lambda^\circ pK^+\pi^-$	42	4 ± 4	32 ± 10	64 ± 11

(ii) The final state $\Sigma^- pK^+$ has a peaking at 1800 MeV/c² in the $\Sigma^- K^+$ mass spectrum which is not reflected into an enhancement in the $\Sigma^- p$ mass spectrum at the high mass region (see figure 44). This is in marked contrast to the analogous reaction $pp \rightarrow \Sigma^+ nK^+$.

(iii) The reactions $\Lambda^\circ nK^\circ\pi^+$ and $\Lambda^\circ pK^+\pi^-$ are characterised by a very high (46 per cent) Y* (1385) production. The highest observed in similar pp channels at comparable momentum is 34 per cent.

Figure 44. Mass distribution of 95 events of the reaction $np \rightarrow \Sigma^- pK^+$. The curves were generated by a Monte-Carlo programme that included the variation in momentum of the incident neutrons (Experiment 30).

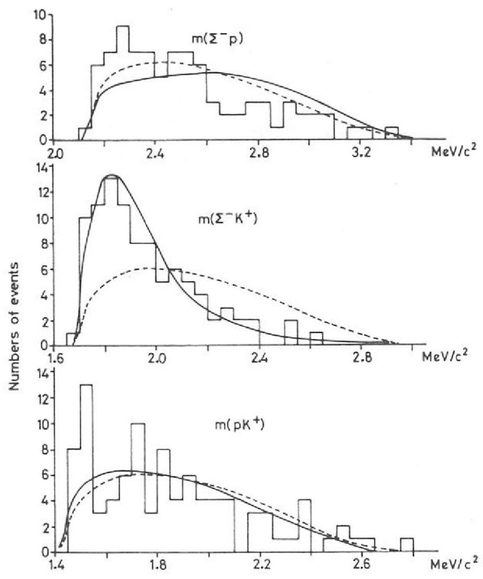

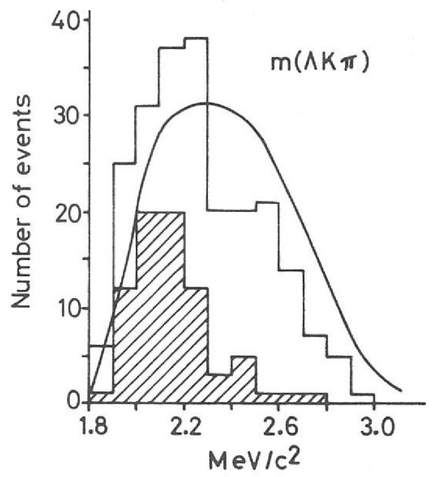

Figure 45. Three body invariant mass distribution of all $\Lambda NK\pi$ final states from np interactions in Experiment 30. The shaded portion contains events with $m(\Lambda\pi)$ in the range 1345-1405 MeV/c². The curve is a resonance model which gives the best fit to the two body invariant mass spectra of the same events.

(iv) There is evidence for the pseudo two-body reaction $np \rightarrow N^*p$ in the three body channel Y* (1385)pK (see figure 45). It is not certain whether this is due to N* (2190) or Δ (1950), as there are too few events in the selected region to give the peak positions accurately.

(v) There are about 120 events which have identified strange particle decays, but no satisfactory solution. It is estimated that 20 of those will be due to interactions of Λ° produced in the chamber, and another 30 may have been produced by K_L° emerging from the target. An example of the former type was shown in last year's report, and it is hoped that enough events of this type will be found to form the subject of a separate publication.

Single and multiple pion production

(i) $np \rightarrow pp\pi^-$ between 1 and 7·5 GeV/c

The study of this reaction has now been completed. About half of the film was useable and yielded a sample of 27,100 three-prong events. These were tested against the 3-constraint hypothesis $np \rightarrow pp\pi^-$, 3658 events giving satisfactory fits. Using the known cross-section for the reaction as a function of neutron momentum, the momentum spectrum of the neutron beam was deduced from the momentum distribution of the incident neutrons. This spectrum was used in the evaluation of the cross-sections tabulated above.

The events were divided into four momentum ranges and the properties of the reaction studied from threshold up to 7·5 GeV/c. Particular results of interest are:

(a) The existence of the N* (1470) in the $p\pi^-$ mass distribution at 7·0 GeV/c, reported by other workers, could not be confirmed. Our results in the corresponding momentum range are more consistent with the diffraction dissociation model.

(b) At lower momentum, there is clear production of the Δ° (1236) and N* (1688)

(c) There is a forward-backward asymmetry in the c.m.s. which increases with incident momentum. From isospin considerations, this appears to be inconsistent with the present cross-section data for $np \rightarrow pp\pi^-$ and $pp \rightarrow pp\pi^\circ$.

(d) OPEM and DRM predictions for the reaction have been evaluated (including a variable beam momentum) and compared with the data. After suitable adjustments to the OPEM form factors, satisfactory fits were obtained. DRM fits were less satisfactory.

(ii) $np \rightarrow pp\pi^+\pi^-\pi^-$ and $np \rightarrow pp\pi^+\pi^+\pi^-\pi^-\pi^-$ between 1 and 8 GeV/c.

In January 1969 112,000 pictures of n-p interactions in the 1·5m hydrogen bubble chamber were taken, using a full 8·3 GeV/c extracted proton beam striking a Be target approximately 7·8m from the chamber to produce a beam of neutrons. A sample of this film is being processed to examine the reactions $np \rightarrow pp\pi^+\pi^-\pi^-$ and $np \rightarrow pp\pi^+\pi^+\pi^-\pi^-\pi^-$. To date 7353 events of both topologies have been measured, of which 2-3 per cent are 7 prongs. 26 per cent of five prongs, and about 50 per cent of 7 prongs, fit as the above reactions (3C fits). The general features of these reactions are being analysed, and together with data on $np \rightarrow pp\pi^-$ will be compared with predictions of the multiperipheral model. Further light may be thrown on the existence of the N* (1470) observed in 7 GeV/c pd collisions. Results for the channel $np \rightarrow pp\pi^+\pi^-\pi^-$ will be compared with those of $pp \rightarrow pp\pi^+\pi^-\pi^-\pi^\circ$.

Experiment 31

UNIVERSITY OF LIVERPOOL
RUTHERFORD LABORATORY

$\overline{p}p$ Two-Prong Interactions

At the end of 1968, a Rutherford Laboratory group joined physicists of the University of Liverpool in a study of anti-proton-proton interactions in an energy region near the mass of the T-meson first observed by the CERN Missing Mass Spectrometer Group. The CERN 2m liquid hydrogen bubble chamber was exposed to anti-protons at momenta of 1·28, 1·34, 1·39 and 1·47 GeV/c. A scan of approximately 50,000 pictures was carried out at RHEL for all two-prong interactions; the 75,000 events yielded by the scan were then digitized in preparation for measurement on the HPD. The measurement was completed in late 1969 and the remeasures were almost complete at the end of the year. Use was made of automatic ionization measurements obtained from the HPD to resolve final state ambiguities, reducing the amount of scan-table examination of events by about one-half. An on-line light-pen facility was also used to fix some of the geometry failures, hence reducing the number of remeasures. Physics analysis is now beginning. It is hoped that the presence of T-meson formation will be observed in the large-scale elastic scattering data and/or in the $\pi^+\pi^-$ and K^+K^- annihilation channels.

Experiment 32

UNIVERSITY OF CAMBRIDGE

Anomalies of Electromagnetic Processes

A study has been made of pair production and bremsstrahlung losses using pictures taken in the 1·5m hydrogen bubble chamber in January and September 1969. Using the X1/K9 beam line, separated beams of approximately 1 GeV/c 'electrons' were produced. The results suggest that particles lighter than the muon other than electrons may have been present in the beam.

Anomalies have been observed in the distributions of the following three quantities:

(i) Pair α- Anomaly

α is defined as $(p_+ - p_-)/(p_+ + p_-)$ where p_+ and p_- are the momenta of the positive and negative tracks of the pair. No anomaly was found in the film exposed in a neutral beam of the distribution of α for pairs which can be assumed to come from π^o- decay gammas. The histogram of $|\alpha|$- values for all pairs with $(p_+ + p_-) > 100$ MeV/c on the January film is shown in figure 46. The Wheeler-Lamb theoretical spectrum with measurement errors folded in is shown for comparison. When the theoretical and experimental distributions are normalised to give the same total number of events, the experimental distribution is found to be consistent with theory only at a level of 1 part in 10^3. There appears to be an excess of events concentrated between $|\alpha| = 0{\cdot}3$—$0{\cdot}6$.

(ii) Pair Energy Anomaly

Writing k for the pair energy $(p_+ + p_-)$ and E_o for the incoming beam momentum we have examined the distribution of the ratio k/E_o. Considering all pairs from both runs, a smoothly decreasing spectrum is obtained except for an enhancement in the range 0·80—0·86. Four different sets of beam entry conditions into the chamber involving differing amounts and types of material were used. In figure 47 is shown the k/E_o spectrum corresponding to the presence of about 1·5 radiation lengths of material placed in front of the chamber beam entry window.

(iii) Bremsstrahlung Anomaly

A plot of R, the ratio of final to initial momentum for particles entering the bubble chamber with approximately full beam momentum is shown in figure 48. The theoretical curve, calculated using Monte-Carlo techniques, is shown for comparison, and has been normalised to the experimental distribution in the range 0·22—0·90. An enhancement in the range 0·16—0·22 is apparent.

It is planned to take more pictures in the period February-March 1970. This will enable a more detailed investigation of the above phenomena to be carried out. The fact that the enhancements in R and k/E_o are complementary may indicate that they are related phenomena.

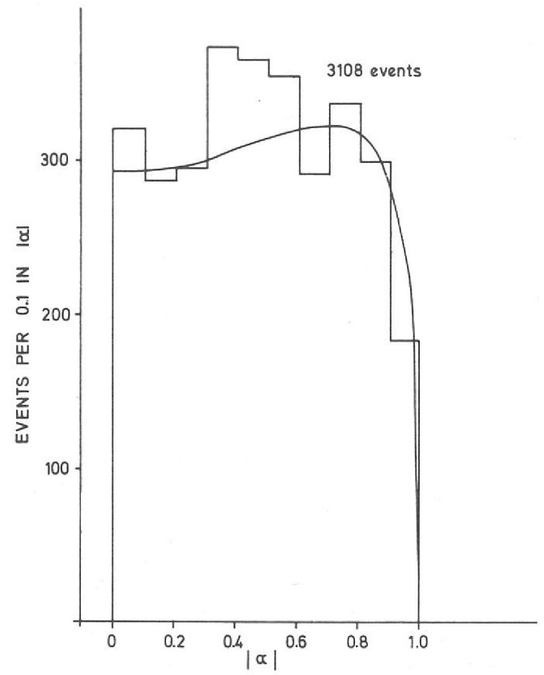

Figure 46. Histogram of $|\alpha|$ values for all pairs found with momentum greater than 100 MeV/c in the January film of Experiment 32. The solive curve is the Wheeler-Lamb theoretical spectrum with measurement errors folded in.

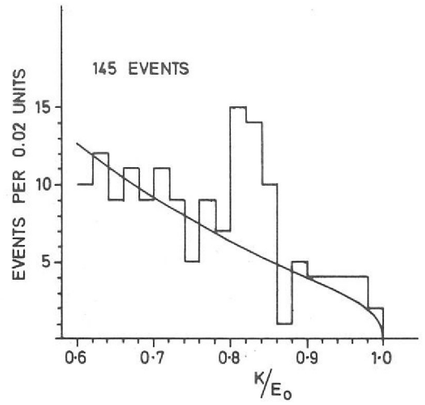

Figure 47. The measured k/Eo spectrum corresponding to the presence of about 1·5 radiation lengths of material placed in front of the chamber beam entry window (Experiment 32). The theoretical curve is shown superimposed.

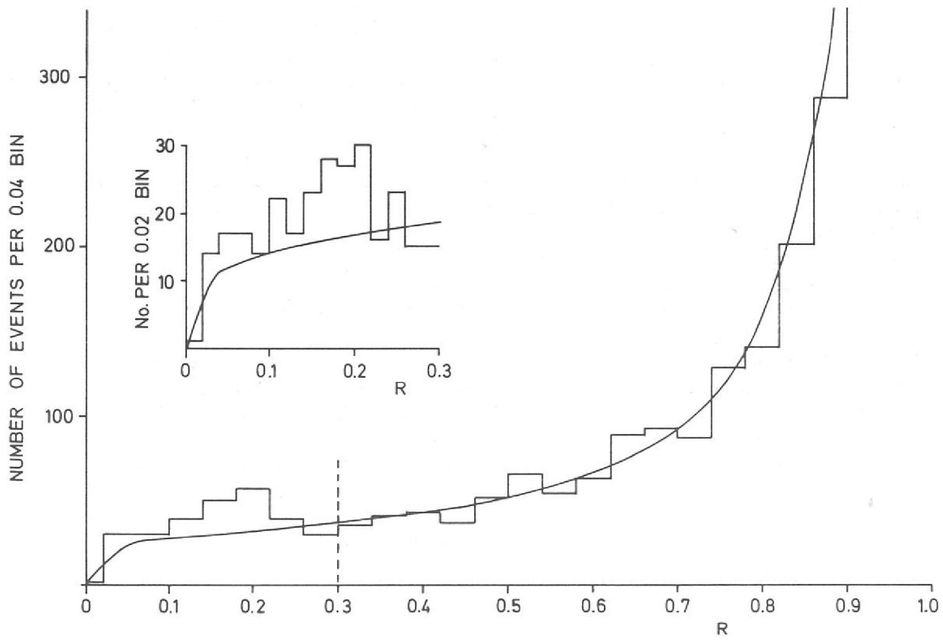

Figure 48. A plot of $R = \frac{\text{Final momentum}}{\text{Initial momentum}}$ for particles entering the bubble chamber (Experiment 32), with approximately full beam momentum. The theoretical curve was calculated using Monte-Carlo techniques and has been normalized to the experimental distribution in the range 0·22-0·90.

Experiment 33

RUTHERFORD LABORATORY
CERN
UNIVERSITY COLLEGE, LONDON

Beta Decay of Λ° *using Neon-Hydrogen Target Facility*

This experiment takes advantage of the sensitive target facility in the 1·5m chamber (see page 96) to study the β decay of the Λ° hyperon. A beam of 1·035 GeV/c π^- mesons is injected into the target which is filled with hydrogen. The associated production reaction $\pi^- p \rightarrow \Lambda^\circ K^\circ$ yields a sample of highly polarized Λ°'s.

The decay spectrum for the β decay of the Λ° in the V-A theory has the form

$$dN = C\,(p_e^{max} - p_e)_e^2\; p^2{}_e\,[1 + \alpha \cos\phi_{e\nu} + P\,(\beta_e \cos\phi_e + \beta_\nu \cos\phi_\nu)]\; dp_e d\Omega_e d\Omega_\nu$$

where $\alpha = \frac{1-x^2}{(1+3x^2)}$; $\beta_e = \frac{2x(1+x)}{(1+3x^2)}$; $\beta_\nu = \frac{2x(1+x)}{(1+3x^2)}$ and $x = C_A, C_v$ where C_A and C_V are the axial vector and vector coupling constants. p_e and p_e^{max} are the momentum of the electron and its maximum value, P is the polarization of the Λ°, $\phi_{e\nu}$ the electron neutrino angle, ϕ_e the angle between the electron momentum and the Λ° spin, and ϕ_ν the angle between the neutrino momentum and the Λ° spin direction.

The experiment is aimed at determining the parameter x which is related by the Cabbibo theory to the coupling constants in other hyperon β decays and to the rates. Clearly the distributions in $\cos\phi_{e\nu}$, $\cos\phi_e$, $\cos\phi_\nu$ have sensitivities to the value of x. In particular $\phi_{e\nu}$ is not sensitive to the sign of x.

The target system is used in order to detect a sample of β decay events against a background of 800 : 1 normal $\Lambda^\circ \rightarrow p\pi^-$ decays. The design of the target system is shown in figure 49. The target is constructed of 2mm thick perspex, is 4cm deep by 30 cm high and extends the full length of the chamber. Thus the beam particles are contained in the target and interact only with protons whilst the secondary particles (i.e. the products of the Λ° and K° decays) pass through the walls of the target into the main chamber volume. The main chamber is filled with a 50 molar per cent neon-hydrogen mixture. Operating conditions are then chosen so that the mixture in the chamber and the hydrogen in the target are simultaneously sensitive.

The leptonic Λ° decays ($\Lambda^\circ \rightarrow pe^-\nu$) are detected by the radiation loss of energy of the electrons in the neon-hydrogen mixture. The radiation length of the mixture is about 70cm which is sufficient to allow the detection of the electrons by the characteristic appearance of their tracks, without introducing too much multiple Coulomb scattering error into the energy determination. During 1969 two test exposures were made using the target system. A picture from such an exposure is shown in figure 50. Clearly the two phase operation of the chamber is successful since both the beam tracks and the secondary tracks outside the target are of good quality. The optical quality of the pictures is excellent. The perspex surfaces do not present any problems since they are plane and nearly normal to the axis of the cameras. The expansion is transmitted to the hydrogen by movement of the perspex walls; since however an expansion ratio $\Delta V/V \lesssim 1$ per cent is required for sensitivity, the walls only move about 0·2mm, i.e. one tenth of their thickness.

In order to achieve useful statistics on the Λ° decay process it is necessary to run with a high number of beam tracks. In addition to the target tests a sample of pure hydrogen pictures were taken in 1969 to study the scanning and analysis problems of high track density film. From these studies it is concluded that up to 100 π^- tracks per picture are acceptable and will yield, in the total exposure of 700,000 pictures, approximately 150-200 fully reconstructed Λ° beta decays. The main data taking run will be in 1970 and should yield a well defined value for C_A/C_V the ratio of the axial vector to vector coupling constants in the decay.

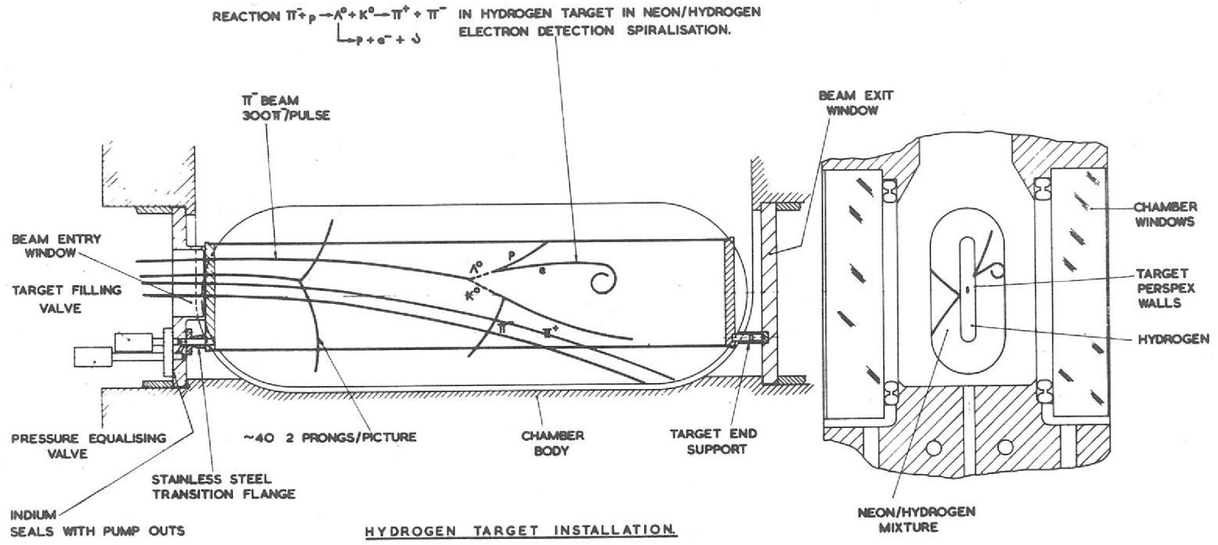

Figure 49. Diagram of the hydrogen target installation for the 1·5m British National Bubble Chamber (Experiment 33).

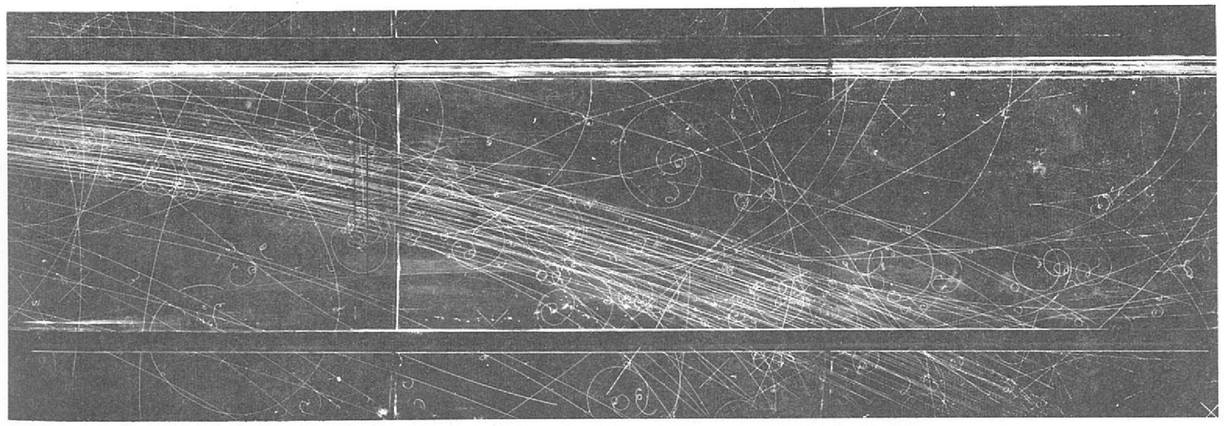

Figure 50. Bubble chamber picture taken during tests with the liquid hydrogen target installation.

Theoretical High Energy Physics

The work and interests of the Rutherford Laboratory's theorists cover a wide range of topics in high energy physics. There is some emphasis on the practical consequences of theory, and their relation to experiment, but formal questions are not ignored.

As usual, there was a summer programme of visitors from other centres in Britain and overseas. The annual December conference was attended by some 200 physicists, mainly theorists from British universities.

The following brief accounts give some idea of the work going on here.

The Veneziano Model

The most exciting area in strong-interaction physics last year was the Veneziano representation. This is a new type of formula, first written down by Veneziano for the rather inaccessible process $\pi + \pi \rightarrow \pi + \omega$, and later extended to other reactions. The reason for the excitement is that in a simple formula two deep theoretical principles and some intriguing experimental systematics have been embodied, namely:

(i) Crossing symmetry: the relation between particle-particle and particle-antiparticle scattering.

(ii) Scattering cross-sections at high energy vary as a simple power of the energy – the power depending on momentum transfer – "Regge behaviour".

(iii) In the spectrum of resonances, the highest spin at a given mass m is proportioned to m^2.

(iv) Analyticity. The formula unites low and high energy scattering in a single well-behaved mathematical function. The connection between high and low energies is not *a priori* very strong, but a simple and bold scheme (the Finite Energy Sum Rules) assuming Regge behaviour at high energy has had amazing success in predicting high energy scattering from low energy data. The Veneziano formula is a realisation of this stronger connection.

There remain many problems. The biggest is that the formula is not unitary; it does not strictly conserve probability. Attempts to put this right have become a major industry, but so far no completely satisfactory answer has been found.

Daughter Structure of Veneziano Model

The predictions of the Veneziano model for π–π scattering have been investigated. In particular, it predicts a vector meson ρ' with the same mass as f°. It was found that the most sensitive test for this object is the forward/backward asymmetry of the $\pi^+ \pi^-$ angular distribution in the f° mass region. None of the present unitarisation schemes give results consistent with the observed asymmetry. It is concluded that if such a ρ' exists, the mass-degeneracy with f° is badly broken.

Resonance Recognition in Veneziano Model (73)

A question of practical importance is how to recognise a resonance, and determine its parameters, from the Argand diagram of a partial wave amplitude varying with energy. A resonance is expected to give a circular arc, but this is not enough: is the resonance energy at the top of the loop, or where? Also there is controversy about the significance of Regge pole exchange contributions, that are known to give Argand loops: are the latter approximations to be true resonance loops, or are they background effects that should be subtracted? These questions were studied in a Veneziano model for the process $\pi\pi \rightarrow \pi\omega$. This model has many realistic features, also the true resonance parameters (and the Regge pole terms) are known. It was found that the only reliable criterion for determining a resonance energy is to take the maximum of velocity in the Argand diagram. Regge poles do not in general give good approximations to the resonance loops (in the jargon, local duality does not occur), but neither is there any advantage in subtracting them as a background.

The Z Enigma (161)*

A Z* resonance is one which has strangeness +1 and would therefore be labelled exotic from the simple quark model viewpoint. An obvious place to look for such objects is in K^+p elastic scattering; in consequence there was much activity in analysing new data in this channel as it became available throughout the year. Polarization measurements now extend from 0·9 to above 2·0 GeV/c while from the University College, London/RHEL experiment (Experiment 4, page 29) preliminary differential cross-section data will shortly be available above 1·4 GeV/c.

Previous analyses both at RHEL and other laboratories indicated a possible Z* resonance in the $P_{3/2}$ state. However the uniqueness of this resonant solution is by no means certain, especially as the data currently available is still at widely spaced momentum intervals. It is hoped that future data from Experiments 3, 4 and 8 (see pages 28, 29 and 33) will go a long way to settling this question.

πN Scattering (61, 160)

A recent high statistics experiment by a Bristol/RHEL collaboration (Experiment 1, page 26) provided π^- p differential cross-section data from 1·2 GeV/c upwards. Working in collaboration with members of the experimental team an analysis was performed to see what alterations to the CERN I THEORY phase shifts were needed by the new data.

The results were a strong confirmation of the P13 (1860) resonance and further support for the D13 (2030). Possible existence of an F17/G17 parity doublet and of a P33 resonance all around 2000 MeV were indicated.

Duality and Regge Cuts (6)

The concept of duality has proved very successful in correlating different experimental data. According to duality, the resonances that appear in low energy scattering and the particle exchanges (Regge poles) that describe high energy scattering are in some sense the same thing. They give alternative, equally valid, descriptions of the imaginary part of the scattering amplitude. Thus to add both contributions is double-counting. Also, if there are no resonances in a certain process, the Regge exchanges should be absent or cancel out; this sort of correlation is in fact found quite widely.

On the other hand, Regge cuts (representing multiparticle exchanges) are now known to be important in high energy scattering. They do not obey the same rules as Regge poles, in general, and spoil the tidy duality picture. Fortunately, one show that at least the leading Regge cuts do follow the same systematics as the Regge poles, and can be included with them in duality.

Regge Cuts in Kp Scattering (65)

The available K^-p backward scattering cross-sections (up to 3 GeV/c) fall very rapidly with increasing energy, ($d\sigma/du \sim s^{-10}$, where s and u are the squares of energy and momentum transfer). This is consistent with the absence of any relatively light particles that could be exchanged (i.e. no high-lying Regge trajectories in the u-channel). However, double-particle exchanges (Regge cuts) can occur, and are expected to give a contribution falling only as s^{-3}. The apparent contradiction between this and the data above is explained by a model calculation according to which the cut contributions are smaller than the presently measured cross-sections, and become dominant only above 5 GeV/c.

$\pi\pi$ Scattering (71, 97, 146)

There has recently appeared additional experimental information relating to S-wave $\pi-\pi$ interactions, making it worthwhile to pursue further the theoretical analysis via forward dispersion relations described in last year's Report. Taking the experimental and theoretical information together, an almost unique picture of $\pi-\pi$ scattering emerges for dipion energies up to 850 MeV, although certain questions remain.

Chew-Low Extrapolation (37, 147)

Empirical evidence on $\pi-\pi$ scattering comes mainly from experiments on peripheral dipion production and the most model-independent way of extracting elastic $\pi-\pi$ parameters is afforded by the Chew-Low Extrapolation method. Recently reported analyses have put into question the usual practice of assuming that the extrapolated intensity function vanishes for zero-momentum transfer as it would for pure one-pion exchange. A modified method has been prepared incorporating a model for the non-vanishing background. An application has been made with interesting consequences for the Vector-Dominance (or rho-photon analogy) Model.

High Energy Elastic Scattering and the Shadow of Inelastic Processes (43)

An s-channel approach has been employed to analyse the differences between the high energy total cross-sections and elastic scattering of K^-p and $\bar{p}p$ and their counterparts under crossing K^+p and pp. The idea is to attribute the difference to the shadow of specific inelastic channels open to the former and closed to the latter, e.g. annihilation.

CP in Radiative τ Decay (29)

The 2π decay of the long-lived neutral kaon provides evidence for CP-noninvariance. If, however, the CP-odd interaction is even under space-reflection, $K \to 3\pi$ decays which are parity conserving offer a natural place to look for CP-noninvariant effects. Due to conditions imposed by TCP-invariance, it is better to consider the radiative channels. This work is devoted to a phenomenological discussion together with an estimate of the magnitude of these effects in $K^{\pm} \to \pi^{\pm}\pi^+\pi^-\gamma$ decays; one should observe asymmetries between the K^+ and K^- modes.

CP in Radiative θ Decay (92)

CP-noninvariant effects in $K^{\pm} \to \pi^{\pm}\pi^{\circ}\gamma$ decays may arise due to interference between the inner bremsstrahlung amplitude and the electric and magnetic direct amplitudes. This work is devoted to an estimate of the magnitude of the strength of the magnetic direct radiation term by relating it to the τ^+ decay rate and by using the Veneziano model to give the off-mass-shell dependence of the amplitudes. This term is found to be negligibly weak; the asymmetry after polarization summation between the radiative $\theta^{\pm}$ modes then depends essentially only on the electric direct term and the bremsstrahlung amplitude.

CP-Nonconservation (2, 29, 47, 48, 49, 135)

Work continued on problems associated with CP-nonconservation. It was noted that charge-asymmetry in "η" decays due to background interference (Yuta-Okubo effect) could be suppressed by choosing η-production mechanisms with no I = 2 background. The measurement of the phase of η_{oo} was shown, by the application of previously published ideas (1968 Annual Report, page 56), to demonstrate T-invariance. The arguments proving that experiments on $K_2^{\circ} \to 2\pi$ decay cannot be understood except by giving up CP-invariance were summarised. Information on the possible occurrence of CP-noninvariant interactions which conserve parity may be obtained from a study of $K\pi 3$ decays. A phenomenological analysis was made of radiative $\tau\pm$ decays, where appreciable charge-asymetries indicating CP-noninvariance may occur. A graphical representation was given of CP-nonconservation parameters in K° decay, which improves on the one proposed by Wu and Yang.

A systematic analysis of all possible tests of TCP-invariance from K° partial decay rates was also made. An exact formula was devised for the phase of the mixing-parameter in superweak theories, showing that a single real parameter determines all CP-noninvariant phenomena in this case. A review of the current situation in CP-nonconservation was given at a NATO Summer Institute in Karlsruhe.

Form Factors (44)

Cross terms between electric and magnetic scattering in electron-proton scattering, which can help to determine the poorly-known electric form-factor GE, was shown to be determinable from measurements of the recoil proton polarization from polarized target protons.

Intermediate Bosons

Restrictions imposed on the theory that the hypothetical intermediate boson of weak interactions possesses quadratic strong interactions, by the low meson flexes found in the gold-mine experiments have been considered.

NUCLEAR PHYSICS ON THE PLA

Nuclear Physics on the Proton Linear Accelerator

With the closure of the PLA towards the end of the year use of the accelerator has been on a gradually diminishing scale. Despite this however the machine continued to run extremely well right until the end. To allow a gradual phase out of the machine prior to its final close down and to allow some of the staff to be redeployed to other projects the machine was operated on a three week cycle consisting of an average of two weeks scheduled for experiments followed by a shutdown period of one week. During the shutdown week any necessary maintenance work was carried out on the machine and on average three days were allocated for this purpose.

During the year a total of 4556 hours of machine time were scheduled for experiments. Of this time the proton beam was available to the experimenters for 3921 hours representing machine availability of 86%. This figure compares very well with that for the previous year (see table 1) of 91% considering the much reduced maintenance carried out on the machine.

Some further work was carried out on the polarized proton source as a result of which a beam with maximum intensity $2{\cdot}3 \times 10^9$ protons/sec. and polarization of 63% was obtained to be compared with figures of $1{\cdot}7 \times 10^9$ protons/sec. and 53% recorded during the previous year. The improvement in performance of the polarized beam since the first installation of the polarized source is summarised in table 2. No other development work was carried out on the machine during the period under review.

On 3rd October 1969 at 11.00 a.m. the machine was closed down in a simple ceremony by the present Director of the Rutherford Laboratory Dr. G. H. Stafford assisted by Mr. J. M. Dickson previously leader of the PLA Accelerator Physics group. During its 9 years of operation the PLA produced 42,658 hours of beam out of a total scheduled time of 51,291 hours representing an overall machine availability of 83%. During this time the performance of the machine in terms of output current and energy spread were considerably improved and the accelerator became one of the principal centres for nuclear structure physics research. Over 40 PhD theses and 120 published papers have been written on experiments carried out on the PLA.

With the closure of the machine imminent the experimental work has principally been concerned with the completion and analysis of experiments already in progress or with the extension of well established studies (e.g. elastic and inelastic proton scattering) to other target nuclei or energy levels. However two experiments which were largely carried out in the year under review were the measurement of the polarization in proton-proton scattering at 10 MeV and the measurement of the D parameter for proton-nucleus scattering at 50 MeV. These two experiments will be described in some detail and the remaining work briefly summarised. All the experiments, together with the associated experimental techniques and theoretical studies are very fully described in the 1969 Final PLA Progress Report (RHEL/R187) which is freely available.

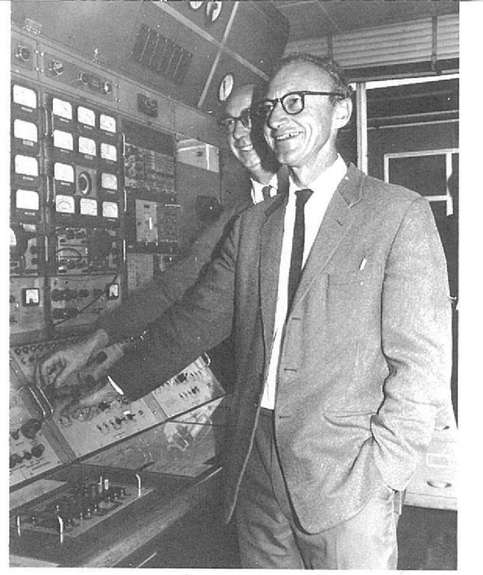

Figure 51. Dr. G. H. Stafford and Mr. J. M. Dickson switch off the Proton Linear Accelerator for the last time on October 3rd 1969.

Table 1

Running Time 1960 – 1969

	Hours Scheduled	Hours Available for Use	Availability(%)
1960	1,420	980	69
1961	2,240	1,169	52
1962	5,544	3,971	72
1963	5,453	4,405	81
1964	5,573	4,664	84
1965	6,128	5,260	86
1966	6,303	5,605	89
1967	6,521	5,847	90
1968	7,553	6,836	91
1969	4,556	3,921	86
	51,291	42,658	83

Table 2

Polarized Proton Beam

Source	Date	Intensity(I) p/sec	Polarization(P) %	IP^2
I	1961	$1{\cdot}5 \times 10^7$	31	$0{\cdot}014 \times 10^8$
		6×10^7	22	0·029
	1962	6×10^7	32	0·06
II	1963	6×10^7	35	0·074
	1964	2×10^8	40	0·32
III	1965	$1{\cdot}3 \times 10^8$	51	0·34
	1966	$5{\cdot}3 \times 10^8$	52	1·44
		$5{\cdot}3 \times 10^8$	61	1·88
	1967 Maximum	$1{\cdot}3 \times 10^9$	50	3·25
	Average			2·5
	1968 Maximum	$1{\cdot}7 \times 10^9$	53	4·8
	Average			3·2
	1969 (Jan.)	$2{\cdot}3 \times 10^9$	52	6·2
	1969 (Aug.)			
	Maximum	$2{\cdot}3 \times 10^9$	63	9·1
	Average			6·0

Experiments at the Proton Linear Accelerator

Number	Experiment	Group
1†	Proton-proton polarization measurements at 10 MeV	University of Oxford
2†*	The D-parameter for proton-nucleus scattering at 50 MeV	Rutherford Laboratory
3†	Precision measurements of the polarization in elastic scattering	University of Minnesota, USA University of Birmingham
4†	Polarization in elastic and inelastic scattering	University of Birmingham
5†	Triple scattering parameters for proton-deuteron elastic scattering	Queen Mary College, London Kings College, London Queen's University, Belfast
6†*	Cross-sections and polarization for elastic and inelastic scattering	King's College, London West Ham College of Technology
7†	Backward angle scattering of 50 MeV protons	King's College, London University of Kent
8*	Elastic and inelastic scattering of protons	University of Manchester Rutherford Laboratory
9†	Elastic scattering of protons from O^{16}	University of Birmingham
10†	Inelastic proton scattering at 10 MeV from Fe^{54} and Ni^{60}	University of Birmingham
11†	The C^{12} (p,p'γ) reaction with polarized incident beam	University of Birmingham
12*	Pick-up reactions	University of Oxford Rutherford Laboratory
13*	Total proton reaction cross-sections for C^{12}	King's College, London
14	Pick-up reactions on Li^6	University of Oxford
15†	Asymmetry measurements in the F^{19} (p,He^3)O^{17} reaction	University of Oxford
16	Study of the N^{15} (p,α)C^{12} and N^{15} (p,He^3)C^{13} reactions at 49·5 MeV	University of Oxford
17*	The interaction of 50 MeV protons with B^{10}	Queens University, Belfast Kings College, London

† Experiments using polarized proton beam

* Experiments using double focussing magnetic spectrometer

Experiment 1

UNIVERSITY OF OXFORD

Proton-Proton Polarization Measurements at 10 MeV.

Recent measurements of proton-proton polarization at energies between 9·6 and 19·7 MeV at Berkeley yielded a trend towards positive asymmetries at small angles. This was interpreted by the authors as being indicative of the inadequacy of the accepted one-pion exchange model and of the need for a sizeable amount of spin-orbit interaction. Comprehensive phase-shift analyses of proton-proton scattering data in the region of 20 MeV could not be reconciled with the 19·7 MeV Berekeley data. Subsequently polarization measurements at 20·2 MeV were published which were in contradiction with the Berkeley data but in agreement with the phase-shift analyses using tensor splitting of the p-waves characteristic of one-pion exchange. This indicated the desirability of ascertaining the reason for the inconsistency of the Berkeley data and provided the motivation for a new measurement at 10 MeV to compare with the earlier 9·6 MeV results.

The 10 MeV beam was used to bombard a polythylene target $(CH_2)_n$ mounted at the centre of a scattering chamber on the 77° beam line. The beam polarization was measured with the sampling polarimeter, using a beryllium target in the wheel in place of the 50 MeV carbon target. Beam intensities were of the order of 10^{-11} A, and polarizations of up to 60% were achieved in the final run. Scattered protons were detected simultaneously by left and right semi-conductor counter telescopes at equal angles on either side of the beam.

Successive runs were performed with "spin up" and "spin down". The use of the symmetric detector system removes the need for beam monitoring and eliminates most false asymmetries.

Results of the polarization measurements are shown in figure 52 together with the Berkeley data. Included in the figure are "theoretical" curves. The solid line curve corresponds to the phases representative of one-pion exchange. The dashed line corresponds to the "fit" chosen by the Berkeley group.

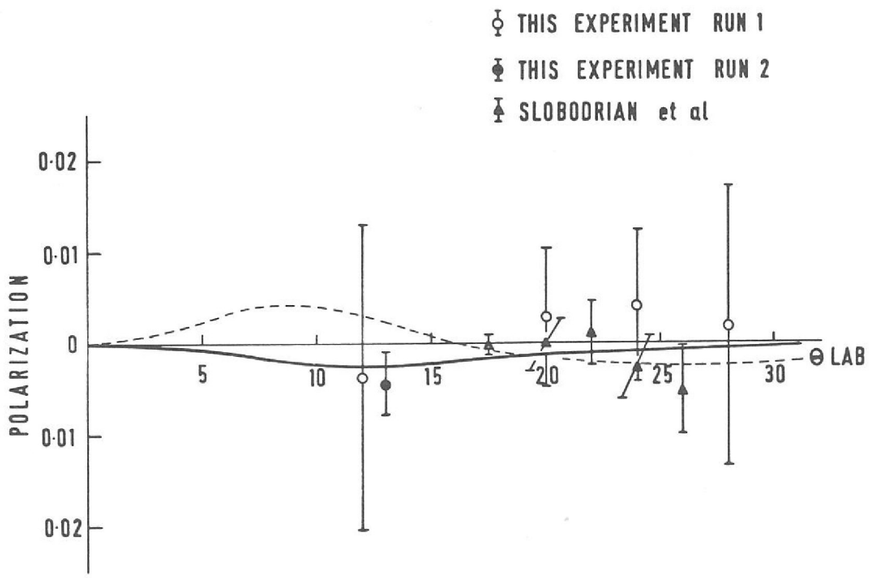

Figure 52. Proton-proton polarization measurements at 10 MeV.

Several measurements were made in a preliminary run over the angular range covered by the Berkeley group as a general check of the experimental technique. Although the statistics are inferior, the results, as shown in the figure, are not inconsistent with the Berkeley data. In a subsequent run, a more definitive measurement with good statistics was made at 13° lab. This is close to the angle where the one-pion exchange potential predicts a maximum asymmetry. The result is consistent with the earlier 12° measurement, and in good agreement with the asymmetry predicted by the one-pion exchange potential. However it is not consistent with the asymmetry using the phase shift set chosen by the Berkeley group. This lends strength to a one-pion exchange description over that advanced by the Berkeley group. It is noted that the Berkeley data at 9·6 MeV is in fact not inconsistent with either set of phase shifts.

Experiment 2

RUTHERFORD LABORATORY

The D-Parameter for Proton-Nucleus Scattering at 50 MeV (13, 172)

In almost all optical model calculations of elastic nucleon scattering the spin I of the target nucleus has been neglected. If forces dependent on the nuclear spin are present they might be expected to have a significant effect on polarization measurements for adjacent target nuclei of different spin. The evidence for such an effect has been considered and it has been shown that any target-spin dependent effects must be small.

This result has been confirmed by recent experiments in which a possible spin-spin interaction between polarized neutrons and polarized Co^{59} or Ho^{165} nuclei has been investigated. The results for 1 MeV neutrons on Ho^{165} show that for a potential term of the form $V_{ss}\ f(r).\frac{\bar{\sigma}.\bar{I}}{I}$ one finds $V_{ss} < 300$ keV.

The other experiments which cover a range of neutron energies are consistent with this result.

An alternative method of determining the existence of a possible spin-spin interaction is through a measurement of the triple-scattering D-parameter. Such an experiment requires a polarized nucleon beam but does not require a polarized target. As a result it is possible to study a much wider range of target nuclei.

Experiments of this kind using polarized neutrons have been considered theoretically and the maximum effect is likely to be observed at the angle of the first diffraction minimum in the elastic scattering cross-section. In the present work measurements have been made of the D-parameter for 50 MeV protons scattered by a wide range of target nuclei.

The D-parameter is measured by scattering a proton beam of known transverse polarization from the target under study. The polarization normal to the scattering plane of the elastically scattered beam is then determined by a second scattering in a polarization analyser. One of the problems associated with experiments of this type is the need to separate the protons elastically scattered in the target from inelastic events. In the present experiment the elastically scattered protons were selected by the n=½ magnetic spectrometer with a slit system placed at the spectrometer focal plane. Only those protons which had been elastically scattered passed through the slit and were measured in the polarization analyser. The polarization analyser was specially designed for this experiment.

For the nuclei studied, which cover most of the periodic system, no convincing evidence for a deviation of the D-parameter from unity was found within the accuracy of the measurements. This indicates that any interaction dependent on the spin of the target nucleus must be small for 50 MeV protons in agreement with the results at lower energies.

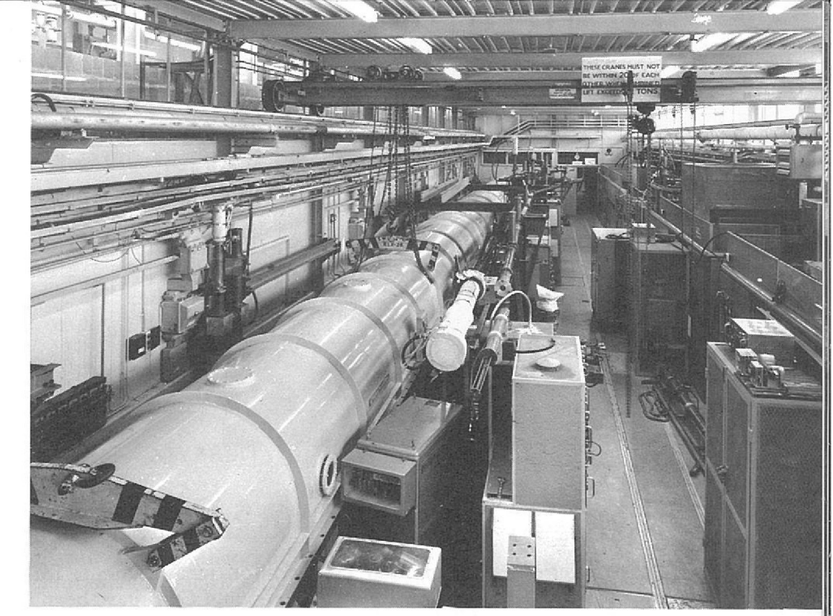

Figure 53. General view of the PLA from the output end.

Experiment 3

UNIVERSITY OF BIRMINGHAM

Precision Measurements of the Polarization in Elastic Scattering.

A theoretical analysis of the precision measurements of polarization in the elastic scattering of 30 MeV protons by Ni^{58}, Sn^{120} and Pb^{208} described in last years Report is being made by Professor Greenlees's group at the University of Minnesota, USA. Further measurements have been made at the Rutherford Laboratory for Ca^{40} and Co^{59} and the analysis of these data is in progress.

Experiment 4

UNIVERSITY OF BIRMINGHAM

Polarization in Elastic and Inelastic Scattering (55, 168, 182, 183)

Data on the polarization in inelastic scattering to several levels was obtained for 30 MeV protons on Ni^{58}, Sn^{120} and Pb^{208} during the precision elastic polarization measurements described in last years report. Further data has also been obtained at 30 MeV for B^{11}, C^{13}, O^{16}, Fe^{54} and Fe^{56}. Analyses of the data have been made using both macroscopic and microscopic models for the interaction. Using a macroscopic model it is found essential for all terms in the optical potential to be deformed; especially the deformation of the spin-orbit term has a significant influence on the shape of the predicted asymmetries. In the microscopic model calculations have been made assuming different configurations for each state and with a two-body interaction derived from the Hamada-Johnston potential.

Experiment 5

QUEEN MARY COLLEGE, LONDON
KINGS COLLEGE, LONDON
QUEEN'S UNIVERSITY, BELFAST

Triple Scattering Parameters for Proton-Deuteron Elastic Scattering (186, 209)

Measurements of the Wolfenstein triple scattering parameter A for the elastic scattering of 50 MeV protons from deuterons have been made. These, together with the measurements of the D and R parameters mentioned in last years Report, completes the experimental programme to help find a unique set of phase-shifts which describe the elastic scattering of protons by deuterons. Final analysis of the data is in progress.

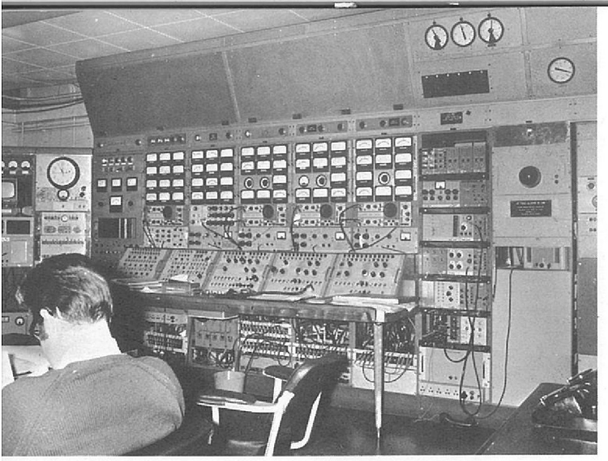

Figure 54. PLA Control Room.

Experiment 6

KING'S COLLEGE, LONDON
WEST HAM COLLEGE OF TECHNOLOGY

Cross-sections and Polarization for Elastic and Inelastic Scattering

Differential cross-section measurements for the elastic scattering of 30 and 50 MeV protons from Cu^{63} and Cu^{65} have been made to complement the polarization data for these isotopes and energies reported last year. Analysis of the raw data has been completed and a theoretical analysis in terms of the optical model made using the difference function method.

To extend these studies of differences in the parameters for neighbouring nuclei further and in an attempt to determine in a less ambiguous fashion the A dependence of the potential strengths, measurements of the differential cross-sections for elastic scattering of 30 MeV protons by target nuclei in the region $54 \leqslant A \leqslant 82$ have been made. Nuclei studied were $Ca^{42, 44}$, $Ti^{46, 48, 50}$, Cr^{52}, $Fe^{54, 58}$, $Ni^{62, 64}$, $Ge^{70, 72, 74, 76}$, $Se^{76, 78, 80, 82}$. Reduction of this very large amount of experimental data is in progress.

Differential cross-sections for elastic scattering of 49·5 MeV protons by Sm^{148} have been measured and will be analysed together with polarization measurements for this nucleus described in last years Report and cross-section measurements made for all the even isotopes of Samarium at Oak Ridge.

Elastic scattering cross-sections have also been made for 49·4 MeV protons scattered by $Mo^{92, 94, 96, 100}$ and for 20·0 and 30·0 MeV protons scattered by $Mo^{92, 100}$. Polarization and asymmetry measurements have also been made for 30 MeV protons scattered from the ground and first 2+ state of $Mo^{92, 96, 100}$. Analysis of the data is in progress. Asymmetries in the scattering of 30 MeV polarized protons from the 3^- states in $Zn^{64, 68}$ have also been measured.

Experiment 7

KINGS COLLEGE, LONDON
UNIVERSITY OF KENT

Backward Angle Scattering of 50 MeV Protons (190)

Measurements have been made of differential cross-sections and polarizations for the elastic scattering of 50 MeV protons using a NaI scintillation counter in conjunction with a sonic spark chamber for angle determination. This detection system is particularly useful for low count rate situations and was designed for large angle scattering measurements so as to make the most efficient use of the available beam.

Cross-section and polarization measurements have been made for Be^9, C^{12}, N^{14} and O^{16}. The backward angle polarization data show a very large variation in magnitude over a small angular interval for both C^{12} and O^{16}. This effect has so far been unexplained. Measurement at large angles of the polarization for Si^{28} and Mg^{24} and of cross sections for Ca^{40}, Pb^{208} and Bi^{209} have also been made.

Experiment 8

UNIVERSITY OF MANCHESTER
RUTHERFORD LABORATORY

Elastic and Inelastic Scattering of Protons

Angular distributions have been measured for the elastic and inelastic scattering of 50 MeV protons by Fe^{54}, Fe^{56} and Fe^{58}; by Pb^{206}, Pb^{207}, Pb^{208} and by the even isotopes of tin, Sn^{116}, Sn^{118}, Sn^{120}, Sn^{122} and Sn^{124}. The analysis of this very large amount of data is at present in progress.

Experiment 9

UNIVERSITY OF BIRMINGHAM

Elastic Scattering of Protons from O^{16}. (54, 167)

From the analysis of data obtained with the PLA for proton elastic scattering from O^{16} the existence of several resonances has been established between 18 and 30 MeV incident energy. The main difficulties in the theoretical fits to these data arose in the fitting of the angular distributions for polarization near the 20·4 MeV resonance. In order to investigate this energy region further the energy dependence of the polarization has been measured at 10 points between 18·75 and 22 MeV for 8 scattering angles. Further measurements of cross-sections and polarization have been made at 26·8 and 28·5 MeV together with the energy dependence of the polarization at 14 points between 25 and 29 MeV for 4 scattering angles. The analysis of the data so far indicates that there are probably two resonances contributing for proton energies in the region of 20·5 MeV. Further analysis is in progress.

Experiment 10

UNIVERSITY OF BIRMINGHAM

Inelastic Proton Scattering at 10 MeV from Fe^{54} and Ni^{60}. (187)

Angular distributions of cross-sections and asymmetries for the reactions Fe^{54} (p,p′)(1·41 MeV) and Ni^{60} (p,p′)(1·33 MeV) and for elastic scattering have been measured using the 10 MeV polarized beam. These results together with proton spin-flip probability data (i.e. the (p,p′α) perpendicular angular correlation) obtained previously using the University of Birmingham Nuffield Cyclotron, are being used to study reaction mechanisms in these nuclei at 10 MeV.

The results indicate that compound nucleus scattering is the predominant effect for Fe^{54}. For Ni^{60} the direct component is dominant, as might be expected from the lower (p,n) threshold for this nucleus. The analysis also shows that the compound nucleus contribution has opposite effects on the inelastic asymmetry and the spin-flip probability, thus enabling the effects of the spin-orbit terms to be separated from the effects of the compound nucleus scattering.

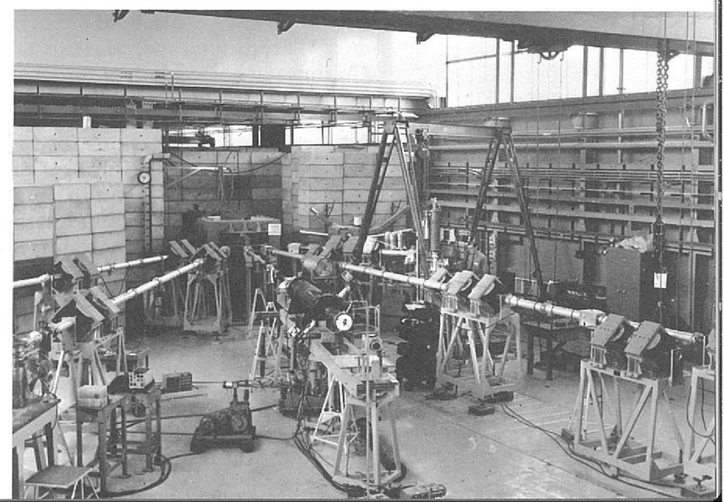

Figure 55. PLA Experimental Area.

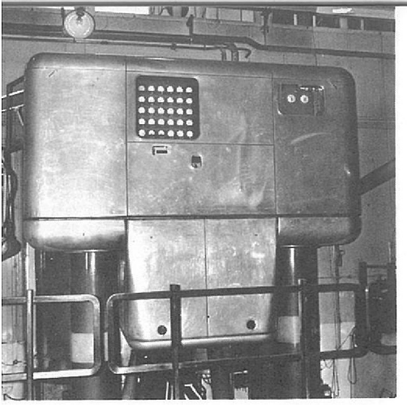

Figure 56. High Voltage Terminal of PLA Injector.

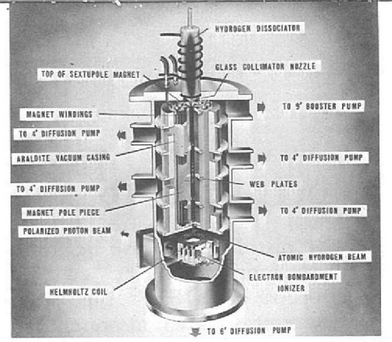

Figure 57. Schematic diagram of Polarized Proton Source which is installed within the HVT shown in figure 56.

Experiment 11

UNIVERSITY OF BIRMINGHAM

The C^{12} $(p,p'\gamma)$ Reaction with Polarized Incident Beam (195)

Measurements of proton polarizations or asymmetries have proved valuable in studies of the spin-dependence of inelastic scattering processes. Additional information may be derived from the observation in coincidence of the γ-rays following scattering. Further information is obtained if the incident proton beam is polarized.

The principal difficulties in such an experiment of the high random coincidence rate and pile-up problems in the γ-ray detector are both aggravated by the low duty cycle of the PLA. However an experiment to measure the correlation for the 4·43 MeV state in C^{12} has been successfully carried out for a range of scattering angles greater than 90°. The results have been compared with the predictions of coupled channels calculations and further analysis of the data is in progress.

Experiment 12

UNIVERSITY OF OXFORD
RUTHERFORD LABORATORY

Pick-up Reactions (62, 164)

The analysis of the Ne^{20} (p,t) Ne^{18} reaction described in last years Report illustrated the usefulness of this reaction in picking out certain characteristics of nuclear wavefunctions. This work has now been extended to the O^{18} (p,t)O^{16} reaction using 50 MeV protons. Analysis of the data is in progress.

The studies of (p,t) reactions on the Nickel isotopes also mentioned in last years Report have been extended to Ni^{58}, Fe^{56} and Cr^{54}. These reactions produce a sequence of nuclei starting from the doubly closed $f_{7/2}$ shell nucleus Ni^{56} to Cr^{52} in units of the removal of 2 protons per nucleus. In connection with this programme of work some measurements have also been made for the Ni^{58} (p,d) reaction.

Experiment 13

KINGS COLLEGE, LONDON

Total Proton Reaction Cross-sections for C^{12}. (194)

Total reaction cross-sections for C^{12} have been measured over a range of energies between 20 and 50 MeV using a new technique in which a mono-energetic beam of protons is brought to rest in a plastic scintillator. Protons which do not give rise to a full light output pulse are either scattered elastically or inelastically, or they react with nuclei in the scintillator. By calculating the distribution of the elastically scattered protons from the hydrogen and carbon then, by a subtraction method, the number of protons which have reacted with the carbon in the scintillator can be obtained. Hence the total reaction cross-section can be calculated. Final analysis of the results is in progress.

Experiment 14

UNIVERSITY OF OXFORD

Pick-up Reactions on Li^6.

The Li^6 (p,He^3) He^4, Li^6 (p,α)He^3 and Li^6 (p,t) Li^4 reactions have been studied at 30 MeV over the angular range from 10° to 50°. The principal objective of this experiment is to look for excited states in the mass 4 and mass 3 system, a subject which has recently been one of considerable controversy. Analysis of this data, and of deuteron spectra from the Li^6 (p,d)Li^5 reaction which were collected simultaneously, is in progress.

Experiment 15

UNIVERSITY OF OXFORD

Asymmetry Measurements in the F^{19} $(p,He^3)O^{17}$ Reaction. (175)

One of the characteristics of the two nucleon transfer reaction is that in certain circumstances the orbital or spin angular momentum associated with the transferred particles is not unique. In these cases the cross-section is obtained by summing the different L or S components of the transition amplitude. The summation over L is straightforward but the summation over S is uncertain. An asymmetry measurement using the polarized proton beam for the F^{19} (p,He^3) reaction leading to the $5/2^+$ ground state of O^{17} has been made. The asymmetries predicted by DWBA calculations are dependent on the extent of the admixture of S=0 and S=1 contributions in the summation of the transition amplitudes. Analysis of the data is in progress.

Experiment 16

UNIVERSITY OF OXFORD

Study of the N^{15} $(p,\alpha)C^{12}$ and N^{15} $(p,He^3)C^{13}$ Reactions at 49·5 MeV.

One of the problems associated with the analysis of multi-nucleon transfer reactions is to establish the relative contributions of pick-up and knock-out processes. The reaction N^{15} (p,α)C^{12} has been studied in order to try to differentiate between these two processes. Whilst the spectroscopic arguments would seem to favour a pick-up type of reaction, knock-out is favoured by kinematical considerations. Using a N^{15} gas target data has been collected both for this reaction and for the N^{15} (p,He^3)C^{13} reaction also. Analysis of the raw experimental data is complete whilst an analysis of these reactions using DWBA theory is being made.

Experiment 17

QUEENS UNIVERSITY, BELFAST
KINGS COLLEGE, LONDON

The Interaction of 50 MeV Protons with B^{10}. (79, 169, 208)

Differential cross-sections for the excitation of a number of states by the reactions B^{10} (p,d)B^9, B^{10} (p,t)B^8 and B^{10} (p,He^3)Be^8 have been measured at 49·5 MeV using the n=½ magnetic spectrometer. The results for the (p,d) and (p,t) reactions have been compared with DWBA calculations. Measurements for the 16·63 and 16·93 MeV levels in Be^8 were analysed to determine the relative contributions of isospin T=0 and T=1 components. The results indicate that only the T=1 components are excited in the (p,He^3) reactions. A possible explanation in terms of a two step excitation process has been proposed.

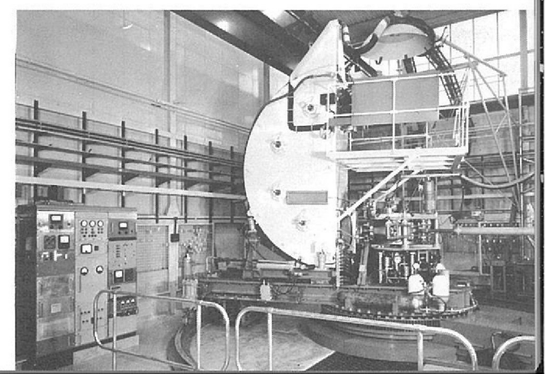

Figure 58. The Double Focussing Magnetic Spectrometer.

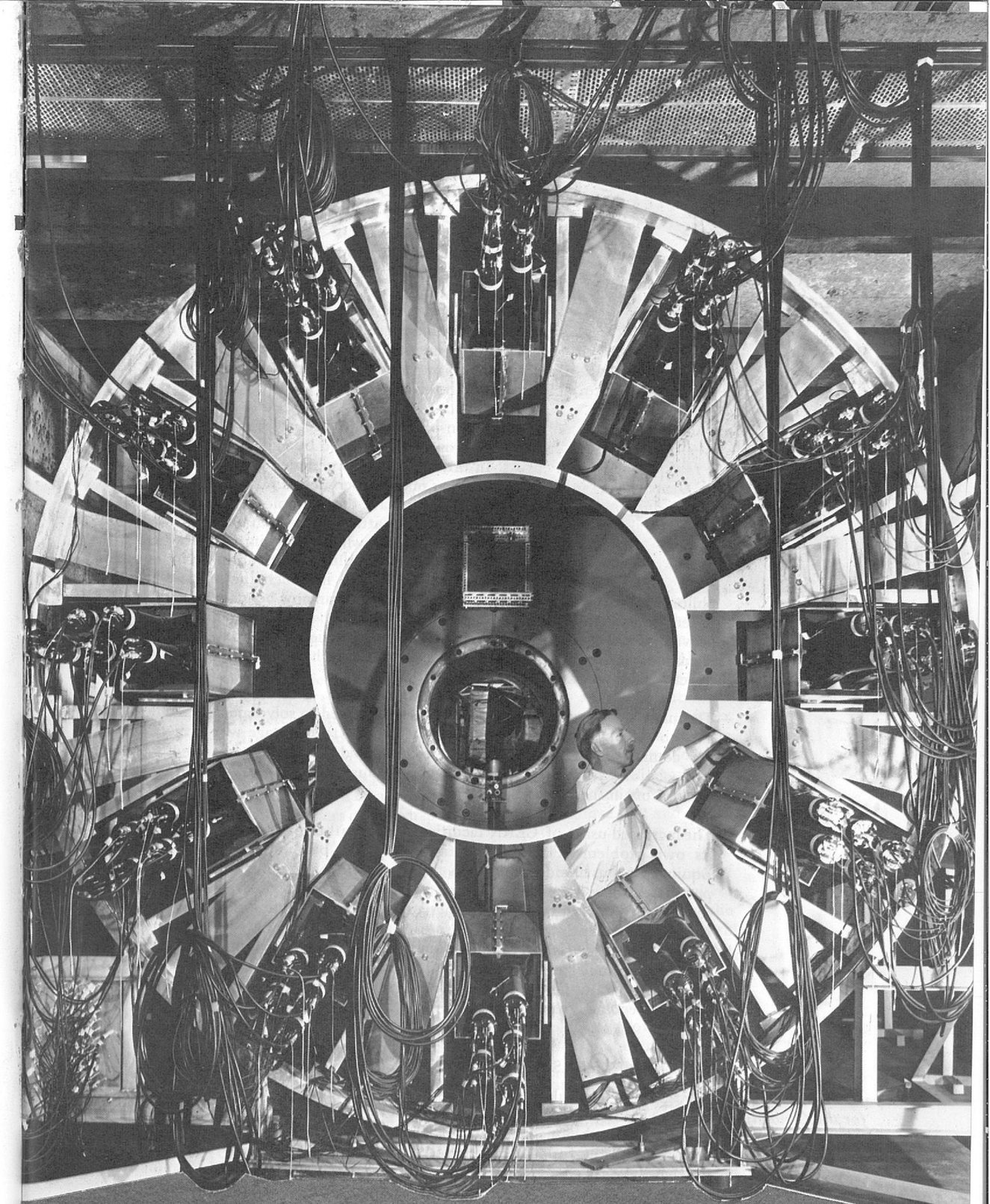

INSTRUMENTATION FOR HIGH ENERGY PHYSICS

Instrumentation For High Energy Physics

This section of the Report deals with the development of devices and techniques (apart from computer applications which are treated separately) that are currently utilised in the Laboratory's fundamental research programme, which has been described in the foregoing pages. This instrumentation work is carried out in several of the Laboratory's Divisions; a substantial fraction of the items described below have been developed by the Nuclear Physics Apparatus Group of Engineering Division, and by way of introduction a short account of the functions of this recently formed Group will be given.

During the design and construction phases of an HEP experiment, problems frequently arise which are more appropriately handled by engineering and technical personnel than by scientists. In order that the experience gained in solving such problems can be made available to as many experimental teams as possible, it has been found organisationally convenient to have the technological support effort in one central pool rather than permanently attached to each experiment. In this way it is often possible to develop equipment which, while initially designed with one experiment in mind, will be of general utility. Fabrication techniques for spark chambers and associated devices is a field in which the adoption of this philosophy has paid dividends; foil spark chambers can now be made up to 4 metres in length, whereas 18 months ago 1·5 metres was the maximum dimension. It has proved possible to develop the constructional techniques to the stage where spark chambers can be made by outside industry instead of having to rely on the skill and experience of laboratory staff.

The many small technological teams that are formed to solve specific problems are able to carry their responsibilities right through to the stage where their devices are commissioned on the 'floor', which in addition to giving them a better appreciation of their work also provides a valuable augmentation of experimental team effort in the setting-up phase.

The increased usage of CERN facilities by the Rutherford Laboratory has brought its own problems. Planning and time-scheduling become even more important. Equipment must be designed with transportability in mind, and as many items as possible made on a "plug-in" basis. It has not been possible, on account of the scarcity of staff with suitable experience, to have a technical support team stationed permanently at CERN. Instead, 'flying-squads' have been available to travel to CERN at short notice as and when required, pending which they take part in the home-based programme. It is expected that this aspect of the Nuclear Physics Apparatus Group's activities will increase when the CERN ISR and Omega projects become operational.

SPARK CHAMBERS

Spark Chamber Array for the C-violation in η Decay Experiment (No.16, page 42)

An array of optical spark chambers has been designed to work inside the M7 magnet (which is described in a later section). The particle beam passes horizontally through this magnet and the chambers are arranged symmetrically about this beam in the form of three concentric, truncated, square pyramids as shown in figure 59. Each pyramid consists of four flat multi-gap spark chambers. The images of sparks occurring within the chambers are reflected into adjacent mirrors and thence into mirrors situated above, below and at the sides of the magnet. Images are finally reflected into vidicon cameras which record the events in 15° stereo view for each chamber gap.

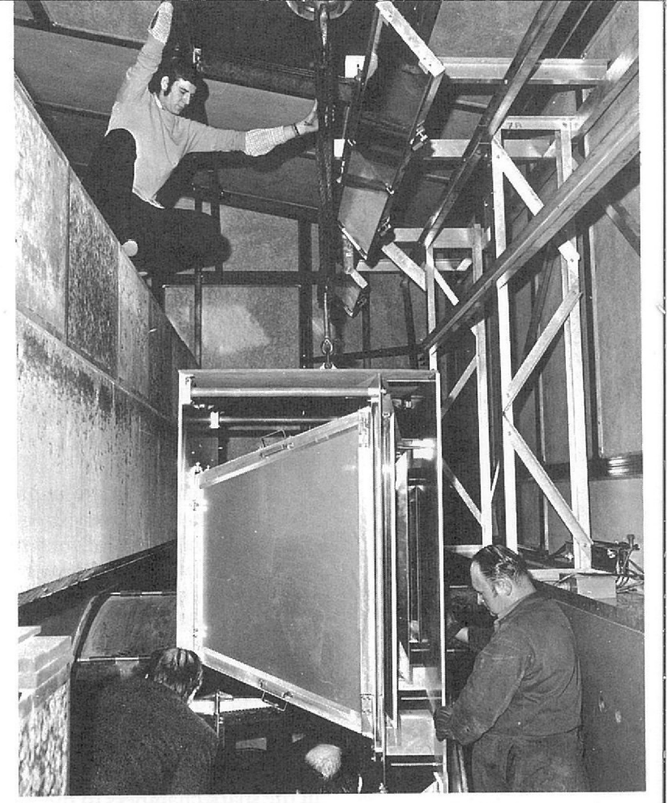

Figure 59. The spark chamber system for Experiment 16 is shown being lowered into position between the poles of a large spectrometer magnet.

The outer and intermediate chambers are constructed from stretched aluminium foil on perspex frames with light alloy supporting frames on each side of the pack. Outer chambers have four gaps of 1 cm, utilise both 0·0005 inch and 0·001 inch thick foils and have an effective area of about 7 square feet. Intermediate chambers have two gaps of 1 cm and 0·0005 inch thick foils are used. The inner chambers are of different construction, consisting of slotted side plates of perspex into which are fitted sheets of expanded polystyrene, 0·084 inch thick, clad on each face with 0·00025 inch aluminium foil. Gaps of slightly less than 1 cm are produced and there are four gaps per chamber. The cross-section of all supporting frames used in the construction of all these chambers has been kept to an absolute minimum. The viewing surfaces of the perspex frames are, of course, flat and highly polished.

The stereo view into the chambers is obtained from the base (upstream) end of the pyramids. All mirrors used throughout are of glass, front surface aluminised. The twelve primary mirrors can be tilted separately and remotely to obtain the correct angle for viewing into each spark chamber. The primary mirrors and all spark chambers are securely held in a carrier frame, and all materials used are non-magnetic.

The spark chambers are electrically isolated from the carrier frame by means of insulating brackets. Electrical connectors and gas manifolds are provided at the downstream end of each spark chamber where access can be obtained through the large hole in the magnet once the carrier frame has been lowered into position. Three large and complex scintillator counters, each covering the effective area of the outer chambers, must be accurately positioned inside the magnet before the carrier frame is lowered. The fourth counter is then assembled above the top spark chambers. Due to the complex geometry of the whole assembly, slow bends in the strips which form the light guide system of the counters cannot be used. An alternative method which uses a perspex prism for each strip has been devised, and right angled joints may be made as well as straight joints. This method has proved successful although it is complicated to manufacture. Claims for improved efficiency of light transfer are yet to be proved conclusively.

Double Gap Sonic Spark Chambers

Fifteen double gap sonic spark chambers have been manufactured for use in Experiment 8 (page 33) which is mounted on the K15 beam line. The smallest chamber has an active foil size of 25 cm × 10 cm and the largest 220 cm × 50 cm. In design they are all similar, each single gap or half chamber consisting of two rigid rectangular aluminium alloy frames, on to one of which is stretched an aluminium earth foil. The other frame carries the high voltage composite foil of mylar and aluminium foil. The frames are spaced 1 cm apart, and the gap between them is sealed by means of a cellular neoprene 'O' ring, making an envelope to contain the helium or helium-neon mixture gas filling.

Unlike most spark chambers these do not have another membrane attached to the outer faces of the frames to equilise the pressure on the active foils. Omitting these has decreased the quantity of gas required and simplified the gas flow problems. This, coupled with an improved gas distribution system and gas tightness has reduced the time from first filling with gas to sparking by a substantial factor. Should the absence of membranes allow impurities from the atmosphere to permeate the foils, a 0·005 inch laminate of mylar and diophane may be attached to the frames, though so far this has not been necessary. Another new feature has been the method of attaching the 75 mm × 1 mm piezoelectric crystals to the sonic detector bars (described in detail in the next section). This has considerably improved the output signal compared with that obtained from parallel connection crystals mounted straight onto the backing bar.

Methods used to manufacture these sonic bar assemblies have produced lengths of mounted crystals straight to within ± 0·002 inch over 36 inches. Installing the bars in the spark chambers to the same order of accuracy has enabled spark co-ordinates to be measured to within about 0·25 mm.

Improvements in Microphone Systems for Sonic Spark Chambers

Improvements in the performance of the piezoelectric strip microphones used as detectors in sonic spark chambers have been made, thus enabling larger spark chambers of this type to be constructed.

As the dimensions of sonic spark chambers are increased the length of microphones required and the distance in gas which the sonic signal must travel are also increased. This results in a rapid attenuation of signal amplitude, and for large chambers it is therefore necessary to increase the sensitivity of the detector system. There are many problems in designing very high gain factors into the sonic amplifier and some increase in microphone sensitivity is necessary if significant improvements are to be obtained.

The strip microphones in use were constructed by mounting individual strips of PZT 5A (Brush Clevite Ltd) on a brass bar using conducting araldite and connecting the strips electrically in parallel. Although this is convenient from a manufacturing point of view and gives an extremely robust microphone, it has the disadvantage that for long microphone bars the output signal is attenuated by the loading effect of the strips that are not excited.

This attenuation effect can be overcome if the individual strips are connected electrically in series. However it is necessary in this case to ensure that stray capacitive effects along the bar do not negate the series connection; also, to minimise the noise signal, the loop produced by the series connection must be made as small as possible.

The technique adopted was to produce a basic module consisting of two series connected strips fixed to an accurately cut length of float glass with Araldite type AV 100, and to form the microphone strip by mounting the required number of such modules on a metal bar using AY111 Araldite; the modules can then be recovered after use by gently heating the metal bar. Measurements on microphones constructed using this technique indicate that the surfaces of the individual strips can be made flat and parallel to the mounting reference points of the bar to within 0·1 mm.

As a result of the series connection of strips, the microphone impedance is much higher than with the previous configuration, but results obtained with prototypes show that units having high sensitivity and acceptable impedance can be constructed using 4 mm × 3 mm × 75 mm strips of PZT 5H material. The high impedance of the microphone is an important factor influencing the design of the sonic amplifier, and a unit employing an FET device in the input stage has been designed for chambers using this type of microphone.

The initial tests were carried out on a chamber 130 cm × 70 cm having an active area such that measurements in the 130 cm plane required a microphone 50 cm long. Using the original type of microphone and a sonic amplifier having a gain of 200, the signal amplitude obtained at 120 cm distance in NeHe was 50 mV. As the level of noise in the detector system was approximately 40 mV under optimum operating conditions, discrimination was exceedingly difficult and chamber operation unreliable. When fitted with the detector system described, a twenty-fold gain in signal amplitude was obtained; the noise level did not exceed 50 mV making discrimination relatively simple. Detectors of this type have now been used successfully on chambers of up to 250 cm × 75 cm and it is planned to produce larger chambers by mid 1970.

Magnetostrictive Delay Line Read-out System for Wire Spark Chambers

A requirement arose during 1969 for the provision of this read-out system for wire spark chambers. Investigations were carried out on the following points, which were expected to affect the performance of the read-out system: delay line material and dimensions; variation of coupling between input coils and delay line; damping of acoustic pulse reflections at delay line ends. Attention has also been given to matching and pre-amplifier requirements and to multiple signal resolution.

The alloy 'V-Permendur' (49% Fe, 49% Co, 2% V) appeared to provide the most efficient magnetostrictive material that was readily available. Acceptable output signals were obtained for delay line lengths up to 1 metre from either tape 0·015 inch × 0·004 inch or wire 0·006 inch diameter. In excess of this length it was necessary to use wire of 0·004 inch or 0·006 inch diameter to minimise degradation of the output signal because of the dispersive effect that occurs when extensional mode transmission is employed. A delay line length of 4 metres is probably the maximum feasible in this mode. Attempts have also been made to utilise torsional mode transmission, which operates in a non-dispersive manner, though so far the output signal obtained has proved to be unacceptably small.

The usual form of output transducer was used consisting of a coil of 200 turns of 0·001 inch wire with a bore of 0·020 inch and length 0·020 inch, either encapsulated or former wound. In the latter the barrel thickness was not greater than 0·005 inch. The concentric bias magnet was formed from rubber bonded Barium Ferrite material, which is easily worked and exhibits good coercivity characteristics. Tight magnetic coupling with the delay line was a prime requirement. The reflected accoustic pulse was damped to a value of less than 4% of the output signal pulse amplitude by means of a simple, mechanically clamped, synthetic rubber, PTFE tape sandwich.

Because each spark chamber wire constitutes a single turn input signal coil, tight magnetic coupling with the delay line is necessary. Separation of the two had to be limited otherwise marked attenuation of the output signal occurred. Where the delay line was required to work on the HV plane of a spark chamber this juxtaposition of chamber wire and delay line required elimination of insulation voids, provision of adequate tracking distances and radiused edges.

The pre-amplifier circuit used was based on the μA 702 differential amplifier in the non-inverting configuration. The twin negative lobes of the characteristic magnetostrictive pulse were clipped, and a gain of approximately 100 provided an output pulse of 1 volt peak when the minimum obtained signal from the output transducer was applied.

A number of prototype 20 cm, 35 cm and 1·5 metre devices ("wands") have been constructed for the purpose of evaluation.

Vacuum Evaporation for Spark Chamber Production

Preliminary investigations into the use of vacuum evaporation as a means of producing spark chamber foils shows this to be a possible alternative to the stretching techniques used at present.

The initial tests were carried out using equipment made available by Edwards High Vacuum Ltd. Several samples of aluminium deposited on a 0·001 inch melinex film substrate were prepared using this equipment and aluminium films 0·00075 inch thick were easily achieved. The edge definition of the aluminium pattern obtained using a simple mask was very good and higher edge definition (if required) seems possible with more sophisticated methods. Sparking tests on the sample foils indicate that results comparable to rolled aluminium foil can be obtained, but care must be taken to remove any static from the melinex film prior to evaporation and to ensure a very clean system during the evaporation process.

To enable further tests to be carried out on larger samples, an evaporation plant capable of processing work units of up to 40 inches in size has been constructed and it is hoped to have this equipment in operation by April 1970.

Gas Recirculating Rig for use with Spark Chambers

The dimensions of spark chambers have increased rapidly in recent years and the problems and costs involved in purging and operating large arrays of such chambers have resulted in the need for a suitable gas recirculating rig to minimise purging times and gas costs.

To satisfy this demand a prototype equipment similar to that described in UCRL 18666 was manufactured for evaluation both in laboratory tests and in experimental arrays on the beam lines. The equipment used consisted of a gas pump of the diaphragm type which, in conjunction with a pressure regulator system, was capable of recirculating gas through a spark chamber assembly at flow rates of up to 20 litres/min, purification of the recirculating gas (Ne or He) being carried out using a filter system of molecular sieve material part of which was maintained at liquid nitrogen temperature. The results obtained were encouraging but it was apparent that a number of modifications were necessary before the rig could be a general utility device capable of working with minimum supervision.

A second version of this equipment incorporating the results of operational experience has been designed and is in the process of manufacture. It is hoped to install this unit on an experiment and to prove the system by mid-1970. Further units will then be produced as standard laboratory equipment.

Gas Purity Monitor System for use on Spark Chambers

Tests on gas purity monitor systems for use with spark chambers have been carried out using the device described by Pisarev and Sheshunov in JINR Report P13-4446. The sensing element used in the system is an electrical discharge cell operating in a relaxation circuit. This gives a fast response to changes in gas composition making the device suitable for use as a monitor of gas purity. The results obtained show this type of monitor to be robust and simple to operate. However, the chosen operating frequency of 40 Hz is not compatible with existing laboratory counting equipment and, at this frequency, measurement of the device characteristics was extremely difficult.

A modified version operating at 2 kHz and capable of driving a standard ratemeter (95/2134) has now been produced. In operation this unit has proved to be very stable, drifts of less than 10 Hz per day being observed, and the sensitivity to variations in gas flow being 1 Hz/litre/minute. The performance is however very much determined by the stability of the HT power supply, the unit having a sensitivity of 1·5 Hz/volt; a high stability HT supply is therefore essential.

At present work is being continued on calibration of the unit to measure the sensitivity to impurities and to assess the long term operational performance of the device.

Electroluminescent Lamps for Spark Chamber Fiducials and Data Boards

The present spark chamber fiducial marks and data boards are illuminated using low voltage filament lamps of the festoon type. The data taking rate in this system is limited by both the rise and fall time of the lamp filament and the poor light output of the lamps, requiring long exposure times of up to 1 second. To overcome these limitations, experiments on systems employing electroluminescent material for illumination have been carried out. The light output obtained from this material is dependant on the frequency and magnitude of the applied voltage and a typical set of characteristics is shown in figure 60.

The data in figure 60 is for continuously rated systems and tests have shown that, for the application required, the light output could be increased by a factor of two without any decrease in reliability by operating the material under pulsed conditions at higher than rated voltage and frequency. Figure 61 shows the increase of light output with increase of frequency and this indicates an optimum frequency in the region of 2 kHz.

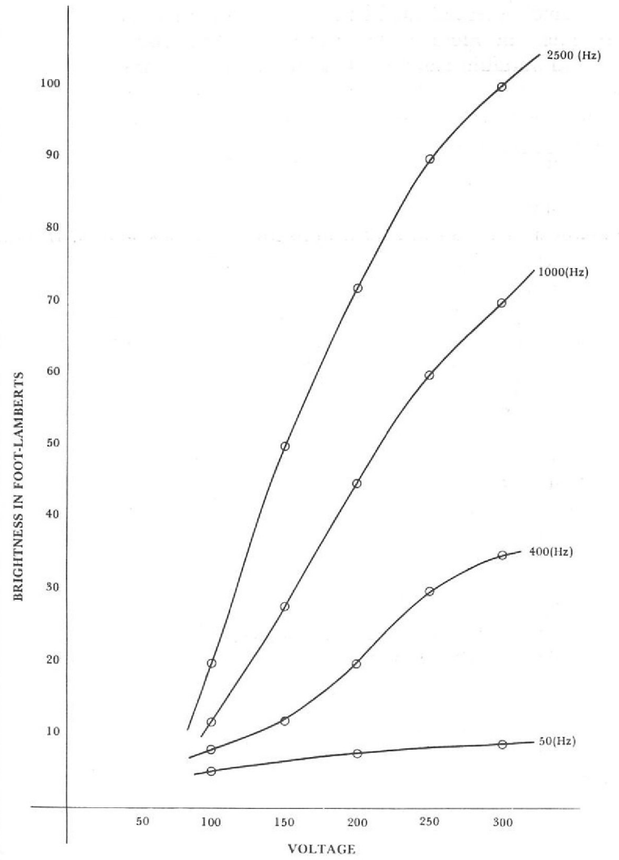

Figure 60. Characteristic curves for green ceramic lamps.

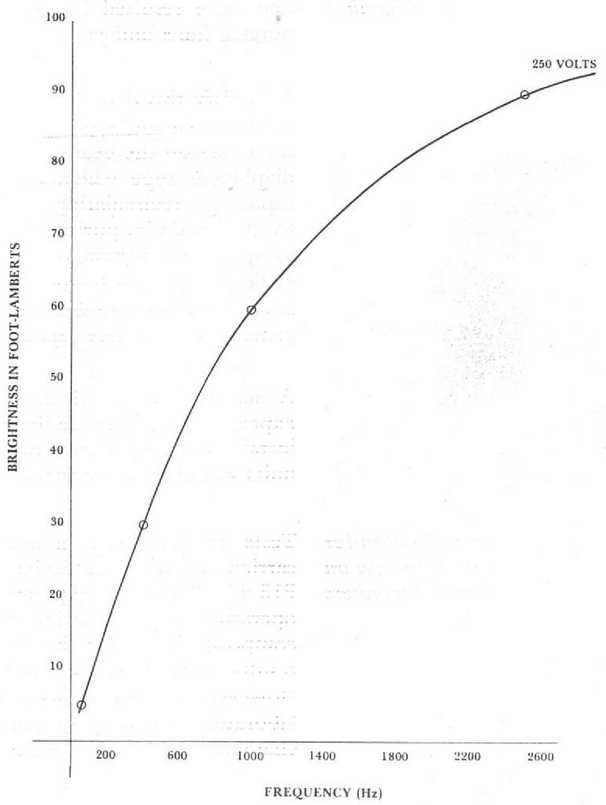

Figure 61. Increase of light output with frequency.

As a result of these tests a fiducial and data board system was constructed employing plastic encapsulated material rated continuously at 120V, 60Hz but operated under pulsed conditions at 240V, 2 kHz. Tests on this system showed the material to be reliable after several million pulses of 100 millisecond duration at a repetition rate of 2 pulses per second.

Test exposures taken on the K13 beam line gave encouraging results for exposure times of 150 milliseconds at f16 aperture using Kodak 2496 film. The edge definition obtained was extremely good and data rates of 3 events per Nimrod cycle seem possible. To date the equipment has operated with a high reliability and the only disadvantages appear to be long delivery on material and the provision of suitable power supplies.

NEUTRON COUNTERS

Neutron Counters for the C-violation in η Decay Experiment (No.16, page 42)

The purpose of the neutron counter is to detect and measure the angle of scatter of neutrons displaced from the hydrogen target. It consists of a deep ring of plastic scintillator material, the depth along the line of flight of the neutron being 12 inches. The whole ring consists of 60 scintillator counters each with its own photomultiplier. Figure 62 is a photograph of the ring looking upstream, and its location relative to the rest of the apparatus may be seen in figure 63 (page 89). These counters are placed in batches of five in twelve equi-spaced positions in a circle around the beam centreline, making in effect five rings of individual counters. Each counter is 2·5 inches thick and 12 inches wide and each is precisely placed so that its centre plane radiates from the hydrogen target. Each five counter unit is housed in an aluminium box which is supported between two lead screws so that the diameter of the circle of counters can be varied from 66 to 120 inches to an accuracy of a few thousandths of an inch. In addition, the angle of each box can be changed so that it can be aligned with the target. The whole counter assembly is mounted on an aluminium framework about 12 feet in diameter. This framework is readily movable so that the distance to the target can also be varied. By means of this arrangement of counters, a very wide range of spatial positions and flight angles can be covered.

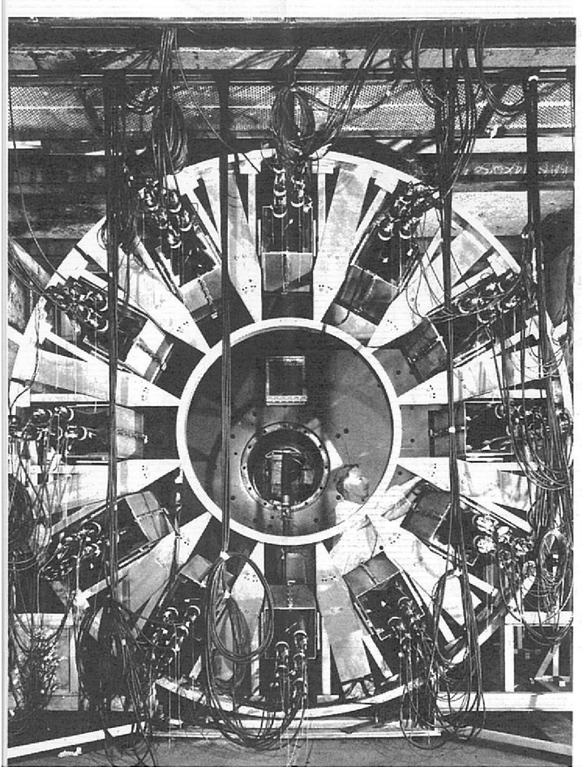

Figure 62. The ring of neutron counters used in Experiment 16.

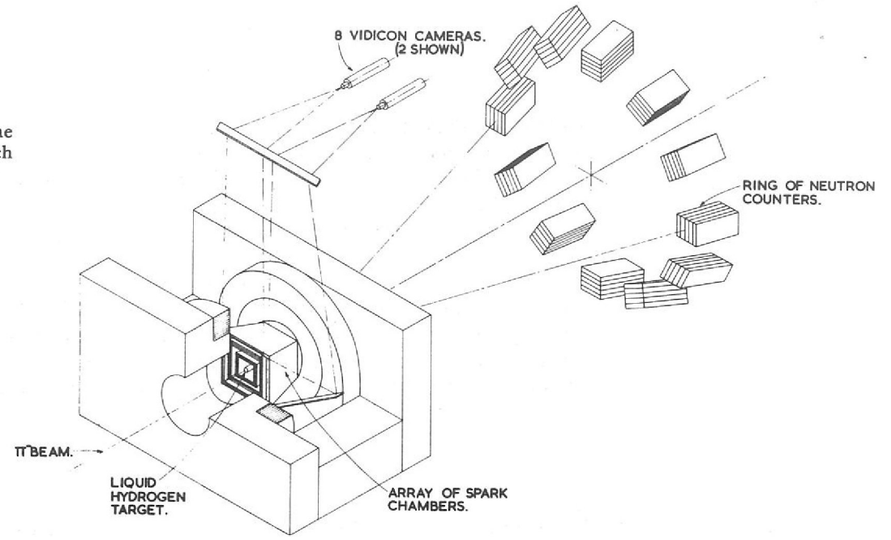

Figure 63. A diagram of the apparatus used in the search for charge asymmetry in η decay.

ELECTRONIC INSTRUMENTATION

Counter Electronics (41, 42, 231)

Most of the experiments use counter hodoscopes and the pattern of scintillator hits is transmitted to a computer. CAMAC is now generally accepted as providing a standard interface for data acquisition and there would be obvious advantages if the special class of simple hodoscope electronics were available within this standard. Such a unit has been developed to process the signals from 8 photomultipliers and to present them in a standardised form on the CAMAC dataway. Each channel includes a discriminator, a strobed gate and a data store. The inherent access to a dataway simplifies the introduction of test facilities which are included in the module. There is a more general interest in automatic testing and remote control of elements within the chain leading from the scintillator to the event trigger and final data acquisition. To fill this need, modules are under development which can be used to route pulses for light diodes and to vary photomultiplier EHT. Other modules can be used in conjunction with commercial modules to vary channel delay and attenuation.

Spark Chambers

A CAMAC unit for use with sonic spark chambers has been developed. This contains 16 channels of amplifier, discriminator and clock gate with control and test facilities.

Proportional Mode Wire Chambers

The requirements and implementation of amplifier channels for this new detector has been investigated. A sensitivity of 0·5 millivolts and a dynamic range of 100 to 1 has been chosen as a general specification and several designs have been tried. None have shown the economic breakthrough which may be necessary before the wide scale use of this detector is viable.

CAMAC Electronics (232)

CAMAC has now been accepted throughout Europe as a preferred standard method of handling the many facets of instrumentation which largely involve digital data transfer. Many modules are now available from commercial sources. In addition to the hodoscope module mentioned previously, specifications have been issued and equipment acquired based on previous COMUS experience. The principal units involved are a 50 MHz, 16 bit, 4 channel scaler, a dual 16 bit gated register and a readout and display system. The scaler and the register include a control register which can be used to control common functions such as clear and inhibit.

General Development

As always considerable effort has been devoted to the design and manufacture of special equipment. Most of this has related to the attachment of additional peripherals and data acquisition electronics to small computers. New design work is being undertaken in collaboration with the Bubble Chamber Research Group, to provide an integrated control system for precision film measuring machines.

MAGNETS FOR HEP EXPERIMENTS

M7 Spark Chamber Magnet

This large gap magnet has been commissioned during the year and is now being used in the C-violation in η decay experiment (No.16, page 42) on the $\pi 8$ beam line in Hall 3. The magnet configuration is very flexible, and it will be possible to utilise it in other experiments.

From the illustrations (figures 63 and 64) it will be seen that this is basically a C-magnet with pierced poles. These pole piece holes can be reduced from the 54 inch maximum diameter by means of a series of inserts; the gap is 40 inches, within which a magnetic field of up to 10 kilogauss can be generated. The magnet weighs 180 tons and special equipment is available to tilt and transport it.

The exciting coils, which are 9 feet in diameter, are of copper, wound with epoxy resin bonded layers of mica-glass composite tape. Prototype coils were subjected to rigorous thermal and insulation tests. The coils are energised by a static power supply rated at 3000A, 200V, with a stability of ± 0·1%.

Figure 64. The large spectrometer magnet being assembled. In the experiment a complicated system of spark chambers and a hydrogen target lie between the pole pieces of this magnet.

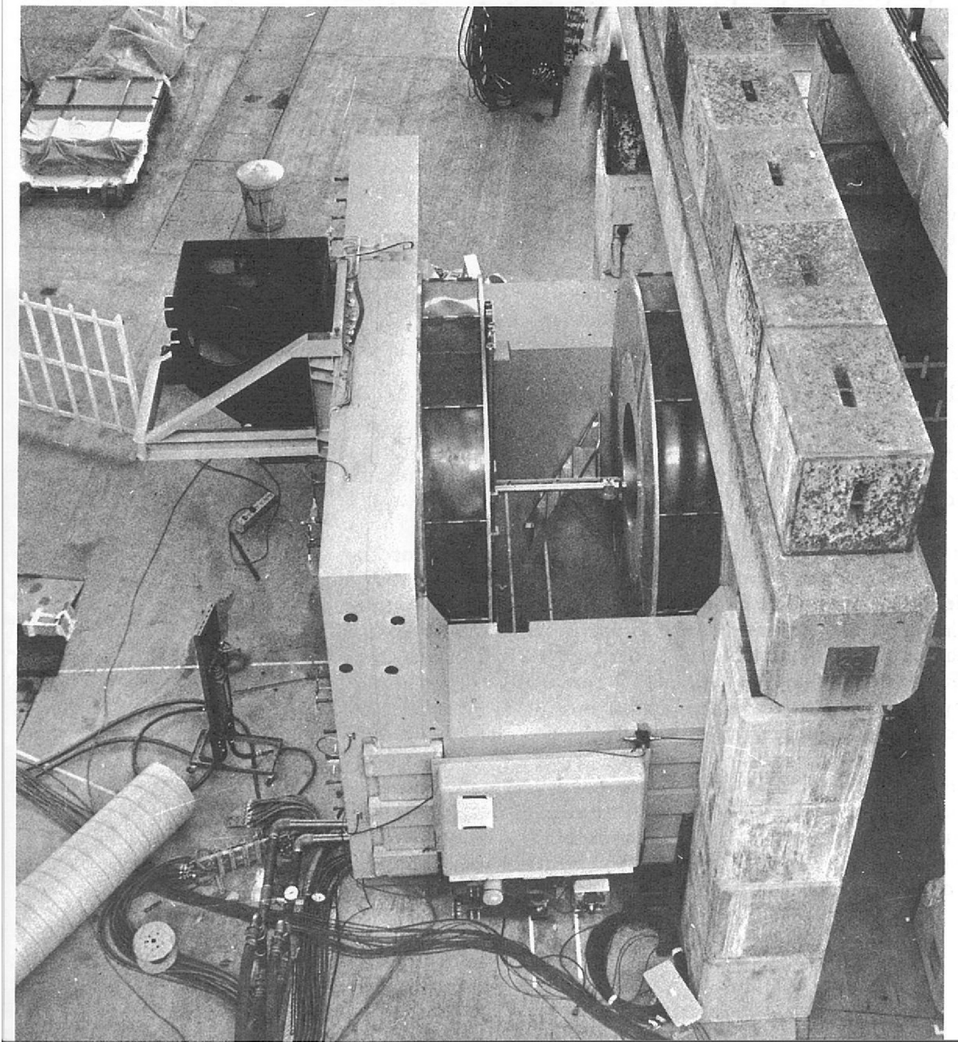

Other Experimental Magnets

Two 400 kW power supplies for use with modified (40 inch gap) M5 spectrometer magnets are at present undergoing tests. They will enable gap fields of 5-6 Kilogauss to be achieved.

A 1-2 MW supply has been ordered to enable the magnet from the Heavy Liquid Bubble Chamber (which has now been dismantled) to be used as a spark chamber magnet.

Magnetic Field Measurement

A semi-automated magnetic field survey unit (based on a Daresbury design) has been constructed to enable 3 dimensional field surveys to be carried out on large magnets such as those used for spectrometric purposes. The unit is transportable and the data output is by print-out and paper tape.

Inexpensive magneto-resistance probes have been developed to monitor (and perhaps, eventually, to control) beam line magnets. Readout is by digital voltmeter and the present accuracy (thought capable of improvement) is about 0·1%.

TARGETS FOR HEP EXPERIMENTS

Polarized Proton Targets

The polarized proton target is currently in use in a π-p experiment (No.7, see page 32), and HEP data is being taken. Preliminary analysis of the polarization recorded during the first cycle indicates proton polarization in the region of 75–80% in LMN which is a substantial increase over that measured in previous targets built at this Laboratory. This increased polarization can be attributed directly to recent improvements made to the target. The NMR system developed during the last year has now been fully tested in practice and found to operate satisfactorily. This system enables accurate measurements of polarization to be made, free from dispersive errors. A new data collecting system is virtually complete enabling data to be collected continuously from the target.

A new type of polarized proton target is under construction aimed at providing good angular access for HEP experiments. In this new system the hydrogen-rich target is first polarized under optimum conditions for polarization by the solid effect at a temperature in the 0·8°K region and a magnetic field strength of 25 kG. The target is then rapidly cooled to about 0·3°K in order to greatly reduce the rate of depolarization from spin relaxation. In this frozen state the highly uniform magnetic field used for polarization is replaced by one of lower uniformity but providing large angular access to the target. The design of the cryogenic system is well advanced and the magnet design is almost complete.

Target Materials for Polarized Proton Targets

Research on target materials has been mainly concerned with dilute solutions of porphyrexide in a butanol-water mixture and with the glycol-chromium V complex in the parent diol. Promising new results have been obtained at 3 cm wavelength using chromium V in pinacol rather than glycol. Electron spin resonance, proton polarization enhancement and relaxation time measurements have been carried out. The dependence of these quantities on the method of preparation of the complex has been studied; variation of reaction time, reaction temperature and the presence or absence of light have all been shown to have a marked effect. The results show that it should be possible to optimize the method of preparation to obtain the best ratio of polarization to proton relaxation time, with direct application to the new frozen target under construction.

Electron spin resonance equipment, operating at a wavelength of 4mm and using a superconducting magnet, has been built. This has been designed for pulse saturation measurement of the electron spin relaxation time, in addition to observation of the ESR spectrum. So far the spectra of dilute solutions of DPPH, porphyrexide and the CrV-pinacol complex have been obtained.

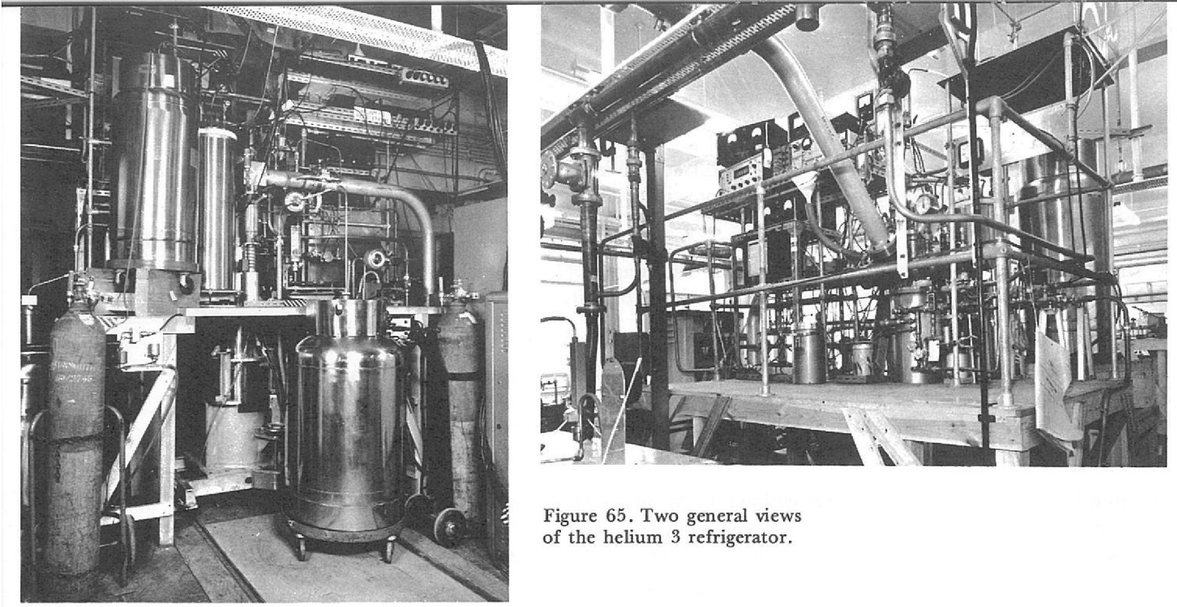

Figure 65. Two general views of the helium 3 refrigerator.

Helium-3 Refrigerator

A helium-3 refrigerator was brought into operation during the year, enabling research to be extended to the difficult temperature range below 1°K. The low temperature is obtained by evaporating liquid helium-3 at reduced pressure, the lowest temperature reached so far being 0·27°K. The refrigerator is designed to operate on a continuous basis, providing refrigeration capacities of about 1 watt at 1°K down to 50 micro watts at 0·3°K. Helium-3 gas is cooled by heat exchange with cold helium-4 gas and then condensed in a tube coil immersed in liquid helium-4 boiling at 1·5°K under reduced pressure. The liquid helium-3 is then expanded through a needle valve into the low temperature region. The evaporated helium-3 can be pumped by either a Roots pump or an oil diffusion pump; the compressed gas is returned to the refrigerator for re-liquefaction.

The low temperature region containing the specimen is at the bottom end of a long cryostat tail which can be placed within the field either of an electro-magnet, or of a 50 kilogauss superconducting magnet which has been designed and constructed for this purpose. Simultaneously the specimen can be subjected to a microwave field, the necessary power being fed to the specimen by a coaxial line or waveguide. Carbon resistors have been used to measure the low temperature.

Liquid Hydrogen Targets

Liquid hydrogen is extensively used as a target material in high energy nuclear physics experiments as it provides a dense concentration of free protons for interaction with incident particle beams. Ideally the liquid hydrogen mass, of specified length and cross section, should be positioned in space in the path of the beam, with no other material present to produce spurious interactions. In practice the liquid hydrogen is held in a double walled container, with a vacuum interspace for thermal insulation. The inner container must be designed as a pressure vessel suitable for low temperatures and the outer container as a vacuum vessel.

Liquid hydrogen has a low density compared with constructional materials so that even quite thin container walls can give rise to significant background effects. These have to be measured separately and subtracted out, and to avoid serious degradation of accuracy the background must be kept low.

Polyethylene terephthalate (melinex) film is widely used for the manufacture of liquid hydrogen container flasks, since it has a low density compared with any metal and possesses high strength at both room and liquid hydrogen temperatures together with a high elastic modulus. It can be heat formed and joined with epoxy adhesives to form thin walled vessels. These combined properties make it the most satisfactory plastic material currently available for the construction of container flasks.

In general, target flasks take the form of a closed ended cylinder, with its axis along the beam. The cylinder is produced in melinex film with an epoxy adhesed lap joint, the closing ends, also of melinex, having been heat formed to a suitable pressure vessel shape. The ends are also glued to the cylinder or metal support structure.

Recent developments have been directed toward improving the ease of manufacture and strength of flasks and the removal of extraneous material from the beam path. The end forms are produced by the 'cold punch' technique, where a melinex film is clamped in a die and heated to 160°C. An ambient temperature punch is then inserted to press the film into the correct form. This technique produces a formed end having a uniform wall thickness. Previous forming methods produced serious reduction in thickness across the pole of the section. In an effort to remove unwanted material from the path of the beam, a re-entrant beam inlet window is incorporated when ever possible, (figure 66). This window is positioned in the metal target supporting frame such that the incoming beam meets the liquid hydrogen in a position which is clear of the support material. The beam, and also side scattering particles, see only the melinex portion of the target flask. The stainless steel support is arranged to have a flanged joint to allow the flask to be constructed in two separate sub-assemblies. This feature gives a greater control of the joints during manufacture.

The vacuum vessel enclosing the flask is designed for minimum cross section (density × thickness) against the collapsing condition under external pressure. It may be required for wide angle scattering systems, when a thin walled metal cylinder is used. Under these conditions a high strength aluminium alloy (H15 WP) billet is machined to the required shape and wall thickness. The determination of the wall thickness for a given cylinder length and diameter is governed by the collapsing pressure, which is required to be at least twice the working pressure. A series of tests on typical aluminium alloy vacuum vessels has been undertaken to compare with the Southwell equations for the collapse of thin wall vessels. The results of this work have enabled the minimum permissible wall thicknesses to be calculated more accurately.

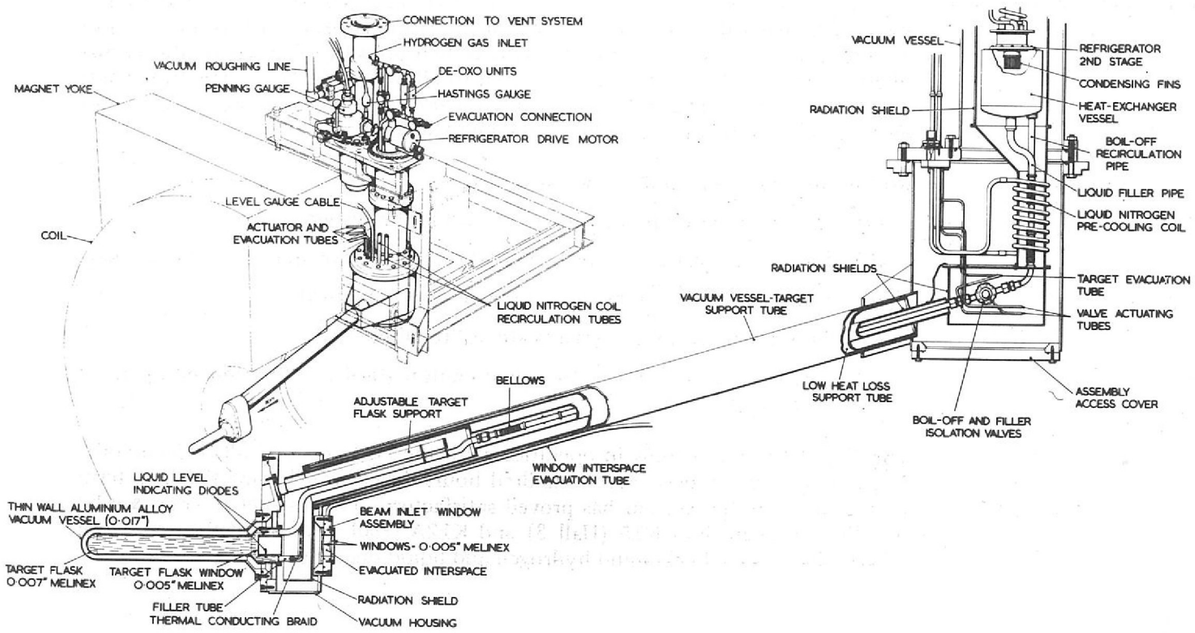

Figure 66. The type II liquid hydrogen target.

Liquid Hydrogen Condensing System

High Energy Physics experiments on Nimrod are tending to require increasing data accuracies, which leads to complex and crowded arrays of counter equipment. This confinement, when associated with a liquid hydrogen target, presents an increasing possibility of an explosion in the event of a burst target flask. This experimental trend, together with a general effort to improve safety standards, has led to the introduction of the Type II liquid hydrogen target condensing system which limits the amount of liquid hydrogen present at any time to that contained within the target flask.

A typical Type II assembly consists of a target appendage vacuum vessel enclosing the target flask, a heat exchanger and a refrigerator, all mounted on an adjustable support frame. Pipe and cable looms connect this unit to a standard vacuum pump trolley, operating panel and refrigerator compressor unit. The appendage and other hydrogen filled components are contained in a ventilated 'hyve' (see below). The target flaks, designed to suit individual experimental requirements, is suspended below a heat exchanger vessel by means of a filler and boil-off recirculation tube. The heat exchanger vessel has a volume slightly larger than the target flask, and there is provision for transferring the liquid hydrogen from the flask into the heat exchanger vessel when experimental background measurements are required. The heat exchanger is connected to a gas container, which is pre-filled with purified hydrogen to a pressure of approximately two atmospheres absolute; the gas system is then isolated to provide a closed system. A mechanical refrigerator, attached to the heat exchanger, condenses just sufficient gas to fill the target flask, so reducing the pressure of the gas system to 1·1 atmospheres absolute. Automatic control of the refrigerator maintains the system pressure and the temperature of the liquid hydrogen.

Remote operation is provided via the system's control panel situated in the experiment's Local Control Room. All valves and instrumentation for normal system operation are sited remotely and the system is interlocked in such a way that any fault condition is immediately displayed on the control panel. During routine target operations, it is unnecessary for personnel to enter the target region.

An evacuated vent system is attached to the vacuum vessel via a low pressure relief valve. This has sufficient volume to contain all the hydrogen gas resulting from a target burst and yet maintain the total system pressure at less than one atmosphere absolute. This system is introduced to allow hydrogen gas, resulting from a target burst, to be pumped out (eventually) at a controlled rate, also to maintain an external pressure on the fragile beam inlet windows.

The advantages of the Type II system are:—

(a) A minimum of liquid hydrogen is used in the system

(b) Provision is made for remove operation from a safe area

(c) Under fault conditions the hydrogen gas is contained

(d) Bulk cryogenic liquid services are not required

(e) The system is designed to operate automatically, with reduced operator servicing time.

The Type II system is now in operation with the $\pi 8$ target in Hall 3 (figure 66). It has operated for over eleven hundred hours during which time the long term performance of the system has proved satisfactory. Two further targets, will be installed in beam lines K15 (Hall 3) and K12A (Hall 1) during February 1970; K12A will be using both liquid hydrogen and liquid deuterium.

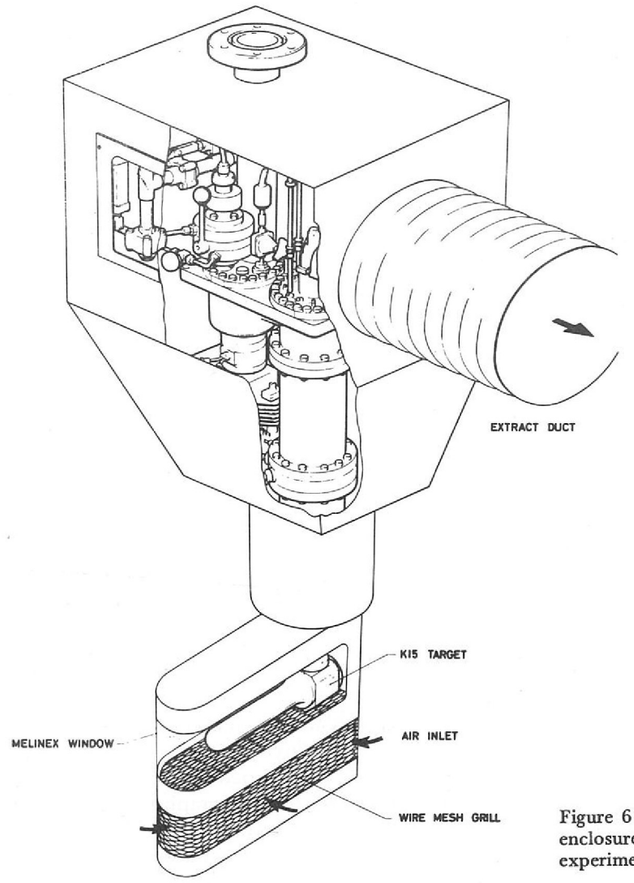

Figure 67. Hydrogen ventilated enclosure (HYVE) as fitted to experiment on K15 beam line.

Hydrogen Ventilated Enclosure (Hyve)

This device is designed to contain and remove the contents of a liquid hydrogen target in the event of a rupture. Its adoption has made it possible to dispense with pressurised containment for counter equipment near the target, which makes for greater experimental convenience and flexibility.

As mentioned in the above accounts of targets and condensing systems, the volume of liquid hydrogen is now kept to a minimum; the actual volume depends on the requirements of each individual experiment and is typically in the range 1—10 litres. The hyve is provided with a suitable catchment tray which contains mesh material with sufficient heat capacity to completely vapourise the entire target contents. A forced ventilation system rapidly dilutes the gaseous hydrogen to below the lower explosive limit.

Figure 67 is an illustration of the hyve provided for the experiment on the K15 beam line. The target (of 1 litre capacity) and its vacuum vessel are enclosed in a cowl constructed from flame retardant material. This cowl is connected via ducting and a 4000 ft^3/min fan to the roof outlet station. A tubular melinex sleeve projects down from the cowl to enclose the target appendage, the wire mesh filled containment tray being situated at the base of the sleeve. The sides of the tube above the tray are left open as air inlets. Tests were carried out in which a litre of liquid hydrogen was emptied into the container section to check on the completeness of containment and removal of hydrogen. These tests were made without the forced ventilation system operating, its efficiency being proved by subsequent smoke tests.

Liquid Level Indicator and Temperature Sensor

A new cryogenic liquid level indicator and temperature sensor, using a silicon diode as the sensitive element, has been developed and patented. The unit has been installed in three liquid hydrogen targets, and has proved highly reliable.

BUBBLE CHAMBER OPERATIONS AND DEVELOPMENT

During the year, two of the Laboratory's bubble chambers have been used in the High Energy Physics programme on Nimrod. The Heavy Liquid Chamber completed the exposure for the University College group in which a beam of 2·3 GeV/cK^+ mesons was used with a chamber filling of 43% Propane, 57% Isceon 13Bl (CF_3Br) mixture. The chamber achieved a high operating efficiency (in excess of 80%) and 336,000 pictures were obtained. The interest of the user group is now turning to exposures in the very large heavy liquid chamber "Gargamelle" at CERN and as there are no other proposals for exposures in the Laboratory's chamber, the instrument is being dismantled for storage. Its large electro-magnet will be used in a spark chamber installation.

The 1·5 m metre cryogenic bubble chamber has been engaged in several different experiments. Standard exposures have been made with hydrogen and deuterium fillings but the main area of technical development has been the collaboration with CERN on the use of track-sensitive hydrogen filled targets within the chamber, which is filled with a neon-hydrogen mixture. In the target development programme, semi-rigid perspex targets have been used, the volume being 20-30 litres. The targets are filled with pure hydrogen gas which condenses as the chamber surrounding the target is filled with liquid hydrogen/neon mixture. When the target is completely filled with liquid hydrogen, it is isolated from its control system by actuating a cryogenic valve in the supply line. The bubble chamber pressure is pulsed and the target pressure reproduces the pressure variations in the chamber as the flexible perspex walls deflect. By careful choice of the neon/hydrogen concentration and the chamber operating temperature and pressure, simultaneous sensitivity can be achieved in the target and the surrounding mixture. A photograph taken during a target development technical run is reproduced as figure 68; the neon concentration was 40%. This new technique can widen the scope of experiments that may be performed in a bubble chamber because the advantages of a pure hydrogen target can be coupled with the high γ detection efficiency in the dense neon hydrogen mixture. During 1970 it is planned to extend the technique further by filling the target with deuterium and using approx. 95 mole % Neon/Hydrogen mixture in the chamber.

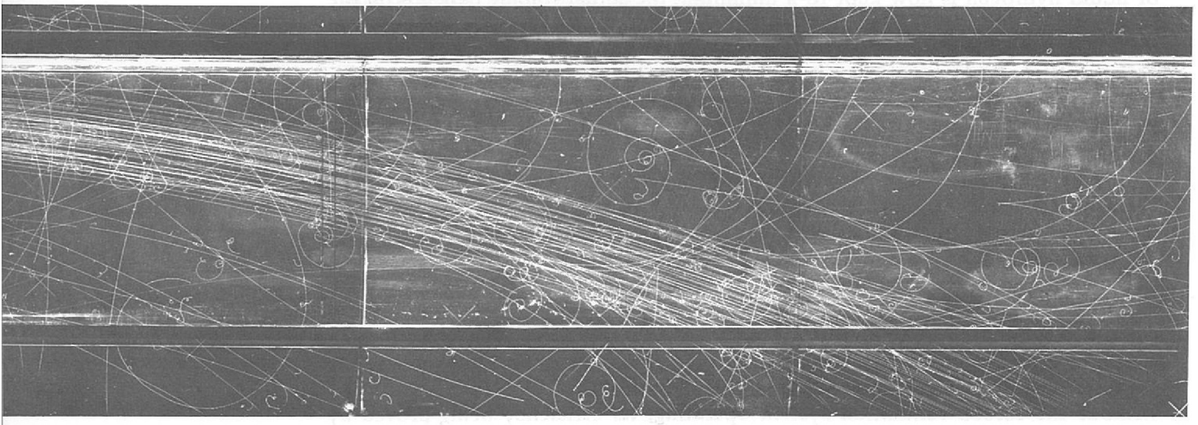

Figure 68. Bubble chamber picture taken during tests with the liquid hydrogen target installation.

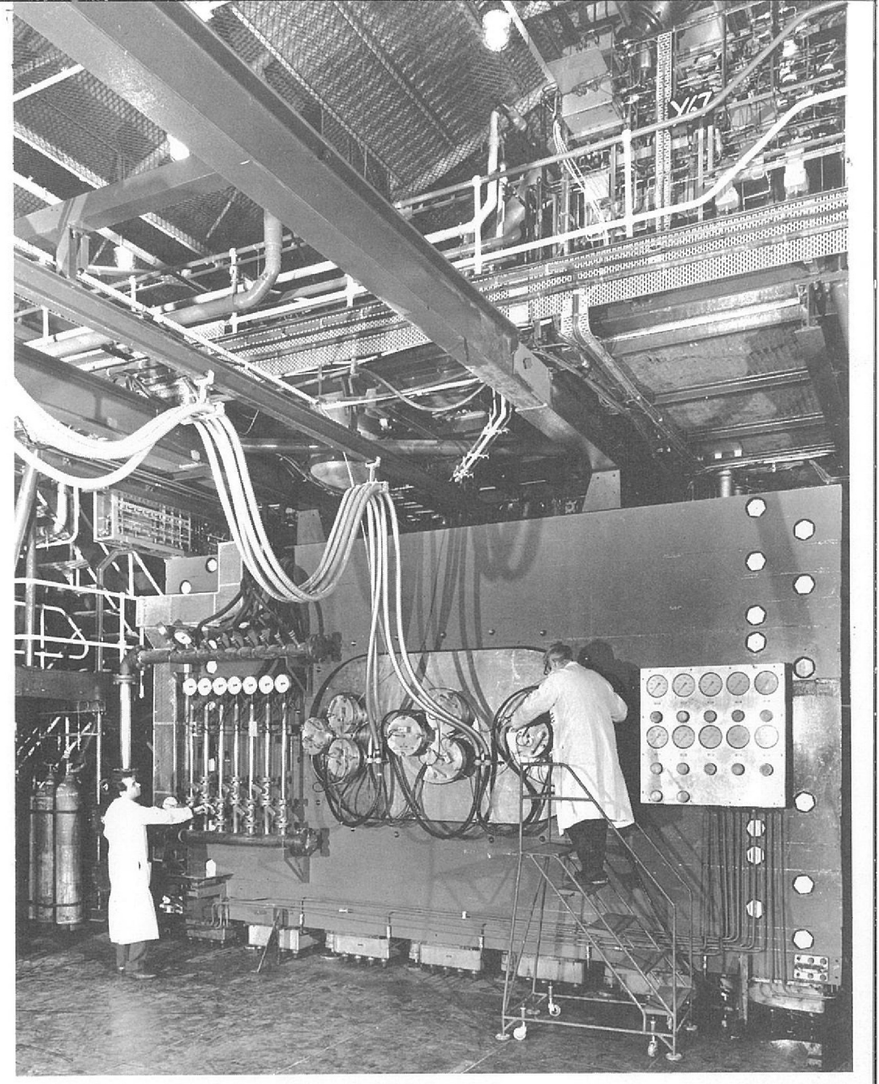

Figure 69. The 1·5 metre cryogenic bubble chamber.

Other improvements are being made to the 1·5 m chamber. A PDP 8.I computer has been obtained and this is being installed as a real-time data logging and control facility. Development is continuing in this field and it is expected that by 1970/71 much of the routine log taking and book keeping will be automatically dealt with by the computer.

A vertical beam bending magnet has been designed and is in process of installation; this will allow better trajectories to be obtained in the chamber with low momentum beams.

Work has continued through the year on the major modification to the chamber in which the present expansion system will be replaced by a hydraulically actuated multiple piston system. With this new system, which will be ready for installation in late 1970, the chamber will be able to operate in a multiple pulsing mode in which two photographs can be obtained for each Nimrod cycle. To realize the full potential of the new expansion system the illumination equipment has been completely rebuilt during the year to make it suitable for multiple pulsing.

During the year, routine data taking runs have taken place alongside the technical runs for development work on the targets. 382,000 photographs have been taken with hydrogen filling and 400,000 in deuterium. With the heavy liquid chamber run, this makes a total of 1,118,000 physics photographs taken during the year.

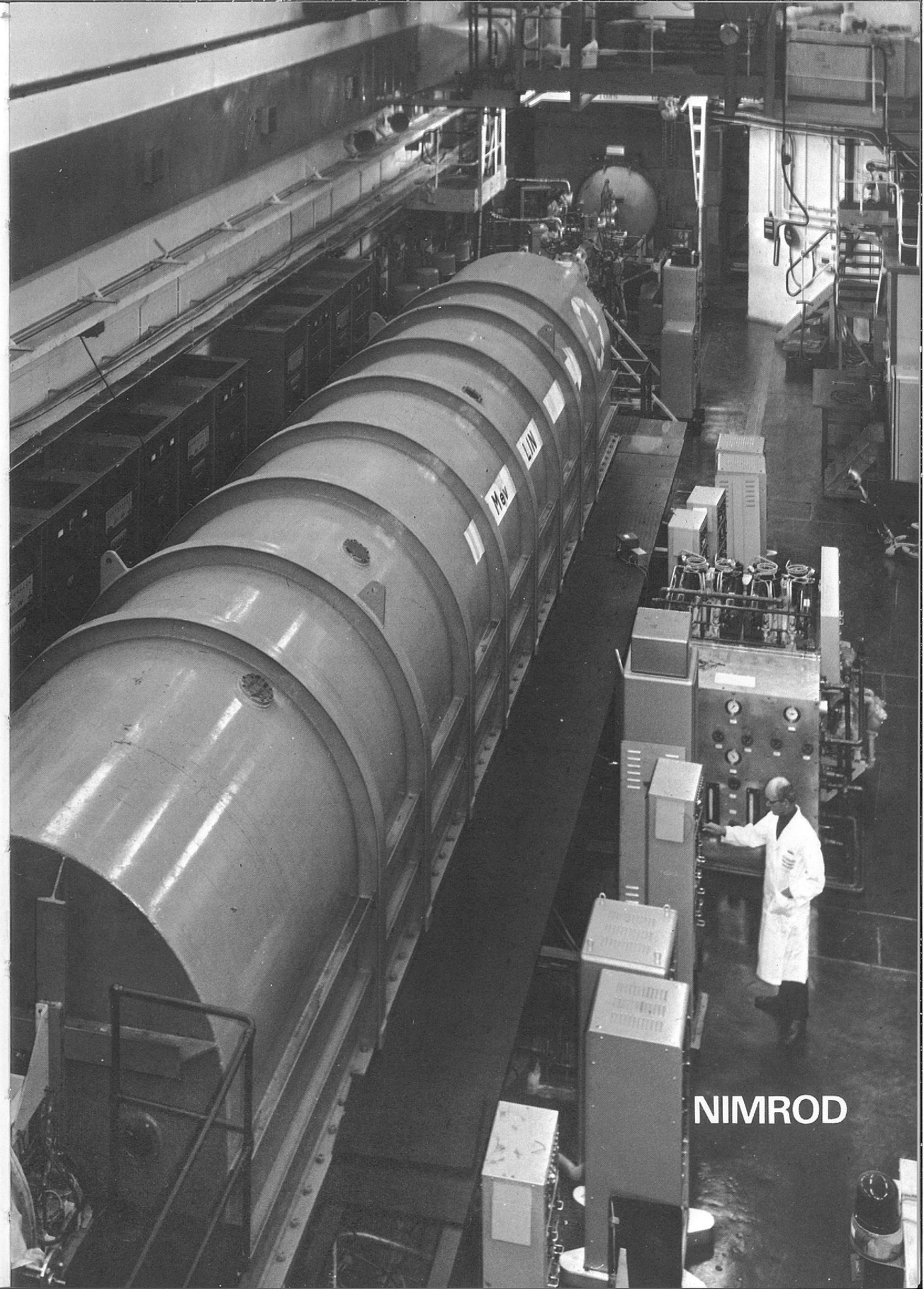
NIMROD

Nimrod

OPERATION OF NIMROD 1969

(219, 220, 221, 222)

Nimrod has operated well throughout the year. Pulse repetition rates have been between 19 and 23 ppm (generally the higher) except for one cycle which was at 10 ppm. Beam intensities of 2×10^{12} protons per pulse have been observed over long periods.

Operation has continued in a three-week cycle, nominally 404 hrs for High Energy Physics and 100 hrs for accelerator development and maintenance. Time devoted to routine maintenance has been somewhat higher this year, primarily because of requirements of swash pump replacement on the plunged extraction magnet system. These on the Mk. I mechanisms are now changed on a routine basis after about 10^6 operations (i.e. about once a month).

Extracted proton beams were run throughout the year except for one cycle (when K10S target radius requirement precluded EPB use). Switched E operation on X1/X2 was the rule and functioned very well indeed, with negligible fault trouble. This system permits the running of two separate extracted proton beams at full energy during the same machine burst. The third extracted proton beam, X3, used to service Experimental Hall No. 3, was commissioned during the middle of the year. Foil measurements on the external target have given intensities of $5{\cdot}6 \times 10^{11}$ ppp with a circulating intensity of $\sim 1{\cdot}8 \times 10^{12}$ ppp. (All Nimrod's beam being spilled onto the machine internal target).

Since X3 was commissioned the normal mode of operation of Nimrod has been

X1 every pulse
X2 with internal targetting beams 4 pulses out of 5
X3 one pulse out of 5

Nimrod's operating record is as follows. Out of the 8760 hours in the year, 2140·26 hours (24·43%) were taken up by major scheduled shutdowns and 316·82 hours (3·62%) by scheduled maintenance. 5144·57 hours (58·73%) were scheduled for HEP; beam was available for 4521·45 hours (due to 608·70 hours of faults and 14·42 hours of setting-up) and was actually utilised for 4511·63 hours. As percentages of HEP scheduled time, the available and utilised times were 87·89% and 87·70%. The remaining 1158·35 hours of 1969 (13·22%) were allocated to machine physics and development, and beam was actually available for these purposes for 831·57 hours (due to 326·78 hours of faults). The lower availability of beam during accelerator development time (71·79%) is, in the main, accounted for by the inclusion of start-up time and by special repairs, principally to plunging mechanisms.

Variation of machine efficiency throughout the year is plotted in figure 70.

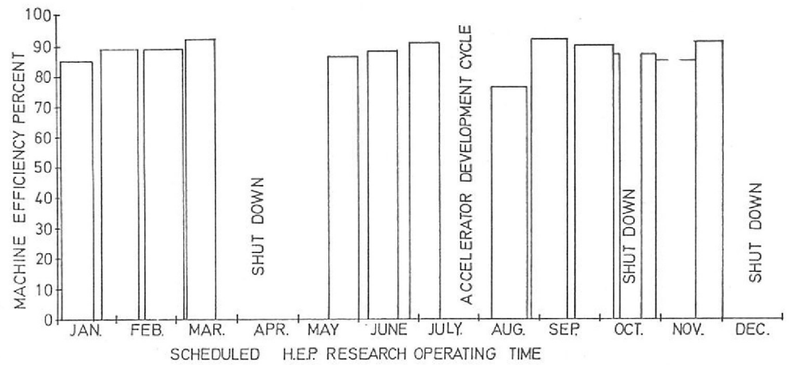

Figure 70. Nimrod efficiency during HEP research scheduled operating time, January to December 1969.

The faults causing loss of beam time have been analysed as follows

Fault Area	Lost Beam Time (hours)	% of Total Scheduled Time	% of Total Lost Beam Time
*Extraction systems	271·34	4·30‡	29·01
Injector	94·38	1·50	10·09
Targets & target mechanisms	74·55	1·18	7·97
*Vacuum	71·82	1·14	7·68
Coolants	70·74	1·12	7·56
Nimrod magnet power plant	69·07	1·10	7·38
Synchrotron r.f.	36·78	0·58	3·93
Inflector	31·43	0·50	3·36
Pole face windings	25·53	0·41	2·73
Nimrod magnet	12·61	0·21	1·35
Public electricity supply (mains dips)	12·18	0·19	1·30
Diagnostics	5·08	0·08	0·54
Beam control	0·85	0·01	0·09
Miscellaneous	47·72	0·76	5·10
†Start-up	111·40	1·77	11·91
	935·48ϕ	14·84	100·00

* Includes routine inspection time

† This is not due to equipment malfunction, but is a non-utilisable part of scheduled time just like fault time.

‡ 5·3% of scheduled EPB time.

ϕ 608·70 hours during the 5144·57 hours scheduled for HEP (i.e. 11·83%) and 326·78 hours during the 1158·35 hours scheduled for MP (i.e. 28·21%).

There were two major scheduled shut-downs during the year, the work undertaken in each being listed below.

March/May 1969 Shut-down

There were two prime objectives in this shutdown:

1. To replace an existing keyed laminated type pole rotor, in one half of the Nimrod Magnet Power Supply, with a solid pole type rotor.

2. To install and commission the two plunging mechanisms associated with Nimrod's new extracted proton beam into Hall 3.

Both these objectives were successfully completed.

December 1969 January 1970 Shut-down

The following projects were undertaken and were proceeding to schedule as the year ended.

1. Installation of a programmed 21,000A transistor regulator which forms part of the power supply for the plunged extractor magnet of the new X3 thin septum extraction system.
2. Installation of the power supply for components of the resonant extraction system.
3. Installation of thin septum scheme magnets XM9 and XHQ2 in Nimrod.

4. Improvements to the MkI plunging mechanisms in Straights 2 and 7. These are part of the XI/X2 EPB system and smoother operation was needed.
5. Injector improvements including a stand-by EHT platform alternator system, a new ion source and an improved temperature monitoring system.

Vacuum System Booster Pump Failure

Routine inspection of fault incidence on 24 inch pumping units showed that rotary pump failures were at a significantly higher rate than other faults and higher than would be expected from the type of equipment, the maintenance quality, or the running conditions; this fault was rising alarmingly.

A chemical analysis of the deposits found in the faulty rotary pumps proved them to be ferric chloride, the most probable cause of which appeared to be corrosion of the booster pump by the operating fluid 'arachlor' a chlorinated diphenyl. A booster pump was dismantled and showed considerable corrosion and lumpy deposits of iron and chloride, and it was decided to clean out all the booster pumps thoroughly and replace the operating fluid with 'Apiezon G', a straight hydrocarbon oil; tests using the new fluid proved satisfactory. No evidence is available yet to show if these measures will successfully eliminate the high incidence of rotary pump failure.

Radiation Dosimetry

Hydrogen pressure dosimeters have continued to be used for measuring the radiation dose received by the Nimrod vacuum vessels which, being of epoxy-glass construction, are susceptible to radiation damage. There have been no significant changes to the pattern recorded previously, the highest dosages being of order 200 megarad in the region of Octants 7, 8 and 1. These doses have been produced by the acceleration of about $3{\cdot}5 \times 10^{19}$ protons.

The radiation dose to the coil clamping pressure bags has also been estimated; the mean dose since start-up is less than 15 megarad.

NIMROD MAIN RING MAGNET POWER SUPPLIES AND ANCILLARY PLANT

During 1969, the magnet has been pulsed from the complete magnet power supply with the exception of the three-week period from mid-September when the magnet was energised by half the power supply only.

The mercury arc convertor plant has continued to perform very well with a very low arc back rate of 1 in about 350 hrs for the whole installation.

Early Operational Experience with the First Solid Pole Alternator Rotor

During the April/May shutdown No. 1 alternator laminated pole rotor was removed and the new design of solid pole rotor was installed in its place. This has poles which are forged integrally with the body, and was mentioned and illustrated in the 1968 Annual Report.

There was some doubt as to whether the characteristics of the system using one solid and one keyed rotor would permit the same range of pulsing modes as were possible with two keyed rotors.

It has been found, however, that the solid pole rotor machine operates extremely well in conjunction with the laminated pole machine when the two shaft systems are solidly coupled. This, however, is not a very desirable operating mode and it has also been found possible to operate the two dissimilar machines in electrical parallel and with separate shaft systems. There is a longer interchange of power between the two machines when pulsing compared with that experienced with machines having similar rotors. This, of course, was expected, but it was necessary to carry out a series of tests to determine whether the increase in power interchange between the two machines remained at an acceptable level.

The pole shoe temperature of the solid pole rotor at the end of a 12-hour duration, full thermal loading 7 GeV pulsing period was 50°C. Vibration levels on bearing pedestals did not exceed 0·001 inches peak to peak, shaft eccentricity levels were low and, in general, the operation of the solid pole rotor machine at this early stage looks promising.

In April one of the two 30 ton flywheel assemblies was removed, dismantled, inspected and several minor improvements made to the shaft to flywheel disc keying arrangements.

High Speed Electronic Analogue Wattmeters (230)

The power interchange measurements mentioned above were made possible by the use of specially developed high speed electronic analogue wattmeters feeding into a data logger and the information then processed by computer.

These wattmeters were first mentioned in the 1968 Annual Report, and a provisional patent specification was filed in May 1969. The equipment was demonstrated at the 24th Annual Electronics, Instruments, Controls and Components Exhibition and Convention, Manchester, in September 1969.

Spares Policy — Nimrod Magnet Power Supply Rotating Plant

In order to ensure operation of Nimrod at full repetition rate it has been decided to order the following additional plant.

Spare 5,100 HP Drive Motor Although these motors have given excellent trouble-free service since being commissioned, it would not be abnormal for a serious fault to develop within the next six years. It has therefore been decided to order a special motor with certain design changes to enable it to operate at either of the existing locations.

A second solid pole rotor for the 42 MVA alternator This is considered to be mechanically superior to the keyed pole form of construction and, as mentioned above, the early operating experience of one of these rotors is very encouraging. A second solid pole rotor has therefore been ordered and when this is received the power plant can again operate with two similar machines with similar inertias and synchronous machine quantities, thus load sharing should then be much improved.

A spare stator for the 42 MVA alternators Since rotor breakdowns can cause major damage to stators, quite apart from genuine stator faults, and since rewinding time takes nearly one year, it has now been decided to order a spare stator.

Two new flywheel assemblies The existing flywheels have shafts keyed to the flywheel discs. Fretting inevitably occurs in this form of construction. Should a flaw be suspected at any time on a flywheel assembly it is possible – even probable – that pulsing would have to cease until replacements of these 30 ton assemblies could be obtained. This delivery period could be as long as two years and this risk, even if a remote one, is not acceptable. Two new flywheel assemblies, have therefore been ordered and in the new design fretting problems will be very much reduced.

Pole Movement on No. 2 Laminated and Keyed Alternator Rotor

During a routine inspection in September it was noticed that five poles on No. 2 alternator rotor had moved axially along the forging; in the case of one pole the movement was about $\frac{5}{8}$ inch. This rotor was removed and replaced by a similar spare rotor. This kept half the power supply out of action for 3 weeks and during this period Nimrod was pulsed at only 10 ppm.

It is believed that the movement occurred because the keying techniques used during the last rebuild of this particular rotor were changed. The change was made in order to achieve a rapid return to service. However, other possible causes exist.

Since a second solid pole rotor is scheduled for delivery in December 1970, only minimum repairs will be made to No. 2 laminated rotor. The latter is due to be returned to site in February 1970, and it will be retained as a low grade spare unit.

Alternator Rotor Vee Coil Support Bolt Design

During this year the new Vee coil support bolts have been subjected to a detailed assessment using conventional fatigue testing techniques on a specially developed rig and photoelastic tests on three dimensional, twice full size models of the bolts using the frozen stress technique.

The results of these tests not only confirmed the superiority of the new design, but also indicated that a worthwhile gain is made by using vacuum melted rather than air melted steel. Vacuum melted steel has therefore become standard for these components on the Nimrod power plant.

When examining the Vee coil support bolts after the pole movement mentioned earlier, it was found that fretting had occurred on the shank of the Vee coil support bolts due to relative movement between the bolt and the glass insulation bonded to it. This tendency has been found to exist on the second laminated pole rotor and efforts are being made to eliminate this problem which will shorten the fatigue life of the bolts. It appears that if a layer of 'Adiprene' is applied to the bolt shank, followed by the glass insulation, the effect may be overcome.

Mercury Arc Convertor Plant Control Systems

A start has been made in equipping of the A1 convertor plant with the modified grid control units which permit access to the grid control circuitry when the plant is operational. A number of other modifications have been made to the control systems to give greater freedom from arc through faults. Adjustments and certain changes have been made to the convertor plant and the master timer to enable operation at 6 GeV with long flat tops of 3 seconds duration to be achieved.

Static Ripple Filter System

A static ripple filter system has been developed and installed to give a much greater ripple reduction than that which is obtained with the existing dynamic ripple filter. With the new system the dynamic ripple filter operates during the current rise period of the magnet pulse, but it is switched out during flat top and replaced by the static filter.

The system is greatly complicated by using the existing ripple filter chokes for both dynamic and static operation. However, acceptance of this complication gives very great financial gain. Early experience ot the new ripple filter system shows it to be a great improvement on the older system, the ripple reduction at 1200 Hz, for example, being ten times greater than that previously obtained. Some difficulties have been experienced with the switching arrangements associated with the new system, but developments are in progress which should overcome these early in 1970.

Ancillary Plant

Demineralised/Raw Water Heat Exchangers for Magnet and Experimental Areas Two of the eight heat exchangers were examined in April and both shells were found to be deeply pitted – in places to half the shell thickness. In addition, one of the tube rests was so badly corroded that a complete rebuild at the manufacturer's works was required. The shells were treated with an epoxy resin paint and returned to service. A complete new heat exchanger has been ordered and a programme of heat exchanger examination has been arranged for December.

New 100 ton Worthington Chiller This new chiller unit has been ordered and installation is due to commence early in 1970. A second chilled chromate water pump has been delivered and installation is scheduled for December.

Electrical Layout and Instrumentation An extensive programme of work has been commenced during the year on: modifications to the electrical distribution systems to facilitate the overhaul of more items of plant during normal operational periods; making changes and/or additions to a variety of control and/or instrumentation systems to achieve greater reliability and significant economy in operation; and the provision of a 40 channel alarm annunciation system to be installed in the Magnet Power Plant Control Room to provide warnings of abnormal operating conditions on important plant parameters.

Hall 3 Demineralised Water System This is not yet satisfactory and, indeed, is not yet handed over; it has nevertheless recently been placed in partial operation for reliability trials.

GENERAL ACCELERATOR DEVELOPMENT

Circulating Beam Monitoring

Because of the planned removal of the beam induction electrodes from Nimrod Straight 3 during 1970, a further set of induction electrodes has been constructed and installed in Straight 6. Field effect transistor head units have been built, and a temporary system of amplifiers was installed in order that the overall system could be checked as far as the Main Control Room. This has proved satisfactory.

A final system of amplifiers has now been built and will be installed early in 1970. This provides remote switching of the amplifiers from the Main Control Room in order that a wide range of beam intensity can be covered. The overall bandwidth of the system is 80 MHz, and it provides r.f. signals from the individual electrodes, the sum of these two, and also their difference. The range of beam intensity covered is from 1×10^{10} to 6×10^{13} particles per pulse.

Studies on Window-Frame Bending Magnets for 300 GeV Accelerator

Magnetic field calculations to find suitable cross-sections for iron-yoked window-frame synchrotron bending magnets have been made using the computer programme TRIM. The magnet specifications were decided by the Magnet Study Group for the European 300 GeV accelerator. More recent work has been concerned with magnets for a "missing magnet" lattice.

Insulated Target Monitors

As an aid to the setting up of target sharing arrangements, work is continuing on the insulated target monitoring system. The beam, on hitting the target, causes the ejection of secondary electrons, leaving the target with a net positive charge. The target is electrically insulated and the measured signal is an indication of the amount of beam hitting the target.

The majority of tests carried out so far have been with internal copper targets, giving large easy-to-measure signals with good linearity and reproducability. Suitable electronics is under construction with a view to having a computer controlled display system giving pulse by pulse indication of percentage beam on each operational target. Design work is also being carried out on flexible coupling leads for azimuthally and radially varying target mechanisms.

Rapid Cycling Booster

A study has been made of a rapid cycling 250 MeV booster synchrotron to provide increased intensity for Nimrod; a possible location is in Hall 2.

The basic idea is to inject four successive booster bunches per Nimrod cycle with the bunches synchronised and matched to Nimrod. In particular this requires accurate control of the Nimrod guide field over an extended injection platform and the use of large aperture beam transport elements for matching into Nimrod. A preliminary design has been evolved for a 10 Hz booster. The choice of a final booster energy of 250 MeV was made following consideration of injection and matching into Nimrod and injection and space charge effects in the booster. It has

not, however, been found possible in the space available to achieve a practical design for the booster – Nimrod beam transport. The conclusion is that Hall 2 is probably not a suitable site. The straight sections available for injecting into Nimrod are on the opposite side of the magnet hall from Hall 2, and the natural site for a booster is on the side of the 15 MeV linac away from Hall 2. This possibility will be explored next. The problem of the regulation of the Nimrod field is being studied.

Power Supplies For Control of n Correction Currents

These were designed for the control of n correction currents throughout acceleration and slow ejection through the 2/3 resonance and median plane currents at low fields. An arrangement comprising ten 8 kW thyristor inverters with control electronics and Brentford d.c. supplies were constructed, installed and tested during the first half of the year. The inverters operate at 500 Hz, handling currents of up to 70 A each. Control at higher frequencies is provided by low current transistor banks, each a.c. coupled to its respective load, thus combining the efficiency of the inverters with the fast response of the transistor banks. Transistor dissipation is low and these components are well protected. The system is compatible with the present low field n supplies and the changeover can be effected by means of moveable links on a patching panel. Commissioning measurements have shown that beam intensity with the new supplies is comparable with that obtained with the present low field supplies. Beam intensity is somewhat less stable from pulse to pulse due, it is thought, to some low amplitude ripple in the controlled current. Modifications to the feedback loop show that a considerable reduction in ripple is feasible at the price of a tolerable reduction in bandwidth of the feedback loops, and further tests indicate that improved operation can be obtained if the Brentford d.c. supplies are pulsed linearly from a low voltage (at injection) sufficient for low field n currents to a high voltage at extraction for the high field n current. Work is in progress to control the Brentford supplies from an external control function derived via a chopper isolator in the reference circuit of the Brentford control loop.

Time Structure Analyser

Electronic circuits have been developed for use on the PS at CERN and on Nimrod for displaying, as a histogram, the distribution of time intervals in a train of pulses which, although ideally random, may have unwanted structure. In such a display random pulses would produce a portion of the Poisson distribution depending on the range of the device. Structure would appear as a periodic component in the histogram. Such a display is commonly derived from a time-to-amplitude converter via a pulse amplitude analyzer. However, both these devices have dead times of several microseconds; data is thus lost and the time to accummulate significant amounts lengthened. In the new device the time intervals are measured using a 100 MHz clock, thus giving a resolution of 10 ns. Three counters are employed cyclically, each counting, reading-out and re-setting in turn. A 256 channel Bin Store is loaded with the read-out counts thus covering a range of approximately 2·5 μs at 10 ns/channel. The Bin Store outputs are in the form of analogue voltages proportional to the number of counts received by the respective bins. The voltages are transmitted via a multiplex switch to an oscilloscope displaying the histogram. The circuits employ high speed emitter coupled logic elements capable of operation up to clock frequencies of 300 MHz. The circuit cards will fit into a single CAMAC crate employing the Dataway to link the Bin Store cards with the counter and decoder circuits. With minor modification to the input circuits the device can be operated with independent start and stop inputs. Further modification of the counters would permit operation at the maximum clock frequency and a resolution of 3 ns.

Slow Spill

The slow spill noise servo has been modified by the addition of a re-designed function generator and noise source input circuit, using field effect transistor switches and integrated circuit operational amplifiers to generate the required function from the beam intensity signal. As a result the slow spill is more stable and less dependent on the varying conditions of fast spill which precedes the slow spill.

To provide a facility for the rapid measurement of spill duty factor by experimental teams, a 2000 series module has been developed. This accepts an input of Type 3 pulses from beam line monitors and develops a voltage proportional to effective spill time which is updated after every slow spill burst. Two prototype modules have been completed and are being evaluated by beam users.

Pole Face Winding Current Monitors

Differential amplifiers linking the n sheet current shunts to analogue-to-digital converters have been provided for use with the X3 computer monitoring system. The amplifier outputs will be made available in the Main Control Room to provide better monitoring facilities than those at present in use for the n and median plane currents.

Induction Electrodes

An improved system has been installed in Straight 6 and tested satisfactorily. This will shortly be put into use with the machine and will replace the existing system in Straight 3, so that this latter box will be freed for use by resonant extraction equipment.

DEVELOPMENT OF EXTERNAL PROTON BEAMS

X3 Commissioning

Nimrod's third external proton beam (EPB), X3, was commissioned with noteworthy success during July 1969. A flux comparable with X2 was achieved – about 5×10^{11} protons per pulse at the external target, corresponding to an average 28% overall extraction efficiency. The beam is exceptionally stable.

As may be seen in figure 56, X3 is the only source of primary particles for the new experimental area, Hall 3. Initial exploitation is by the two secondary beams π8, and K15, which work at production angles of 6·5° (achieved using the new septum magnets, M8, M9 and M10). Later, X3 may be extended and re-focussed on to a second external target to serve further secondary beams.

In its present form, X3 is a chromatically-corrected energy-loss system, similar to the earlier beams, X1 and X2. During 1970, it will be used to test two new schemes: "thin-septum" energy-loss, and resonant extraction. Both are aimed at achieving greater proton fluxes.

The present extraction components consist of an energy-loss target (22·5 millimeters of beryllium) located 14° into Octant 5, a plunged extractor magnet (XM) in Straight 4, and a plunged correction quadrupole (XQ) in Straight 1. The plunging systems are the new Mark II mechanisms. The Straight 1 vacuum box was re-built to accommodate XQ as well as the 15 MeV inflector.

As in the case for X1 and X2, protons are turned parallel to the beam axis by a quadrupole multiplet located just outside Nimrod's vacuum header tank, and are re-focussed by a similar multiplet 2·5 m in front of the external target in Hall 3. The chief feature of X3 is the long parallel beam drift length between multiplets – about 50 m.

Tuning devices such as ray-tracing collimators, scintillating probes and wire-scanning chambers were incorporated into the X3 design from the early planning stages, and led to rapid and successful commissioning. A more striking feature was the employment of computer control techniques *ab initio*, using a PDP8 computer, for scanning, monitoring and logging, see page 110. As far as we are aware, this is the first occasion on which computer control has been used for beam commissioning as opposed to routine operation. In conjunction with the new EPB monitoring system described below, the technique proved to be very successful.

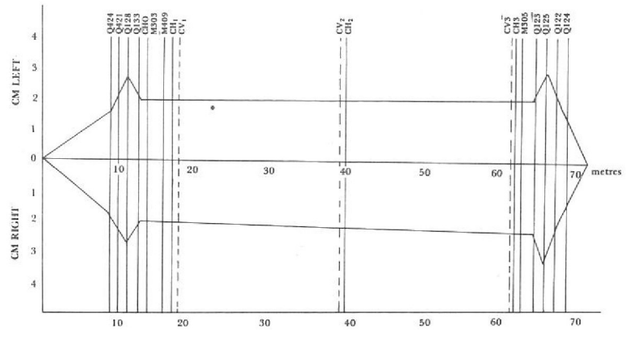

Figure 71. X3 ray traces in horizontal plane.

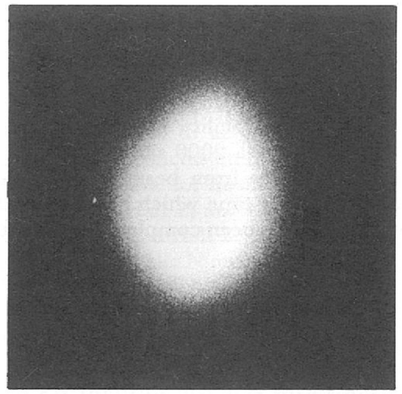

Figure 72. Film trace of the beam upstream of the external target.

Measured beam properties are illustrated in figures 71-74. The interpretation of ray-traces in the horizontal plane is shown in figure 71: the rays differ from the computed trajectories by displacements less than 2·5 mm at the end of the 50 m drift length. Figure 72 is a film trace of the beam upstream of the external target, and figures 73, 74 are scans carried out at the mid-target focus using a 0·1 mm diameter wire. They show that the beam is focussed within a 4 mm diameter spot, with half-height widths of 1·5 mm horizontally and 2·15 mm vertically.

In the final stages of commissioning, beam sharing conditions were established in good agreement with calculation. In particular, it was verified that a selected percentage of beam could be delivered in fast spill to either X1 or X2, followed by slow spill down X3 (this is a complex manoeuvre since it involves programming two sets of plunging magnets). It may be accomplished with zero net loss in efficiency. Alternatively, selected pulses may be delivered to whichever EPB is required, and sharing ratios with internal target users may also be programmed.

EPB Diagnostics Extensive use of external beams in such complex sharing programmes has necessitated development of a new centralized EPB monitoring system: this was installed during the summer shutdown and used for X3 commissioning. The system, illustrated schematically in figure 75, operates automatically under control of the main machine programming unit. Signals from EPB devices, such as the Secondary Emission Chamber flux monitors (SEC's) are processed by the Monitoring Unit which converts them to digital form and subtracts the effects of zero error and drift in their head amplifiers. The signals are gated by the Timing Unit and fed out to the secondary beam users, to the Main Control Room display, and to the computer interface.

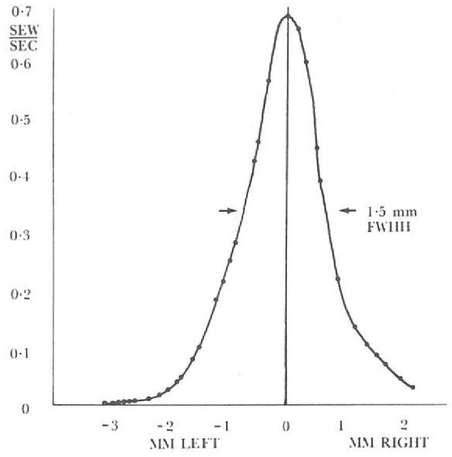

Figure 73. Horizontal wire scan at X3 external target.

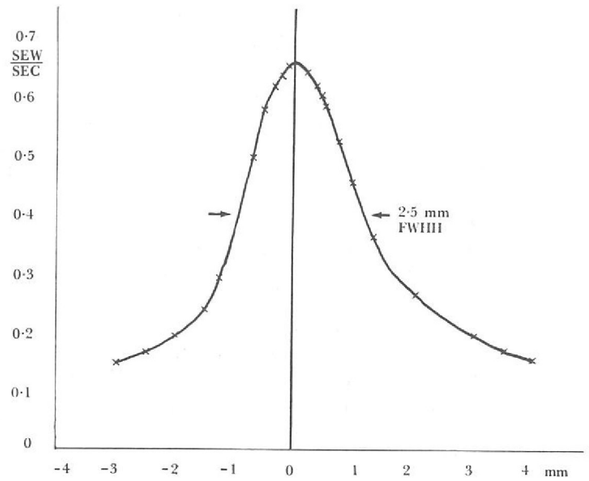

Figure 74. Vertical wire scan at X3 external target.

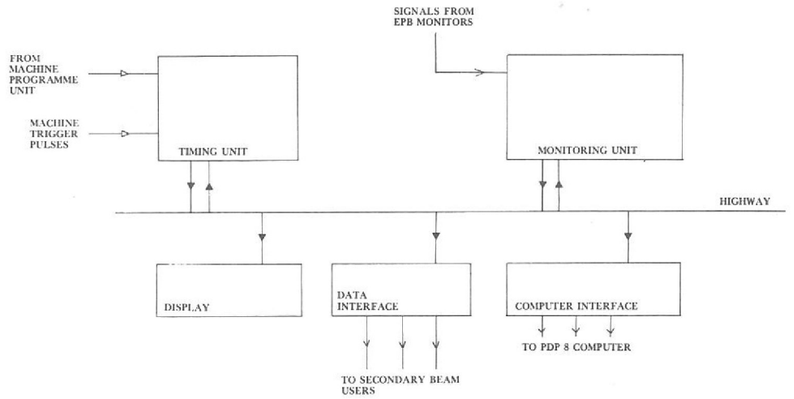

Figure 75. Schematic diagram of the EPB monitoring system.

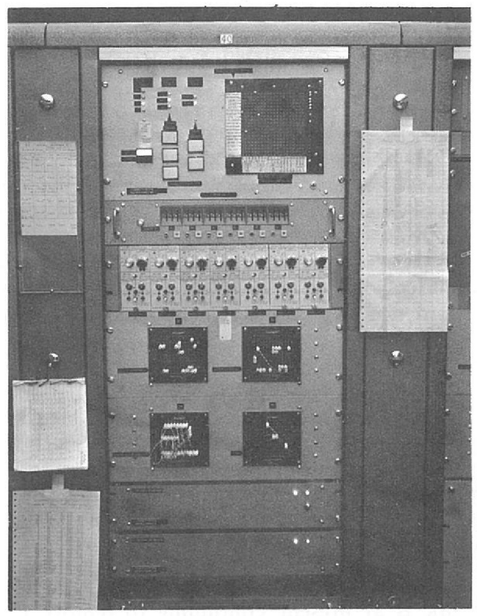

Figure 76. General view of the Timing Unit and Part of the Inter-rack Highway.

The system is modular, and all interconnections are made via a 96-channel inter-rack highway: most of the signals may be patched out readily for 'scope display. Figure 76 is a general view of the Timing Unit and part of the Inter-rack Highway.

The SEC flux monitors are now extremely reliable both in terms of long-term stability and linear response, as evidenced by calibration against aluminium foil exposures. Their amplifiers have been adjusted to give a digital output reading directly in protons $\times 10^{-8}$.

New Extraction Methods – Thin-Septum and Resonant Schemes (107, 225)

Design of the thin-septum and resonant extraction systems, (see 1968 Annual Report), was completed during 1969. Some of the hardware is already available and the remainder is on order. It is hoped that enough should be ready for installation during the December 1969-January 1970 shutdown to enable the main features of the thin-septum scheme to be studied. This system uses an energy-loss target at the end of Octant 4, a 1 cm septum magnet in Straight 4, and powered shims in the Octant 5 header vessel; it dispenses with the correction quadrupole (XQ) used in the existing EPB's.

The resonant system is to be tested later in 1970. In this method of extraction the beam is guided onto resonance by programming particular Nimrod poleface windings, the power supplies of which have been modified to reduce current ripple to about 1% of the predicted operating currents.

X3 COMPUTER CONTROL SYSTEM

(236) During 1969, the first stage of the computer control/monitoring system for the X3 beam line was completed and commissioned.

Hardware The completion and commissioning of the data transmission system (STAR), the magnet interface unit providing monitoring and control functions, a scaler acquisition system, interface and drive unit for an output typewriter (IBM) and the numerous small units (test boxes etc.) that are associated with such a system.

Software (119, 215) Virtually the whole of the basic computer software for driving the X3 system was written during the first six months of the year. The basic PDP8 computer was augmented during this period by a high speed reader/punch and a 32 K disk which both speeded up the software development and allowed a much more sophisticated approach to be adopted.

The work outlined above allowed magnet currents to be set or varied over a range of values (scanned), deviations of magnet currents from set values to be printed out, standardised logs to be obtained and various simple experiments to be run automatically. The experiments involved scanning a parameter of the extraction system while recording other parameters, performing a measure of data reduction and printing out the results in a standardised tabular form. These facilities undoubtedly helped in the speedy commissioning of the X3 beam line. Much valuable experience was gained in the field of computer control of equipment and in operator/machine interaction.

The major shortcomings of the system were that insufficient core space in the computer prevented on-line plotting of the results; many of the system subroutines and nearly all of the user programs had also to be restricted. Similarly the scope of the work was limited by the fact that not all of the magnet power supplies and none of the collimators were computer controlled. The output facilities were also very primitive.

Work is at present continuing to remove these shortcomings. The addition of another disk and a further 4 K of core store have removed the computer store restriction, but have necessitated a large amount of re-programming, which will, however, greatly improve the software and versatility of the system. A CRT display has been obtained to improve the communication between operator and computer. At the same time, to prepare for the next stage of the X3 system, a considerable extension to the STAR system, further interface units, scalers and numeric display units are in the process of completion and are due to be commissioned about the end of this year. The users of the system, in particular the Nimrod operators, have experienced little difficulty in adapting to the new control techniques.

Collimators Each jaw of the 7 collimators in X3 has been fitted with a digitizer providing a continuous digital readout of position; the jaws are driven by ordinary a.c. motors (not stepping motors). An interface unit has been designed and constructed to buffer the input settings and position readouts between collimator and computer. Any overshoot of the final position is corrected by the interface before instructing the computer that the required setting has been achieved. Both jaws of a particular collimator may be controlled simultaneously. A control panel enables the operator to monitor the computer operations and to override them if necessary.

Following the success of X3 computer control, a study is in progress to examine the benefits and costs involved in computer control of the K9 separated beam.

EXTRACTED PROTON BEAM COMPONENTS

MkI Plunging Mechanisms

This original design of plunging mechanism is still in use in two positions on Nimrod, despite the undesirable features that have been mentioned in previous Reports. Most of these are due to shortcomings in the swash pumps, which are now replaced every 4-6 weeks. Detailed modifications to extend the period between overhauls have been made. Other improvements include the use of flexible oil pipes to reduce vibration, modifications to the undercarriage wheels to reduce wear and the provision of ram pressure measurement. The control loop system has been converted to the MkII design and smoother operation is expected.

MkII Plunging Mechanisms

During the year two MkII plunging mechanisms were installed Nimrod Straights 1 and 4. They carry a quadrupole and an extraction magnet respectively, and with a target in Octant 5 form a Piccioni extraction system for the X3 beam serving Hall 3. The design is aimed at satisfying two main criteria, both connected with minimising fault time (which, for extraction systems in 1969, amounted to just over 270 hours (see table on page 101)). The first criterion was to ensure that all components were of high reliability, and the second was to ensure that access and interchangeability were optimised. This ensures that, in the event of a breakdown, repairs can be made quickly; this not only reduces beam-off time, but also minimises the time for which personnel have to work in areas of high radiation level. The success of the new design may be judged by the fact that the time taken to replace a magnet is now measured in hours rather than days.

The MkII mechanism is shown diagramatically in figure 77. The services over the cable arch and through the ram tube carry cooling water and excitation current of up to 17,000A to cater for the requirements of thin septum magnets XM9 and XM10. The total electrical resistance of the XM9 system is 1·3 mΩ; this matches the power supply which is described later together with the magnets themselves.

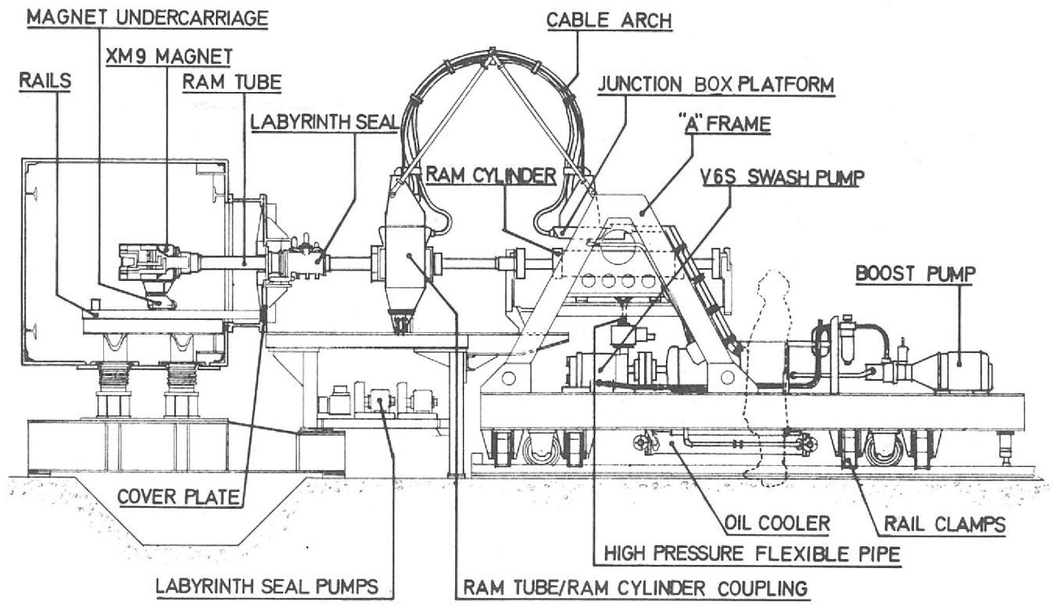

Figure 77. MkII Plunging Mechanism.

The magnet undercarriage wheels are independently suspended to accommodate any misalignment between magnet and rails. The undercarriages operate in high vacuum and in high radiation levels; lubrication and the avoidance of wear are problems which are still demanding attention. Swash pump troubles are expected to be much reduced in comparison with MkI, the pump (type V6S) having been redesigned from the original type VW20 on the basis of the MkI experience.

Other design changes include mounting the entire assembly on rails, the use of flexible piping in the hydraulic circuit between pump and ram to reduce vibrations, anti-wear modifications to the ram and an improved labyrinth seal on the ram shaft. Provision has also been made for diagnostic aids such as ram pressure measurement and end-position sensing.

Except for the undercarriage trouble mentioned above the MkII system reliability has been good. The action is smoother than MkI and a shorter stroke time (400 ms) is available. End position accuracy is of the order of ±0·5 mm and each of the two mechanisms has executed about 1·3 million strokes since installation.

XM9 Extractor Magnet

This magnet, which is now in use, weighs 14 cwt, and is illustrated in figure 78.

The yoke is 12 inches by 12 inches by 27·75 inches long and consists of 105 quarter-inch laminations, interleaved with 0·005 inch melinex. The 4 inch aperture was machined to a tolerance of 0·0012 inch, the central field being 9·8 kilogauss with a gradient of 185 gauss/cm.

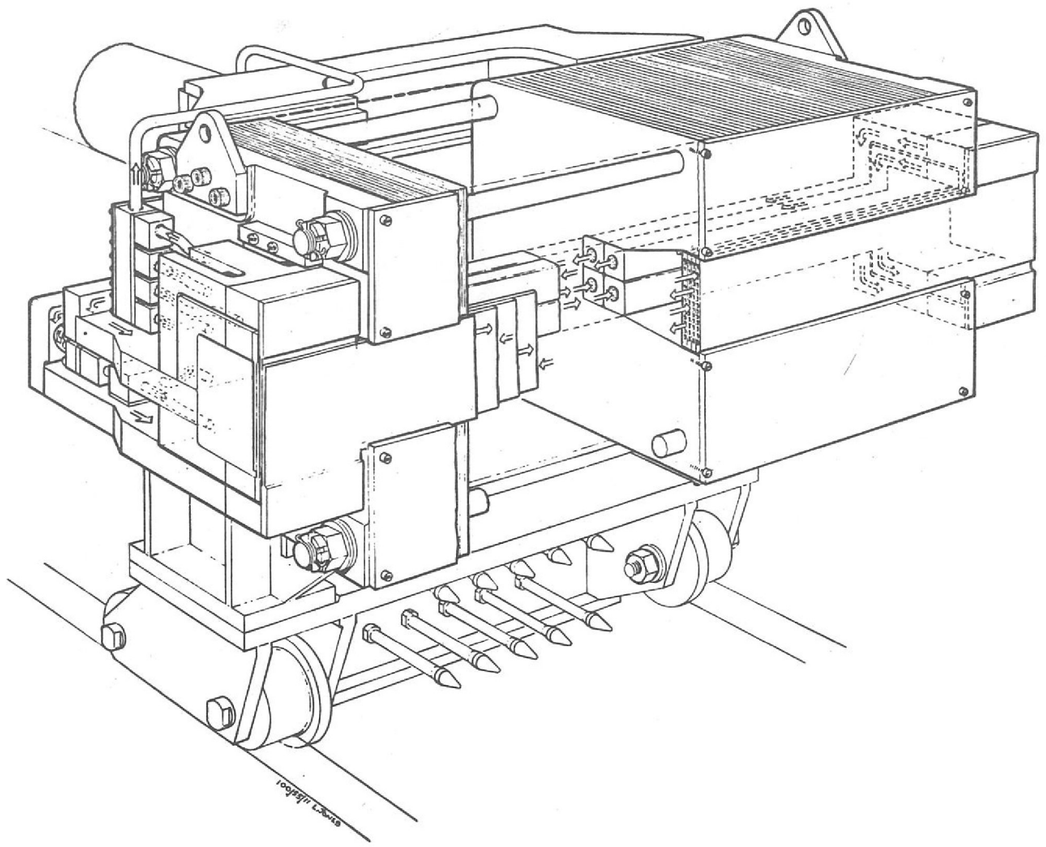

Figure 78. XM9 Magnet.

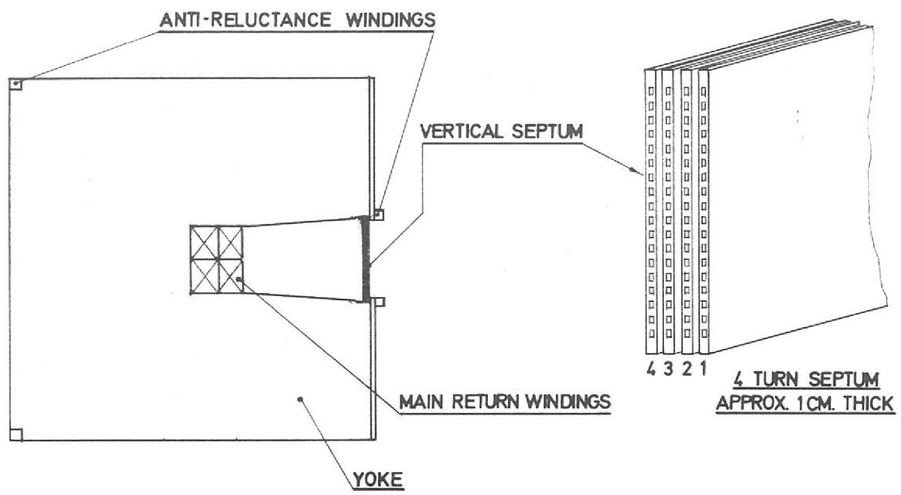

Figure 79. XM9 Magnet cross-section.

The conductor configuration is seen more clearly in figure 79. The septum is nominally 1 cm thick, consisting of 4 turns each with 18 water channels. The water flow rate of 3·6 gall/min at 100 psi gives a temperature rise of 15°C. The exciting current of 14,000A for 600 ms is pulsed every 2-4 seconds, giving an rms current of 7,000A. The rms current density is 4070A/cm^2 . The 4 turn anti-reluctance winding carries 100A.

The septa are manufactured by the "lost indium" process, in which the coolant channels are initially grooves machined in a copper bar. These are then filled with indium, following which this surface of the bar is electroplated with copper to a minimum thickness of 1·5 mm. After machining to size the septum is stood upright in a 200°C oven to melt out the indium, and when the passages are clear the end caps and manifolds are brazed on.

In use, this magnet has developed pin-hole water leaks both at brazed joints and in the main body; alternative septum fabrication methods are being investigated, two of which are depicted in figure 80 (a) and (b). The first of these was fabricated from readily available copper sections and has been fitted to magnet XM10. The brazing process was complex, and necessitated the use of special jigs and a low temperature, high strength silver braze. A better design (figure 80 (b)), at present under construction, uses $\frac{3}{8}$ inch square copper tube bonded together with glass tape and epoxy resin. This type of construction has no water joints inside the Nimrod vacuum system, though some changes to the ram tube services are required.

The magnet has been pulsed up to 16,000A, and field measurements are in good agreement with calculations using the TRIM program.

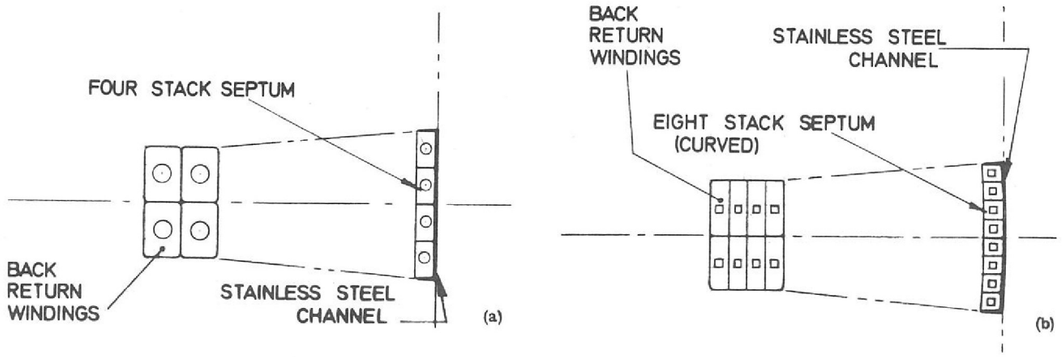

Figure 80(a) and (b) Alternative septum fabrication methods.

XHQ2 Header Vessel Quadrupole

The XHQ2 quadrupole is located in the fringe field of the Nimrod main magnet, where it provides radial focussing for X3 extracted proton beam. It is not a plunged magnet, although it is mounted on a ram to facilitate installation, removal and adjustment.

The magnet itself, illustrated in figure 81, weighs about 1 ton and is approximately 1 metre long. It is fabricated from ¼ inch low carbon (0·08%) steel laminations with 0·005 inch melinex inter-leaving. The neutral pole is of 38% cobalt steel. The exciting coil consists of 120 turns of ¼ inch square copper tube with 0·005 inch epoxy-glass insulation. The exciting current of 160A gives a field of 4,000 gauss in the centre of the aperture, with a gradient of 800 gauss/cm.

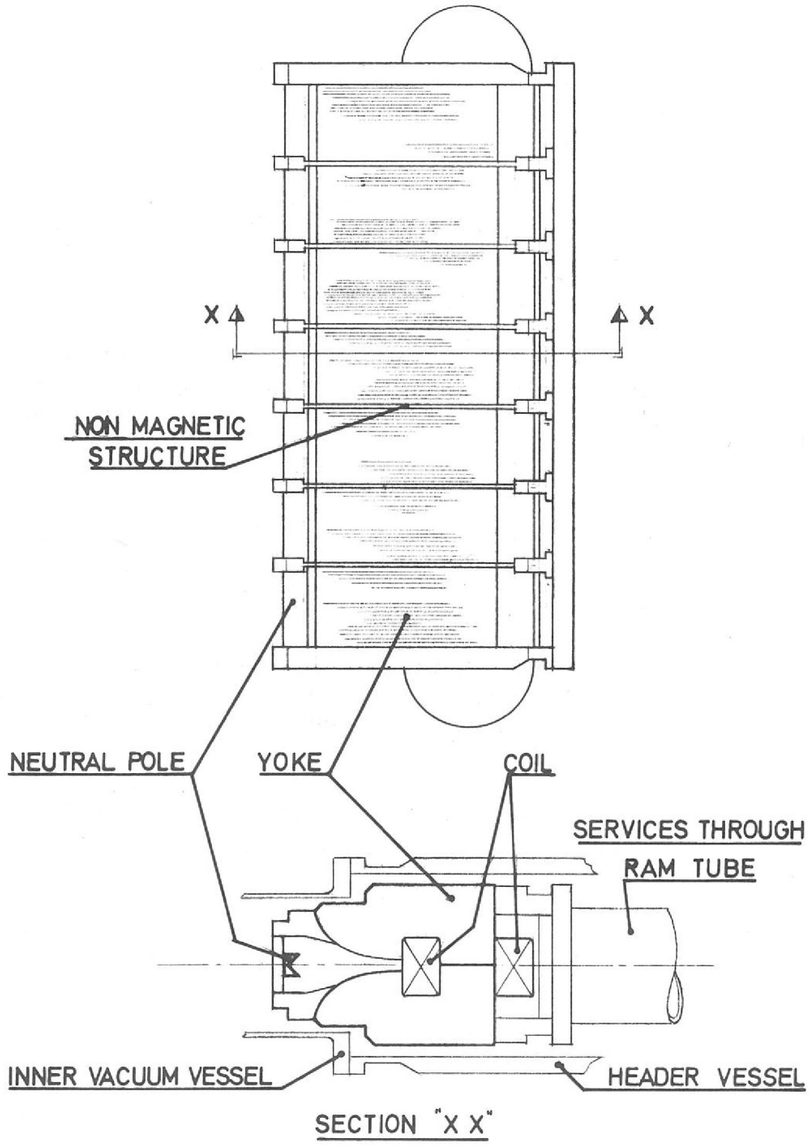

Figure 81. XHQ2 Magnet.

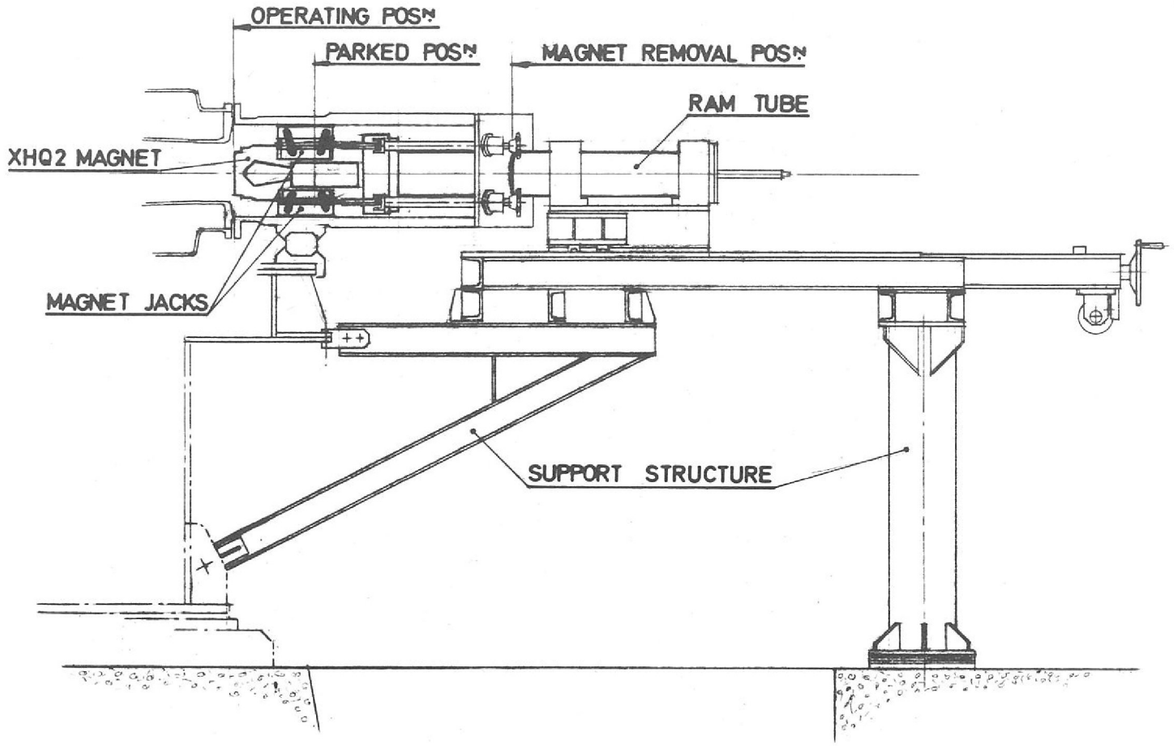

Figure 82. XHQ2 Magnet and support structure.

The support system is shown in figure 82. The magnet is cantilevered from an 8 inch stainless steel tube through which the services are fed, and this part of the system has been designed so that there are no water joints inside the Nimrod vacuum system. The operating position of the magnet is just inside the inner vacuum vessel; a small amount of angular adjustment is available here in addition to the radial movement. There is also a 'parked' position 12 inches out where, as in the operating position, the magnet can be clamped by means of jacks.

XHQ2 is located in Octant 5 and is sometimes referred to as a "powered shim" since it provides a field which, in conjunction with the main magnet fringe field, is linearly focussing. A similar magnet, XHQ3, is also needed in the complete thin septum extraction scheme; delivery is expected in mid-1970.

Other EPB Magnets

A laminated extractor magnet (XM7) was installed in the autumn in Straight 2. It replaces a solid yoke magnet forming part of the X1/X2 EPB system. The laminated construction has resulted in a shorter time-constant with the result that the fields obtained during the switched extraction mode of operation more closely resemble the fields obtained in the unswitched mode. This modification has led to an increase in extraction efficiency.

The soft kicker magnet for the resonant extraction scheme, RX3, has been pulsed up to 10,000A, and its plunging unit is being fitted with remote positioning control. Installation in Straight 3 is scheduled for Spring 1970. The present design embodies a 2·5 mm septum, but development work is in progress on a 1·2 mm edge-cooled version.

As a safeguard against magnet failure, a policy of having one complete spare magnet assembly of each type was implemented and the desired objective has now been achieved.

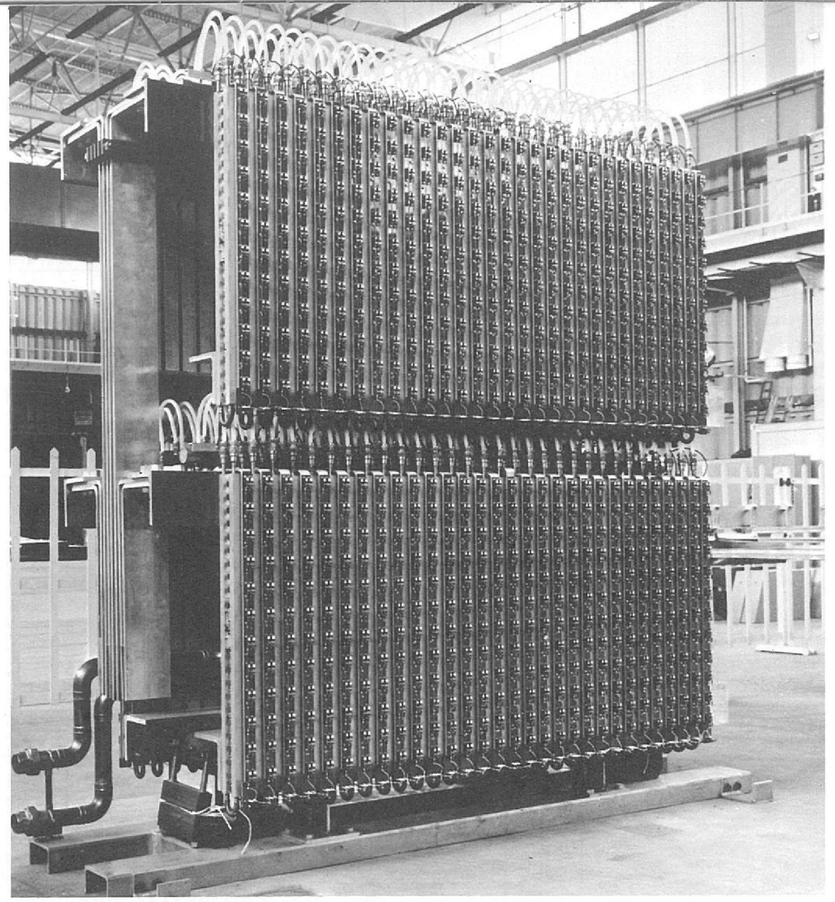

Figure 83. 21,000 A transistor regulator for the XM9 magnet.

EPB Magnet Power Supplies (110)

The X3 thin septum Piccioni system plunged extraction magnet (XM9) will be powered initially by a 250 kW rotary power supply feeding a programmed 21,000A transistor regulator which is to be located in the catacombs of the magnet monolith to shield it from radiation. This power supply (limited by the generator to 16,000A in pulsed operation) is only a temporary installation to allow the thin septum scheme to undergo preliminary commissioning. The permanent system embodies a homopolar generator which is due to be delivered in the first half of 1970. This machine is rated at 40V, 15,000A (600 kW) continuous or at 40V, 21,000A (840 kW) in pulsed operation at 25 pulses per minute. The power supply for the plunged magnet RX3, which forms part of the resonant extraction system at present under development, is based on a 300 kW d.c. generator. The control system will be similar to that of the homopolar generator mentioned above. The generator has been pulsed up to 7,000A, the predicted requirement being 5,000A. Space limitations make it necessary for the power supply to be located some 200 feet away from the magnet and to ease the installation problems it has been decided to use water cooled cables for the interconnection rather than conventional cables or bus-bars. There are three cables in parallel per pole.

Targets and Target Mechanisms

Solid targets are used as energy-loss elements in the extracted proton beam systems, and also to produce secondary particles both within Nimrod and in external beams. Target materials have included copper, beryllium, 'heavy metal', lead and uranium-zirconium alloy. Internal targets have continued to give trouble (losing nearly 75 hours of beam-time during 1969) due to failure of target head bearings. These have to withstand millions of operations in a hostile environment (high vacuum and high radiation levels). It has been noted that the failure rate depends on both beam intensity and number of operations. A planned maintenance system is now in operation, whereby targets are changed after 2 million flips, or immediately before a high intensity cycle (e.g. 10^{12} protons per pulse onto a 10 cm copper target). Standardisation of targets, target arms and other components has been taken as far as possible in order to simplify the stocking of spares. A selection of components is shown in figure 84.

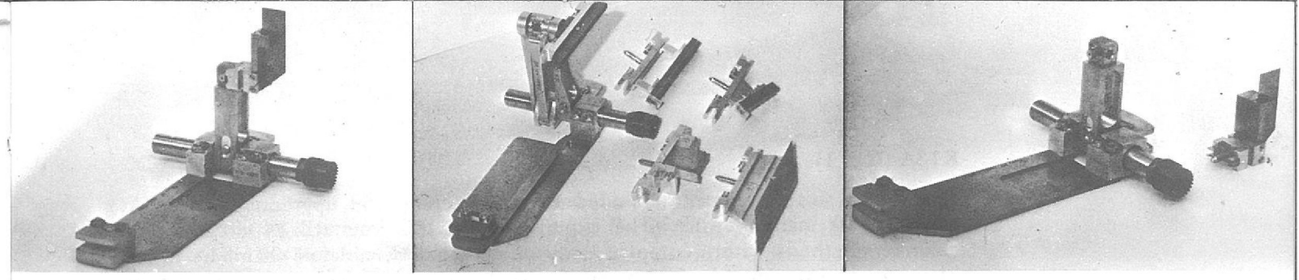

Figure 84. A selection of components for targets and target mechanisms.

The remote removal system fitted to MkIc target mechanisms has been extensively used for X3 target changes during the development phase; the saving in machine time was considerable. Similar facilities are to be provided on the MkIII mechanisms, for which an insulated target has also been developed. This permits measurements of beam intensity to be made and involved overcoming many problems associated with running electrical signal leads to a target capable of complex movements both during operation and setting-up.

A type IV external target mechanism has been manufactured. It can carry 8 targets in a remotely operated indexing head which can be adjusted both vertically and horizontally. Further development work has been carried out on the type I external target mechanism; pneumatically operated controls have been fitted, resulting in a simpler and more compact unit.

BEAM LINES AND EXPERIMENTAL AREA DEVELOPMENT

Installation of new beam lines and HEP experiments, and the modification of existing ones has gone on throughout the year, as experimental requirements and the availability of new equipment required. Some of the devices mentioned as having been installed are described in detail in the section of this Report dealing with instrumentation (pages 82-97).

Existing Beam Lines

K11 (Hall 1)

This beam line which fed the Heavy Liquid Bubble Chamber, has now been dismantled since the chamber is no longer required. Its magnet is to be used on the K16 beam line (see below).

K9 (Hall 1)

This line feeds the Hydrogen Bubble Chamber and preparations were made to incorporate a high field pulsed magnet close to the chamber as part of a system for producing neutral hyperons. Installation has been deferred, however, due to a rearrangement of the bubble chamber programme.

K12A (Hall 1)

Following the completion of the original experiment on this line, a proposal was accepted for another experiment utilising the same front end of the equipment, but with a new spectrometer-detector system. Increasing the spectrometer performance to 8 kilogauss over a 14·5 inch aperture has necessitated the installation of a special multistage water pump which is shared with the K13A line. A MkII liquid hydrogen target and a hyve have been installed.

K13A (Hall 1)

Changes to this experiment included spectrometer magnet upgrading to 6 kilogauss at 40 inch aperture. The experiment on this line utilises visual spark chamber methods with a complex array of mirrors to enable all chambers to be photographed on one film frame. An air circulation system, incorporating electrostatic precipitation filters, is being installed to keep the mirror system free from dust.

P71 (Hall 1)

The experiment for which this line was built has completed data taking; the line is being left intact although there are no immediate plans to use it again.

π8 (Hall 3)

This beam line, and K15 (see below) were brought into operation during the year. Items installed on π8 included the M7 spectrometer magnet and the first MkII liquid hydrogen target system (with hyve). Other experimental requirements made it necessary to site the hydrogen refrigerator rather a long way from the target and, although conventional cryogenic piping methods were successfully used, development of new interconnection methods has been initiated in case this problem occurs elsewhere in a more acute form. An anti-dust system, similar to that on K13A, is to be provided.

K15 (Hall 3)

The experiment on this line uses a type M5 spectrometer (up to 14 kilogauss at 12 inch aperture), a MkII liquid hydrogen target and a specially designed hyve which was proof tested, with liquid hydrogen, in the Hazardous Test Area.

Future Development of Hall 3

The X3 beam is to be transported further into Hall 3 to a second target blockhouse (designated X3X) instead of being dumped after the first blockhouse (X3) as at present. The first blockhouse, serving the π8 and K15 beam lines, will remain essentially undisturbed (see figure 85). Procurement of equipment for this Phase II development is in hand, the target date for commencement of installation being mid-1970.

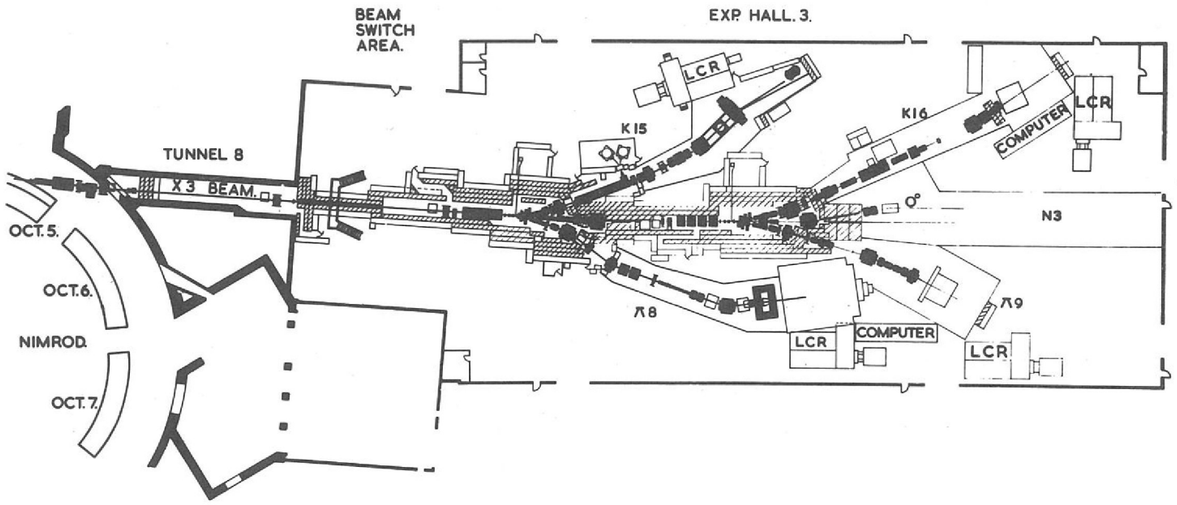

Figure 85. Experimental Hall 3. Phases I and II.

X3X Blockhouse

This will consist of 4,300 tons of iron and steel and 1,600 tons of concrete. 1,300 tons of steel have been found in the shape of the magnet yoke of the Liverpool University 156 inch synchrocyclotron which was recently closed down. This is now being cut and drilled to meet the requirements of its new role. The X3X blockhouse will serve 2 beam lines (K16 and π9) with the possible future addition of a neutral beam.

K16 (Hall 3, Phase II)

The beam line elements will include a superconducting radio-frequency particle separator (see page 120). The experiment itself will utilise the magnet from the Heavy Liquid Bubble Chamber as a spark chamber magnet, and appropriate modifications are being carried out.

π9 (Hall 3, Phase II)

In order to reduce further the congestion in Hall 1, it is proposed to rebuild the experiment at present on the K14A line on π9. The opportunity will be taken to replace the present polarized target with another having easier access for detectors. This new target, known as PUT, is described on page 91.

Pion Beam for Biological Research.

Consideration is being given to providing a pion beam for biological research by parasiting from X3 blockhouse, when the present Radiation Protection experiment on radiation transmission through tunnels is completed.

Beam Cut-off Units

A new type of beam cut-off unit was installed in the X3 blockhouse, enabling either π8 or K15 line to be isolated (e.g. for maintenance purposes) without affecting the other line. It consists of a series of steel discs with off-centre holes; by rotating the discs the beam can be obstructed or not. The unit is pneumatically operated and fails safe to the closed position. It operates in vacuum and its external dimensions conform to the shield block module sizes; it can therefore be used as part of a radiation shield wall. The X3X blockhouse will also embody these devices.

D.C. SEPARATORS AND HIGH VOLTAGE RESEARCH

Wire-mesh Electrodes

The most exciting development occurred towards the end of the year when tests disclosed the great potential advantages of wire-mesh electrodes for d.c. particle separators.

Wire screen electrodes have been discussed during the past year in connection with ultra-thin septa for accelerator ejection magnets. As reported in the 1968 Annual Report, research at the Rutherford Laboratory has shown that the multiplicative ion exchange process plays a large part in limiting separator performance, and it was realised that the effects would be greatly reduced by using a grid structure for one or both of the electrodes.

An experimental stainless-steel wire-mesh separator electrode was constructed and installed as the anode in the test separator tank. It quickly reached 650 kV across a 10 cm gap, (to be compared with the 500-550 kV to be expected with plane stainless-steel electrodes, and with the 700-750 kV with a heated glass cathode). This voltage was attained after 24 hours conditioning time, (compared with about 7 days for ordinary stainless-steel and 3-4 weeks for glass). Further, the performance

was completely insensitive to deliberate contamination by organic materials which would have been catastrophic with other types of electrode.

Development of mesh electrodes is being actively pursued on the grounds that they promise advantages in ease and reliability of operation which could more than compensate for the slightly lower electric field than is attainable with glass cathodes.

Electrode Support Insulator

The new design of insulator mentioned in the 1968 Annual Report has been subjected to an accelerated life test at high voltages: a set of 4 such insulators withstand a 4-week test at about 6 sparks/hr at 350 kV and 80°C, equivalent to more than one year of normal operation.

High Voltage Lead-in Insulator

Running at the above high voltages, sparking rates and temperatures revealed a weakness in the high-voltage lead-in insulators, and failures occurred under 380 kV, 80°C conditions. Calculations revealed the reason for such failures, and a new lead-in termination assembly has been designed to overcome them. A computer program using a relaxation technique was used in the design to minimise the radial and longitudinal electric stresses. A prototype of the new design has been delivered, and will be tested shortly.

600 kV Precision Potential Divider

The balancing technique proposed in the original design report has now been tested, and proves to be very successful. The metal film resistors in the measuring chains are not reliable at voltages above 400 kV and will be replaced by simpler units.

Basic Vacuum Breakdown Research (78)

Further experiments during 1969 have given additional information on the effects of ion exchange phenomena in the breakdown of separator type vacuum systems. They indicate that residual pressure in the system can cause ions to be lost from the process by charge exchange with the residual gas molecules. It has also been demonstrated that mesh electrodes suppress the ion exchange process.

Particle Separator Vacuum Systems

Operating difficulties with the particle separator diffusion pump units have continued and since turbomolecular pumps are now giving reliable service, diffusion pumps are being replaced by them. After the December shutdown only one separator, that in the K14 beam, will still have diffusion pumps and it is hoped to replace these in mid-1970.

SUPERCONDUCTING R.F. SEPARATORS

Cavity Parameters

The particular requirements of r.f. separated beams at Nimrod lead to the choice of 1300 MHz disc-loaded cavities operating in π-mode. From an assessment of possible geometries, a final structure has been selected – representing a compromise between increased beam acceptance and shunt impedance on the one hand, and reduced peak magnetic and electric fields on the other. Salient parameters are:

Maximum Deflecting Field: (E_o)	=	3·6 MV/m
Aperture: (2a)	=	10·5 cm
Disc Thickness: (t)	=	3·95 cm
Peak Magnetic Field for above E_o: (H_p)	=	540 G
Peak Electric Field for above E_o: (E_p)	=	13·8 MV/m

Tests are at present under way to determine the suitability of lead plating for these conditions. A preliminary layout drawing of a deflecting cavity in its cryostat is shown in figure 86.

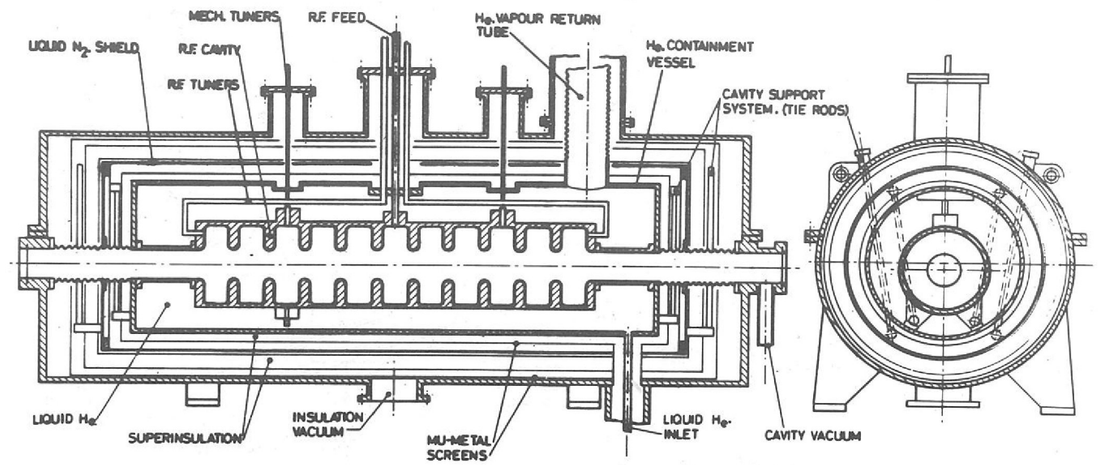

Figure 86. Proposed r.f. separator cryostat assembly.

Measurements

Measurements of R/Q agree with theoretical prediction to within 3%; surface fields have been measured and confirm results obtained elsewhere. A mechanical tuner has been designed, constructed, and tested, giving 126 kHz per mm penetration, in one cell. A further tuner is being constructed. Two tuners per cavity will be used.

Since the beam pipe diameter is a significant fraction of a cut-off wavelength, it presents a considerable shunt reactance to the cavities. This has been measured and tuned out by increasing the length of the terminal half-cells by about 4 cm. Losses in the end cells have also been measured, and correspond to a 6% reduction of Q in the final structure. Cryogenic microwave windows have been constructed and tested, and design drawings for windows on the final cavities are being prepared.

Improvement Factor

The maximum theoretical improvement factor is $I_{th} = 5{\cdot}6 \times 10^5$: the initial aim for a practical system was chosen to be $I = 10^5$, implying a lead impurity of about 2 parts in 10^5, and an ambient magnetic field below about 7 mG. A programme of low-power tests in S-band cavities has now been completed, with the result that a satisfactory plating schedule has been achieved, giving Q values in the range $1 - 7{\cdot}5 \times 10^9$ at 1·6°K. Scaling to 1300 MHz, the corresponding improvement factor is up to 4×10^5. Currently, a 2-cell wrought-copper 1300 MHz cavity, and a similar electroformed cavity, are being prepared for high power tests; both are being plated with lead.

Extra-mural research is under way at the University of Liverpool, to study the growth of microprotrusions and their field enchancement effects in lead and niobium.

Refrigeration and Cryogenic Systems

The refrigeration requirements for a two-cavity separator system are a power of 25W at 1·85°K, with a temperature stability better than 0·01°K. The chosen temperature is a compromise between the cavity requirements (high Q, therefore low temperature) and the rapidly rising cost of refrigeration as the operating temperature is reduced. Calculations have shown that modifications to the existing Liquid Helium Bubble Chamber refrigerator, including the fitting of an additional Joule-Thompson stage, will yield 40-60 watts at 1·85°K. There should be spare capacity for other superconducting beam elements, and pre-cooling capacity will be available at 4·7°K and 66°K.

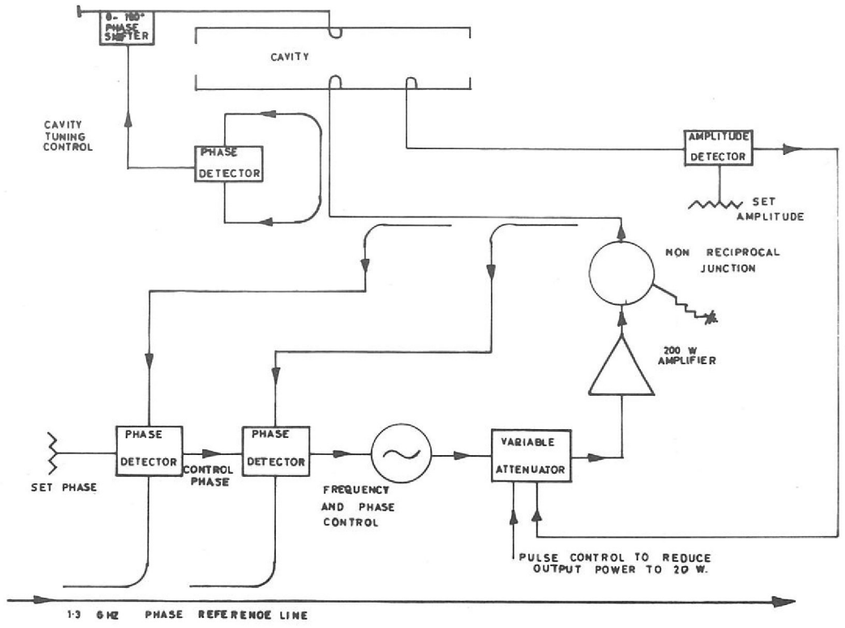

Figure 87. Proposed r.f. system.

A design study of the cryogenic system for a two-cavity separated beam has been carried out, and the choice has fallen on the simplest system considered (gravity flow of the liquid helium, evaporative cooling and a separate gas return) although more exotic systems utilising the special properties of superfluid helium were considered.

R.f. System The proposed r.f. system design is illustrated in figure 87. R.f. sources of 200W peak per cavity will be used, so that solid-state and strip-line techniques can be used throughout. The r.f. power source has been assembled for the first high-power tests, and many prototype components for the full system have already been constructed.

Beam Design Recent beam design studies have concentrated on the application of the superconducting separator to a separated K^- beam in the range 2·0-3·5 GeV/c, centred on 2·7 GeV/c. University College, London have expressed considerable interest in such a beam, which might form part of the Hall 3, "Phase II" complex: see layout of figure 88. Provided no major snags arise in the separator research programme, the beam could be installed during the first half of 1971.

A provisional optical design is illustrated in figure 89: the two 10-cell cavities are spaced about 7·5 m apart.

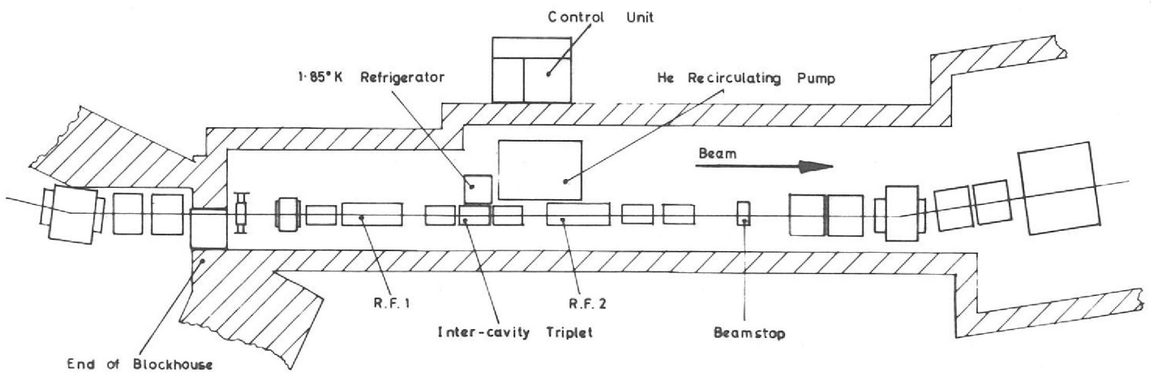

Figure 88. R.f. separator beam layout.

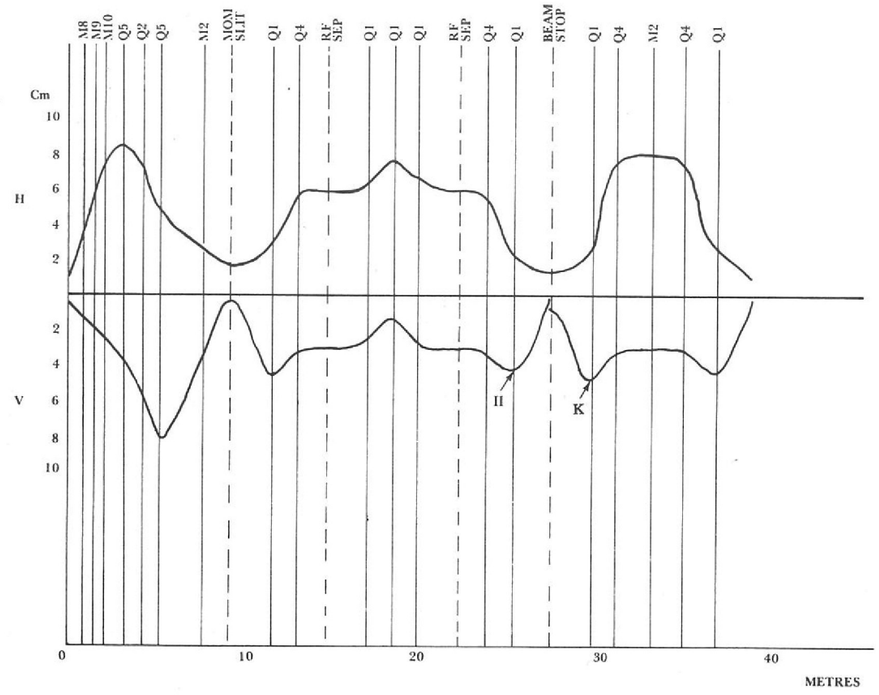

Figure 89. Beam profiles through proposed r.f. separated beam.

SUPERCONDUCTING QUADRUPOLE LENS

The fluxes of secondary particles in Nimrod beams may be increased significantly if superconducting quadrupole magnets prove to be reliable in operation. In particular, their use in r.f. separated beams could lead to an additional factor of about 3 in "wanted particle" flux.

The technical specification of a prototype superconducting quadrupole to be manufactured by Industry has been completed this year, and tenders are being invited. This unit should have an effective length of 33 cm, an aperture diameter of 12 cm, and should operate at a maximum gradient of 6·5 kG/cm. It is intended to install it in the Nimrod experimental area for operational assessment as soon as possible after delivery.

SUPERCONDUCTING SYNCHROTRON MACHINE STUDIES

Theoretical design studies for a superconducting synchrotron to replace Nimrod began in the last quarter of 1969. The initial objective is to assess the capabilities of a machine located in the Nimrod Hall, using the existing power supplies, with injection from a small (conventional A.G.) booster synchrotron, and with two ejected beams serving Experimental Halls 1 and 3 respectively. If possible, energy would be close to 25 GeV and flux would be in the range 2-10 $\times$ 10^{12} protons/second with a duty cycle in the region of 20-25%. Bending fields of about 60 kG and quadrupole gradients of about 9 kG/cm are envisaged.

Lattice studies are under way to meet these requirements, the chief problem being to provide sufficient straight section length.

PULSED MAGNETS

Major emphasis during 1969 has been on the construction and testing of high field pulsed magnets for an enriched Λ° hyperon beam; and on the development of flat-top field switching magnets offering millisecond pulse lengths and microsecond rise times.

Switching Magnets (217)

The development of two types of drive circuit, (outlined in the 1968 Annual Report), has been completed. The initial application of the 250 A triode system is to energise a 500G dipole consisting of 40 air-cored turns in an elliptic cross-section, giving good spatial field uniformity. A more operational development of this magnet is under construction, incorporating a glass/epoxy resin vacuum flight tube with which the coil assembly is integrated. Figure 90 shows a typical current trace.

The 1 Ω delay line system has been used to power a 4-turn 12 μH air cored coil: studies of optimum conductor location have led to a system in which the field is uniform to within 2% over most of the circular cross-section. The current trace shown in figure 91 is typical of the early results.

Studies are under way to examine low-loss laminated iron magnets which would give similar performance when powered by the same drive systems.

Fast Rise End Units

To reduce the step-magnet rise times, a scheme has been developed involving "separate function" leading-edge units of less than 3 μs rise. Trailing edges of the pulse are matched to the front edge of the existing step-magnet waveforms to give an effective fast-rise flat-top field as seen by the particles. No electrical or magnetic coupling is required between the new units and the existing step magnet elements; they are also suitable for addition to other flat-top field devices.

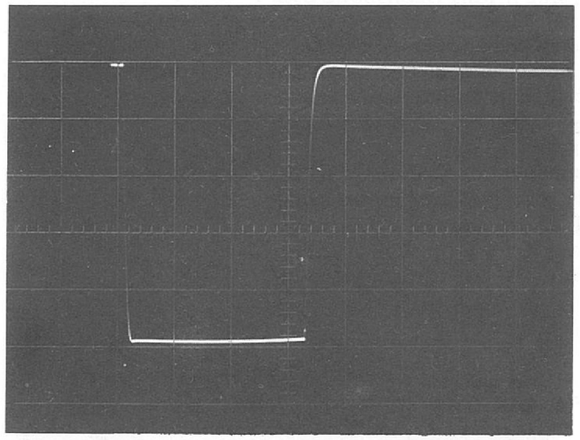

Figure 90. A typical current trace. Time base 100 μs/cm. Vertical sacle 50 A/cm (another correction setting)

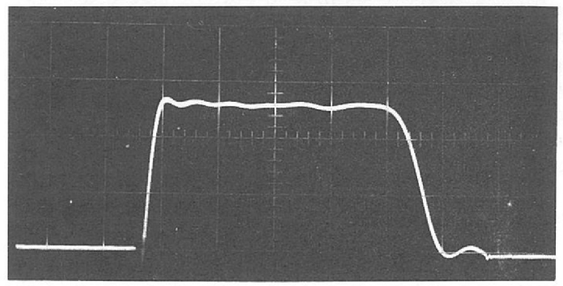

Figure 91. Pulse from 1 Ω delay line system.
Voltage = 6 kV, C = 100 μF,
Time base, 50 μs/cm.
Vertical scale, 1000 A/cm. Field, 0·1 G/A.
Flat-top Ripple = ± 3%.

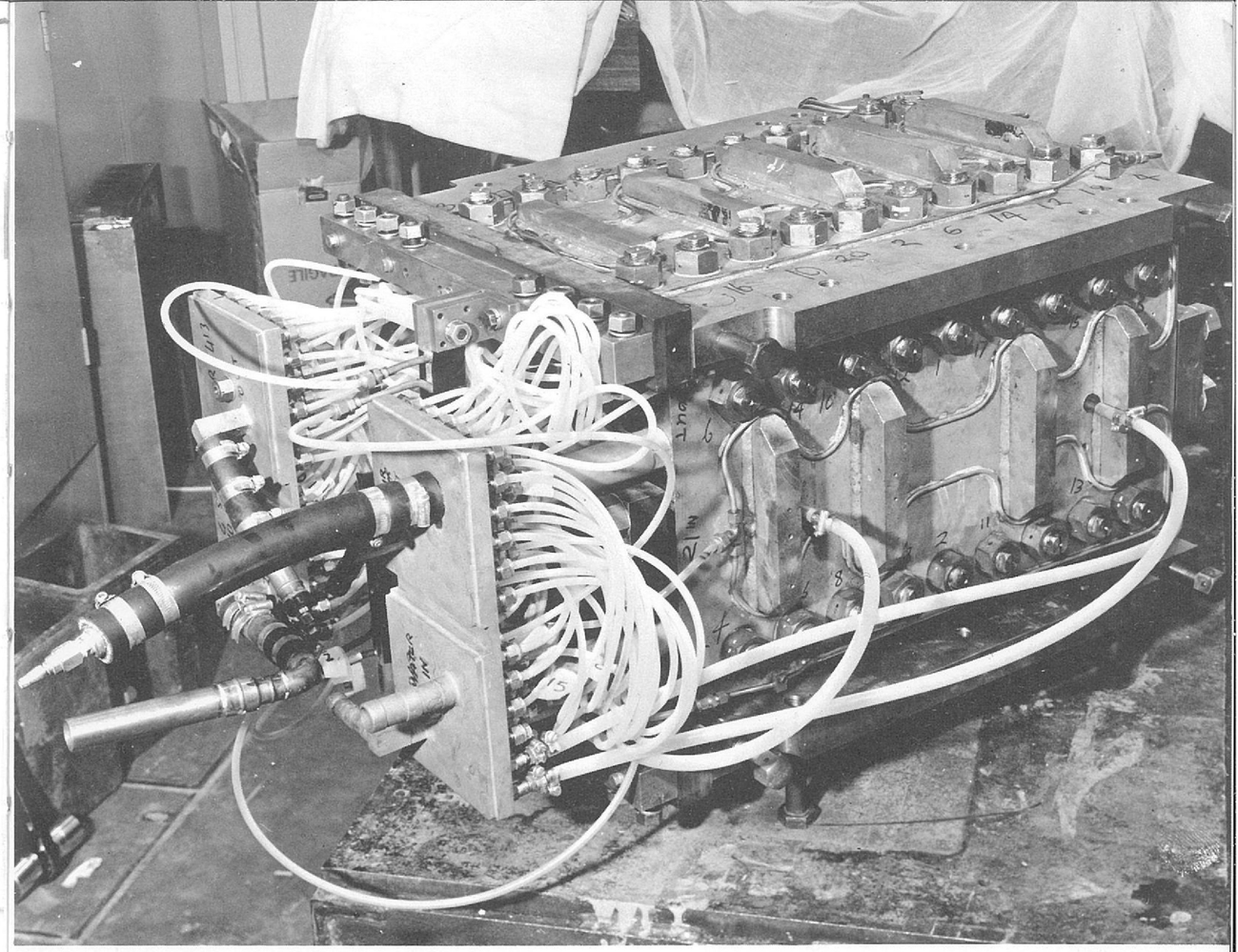

Figure 92. An assembled high field pulsed magnet.

High Field Pulsed Magnets

Two 40 cm Type I high-field pulsed magnets have now been tested for well over 100,000 pulses each, at 70 kG, and one coil has also been operated for an extended period at 100 kG.

More efficient cooling of the laminated uranium collimator inserts has overcome the hazard of ignition, but 'heavymet' will be used in any operation magnets. A further coil has completed its tests prior to beam line operation, and another one is nearing completion. The programme timescale has not permitted a practical demonstration of total lifetime for any of the recent magnets. An assembled magnet is illustrated in figure 92.

COMPUTING AND FILM ANALYSIS

Computing and Film Analysis

COMPUTER SYSTEMS AND OPERATIONS

Central Computer Extension

In May an additional 500K bytes of main core store was added, making a total of 1 M bytes main core plus 1 M bytes of LCS. Four extra magnetic tape decks were added so that the installation now has 4 High Density (1600 BPI) 9 track tape drives, 3 Dual Density (800 BPI/1600 BPI) 9 track tape drives and one 7 track drive. These are attached by a selector sub-channel to the highspeed multiplexor. At the end of the year work was in hand to install a second magnetic tape control unit and another selector sub-channel. (This will reduce the possibility of conflict between jobs accessing magnetic tape.) Early in the year the magnetic drum was brought into operation and allows fast access to much used system data sets.

Towards the end of 1970 the 2311 (small) disks will be replaced by a second set of 2314 (large) disks.

Building Extension

The extension to Building R1 provided a much needed increase in space for the central computer installation. The computer room was extended to allow for the increase in machine size, and the amount of working space and office space for operations staff in the reception area was increased. In addition a spacious data preparation area was provided, and also room for programmers to work in the reception area where there is access to a library of manuals and the data preparation equipment.

Operations

As a result of these modifications, it is now possible to run four batch streams in addition to the on-line work. Allocating one stream to CPU-bound production jobs has increased the weekly average CPU efficiency to over 80% without affecting the turn-round of short jobs, the average turn-round on prime shift being about two hours. The extra magnetic tape drives allow tapes to be loaded in advance and considerably improves the operation of the computer. The total number of jobs per week has increased from about 2500 to about 3500.

Software (120)

The MFT2 operating system continues in use. In August, release 17 of the OS was installed. Its main advantages were the ability to put more system modules onto the drum, and the ability to split partitions between main core and LCS. A consequence of the latter facility is that low priority partitions in LCS are now possible. Economy in the use of main core by long-duration low-activity jobs (such as graphics jobs) is made possible by running part of the job in LCS. Unfortunately full use could not at first be made of the facility because of system troubles in re-defining partitions.

Future Development

A test batch, representative of the work load of the Laboratory, was constructed to allow comparisons of performance between different computers; it was run during the year on an IBM 360/85. The possibility of attaching keyboard terminals to the system is under consideration. The terminals would allow users to update files and enter jobs into the batch stream. Various existing systems such as CRBE, APL are being evaluated.

Accounting (229)

A program has been written to analyse the output from the IBM MUSIC accounting facility. From this a weekly analysis of machine usage is made, by Division and by project and this information is given a wide circulation. The accounting program also provides very detailed information about the efficiency of the system, and the use made of the various system devices. This has been used in conjunction with IBM's AMAP program to construct the system data sets in the most efficient way possible.

Services to Users

The PPE package obtained from CAP, has been used on several long running production programs to pinpoint highly used parts of the program. Throughput can be improved, sometimes quite dramatically, by recoding these parts of the program.

Routines have been written which improve the efficiency with which 7-track tapes written on other computers can be handled. They are particularly valuable in reading tapes containing large numbers of faults due to having been generated under adverse conditions.

The "Computer Introductory Guide and Reference" has just been published to provide a comprehensive guide to the system facilities, and pointers to the source of information necessary for using them.

The library of standard catalogued procedures has been extensively revised, new procedures invented to enable users to submit jobs with as few control cards as possible, and a new library created of special-purpose procedures for groups or individuals. Bulletins have been issued describing these improvements, and giving guidance on the response of the operating system to errors made during the development of new programs.

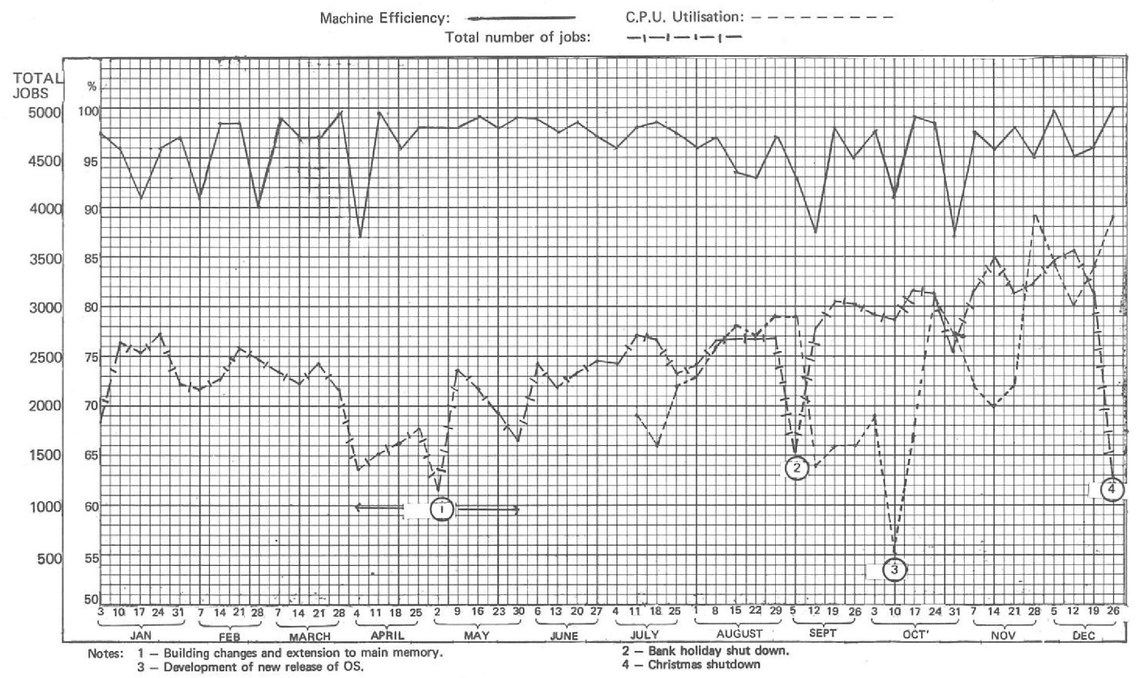

Figure 93. Central computer machine statistics during the period 27 12 68 to 26 12 69.

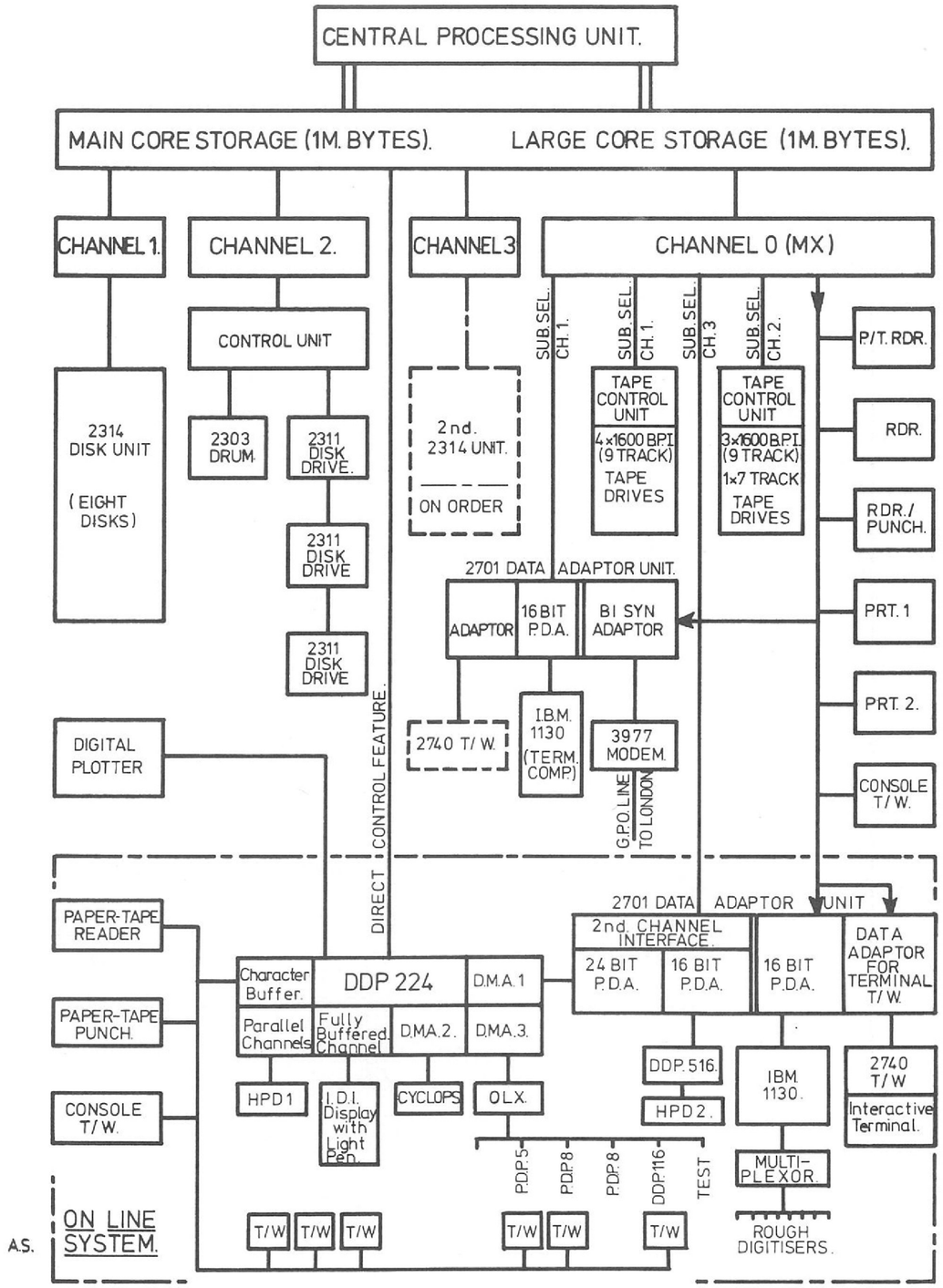

Figure 94. Rutherford Laboratory Central Computer. IBM 360/75.

SYSTEM 360/75 ON-LINE APPLICATIONS

The main on-line applications work of the Laboratory is centred around the coupled IBM 360/75 plus Honeywell DDP-224 computer complex. The DDP-224 controls the following equipment:

(i) HPD 1. A bubble chamber film measuring machine.

(ii) CYCLOPS. A spark chamber film measuring machine.

(iii) IDI display scope. A graphical display with light-pen.

(iv) OLX. A fast parallel data input link to the Nimrod experimental area.

(v) Calcomp plotter.

(vi) Paper-tape equipment.

(vii) 7 IBM typewriters.

The DAEDALUS operating system, which has been developed at the Laboratory, is used to control the complex. It allows the transfer of data and messages between user programs running in the 360/75 and the devices attached to the DDP-224. All devices can be operating at the same time.

The complex is maintained and developed by a small support section of four and is scheduled for production operation for 97 hours per week. Availability of the complex as a whole has averaged better than 98%. During the year the OLX link has been transferred to a direct memory access channel to improve the efficiency of data transfer. In addition a multiplexor for connecting several Tektronix 611 storage tube displays has been developed. A detailed schematic layout of the complex is shown in figure 94. Detailed reports on DAEDALUS and items (i)–(iv) are given below.

On-Line Control Programs

The DAEDALUS on-line system has operated reliably throughout the year. Normally 70-80 hours of production is achieved each week and for much of this time there is more than one user. The main users are HPD, CYCLOPS and the IDI visual display. The latter became fully operational at the beginning of the year when the software package to drive the display by the light pen was fully debugged. Since then the system has been used to reprocess bubble chamber and spark chamber events which fail the analysis program. Up to 30 hours per week has been used for this purpose. At the end of the year final checking of software necessary to add a Tektronic 611 storage display unit was being done. This would allow the display of graphical output containing a large number of points but will have no interactive facilities. Facilities have been provided to allow users to enter jobs into the 360 by commands from DAEDALUS typewriters. Development of this is continuing to make it easier to use, and more versatile.

Work has begun on an improved DAEDALUS system which will be able to control many satellites. The first two computers to be added would be an IBM 1130 computer which is to be used as a terminal facility in the experiment Hall and the DDP 516 which will control HPD2. Later the existing IBM 1130 which controls the rough digitizers will also be incorporated in the system.

HPD (214)

The HPD has been used this year for measuring film from two experiments in the CERN 2-metre hydrogen bubble chamber.

Antiproton film, exposed during 1966 and later, was measured intensively from January-July; by early August 76,000 events had been measured (all of 2-prong

topology). In April the rate was increased by measuring all events on a frame (up to a limit of four) on a single normal scan, and during nine successive weeks in May-July, more than 3,000 events were measured every week (over 35,000 in the period), with a peak of over 5,800 in one week.

The measurements have been processed through two filtering programs (CERN HAZE and RHEL HAZE) in succession, and tracks still faulty were patched-up by using a display and light-pen. The Geometry pass rate after the first (CERN) HAZE averaged 76% (accepting 2-view reconstructions, rejecting helix fit errors exceeding 20 microns) and about 94% after light-penning. These figures exclude rough digitizing faults which are easily found (such as format errors, etc.) but includes cases of bad road-making. Helix fit residuals peak at about 4 microns.

Results from kinematic fitting of these events are satisfactory, the χ^2 probability distributions look good and the full width at half height of the missing mass peak in 4–C events is 22 MeV/c^2.

Since July a new experiment has been mounted, dealing with 14 GeV/c K^-p film taken during February-April of this year. Much more complex events appear in this film – neutral and charged vees, and multi-prong events. Changes were necessary to cope with these, as a result of which the number of events measured so far is only about 6,000, though the measuring rate has exceeded 100 events per hour.

The Geometry pass rate after the first (CERN) HAZE filtering program again reached over 70%, though it is not so good for some early rolls of film taken with a different camera arrangement. Since the maximum helix fit error accepted has been reduced to 13 microns, and there are on average 5 tracks per event instead of 3 in the earlier experiment, this pass rate looks better than before. The helix fit peak is slightly better (except on the early rolls of film).

In addition 12,000 more antiproton events have been measured during this period, as have fiducial marks on 260 spools of K^-p film (30 frames per spool) as a preliminary check on their positional stability.

Improvements have been carried out on the on-line control program, making measurements faster, more automatic, and tolerant of a wider range of film quality. In particular, the digitizing level is now controlled automatically, giving more uniform bubble density measurements.

No radical changes have been made to the hardware of the operational HPD as measurement of existing film has had priority over developments to cater for 'Scotchlite' chambers, etc. A number of improvements have been embodied in the second machine (HPD 2), the installation of which is well advanced. Experience gained from this development work has enabled many detailed changes to be made to the production machine, resulting in a high degree of reliability.

The flying spot that scans the film is generated by a disc rotating at 6000 rpm. To minimise heating and to help maintain a constant speed the disc was run in a vacuum. This proved troublesome in practice and it has been found much better to run the disc in a helium atmosphere; the disc speed is now constant to within the limits imposed by the mains-driven synchronous motor, the demands upon which are now less arduous. Spot quality is also receiving attention, in an effort to reduce fringes and satellite spots which can degrade the output signal.

A new device has been developed for detecting the Brenner marks (fiducials) on the film; it incorporates fibre optics and semi-conductor infra-red detectors, and can accommodate any type of film. Improvements have also been made to the film gate, the servo-controlled hydraulic stages and to a number of other items affecting ease of operation and maintenance.

CYCLOPS

CYCLOPS is a flying spot digitizer used for measuring 35 mm spark chamber film. It scans the film with the image of a fine spot (about 20 microns across) generated on the face of a high-precision CRT. During 1969 it has had another full year of automatic operation, running under the DAEDALUS system for up to 20 hours per day using a 62K byte main core partition in the IBM 360/75 and 48K bytes of large core store. In production, CYCLOPS can measure up to 600 frames per hour where the frame measures 35mm × 100mm. Averaged over the full running time it reaches a figure of about 300 frames/hour and measures between 10,000 and 30,000 frames per week dependant largely on the availability of film. Binary picture numbers are decoded on-line; film positioning and the data are checked before digitized co-ordinates are written to 9 track magnetic tape on the IBM 360/75 for later off-line analysis.

During the year a fully operational system has evolved enabling diagnostic and production running to be performed within the same program. Operators using commands from an on-line typewriter can change the mode of operation and the values of selected variables in the program to enable problems with film and hardware to be diagnosed and overcome. New facilities making the system more automatic and more reliable have been added with the result that the system can now run virtually unattended for hours at a time.

Two experiments have been measured on CYCLOPS during the year. A Daresbury experiment on e-p scattering has been completed. This involved the measurement of some 100,000 events. Magnetic tapes of digitized data were stored and sent to Daresbury for complete analysis.

Measurements on film from the Nimrod experiment on the leptonic decay of neutral kaons (Experiment 14, page 40) was continued and a further 300,000 events have been measured.

Computer Graphics (123)

A set of computer programs has been written for rescuing bubble chamber events which, having been measured on HPD, fail in the Geometrical reconstruction programs. Selected regions of HPD digitizings of these events are displayed on an IDI computer controlled display, and by means of a light-pen, an operator controls the selection and accurate measurement of tracks. The results of these actions are displayed superimposed on the track digitizings, and can be modified or accepted by means of control characters, or 'light-buttons' on the screen. When satisfactory, the track points are written to disk, to be merged at a later stage with the originally successful events.

These events have failed principally because of pattern recognition errors, the commonest causes of which are superfluous tracks very close to, or crossing the required tracks, and small scatters which cause incorrect determination of track curvature. Digitizings within a narrow road (640 microns wide on film) about the bad tracks are stored on magnetic tape, together with the co-ordinates of the three rough digitizings, and the track master points found by the automatic pattern recognition programs.

A batch of these tracks are transferred to disk and then displayed. The three views of a track are displayed side by side, and by means of the light buttons the operator selects which views require attention. With a single view on the screen, the operator either deletes some of the original master points, or causes a simple filtering of the track guided by points selected with the light-pen. New master points are displayed and can be accepted or changed. When satisfactory the co-ordinates of the new points are written to disk.

Over 100,000 track views have been displayed and 'patched up', corresponding to 20,000 failed events from anti-proton and K^- film in the CERN 2 metre chamber. Measuring rate is about 100 tracks per hour, and the display is operated up to 10

Figure 95. Selected events shown on a computer controlled display. By means of a light-pen the operator controls the selection and accurate measurement of bubble chamber events.

hours daily. Of the bad events (which are about 20% of the total measured by HPD) between 50% and 75% are subsequently successful, the remainder being mostly very faint tracks or bad roads.

A film has been made of the 'patch-up' system in action, and has been shown at the 1969 HPD meeting at Amsterdam where it was well received. Copies of the film have been borrowed by CERN, Dubna (USSR) and Argonne (USA). A set of programs is being written for 'patch-up' of events measured under 'minimum guidance' where only the vertex of an event is pre-digitized.

A similar system of programs is under development for 'patch-up' of failed events from the CYCLOPS spark-chamber film device, where the tracks are straight and the problem is one of recognising tracks in two views by means of the spark structure. The spark co-ordinates and widths are displayed for the two views and by means of the light-pen, the operator can redefine end-points and correlate pairs of tracks.

Remote Link to Nimrod Experimental Area

Attached to the DDP-224 is a parallel data communications link which allows data collected by small computers in the Nimrod experiments halls to be transferred into the 360/75 via the DDP-224 (the distance is some 300 metres). Up to five computers can be multiplexed on to the link. During the year the main users of the facility have been the University College group collecting data for the K8 experiment, (Experiment 4, page 29). Data for the experiment was collected by a PDP8 and written to magnetic tape. During 'beam-off' times on Nimrod the data on the tapes was transferred via the link to the 360/75. The data was checked and partially analysed and then written to tape in compressed form. In all some 100 magnetic tapes containing some 4 million events were transferred via the link for this experiment.

On-line Rough Digitizer System (218, 237)

The rough digitizer system which provides guidance measurements for the HPD system is now operational using six machines. Three of these are D-Mac and three Rutherford Laboratory IPD co-ordinate measuring tables. These are all connected to an IBM 1130 computer and data is collected in the computer, checked and then stored on a disk store. At a later stage this data is transferred to disk storage on the IBM 360/75 via an electronic data link. Usually this transfer of data takes place once a day and when sufficient data from a particular roll of film has been collected for HPD a further merging program takes the data from the 360 disk and puts it on to magnetic tape in a form ready for HPD programs.

The system is operated continuously for 124 hours a week and produces some 3-4000 events in that time. To increase the output a further six machines using Mangio Spago digitizers have been built and the electronics connecting those to the 1130 computer is currently being commissioned.

A supervisor program for the 1130 has been developed to allow the overlapped operation of all the devices and to sort data into a form suitable for data checking programs; since this is now operating satisfactorily it is being extended to handle up to 15 devices.

Data checking programs have been interfaced to the supervisor and, in the first phase checking has been limited to logical and format errors. Operators are informed of any errors via a typewriter which is supplied to each measuring station. Further co-ordinate dependent checks are being developed to improve the quality of the data and a system for the on-line calibration of machines is currently being devised.

Machine Maintenance

The Track Analysis Maintenance Section of Engineering Division is now responsible for all the machines used in the measurement of bubble and spark chamber film. An additional 11 machines (of 3 different types) used for spark chamber films have been taken over for maintenance and for the incorporation of new digitizing systems. Machines for bubble chamber film now number 19 (8 different types) with the addition of 4 three channel projector machines using a modified Mangio Spago digitizing system connected on-line to the IBM 1130 computer. 2 Vanguard three channel machines are on order, and 2 Duff machines have been transferred to Durham University.

The scanning and rough digitizing machines are now housed in a suite of adjacent laboratories, with the workshop in close proximity. These changes have enabled reliability and throughput to be increased, as required by the gradual introduction of 24 hour scanning.

FILM ANALYSIS SOFTWARE

Bubble Chamber Analysis System (121, 122, 124, 125, 126, 214)

The Full Guidance system which has been operational on HPD 1 since early in 1968 requires that each track of an event is pre-digitized by rough-measuring three points along its length. During the year two major changes have been made – the introduction of a new filter program, and an automatic track matching program – and parts of the system have undergone continuous modification to achieve maximum economy of computer storage space and CPU time.

The RHEL filter program uses a 'stringing' technique in which the digitizings produced by the HPD are joined to form string, and the strings joined to form track segments, which are then themselves joined; finally one segment is chosen to form the track and master points are calculated. The program is used in normal production to refilter those events which fail to be reconstructed by the GEOMETRY program after the first filtering. In this mode, about 40% of the failed events are rescued, and the remainder are output to be patched-up using a display and light pen.

The track matching program assumes that the vertices are matched by the measurer, but that the tracks at the vertex are measured in any order, and it uses information such as the angle of the track, magnitude of curvature, and rms deviation from a helix to match the tracks. The program is not yet used in the production system, but has been tested on about 800 events. On events which were matched by the measurer, the pass rate is similar to the GEOMETRY pass rate to within 1 or 2%, while on a batch of 230 events which were measured without the measurer attempting a match, the MATCH program found that 17% of 4 prongs and 45% of 6 prongs required matching.

Work is now proceeding on a Minimum Guidance system in which only the vertices of an events are pre-digitized. The rough digitizing rate is greatly increased, but more complex programming techniques are required to find, follow, and match the tracks.

One of the main problems is to reduce the amount of data from each frame to a manageable size. In the Full Guidance system only about 10-20% of the digitizings are kept, the rest being rejected since they are too far away from any track, but in the Minimum Guidance system with only vertex measurements, this is not possible. A program, using the stringing techniques developed for the RHEL filter program, is being written to identify and reject the digitizings belonging to non-interacting beam tracks. It is hoped that this will be possible in real time, so that this method of data reduction can be included in the software for HPD 2.

A Minimum Guidance filter program has been developed in collaboration with CERN and this forms the nucleus of an RHEL Minimum Guidance system. The performance of this program on events measured by HPD 1 is promising, and development work is concentrated on reducing the CPU time and storage requirements by recording some of the key routines more efficiently, and by carefully adjusting the numerous program parameters in consultation with CERN.

Preliminary work has also started on adapting the track matching program for Minimum Guidance, and on developing a patch-up system using the display and light-pen.

Spark Chamber Programs

Data from CYCLOPS stored on magnetic tape requires detailed analysis in order to convert single digitizings first into tracks and finally into complete events.

A general track-finding program was developed further and is now capable of working for any experiment measured on CYCLOPS dealing with straight tracks and showers. The program can search, in areas of the original picture defined via fiducial marks, for tracks and showers. The program is given no initial guidance as to whether the event is good or, whether and where, tracks exist, but by systematic searching it is able to link digitizings to form tracks. If sufficient tracks are found then the event is accepted and data stored on magnetic tape or disk for further analysis.

All events in the K13 experiment (No. 14, page 40) were measured and the track finding was able to find about 95% of the 'good' events whilst retaining some further 'possible' events of which it was unsure. In combining together the various views of tracks in good events for full 3D reconstruction of the event some events fail. These events and the 'possible' events required some manual intervention or patch-up to correct or reject them.

The patch up was done in one of three ways but each method produced guidance information which required re-cycling through the track finding process, when tracks were then found by searching in clearly defined regions. The guidance data was obtained from rough digitizers, Tektronix 611 storage tube with an interactive tracker ball in a DDP 516 or the IDI Graphics system.

At present all the patch-up methods are operational and they all give results better than hand measuring alone. Some 50% of the good events are dealt with automatically and this figure is raised to 80% by 'patch-up'.

To help in the development of the automatic pattern recognition programs much use has been made of the Atlas Laboratory's SC 4020 plotter and programs have been developed to make use of the facility. More recently, work has started to see whether existing programs from track finding and patch-up could be used on data originating from spark chambers using non-visual methods of recording the information. The general problem of tracking particles in spark chambers contained within regions of varying magnetic field is also under investigation.

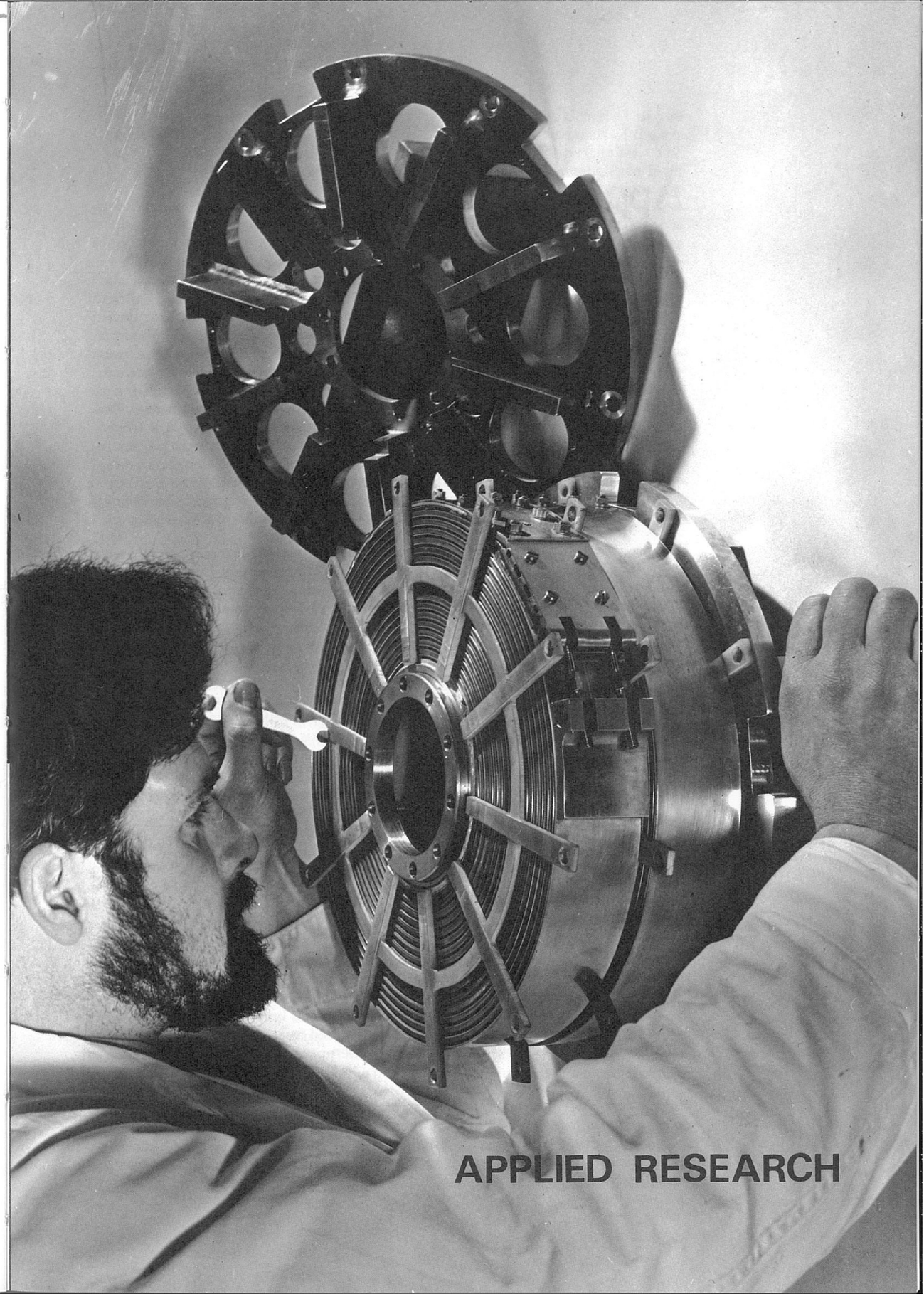
APPLIED RESEARCH

Applied Research

THE PROPOSED HIGH FIELD BUBBLE CHAMBER

The High Field Bubble Chamber has been conceived as a high precision instrument for study of the strong interaction physics of elementary particles. The unique combination of high magnetic field (70 kilogauss), rapid cycling (5 to 10 expansions per second), and optical precision (50 microns in chamber space) which makes this chamber such a powerful physics tool has naturally enough introduced a number of new engineering problems of formidable magnitude. The physics and technical specifications for the chamber were laid down in a Design Study Report published in January 1967, at which time a research and development programme was started to investigate the feasibility of new techniques suggested for incorporation into the proposed chamber. By April 1969 this work was sufficiently advanced for authorisation to complete the design to be sought from and granted by the Science Research Council.

If approval to proceed to the construction stage of the project is given in early 1970, it is expected that the High Field Bubble Chamber will be ready for its initial test run early in 1974. The present programme envisages the installation of the chamber in a temporary building adjacent to Experimental Hall 1 for the initial proving trials, and then reinstallation at CERN where nuclear physics experiments will be performed with the chamber as part of the European Bubble Chamber Programme.

A brief technical specification of the proposed chamber is given in Table 1 and an artist's impression is shown in figure 96. The chamber itself is cylindrical in shape, 1·5 metres diameter and 1·8 metres long with its axis vertical. An optical system consisting of a retro-directive illumination system and four cameras allows the tracks of charged elementary particles in nearly 2,500 litres of liquid hydrogen to be photographed stereoscopically. Provision is also made for the use of deuterium and mixtures of neon in hydrogen as chamber liquids.

The necessary magnetic field is provided by a pair of superconducting coils each of 1·9 metres internal and 3·2 metres external diameter and of length 1·1 metres, the pair being separated by an axial distance of 0·4 metres. A magnetic field of 70 kilogauss has been specified with a uniformity of ±10% throughout the fiducial volume of the chamber.

Although larger superconducting magnets than this have already been built and successfully tested, these have been designed for magnetic fields lower than 30 kilogauss. The High Field Bubble Chamber magnet is the largest superconducting magnet with a field strength as high as 70 kilogauss known to be under design at the present time. Iron shielding will be provided to reduce the stray magnetic fields which would otherwise interfere with the operation of surrounding equipment.

Particle beams will enter the chamber across the median plane between the magnet coils. The momentum of both the incoming beam particles and of the charged secondary particles produced by interaction with protons of the liquid hydrogen will be determined accurately by measurement of the appreciable track curvature occurring in the high magnetic field.

A resonant expansion system is proposed in which the natural period of the expansion-recompression cycle is controlled largely by the moving mass of the expansion piston and the spring rate of the liquid hydrogen in the chamber. The expansion piston will be normally held in a condition of force unbalance from which it will be released by a hydraulic latching mechanism to initiate the expansion-recompression pulse, and subsequently re-latched by the same device. In this way conditions can be set so that the liquid hydrogen in the chamber is superheated for a time sufficiently long to allow the growth of small bubbles along the paths of charged particles, but yet sufficiently short to suppress large scale parasitic boiling in the chamber. The hydraulic system will be capable of repeating this expansion-recompression sequence 10 times per second.

A novel method of sealing the expansion piston to the chamber walls is proposed and this involves the use of bellows made from an electrically non-conducting material. If metallic bellows were used, eddy currents induced by their movement in the magnetic field during the expansion cycle would decay and produce unacceptably high boiling in the liquid hydrogen. If piston rings were used, rubbing friction at the rings would nucleate unwanted bubbles during the expansion cycle. An ideal solution of this difficult sealing problem for a high magnetic field chamber is to adopt plastic expansion bellows since no chamber heating whatsoever should result from their use. Bellows of this type are not available commercially, so an experimental investigation into the feasibility of such components has been carried out and encouraging results have been obtained.

The expansion piston itself must also be constructed from electrically non-conducting material and the use of epoxy-bonded fibre-glass is receiving experimental consideration.

The photographic system which records the bubble tracks consists of four cameras mounted at the base of the chamber. Four telecentric lenses view the chamber working liquid by looking through four sets of so-called fish-eye windows. Each set consists of three concentric spherical glass caps made to optical tolerances and maintained concentric with one another within tight limits. The largest fish-eye glass separates the liquid hydrogen in the chamber from the surrounding vacuum which provides thermal insulation for the chamber. The middle window is a radiation shield cooled at its edges to 25°K, the temperature of the chamber. The smallest fish-eye separates the vacuum space from atmosphere and is maintained at ambient temperature. Within the smallest fish-eye, at the common centre of curvature of all the glass surfaces, the camera lens is mounted. Surrounding this lens is a ring light source fed by light pipes from remotely positioned flash tubes, since the high magnetic field makes it undesirable to operate a flash tube near the lens. The chamber walls adjacent to the working volume of liquid hydrogen are covered with 'Scotchlite', a beaded screen retro-director similar in principle to the material used for cinema screens and motorway signs. Light from the ring source is then retro-directed towards the photographic lens which consequently sees a bright field everywhere except where track bubbles have scattered light out of the returning beam. Particle tracks are then seen as dark shadows against the illuminated 'Scotchlite' and can thus be photographed.

Two refrigeration systems are required for the High Field Bubble Chamber, a hydrogen refrigerator producing 10 kilowatts at 22°K and a helium refrigerator producing 750 watts at 4·4°K. The hydrogen refrigerator will be used to cool down the chamber, fill it with liquid hydrogen, deuterium, or a neon-hydrogen mixture, and then maintain it under precise control at some selected temperature within the range 25°K to 30°K. The helium refrigerator will be coupled to the superconducting magnet to keep the coils at 4·4°K. Because the cooldown and operational procedures for the chamber-magnet system do not call for both the hydrogen and helium refrigerators to be operated at maximum output at any one time, a combined system is now being considered which allows the output of

either refrigerator to be increased temporarily at the expense of the other to overcome a period of peak demand. In this way economies can be made in the size of installed plant. Even so, both refrigerators will be bigger than any yet operating in Britain at liquid hydrogen or helium temperatures.

Table 1

TECHNICAL SPECIFICATION OF HIGH FIELD BUBBLE CHAMBER

Chamber Dimensions		
Diameter of fiducial volume		150 cm
Depth of fiducial volume		100 cm
Fiducial volume		1750 litres
Total chamber volume	approx.	3500 litres
Superconducting Magnet		
Magnetic field at centre of chamber		70 kilogauss
Field uniformity in fiducial volume	approx.	±10 %
Beam Entry		
Across the median plane of chamber between pair of magnet coils		
Optics and Cameras		
Illumination system		bright-field Scotchlite
Four cameras symmetrically placed around base of chamber		
Film size		70 mm
Rapid film advance		10 frames per second
Stereo angle between opposite pairs of cameras	approx.	35°
Objective lens – field angle		110°
Demagnification at front plane of fiducial volume		15
Demagnification at rear plane of fiducial volume		31
Positional Accuracy in fiducial volume		50 microns on HPD master point
Expansion System		
Natural period of pressure oscillation in chamber		adjustable between 50 and 100 milliseconds for hydrogen operation.
Rapid cycling		10 cycles per second
Working Fluids		
Operation permitted with hydrogen, deuterium, neon and neon-hydrogen mixtures		mixtures
Use of track sensitive hydrogen or deuterium targets in neon-hydrogen mixtures also possible.		
Refrigeration		
Refrigeration capacity at 22°K		10 kilowatts
Refrigeration capacity at 4·4°K		750 watts

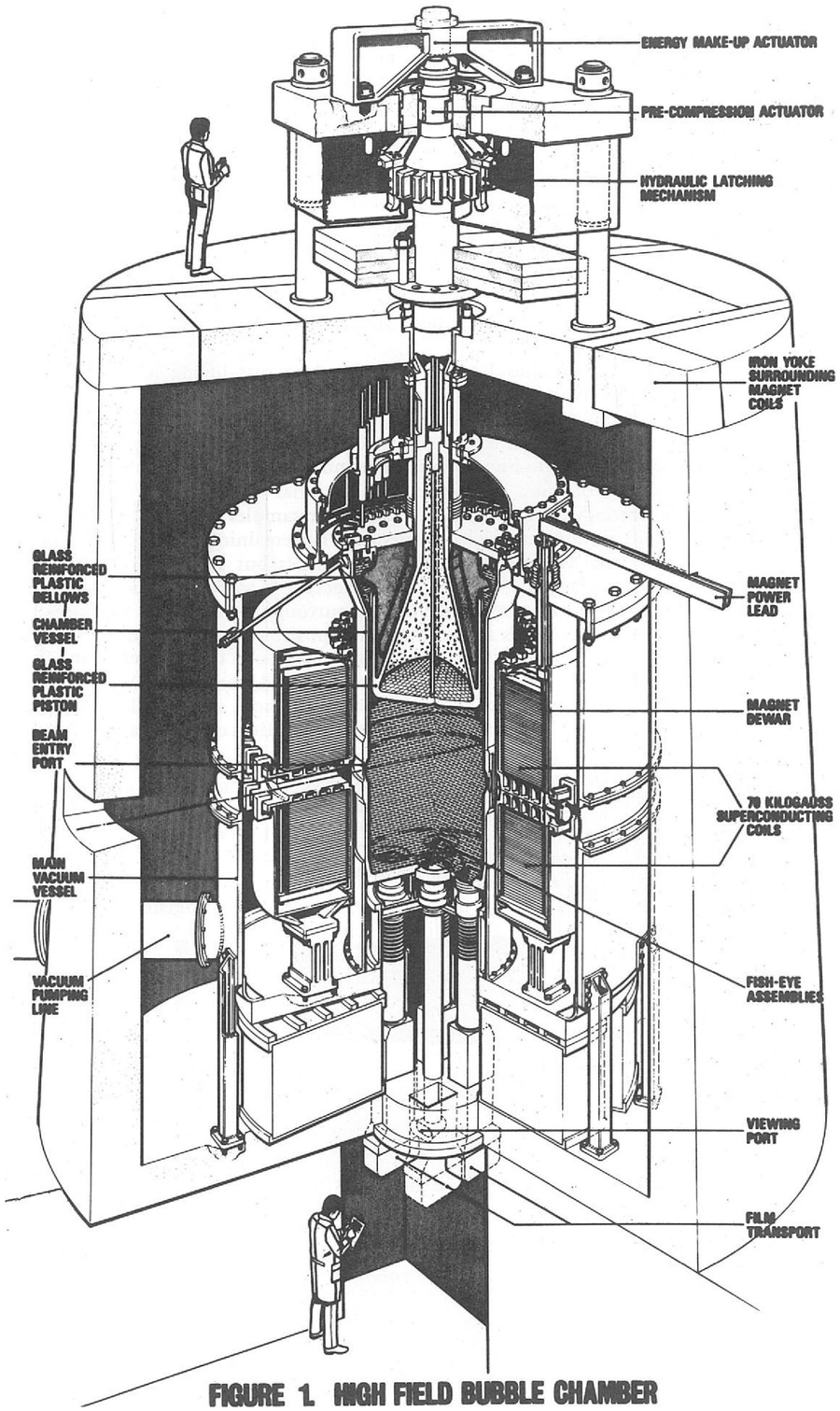

FIGURE 1. HIGH FIELD BUBBLE CHAMBER

Figure 96. Artists impression of the proposed High Field Bubble Chamber.

RESEARCH AND DEVELOPMENT PROGRAMME

As is appropriate for a high field, high precision, fast cycling chamber, research and development work has been concentrated on three aspects of the design: the superconducting magnet, the optical system, and the expansion system.

Superconducting Magnet

The three main problem areas associated with the magnet are the containment of the enormous forces generated within the coils by the interaction of magnetic field and current, the difficulties of winding such a highly stressed magnet, and the development of a suitable composite superconductor capable of being manufactured in quantity at an acceptable price.

During the current year further work has been performed on the third of these topics, the first and second having been successfully examined earlier.

Conductor development has been concentrated on producing a suitable composite of niobium-titanium in copper. This work has been performed jointly by Imperial Metal Industries (Kynoch) Ltd., the one UK producer of this material, and the Rutherford Laboratory. Samples of superconducting strip produced in connection with the High Field Bubble Chamber are shown in figure 97. These samples have part of their copper matrix material etched away to reveal the individual superconducting filaments. The wider samples (a and b) have respectively 36 and 60 niobium-titanium filaments. The remaining samples (c d e and f) produced later have the same number of filaments but these are twisted with respect to one another, the twisting being necessary to reduce the time taken for complete penetration of the strip by the surrounding magnetic field. Evaluation of these conductors has shown that a composite superconductor of the type illustrated in figure 97 e or f is entirely suitable for use in the magnet of the High Field Bubble Chamber. These conductors are specified to carry 7,500 A in a field of 84 kilogauss (the peak field of the proposed magnet), and to allow complete penetration of magnetic field into the conductor in less than one hour after energisation of the coils.

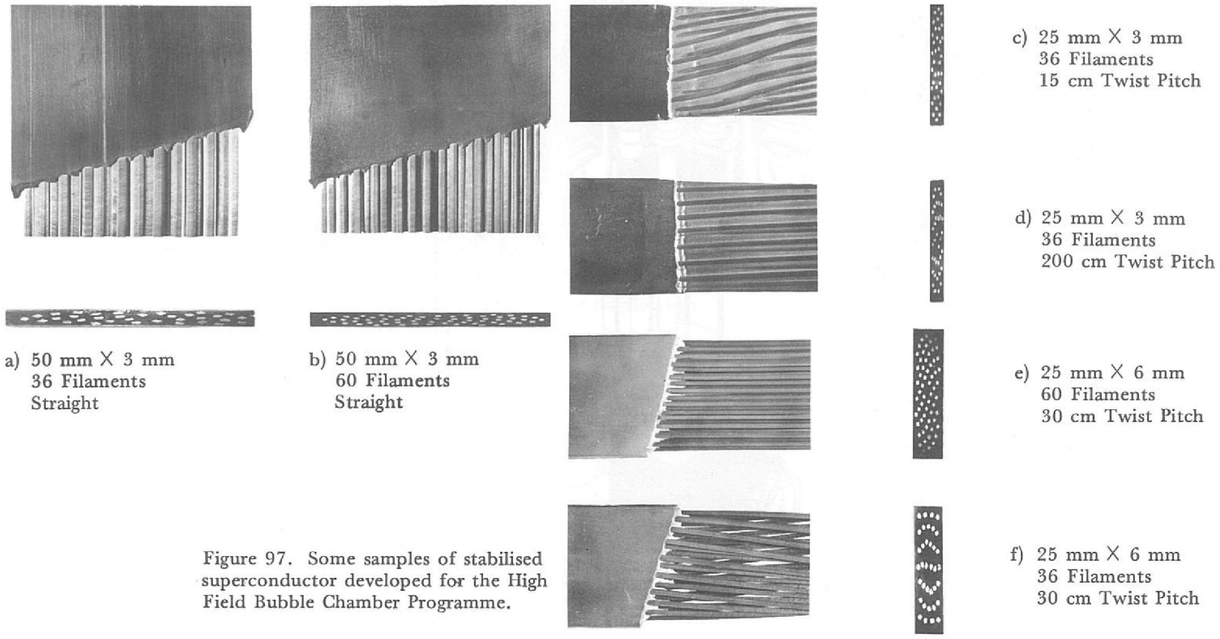

a) 50 mm × 3 mm
36 Filaments
Straight

b) 50 mm × 3 mm
60 Filaments
Straight

c) 25 mm × 3 mm
36 Filaments
15 cm Twist Pitch

d) 25 mm × 3 mm
36 Filaments
200 cm Twist Pitch

e) 25 mm × 6 mm
60 Filaments
30 cm Twist Pitch

f) 25 mm × 6 mm
36 Filaments
30 cm Twist Pitch

Figure 97. Some samples of stabilised superconductor developed for the High Field Bubble Chamber Programme.

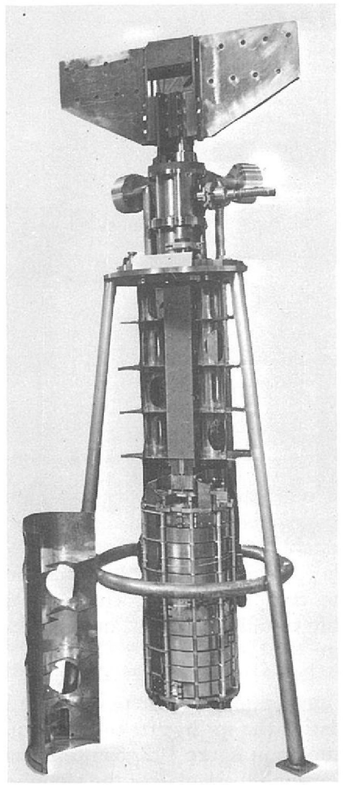

Figure 98. The 'RACOON' superconducting magnet.

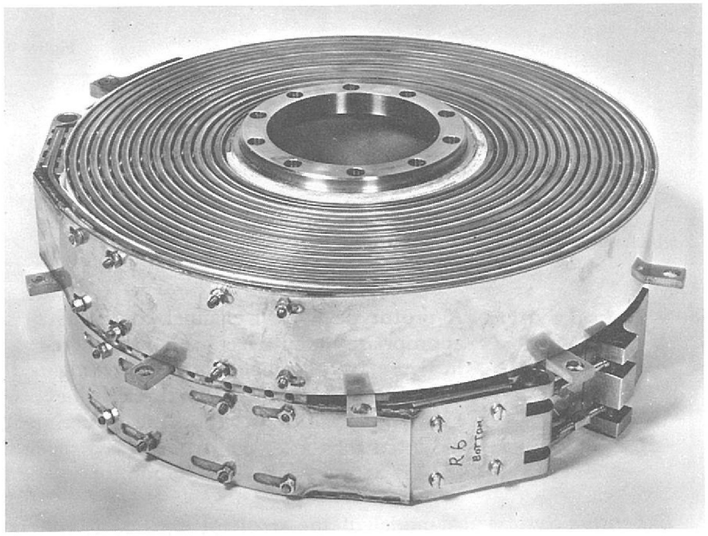

Figure 99. One of the six double pancakes comprising the 'RACOON. test coil.

Manufacture has been completed of a test coil, code-named RACOON, intended to check the performance of possible conductors in a thermal and magnetic environment similar to that which will prevail in the large coils. The assembled RACOON coil is shown in figure 98. One of the six double pancakes comprising the RACOON coil is shown in figure 99. It will be noticed that liquid helium can penetrate freely through the windings allowing cooling of almost the whole of one wide surface and both edges of the 50 mm × 3 mm conductor. The RACOON coil is designed to produce 25 kilogauss with an operating current of 7,500 A, and should also be able to generate almost 50 kilogauss when energised to the maximum current that the superconducting strip is capable of carrying. To date testing has been restricted to 11,500 A, the limit of the presently available power supply. At this current, thought to be the highest ever injected into a superconducting magnet from an external power supply, the RACOON coil produced a magnetic field of almost 40 kilogauss and performed in a most stable manner. During the series of tests the energy stored in the magnetic field of the coil (some 100 kilojoules) was successfully extracted and dumped into a resistance external to the cryostat which contains the coil. It was found that this energy extraction could be completed in a few tenths of a second thereby reducing the dissipation of energy within the coil itself to a negligible level in the event of a section of the superconductor reverting to a 'normal' state due to loss of refrigeration. In this way excessive boil-off of liquid helium can be avoided should it become necessary to extract the stored energy of the magnet quickly following some failure of associated equipment. At a later stage it is proposed to operate RACOON as an insert coil to the CERN superconducting test magnet BRARACOURCIX or a similar magnet. In this test it is confidently expected that peak fields of over 80 kilogauss will be encountered by sections of the RACOON windings thus duplicating the peak field condition of the High Field Bubble Chamber magnet.

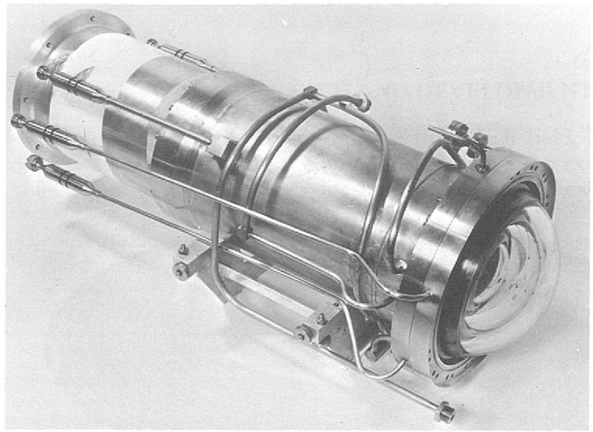

Figure 100. Protype optical channel.

Optical System A prototype optical channel consisting of a set of three fish-eye windows and appropriate mounts has been constructed. The assembled optical channel, shown in figure 100, has been used to investigate the establishment and maintenance of concentricity between the three fish-eye windows under true bubble chamber operating conditions. For this experiment the complete optical channel was mounted into a 25 cm diameter hydrogen bubble chamber now set up as a test facility at the Rutherford Laboratory. (See figure 101).

Expansion System A model of the resonant expansion system to approximately one-tenth scale is being constructed with a double gas spring simulating the spring rate of the liquid hydrogen in the bubble chamber. The test rig, shown in figure 102, comprises an hydraulic latching system, a cylinder and piston assembly simulating the chamber liquid, and an additional (adjustable) mass to give the system natural periods of oscillation in the range 10 to 20 cycles per second. The latching mechanism consists of a pair of fast acting, hydraulically actuated friction clutches operating transversely to the piston shaft. Since some energy is lost from the moving system during oscillation due to bearing friction, etc., a small energy make-up actuator is required and this has been added to the existing rig during the present year.

Tests of the model expansion system had already shown that timing of the unlatching and re-latching mechanism, and therefore the timing of the expansion pulse itself, could be controlled to better than one millisecond, this being more than adequate for the full-size bubble chamber. Testing has been extended to include evaluation of the automatic energy make-up system. It has been demonstrated that the proposed hydraulic expansion system is entirely feasible and highly versatile.

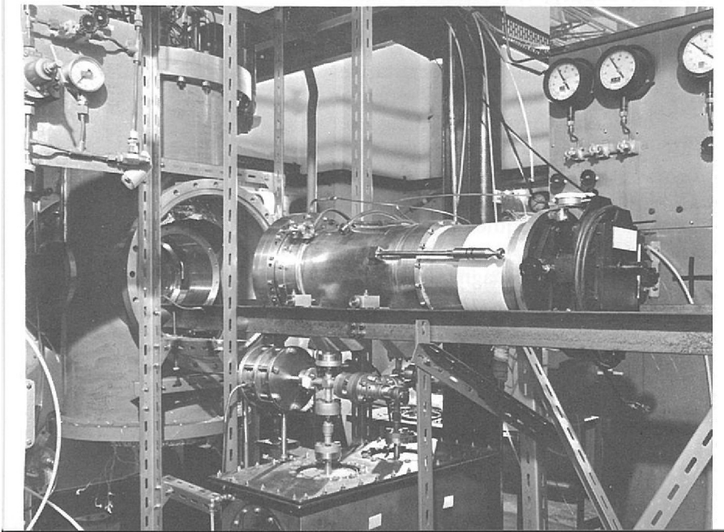

Figure 101. The 25cm Hydrogen Bubble Chamber with fish-eye assembly ready for mounting on to the chamber.

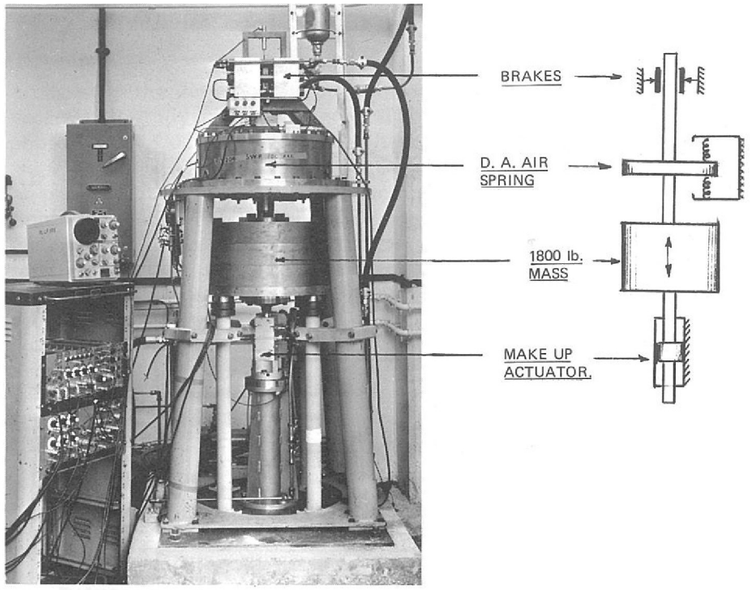

Figure 102. Make up energy test rig for testing the model expansion system.

The required operating parameters are an amplitude of ±0·4 inches and a cycle time of 50 ms. Two methods of controlling the actuator have been considered; these are described below together with the test results.

(i) A closed loop servo-system using one electro-hydraulic control valve for the actuator was tried first. The amount of energy injected into the system is controlled by varying the phase or amplitude of the driving signal to the valve – see figure 103. Control of amplitude could not be made better than 5%. The system was prone to generate large pressure spikes in the actuator, and although these might have been cured on the test rig (by means of more sophisticated electronics) they could be expected to be more severe in the full scale system.

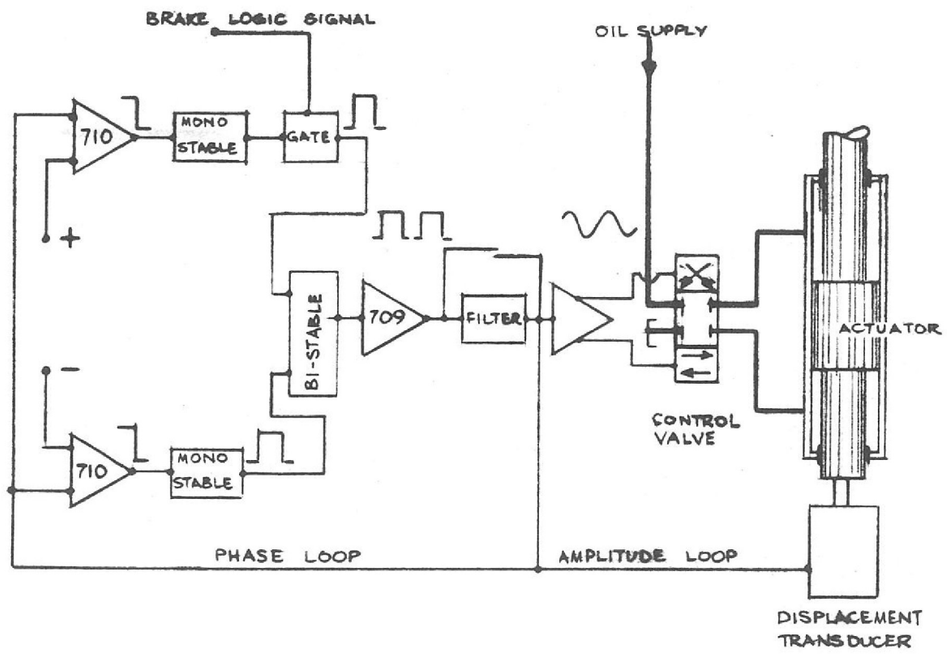

Figure 103. Schematic diagram of the closed loop servo-system using one electro-hydraulic control valve for the actuator.

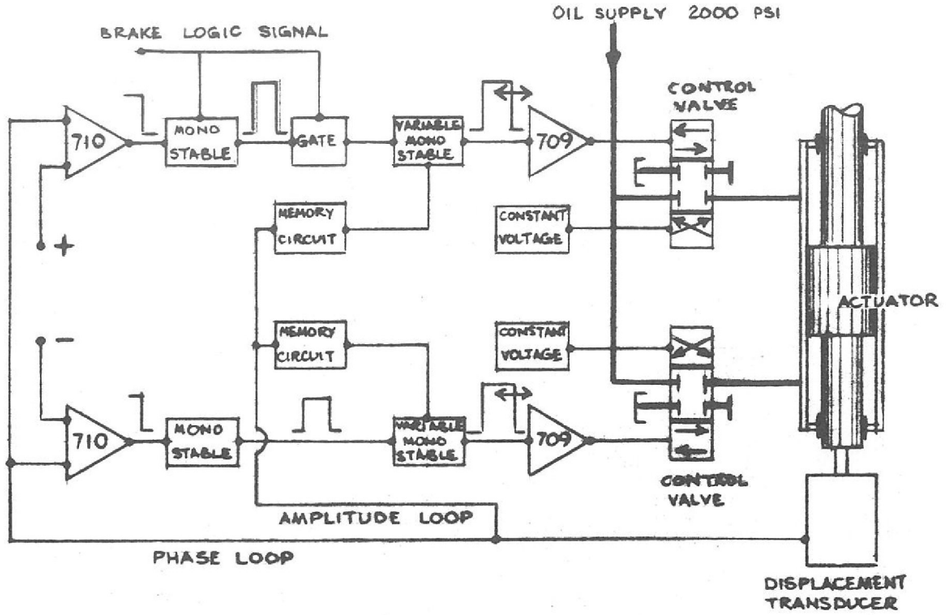

Figure 104. Schematic diagram showing system using two separate electro-hydraulic control valves. A memory circuit is also included.

(ii) In this method, energy is injected in discrete pulses to either side of the actuator via two separate valves, the pulse length determining the amount of energy injected. A memory circuit is included to make small adjustments to the pulse length in order to control and maintain the correct amplitude of the oscillating system as shown in figure 104. It proved to be relatively simple to control the amplitude to better than 0·5% despite a somewhat empirical setting-up procedure. Pressure spikes do not occur since the valves act only as switches; this has the further advantage that the system is not affected by component wear, temperature changes or drift.

Construction and testing of bellows made from fibre-glass cloth bonded with epoxy resin has demonstrated the feasibility of using this material in the expansion system of the proposed chamber. One-fifth scale model bellows have been manufactured and successfully life tested at both room temperature and in liquid nitrogen at 78°K. Testing during the present year has been continued and has been extended to cover one-fifth scale bellows bonded to flanges made of epoxy-bonded fibre-glass. An example of this latest-type of bellows is shown in figure 105. As part of the testing programme bellows have been subjected to both internal and external cyclical pressure variation. They have performed without failure for many millions of cycles with both higher pressures and higher (scaled) deflections than would be required for the High Field Bubble Chamber application.

Figure 105. Model bellows made from fibre-glass cloth bonded with epoxy resin.

Computer Studies of Simulated Bubble Chamber Pictures

To assist in the design of the optical system of the proposed chamber, it has been necessary to study in detail the general appearance of the resulting bubble chamber photographs. Computer programs have been written and used with a two-axis graph plotter to map typical bubble chamber events measured in existing chambers, or predicted events, through the geometry and optical system of the High Field Bubble Chamber. Thus it is possible to study the effect of changes in such parameters as chamber dimensions or lens characteristics on the appearance of the resulting pictures, and to evaluate the ease with which they can be scanned for interesting particle interactions. A set of such computer simulated pictures is shown in figure 106.

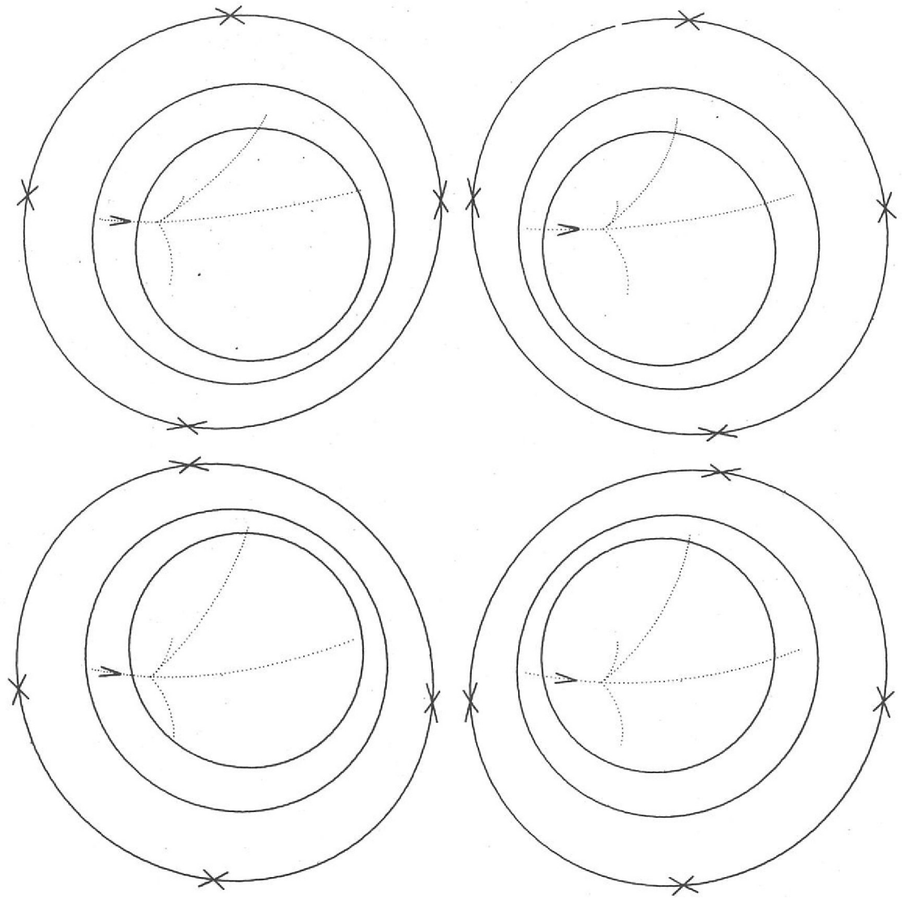

Figure 106. Set of computer simulated bubble chamber photographs.

SUPERCONDUCTING MAGNETS

Objectives (77a)

High energy physics relies extensively on the use of magnetic fields, in particular for the guide field of accelerators, for deflecting and focussing particle beams, and for momentum analysis in bubble chambers and spark chambers. Conventional iron cored magnets are limited typically to the range 10-20 kilogauss. Superconducting magnets offer the possibility of extending this range to 50-150 kilogauss. Although at present still in the development stage it seems likely that they will eventually be used instead of iron-cored magnets in many high energy physics applications.

The most clear-cut and economic case is for large bubble chamber magnets, and a number of such projects are in progress throughout the world. Economic and reliable designs for quadrupole and bending magnets have yet to be demonstrated, although prototype development is now well under way. Progress towards pulsed superconducting magnets, though in the early stages, is also encouraging, the objective being to increase the field strength of a synchrotron magnet by at least a factor 5, thus increasing the particle energy for a given ring diameter.

The development of this new technology involves the study of many unusual materials and engineering problems. The Rutherford Laboratory has been working in this field since the discovery of high field superconductors in 1961, and is now playing a leading role in the development of operational systems.

Filamentary Conductors (77b, 85)

The principal feature of the programme during 1969 was the successful continuation of the study of twisted filamentary composite conductors which were developed during 1967-8 in collaboration with Imperial Metals Industries (figure 107). Such conductors are essentially free from flux jump instabilities, and should operate reliably under both dc and pulsed conditions. Theoretical studies of these composites have been refined and extended to include effects arising from the self field of the wire, approximations to a fully three dimensional analysis, and the presence of more than one normal metal. A detailed programme of measurements on a range of samples and small coils has been completed, and these confirm the theoretical predictions of conductor stability as a function of filament diameter and overall diameter, and also the predictions of required rate of twist for a given normal metal resistivity.

Conductors containing larger numbers of finer filaments have now been fabricated by IMI (figure 108). These are designed to have an ac loss sufficiently low for pulsed operation (down to about 1 second rise time). A programme of coil tests has confirmed that these materials remain stable under ac conditions.

A set of five papers forming a complete review of experimental and theoretical work on these materials is now available as a preprint.

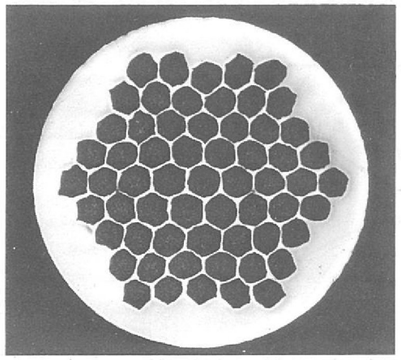

Figure 107. Cross-section of 61 filament conductor.

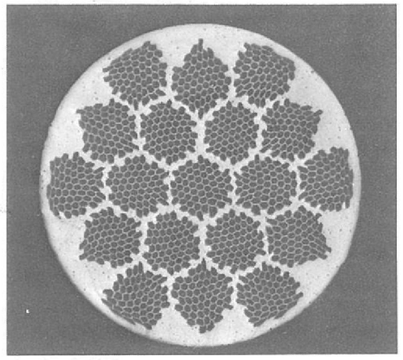

Figure 108. Cross-section of 1000 filament conductor.

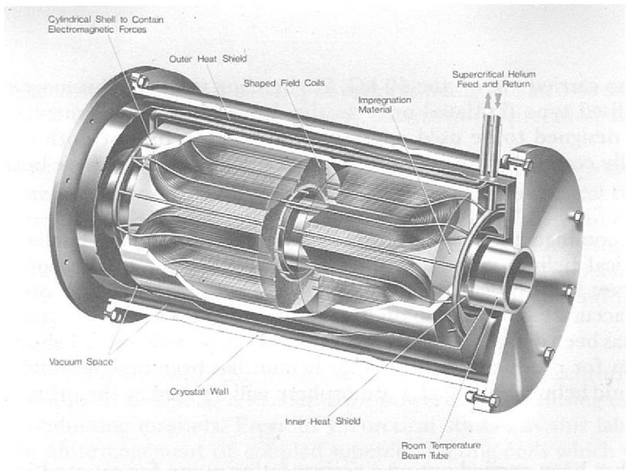

Figure 109. Proposed 40kG Quadruple Magnet.

Magnet Development

A number of 50 kG, 9 cm bore solenoids of filamentary conductor have been wound. These, in conjunction with the tests in smaller coils, confirmed that the material will give repeatable and predictable coil performance provided that internal heating of mechanical origin (e.g. wire movement) is prevented by, for example, vacuum impregnation with a material such as paraffin wax. However, coils potted in epoxy resin have not always reached short sample characteristics. This is believed to be due to internal cracking, releasing the stored energy which arises from differential thermal contraction. Methods of overcoming this difficulty by using loaded resin or other potting materials are being investigated.

To extend this study to full sized coils, a (non-operational) quadrupole type magnet to operate at 40 kG with a 12 cm aperture has been designed (figure 109).

This uses a 1500 A, fully transposed cable formed from 18 strands of 0·4 mm diameter 61 filament composite. A cable development programme carried out in collaboration with Ormiston (London) Ltd., showed that such a cable could be subsequently compacted into a square conductor to improve packing factor and current density.

This cable is being wound into a series of about 16 poles which are subsequently vacuum impregnated with various materials. Initially the poles are being tested separately to determine the most effective material for impregnation; at a later date four of the poles are to be assembled to form a complete quadrupole. During the period under review a series of test windings were made (using copper cable) to establish satisfactory techniques for both winding and impregnating, and manufacture of the first six superconducting poles was completed (figure 110). Full short sample current was reached in the wax impregnated coils, but, as indicated above, coils potted with unfilled resin still showed some degradation.

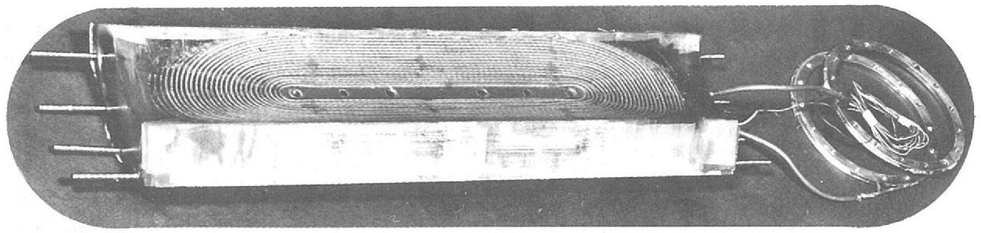

Figure 110. Resin impregnated pole for quadrupole magnet.

Further work was also carried out on the 40 kG, 2m bending magnet. This magnet is of the fully stabilised type (initiated prior to the development of filamentary conductors), and is designed to be used operationally. Manufacture of both coil and cryostat is initially complete; but final assembly and commissioning have been delayed.

Cryogenics

As an alternative to cooling superconducting coils by immersion in liquid helium, the use of supercritical helium circulated through tubes adjacent to the coil is being considered (figure 109). To gain practical experience in this method of cooling, and to obtain more accurate information on heat transfer and flow rates, a suitable horizontal cryostat has been designed for use with the quadrupole described above. In addition, a system for producing supercritical helium has been designed and is now being made. Liquid helium boiling at 1 atmosphere will be used as the primary refrigerant.

Development work has been carried out on a reciprocating pump for supercritical helium, and it is believed that a suitable combination of cylinder and piston materials has been found. Commissioning and testing of the complete system are scheduled for 1970.

Electrical Engineering Aspects

Further development work was required on the mechanical contactor which shorts out the coil when it has been energised in order to set up the persistent current mode of operation. The contactor must be capable of opening at full current (2000 A) to dump the stored energy into an external circuit during fault conditions or on normal shut-down. The persistent current mode requires a contact resistance not exceeding 5×10^{-7} ohms which must be repeatable after many contactor operations. Trouble has been experienced with icing on contacts during cool-down, and it has been concluded that the mechanical contactor cannot be considered sufficiently reliable to be used for this duty. Attention is therefore being concentrated on superconducting switches which are "opened" (i.e. driven into the normal state) by means of a heater coil.

Instrumentation has been developed to control the rate of cool-down so that thermal stresses in the cryostat are kept within acceptable limits. Field sensing devices and a system to monitor the onset of the normal state have also been developed as has a circuit for the regulation of the 2000 A power supply.

Materials (98, 118)

The preceding work is supported by a continuous programme of investigation of low temperature mechanical and thermal properties of materials. Materials studied during the past year include filled and unfilled epoxy resins, waxes, and various proprietary encapsulants, together with composite specimens to determine the properties of typical sections of impregnated superconducting windings.

Synchrotron Studies (111, 113, 227)

Serious consideration is now being given throughout the world to the possibility of using superconducting magnets in proton synchrotrons, both as a means of converting conventional accelerators to higher energy and eventually to reduce the size and cost of accelerators in the multi-thousand GeV range.

The economic and technological requirements for this application were first studied at this Laboratory during 1965-7, and the recent rapid growth of interest has resulted primarily from the successful demonstration that conductors with the necessary very fine filaments (figure 108) can be manufactured at reasonable cost, and will behave as predicted.

Much time has been spent in identifying the large number of problems to be tackled, and analysing their interrelation, and a balanced programme has been planned aimed at assessing the overall feasibility of the synchrotron. In particular

extensive model and prototype work is being initiated to ascertain how both long term reliability and the necessary constructional precision can be achieved.

Theoretical work continued on accelerator lattice design and its interaction with the magnet design and parameters. Preliminary theoretical studies of the optimum rise time indicated that values rather longer than in conventional machines (3-5 sec. instead of 1-2 sec.) might be advantageous from both economic and practical viewpoints. Preliminary assessments have also been made of various stray field effects and possible iron shielding requirements, but it is not yet possible to decide whether or not the latter will be essential.

Superconducting Power Supply

In association with the work on superconducting synchrotrons, the idea has been revived of designing a synchrotron power supply utilising energy storage in superconducting magnets. Previous theoretical studies at this laboratory (in 1967) led to an arrangement of coupled superconducting coils which would allow energy to be transferred reversibly between a superconducting synchrotron magnet and an energy storage coil. The idea as originally proposed is indicated in figure 111. Two mutually perpendicular coils, connected to the synchrotron and the storage coils, are free to rotate in a uniform external field. All the coils are superconducting. By rotating the system through 90° and back, energy can be transferred in and out of the synchrotron. The total energy in the system remains constant apart from frictional and similar losses; thus the external power required is negligible.

The size of the device would range typically from about 3m diameter for an energy transfer of $5 \cdot 10^7$ Joules, to 8m diameter for an energy transfer of 10^9 Joules. Such a system is in principle simpler and more versatile than a conventional power supply of the same output and should turn out to be cheaper.

Figure 111. Superconducting power supply basic energy transfer system.

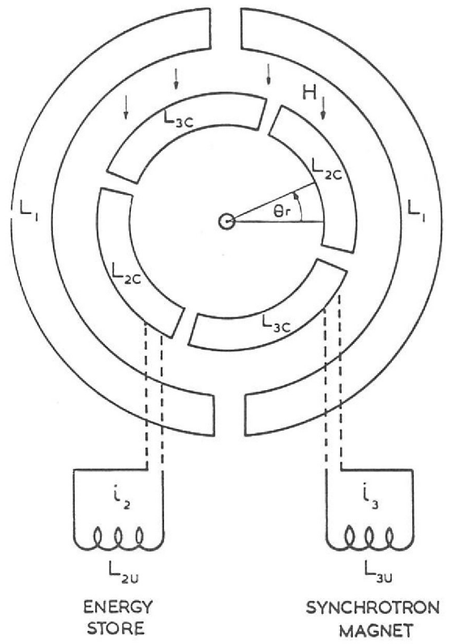

Further work during 1969 has resulted in a number of refinements to the original circuit, which should considerably reduce the constructional and operational problems. These, (indicated in figure 112) are

(a) to combine the energy storage coil with one of the rotating coils. This has the effect of allowing the two coils to be situated at different radii, and only the outer of the two needs to be well coupled to the field coil.

(b) to introduce a superconducting transformer between the power supply and the synchrotron. This allows a full 180° rotation to be used increasing the output by up to a factor 4, and allowing different operating currents and voltages for the synchrotron and power supply.

(c) To include an external variable inductance in the output circuit, which can be used (i) to compensate for errors and asymmetries in construction, and (ii) to produce automatic controlled movement of the rotor without an external drive.

As a result of these improvements the proposal now appears very much more realistic and more detailed feasibility studies are being initiated, including the construction of an electronic analogue to investigate detailed behaviour and control methods.

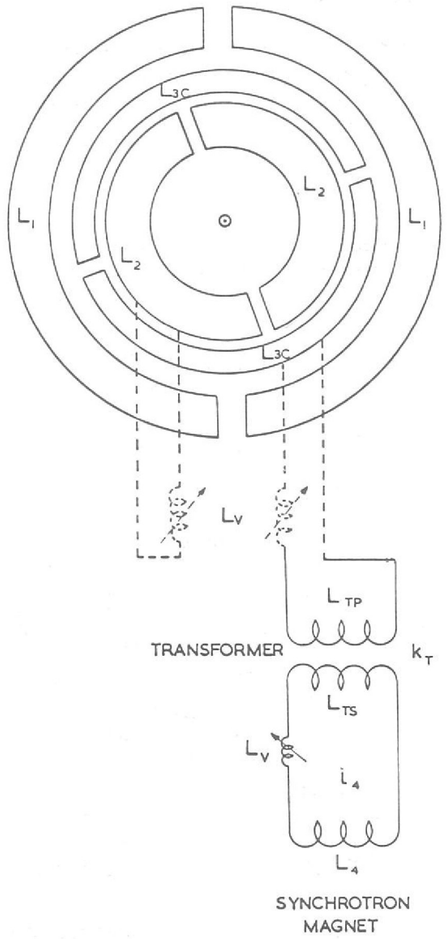

Figure 112. Superconducting power supply improved system.

MATERIALS TESTING AT LOW TEMPERATURES

(98, 118)

Many of the activities described in this Report involve the use of temperatures in the cryogenic range (i.e. 77°K and below). Since many constructional materials have markedly different properties in this region from those at room temperature, test facilities were introduced in 1966 and have been steadily extended and improved.

At present, mechanical properties can be investigated in a cryostat attached to an Instron test machine. This can apply forces of between 50 gf and 5,000 Kgf at various speeds, and specimens can be tested in tension, compression or bending. Deflections as small as 10^{-4} cm may be measured by a strain-gauge extensometer or a displacement transducer as appropriate, and characteristic curves can be plotted on an X-Y recorder. This equipment was demonstrated at the 1969 Physics Exhibition. An additional machine of 10,000 Kgf capacity is under construction. Other equipment to measure thermal conductivity is being designed.

The wide variety of materials studied includes aluminium alloys, stainless steel, bronzes and many non-metallic substances such as filled and unfilled epoxy resin, waxes, various proprietary encapsulants, glass fibre reinforced plastics and composites of these.

CONCRETE INSULATED MAGNETS

(223, 224)

A major problem in the design of some equipment for particle accelerators is that of damage by highly ionising radiation. Materials used for the insulation of magnet coils have shown good radiation resistance, but with future accelerator projects, a better material is required to withstand the considerably increased energies and intensities. The steady increase in performance of Nimrod may eventually impose a limit on the useful life of epoxy resin glass fibre composite insulation of magnets in critical locations. Degradation of an organic insulation results in a loss of strength and bond, a fall in insulation due to moisture absorption and dimensional changes due to gas evolution within the coil matrix.

The design and development has continued of magnets using concrete as an insulator; this material, being non-organic, has superior radiation resistance. A considerable amount of data regarding electrical and mechanical properties of concrete made from various cements and aggregates has been collected during the year, and the long term variations are being investigated.

In magnets using cementations aggregates as an insulating binder, the coils are completely embedded in concrete, which is carefully selected to give maximum insulating properties. The mix of aggregate is selected to permit the mixture to be pumped around the coils and yoke under pressure. Techniques are being developed to ensure that voids do not exist in the filling.

The coils are wound from bare conductor using suitable jigs to give the correct shape. Turn-to-turn spacing is provided by using small pieces of hard insulating material such as alumina or mica-glass sheet placed at intervals. Completed coils are fitted to a suitable iron yoke assembly using more strips of mica-glass to provide the appropriate coil-to-yoke spacing. A flight tube fitted with appropriate end-cheeks is mounted between the poles and the whole assembly is then filled with concrete made from an appropriate cement and a finely graded aggregate. The concrete is allowed to set for a suitable length of time and the whole assembly is then baked to drive off the surplus water not used for the hydration of the cement. The insulation resistance increases during the bake-out process, which is continued until an acceptable value is reached.

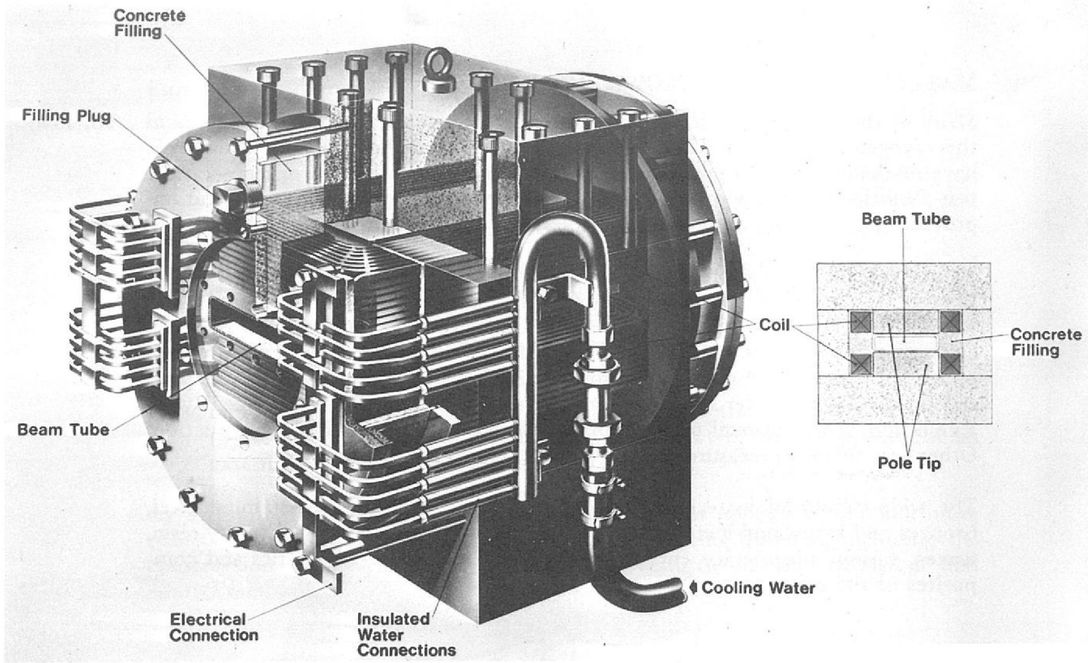

Figure 113. Medium-sized electromagnet using cementations insulation.

Concrete has good compressive strength properties but is poor in tension, and there are considerable advantages to be gained from constructing concrete-filled magnets in the form of a prestressed concrete beam, with the concrete under compressive stress. It is then possible to avoid the small cracks which may appear due to the slight shrinkage during the drying-out process. Problems arising from the differential thermal expansion of coil, yoke and insulating materials are also avoided. The prestressing can be achieved in a number of different ways, the simplest method being to provide a number of tie-bars through plates at each end of the magnet assembly and allow the cement fill to harden while the tie-bars are stressed using an outer framework. An alternative method which is being investigated involves mounting the whole magnet assembly inside a steel tube fitted with end-plates. Concrete is pumped into the tube and allowed to harden under pressure so that the outer steel tube is permanently under tensile stress.

A number of electromagnets have been constructed using the various techniques described. Figure 113 shows a medium-sized magnet which has been made for use in a high-intensity beam line at the Daresbury Laboratory. It is at present undergoing tests there.

The magnet characteristics are as follows:

Field intensity	11,400 gauss (14,800 gauss maximum)
Area of field	32 × 20 cm
Height of gap	5 cm
Cross-section of flight tube	20 × 5 cm
Length of flight tube	50 cm
Normal energising current	375 A (600 A maximum)
Power dissipation of windings	15 kW (48 kW maximum)
Cooling water flow	300 gall/hr
Total weight	600 Kg

The coils were wound in the form of a number of flat "pancakes" fitted with suitable spacers. These were then assembled onto a solid steel yoke into which was also fitted a stainless-steel beam tube to which had been welded heavy end-plates. A strong steel framework which could later be removed was spaced away from the beam tube end-plates, and heavy bolts supported by the framework were screwed into tapped holes in the end-plates. Bolts were also fitted through the clearance holes in the end-plates to screw into the yoke. The outer frame bolts were tightened, stressing the bolts which fitted into the yoke through the end-plate holes. The whole assembly was mounted on a vibrating table and a fine grade of concrete was poured into the magnet. It was allowed to harden, the framework was removed and the assembly was then baked until an acceptable insulation resistance had been achieved. All the exposed concrete surfaces were then sealed to prevent the absorption of moisture.

A second version of this magnet is being constructed using improved manufacturing techniques. A quadrupole magnet based on a DESY design is being produced by outside industry, their work being based on our experience and collaboration.

A variation in the use of concrete for magnet construction was proposed in the design of a magnet for the 300 Gev machine. Here, concrete is used to fix immovably the laminated yoke and to give rigidity to the magnet assembly. In this design it was possible to use organically insulated coils, or coils insulated by any other means, since the assembled yokes may easily be dismantled for coil replacement.

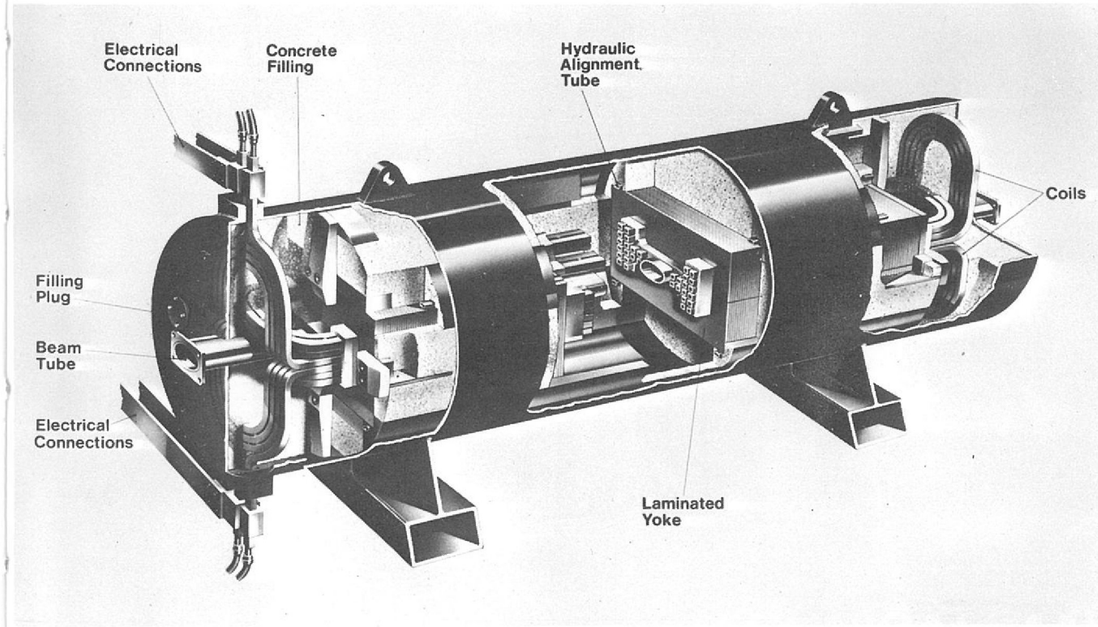

Figure 114. Illustration of proposed concrete insulated magnet for a 300 GeV Synchrotron.

TECHNICAL AND ADMINISTRATIVE SERVICES

Technical and Administrative Services

RADIATION PROTECTION AND OPERATIONAL HEALTH PHYSICS.

The Conference on Radiation Protection in Accelerator Environments, sponsored jointly by the Science Research Council and the Society for Radiological Protection, was held at the Laboratory in March 1969. The Radiation Protection Group was largely responsible for the initiation and organisation of this conference. Members of the Group also presented several papers and edited the proceedings. Over 100 participants, representing a wide variety of accelerator health physics interests, attended the conference.

Research and Development (77, 117, 127, 129, 131)

Studies of accelerator stray radiation field measurement and dosimetry have continued with further examination of the problems of interpreting and correlating data obtained with activation, threshold, emulsion and thermoluminescent detectors. Tissue equivalent dosimetry and LET spectrometry methods are being developed and will also be brought into this work.

Advice in matters relating to radiation safety methods, shielding, induced radioactivity and radiation damage has been given to assist Nimrod development as well as the 300 GeV and other design studies.

A low energy negative pion irradiation facility has been designed. This will be suitable for radiobiological and dosimetric studies directed mainly towards the study of the possibility of using stopping pions in radiotherapy. The Radiation Protection Group hopes to assist and co-operate with visiting radiobiologists in these studies.

During April, a study of the electron-induced cascade in shielding was carried out at NINA by members of the Radiation Protection Group and the Daresbury Health Physics Section. From measurements with activation detectors, thermoluminescent dosimeters and ionization chambers it was possible to deduce the importance of the nucleon-meson cascade relative to the electromagnetic cascade at different depths in typical shielding material.

A large tunnel has been constructed opposite the target of the X3 extracted beam, to enable measurements to be made of the transmission of radiation in a tunnel of very simple geometry. The results obtained are of use in the design of tunnels and ducts in shields for existing and future accelerators.

The analysis of large numbers of activation sample results from these experiments has been considerably assisted by a WANG 362 programmable electronic calculator. This calculator is particularly suitable for work such as this which involves relatively simple calculations on a large number of results.

Personal Dosimetry Service (130, 234, 235)

The six monthly issue of thermoluminescent dosimeters to lightly exposed persons, started last year, continues as a successful routine service. Reported doses have so far been trivial, indicating a correct initial choice of personnel for this service.

The problem of neutron dosimetry in the Nimrod leakage radiation environment has been empirically solved by using a 2 element dosimeter consisting of a neutron track film and a slow-neutron-sensitive thermoluminescent dosimeter. This has successfully overcome the spectrum dependent response of the track film alone.

A pilot scheme, with about 90 persons working in the Nimrod experimental halls, has been in operation since April to test the practical feasability and economics of the method. This has worked well and it is hoped in 1970 to use this method for all neutron track film wearers.

At September 1969, regular dosimeter issues were as follows:

Beta-gamma films (monthly issue)	510
Beta-gamma TLD (6-monthly issue)	320
Fast neutron films (monthly issue)	230
Fast neutron films plus slow neutron TLD (monthly issue)	90

The changes in numbers compared with 1968 are a result of "pruning" the system rather than any significant change in personnel numbers or their activities.

Gamma doses to personnel engaged in the maintenance and repair of Nimrod are expected to show an increase compared with 1968 mainly because of the increased active work load in dealing with three extracted proton beams. None, however, are expected to exceed 5 rem for the year.

Nimrod Environmental Surveys (112, 128, 132)

The commissioning and operation of a third extracted proton beam (X3) during the year has "spread" the pattern of induced activity over a larger area of the Nimrod complex with a consequent increase in the problems of personnel control.

The operation of the X2 extracted beam with its "leaky" blockhouse has continued to be the main cause of significant machine leakage radiation. The X3 blockhouse shielding proved to be adequate and so far there has been no machine leakage problems in Experimental Hall No. 3.

Other Buildings

There have been no requirements during the year to handle work involving significant amounts of loose contamination in the Radioactive Workshop (R52). Prior to its shutting down in October there were no changes of health physics significance on the PLA. All reported personnel doses are expected to be less than 1·5 rem for the year. In the Nuclear Chemistry Wing (R34) only very low levels of loose activity have been handled during the year. There has been an increasing tendency to use large sealed sources (up to tens of curies) for radiation damage studies.

SAFETY

The surveillance and inspection of potentially hazardous situations and equipment (e.g. high voltage and pressurised equipment) has continued to be the main preventative activity of the Safety Group, augmented by safety tours, the publication of "Safety News" and the arrangement of safety show-case displays. Information has been supplied to other institutions on matters in which the Laboratory has special expertise, notably the explosion hazards of flammable gases.

The number of items registered with the Safety Group and requiring periodic inspection increased by one-eighth to 3891, made up as follows: lifting tackle 2145, lifting machines 369, pressure vessels 793, high voltage equipment 384, breathing apparatus and safety equipment 134, fire prevention 66.

During the year a total of 126 (1968-123) injuries involving Laboratory staff were reported, 15 (15) of these resulted in lost time, the average absence being 20·1 (11·3) days. The causes of the accidents were:

Handling goods	42
Stepping on or striking objects	24
Falls of persons	26
Use of hand tools	15
Machinery	7
Falls of objects	2
Electric shock	3
Other causes	7

A nationally used method of representing injury incidence is to compute the Injury Frequency Rate which is defined as (number of injuries × 100,000)/(number of man-hours worked). The figure of 100,000 is the number of working hours in an average man's career; hence the IFR is the number of accidents to be expected during the average man's career. The RHEL figures are 4·61 (4·51) for all injuries and 0·549 (0·551) for lost-time injuries.

ENGINEERING

Building and Civil Engineering

No major works in this category have been called for this year; there has, however, been an increased load of minor alterations and additions to existing buildings to take account of the new requirements as the Laboratory's activities change. In this category come alterations to offices, laboratories, dark rooms and drawing offices in Buildings R1, R2 and R25, and extensions to R1 and R2 for workshops, plant rooms, stores and offices. Work has also been executed for the Atlas Computer Laboratory.

A job with some unconventional aspects was the construction of a steel and concrete blast wall between Hall 1 and the Hydrogen Bubble Chamber Annexe. This must withstand the effects of an explosion yet be moveable to allow heavy crane access into the Annexe. Construction was completed on schedule despite the difficulties of working in this highly congested area.

Mechanical Services

Extensions and additions to heating, ventilating and air-conditioning services have been carried out as required in connection with building extensions and modifications. Changes to site heating services included renewal of the supply pipes to the R12 area, which were among the oldest on site, and a redesign of the system in Building R7 which is a hazardous area since it houses a 10 inch hydrogen bubble chamber. Air conditioning plant for the IBM 360/75 central computer has been upgraded, and a large ventilation scheme for Building R25, to 'clean room' standards in places, was commissioned. Improvements have also been made to these services in the Lecture Theatre, in Buildings R6, R18 and R35, and at the Atlas Computer Laboratory.

Figure 115. The Rutherford Laboratory.

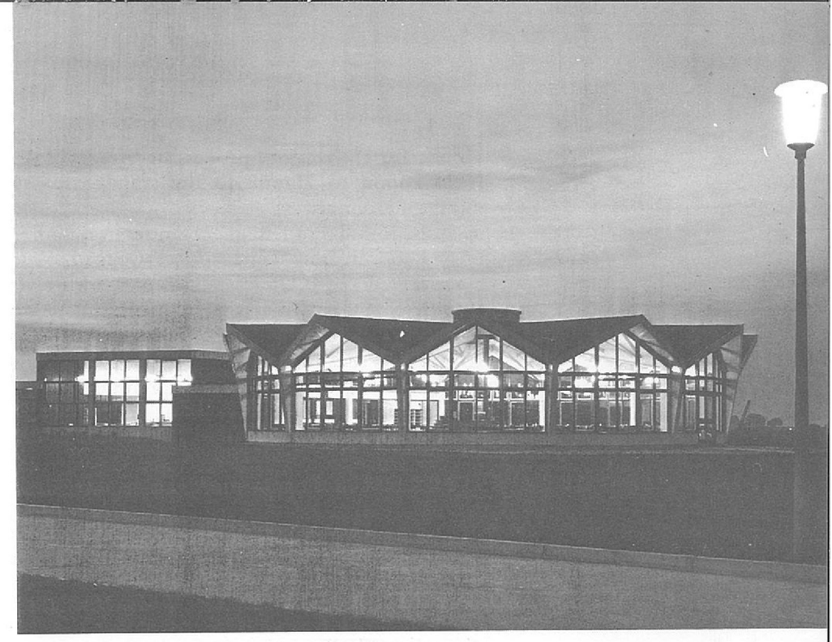

Figure 116. The Restaurant.

The Laboratory uses substantial quantities of liquid helium, and plant for recovering the boiled-off gas for re-liquefaction has been in use for some years. The collection mains have been extended to Buildings R6 (Hall 1), R25 and R55 (Hall 3) and additional high pressure storage vessels have been installed. The central compressor system has been automated, allowing the plant operator to spend more time in the areas where the liquid helium is actually used. A mobile trailer mounted compressor and gas bottle unit has been built for gas recovery from short-term experiments remote from existing installed collection points. A special unit has been built to recover helium from spark chambers, a prime requirement being that the back pressure had not to exceed $\frac{1}{32}$ inch water gauge in order to avoid damaging the fragile spark chamber foils. This was accomplished by use of a bellows-blower unit controlled by a sensitive knife-edge lever mechanism. The blower fed the helium into the site recovery mains via a non-return valve. This installation has already paid for itself by recovering 76,000 cubic feet of helium in 28 weeks.

Permanent platforms have been installed on the magnet room and Hall 3 cranes to facilitate maintenance of ceiling-mounted equipment. Mobile plant has been augmented by the acquisition of 2 new fork-lift trucks and a 45 ton tractor.

Electrical Services

The power distribution system for Hall 3 has been enlarged by the installation of a 3·3 kV, 5 MVA transformer and associated switch-gear in substation 15. Smaller capacity supplies were installed in connection with extensions to buildings and mechanical services, and for specialised purposes such as radiation monitoring. A thyristor control circuit to give smoother control of 5 ton fork lift trucks than is possible with contactors has been proven in service; it has produced other benefits such as reductions in wear, breakdowns and maintenance.

FILM PROCESSING

The Film Processing Laboratory, whose production is based principally on two large OMAC Friction Drive Machines of novel design, has continued in full operation. Basic research, and collaboration with film manufacturers has increased substantially the range of film stocks which may be correctly processed to satisfy the standards required by the various automatic film measuring machines which have come into operation over recent years. Apart from performing normal negative processing of film taken in spark and bubble chamber experiments and film 'printed out' by large modern computers, the Laboratory continues to provide a unique

service for the reversal processing of a large variety of film stocks of varying gauge from 16mm to 70mm, to the standards required by the measuring machines in numerous countries. A service has been provided for the processing of film for users of bubble and spark chambers on Nimrod, and also for the Atlas and Daresbury Laboratories, University of Oxford, Yale and Rutgers Universities USA and a variety of spark chamber groups working at CERN. Film exposed on the CERN 2 metre chamber which is to be measured on PEPR type machines is also processed at the Rutherford Laboratory. A total of $2{\cdot}2 \times 10^6$ feet of film was processed in 1969. The section has been consolidated during the year with the building and commissioning of a new photographic suite and a large film archive adjoining the film processing building. A full and comprehensive photographic service is now available to all users of the Laboratory.

ADMINISTRATION

CERN The experiments in the Laboratory's High Energy Physics programme being conducted at CERN continue to make demands on a number of administrative services particularly those responsible for the transport of stores and equipment and the travel and accommodation arrangements of the experimenters and their families.

The completion of the one experiment on the CERN PS has led to a reduction in the number of furnished apartments leased in Geneva from 20 to 11. 9 of these are sub-leased from CERN and 2 from private landlords. The CERN administration has continued to give valuable assistance in arranging leases and in administrative matters generally.

Accommodation During the year an extension to Building R1 was completed providing additional space for data preparation and offices. Following this it was possible to bring together in Building R1 the whole of High Energy Physics Division (apart from its Electronics Group) and Computer and Automation Division. The scientific teams working on the High Field Bubble Chamber project and on Superconducting Magnets are now accommodated with their supporting engineering teams in Buildings R25 and R50; this has resulted in more efficient co-ordination of effort in these two fields.

Future moves will extend the policy of concentrating associated activities and reducing the spread of individual Divisions among a number of buildings. In this way it will be possible for Divisions to manage their own accommodation on a day-to-day basis. The overall control of accommodation will rest with the Accommodation Working Party on which all Divisions are represented.

Housing During 1969 the open market rents of the Laboratory's 99 unfurnished houses were assessed by the District Valuer and approved by local Rent Officers. Increases in 1969 were limited to 15% or to a maximum of 10/- per week in compliance with the Prices and Incomes legislation, but a further increase in rent will be made towards the end of 1970 making a total increase of 30%.

The Laboratory's furnished houses are let at open market rents which are regularly reassessed. Approval has been given for the conversion of a cottage in the grounds of The Cosener's House as an additional furnished house.

Stores (239) A large proportion of the Stores accounting for higher valued or high turnover items is now processed on the Laboratory's IBM 360/75 computer. Seven programs are in use covering full details of items stocked, records of issues, charges to projects, and reordering. The cost of low value items is charged directly to Laboratory overheads and minimal clerical records are maintained.

Figure 117.

The Coseners House.

Finance

The Laboratory's expenditure for the financial year 1969/70 totalled £7·3 million of which £1·1 million was for capital items and £6·2 million was recurrent, the corresponding figures for the previous year being £7·5, 1·4 and 6·1 million. The items contributing to the total are shown below with last years figures in brackets. The pie chart (figure 118) shows the breakdown of the R & D expenditure; in this case a direct comparison with last year is not possible owing or organisational changes, though there have been no major changes in the spending pattern.

	£ million	
Staff Expenditure	2·51	(2·29)
Research and Development	3·72	(3·81)
Plant and Equipment	0·86	(0·67)
Building Works	0·21	(0·73)
	7·30	(7·50)

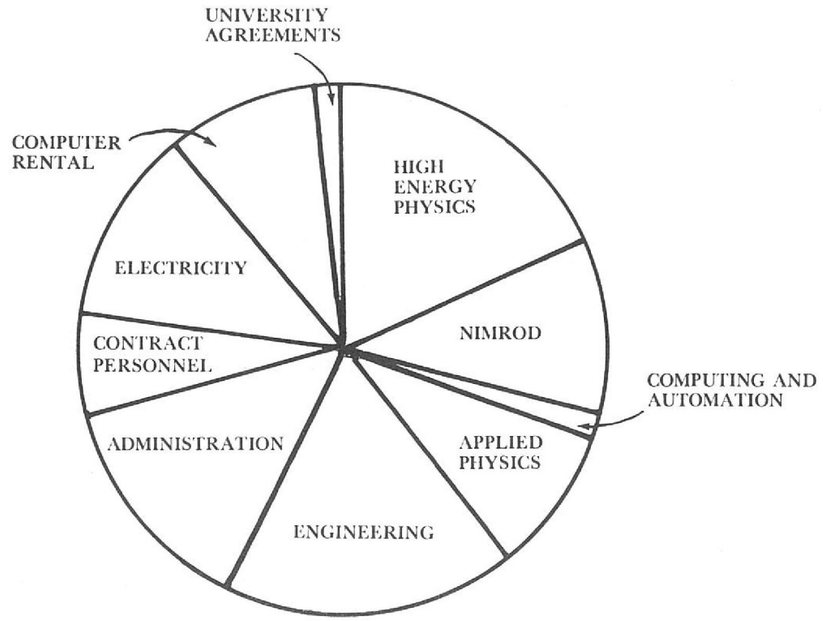

Figure 118. Breakdown of the £3·72 M R & D expenditure.

Staff Numbers The Table below shows the staff position at the beginning and end of the year.

Staff Numbers for 1969

	Opening Strength 1.1.69	Changes during 1969		Closing Strength 31.12.69
		Gains	Losses	
PROFESSIONAL				
Senior and Banded Staff	23	2	2	23
SO class	62	6	3	65
Fixed Term and Research Associates	47	26	25	48
Exp. O. class	126	5	15	116
Engineers I, II, III	100	4	5	99
ADE	5	0	0	5
Total Professional	363	43	50	356
ANCILLARY				
SA and SSA	57·5	9	15	51·5
Draughtsmen	42	7	8	41
Technical class	208·5	7·5	16	200
Non-Techs. and Stores	36	10	2	44
Executive	32	2	4	30
Librarian	0	1	0	1
Clerical	48·5	11·5	12·5	47·5
Secretarial and Typing	28	11	10	29
Photographers	4	0	0	4
Photoprinters	5	1	1	5
Machine Operators and Scanners	52	27·5	12	67·5
Asst. Hostel Manageress	1	1	1	1
Telephone Operators	2	0	0	2
Total Ancillary	516·5	88·5	81·5	523·5
INDUSTRIAL				
Craft	188	24	33·5	178·5
Non-craft	148	29	43	134
Apprentices	34	9	9	34
Total Industrial	370	62	85·5	346·5
GRAND TOTALS	1,249·5	193·5	217	1,226

The figures listed under "changes" include new entrants, resignations and promotions. Staff on sandwich courses, and those working part-time are counted as half.

Staff Relations The local Whitley Committee continued to be a useful forum for exchange of ideas between Staff Side and Management on non-industrial staff matters and working conditions generally. Much important discussion also took place both in associated committees and on an informal day-to-day basis between Official and Staff Side representatives, in order to implement decisions and to keep working agreements up-to-date. The viewpoints of each side on such problems as shift working, car parking and security of property have been freely discussed in the Whitley Committee.

The Restaurant and Suggestions Awards Committees, where Management, Staff Side and Trades Union Side are represented, are examples of participation by management/employee groups to ensure that Laboratory policy is successfully carried out. The future implementation of a proposed local Death Benefit Scheme is a further example of a joint involvement of Staff and Trades Union Sides with the Official Side.

During the year the Whitley Committee introduced and publicised the Civil Service Benevolent Fund to staff and a fine response of membership was achieved. In general the year was a busy one for the Committee which warmly acknowledges the participation by our sister establishment, the Atlas Computer Laboratory, in its activities.

The local Joint Consultative Committee continued to meet regularly during the year and in addition has held several special meetings to discuss and negotiate such subjects as productivity and changes in the pattern of shift working. An innovation has been the training of Shop Stewards through the medium of television when they viewed a BBC-1 series lasting ten weeks on the current topic of productivity bargaining. Ten half-hour broadcasts were viewed followed by a similar period of discussion and question answering. Shop Stewards have also visited the Daresbury Laboratory to view the progress of a pilot study into the feasibility of introducing a productivity agreement for industrial employees in the Science Research Council.

The SRC Joint Negotiating Committee approved and issued the Manual of Industrial Conditions of Employment and a personal Handbook for each employee was awaited as the year ended.

Training The most conspicuous feature of training at the Rutherford Laboratory in the academic year 1968-69 was the unusually large number (eight) of full-time and sandwich course students who satisfactorily completed courses of study. Three of these were holders of Laboratory Awards and the others were on unpaid leave, but receiving industrial training in the Laboratory where appropriate. One MSc in Plastics Technology was awarded and two first degree students were awarded First Class Honours, one in Applied Physics and one in the Physics and Technology of Electronics. The other awards were Upper Second Class Honours in Electronic Engineering, Lower Second Class Honours and Third Class Honours in Applied Physics, one ordinary degree in Applied Physics and one HND in Mechanical Engineering.

The level of day-release, block release and evening concessions for examinable courses showed a fall of 17% compared with last year, perhaps related to the reduced intake of junior scientific and technical grades and craftsmen. The overall pass-rate (related to concessions awarded) of 67% appears very satisfactory. Two day-release students passed the Part II examination for Grad Inst P at the first attempt, a very good achievement in the light of the high standard set in this examination. Staff of the Laboratory have made extensive use of short courses on technical and management topics arranged by the UKAEA, to the extent of 254 out of a total of 344 who attended short courses.

In addition to concessions awarded to permanent staff, thirty-three craft and student apprentices received training in the AERE Apprentice Training Scheme during the year. In the light of current discussion of technician training in the Haslegrave Report it is interesting to observe that slightly less than one third

of all concessions were awarded to grades which can be regarded as trainee grades (SA, CO, CA, MO and apprentices), one third to craftsmen and slightly more than one third to staff already doing technician work in its broadest sense (SSA, the Technician class and some members of the Experimental and Executive classes).

During the academic year the Laboratory provided industrial training for four members of its own staff attending sandwich courses and for 37 college-based sandwich course students in Applied Physics, Applied Chemistry, Applied Mathematics, Computer Science and Electronics. In the period between 1961 and the end of the academic year 1968-69, the Laboratory has provided industrial training for a total of 225 sandwich course students.

Liaison with Schools

In an effort to promote interest in technology and as a contribution towards arresting the drift of students away from science and technology, an experiment has been launched to bring science masters and pupils of nearby schools into contact with the work of the Laboratory. In one sense this is nothing new, for the Laboratory has always been willing to provide, on an ad hoc basis, speakers or assistance and advice on proposed experiments. Some impetus to formalise and enlarge these contacts was given during 1968 by the Reading University Technical Education Unit acting for the Schools Council Project Technology, and during 1969 considerable progress was made.

During July, 9 science masters and 1 6th form pupil spent a period of 4 weeks attached to various groups within the Laboratory. Partly as a result of these work periods, there are now seven schools in the area where senior pupils are undertaking small research projects, the results from which will be of genuine use to the research and development programme. Problems being studied include bearings in vacuum, Hall-plate fluxmeters, magnetostriction, Cerenkov counter gases and scintillation counters. The experience so far gained from this liaison is very encouraging. It is recognised that it is desirable to concentrate the Laboratory's collaboration onto a relatively small number of schools rather than offer what could only be superficial assistance to a larger number.

A number of contributions, including an account of the masters' visit, have been written for the publication "Project" which is published for the Department of Education and Science by the Central Office of Information to keep 5th and 6th formers informed about science, technology and engineering.

Exhibitions

At the 1969 Physics Exhibition held in London during March, the Laboratory displayed three items: automatic data read-out from spark chambers using an on-line digital computer (see figure 119), mechanical testing at 4·2°K, and a high stability Hall-effect fluxmeter. Superconducting magnet technology in high energy physics was the theme of the RHEL contribution to the French Physics Exhibition in December, with emphasis on the utilisation of superconductors in the proposed High Field Bubble Chamber. (See figure 120).

Figure 119. A section of the Laboratory's display at the Physics Exhibition.

Figure 120. Part of the Laboratory's display at the French Physics Exhibition.

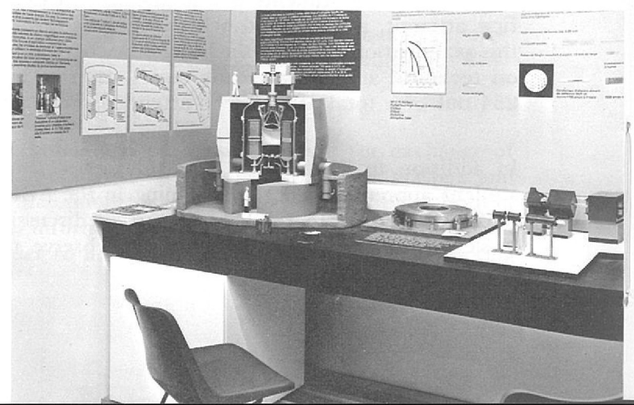

Figure 121. Visit by members of the Science Research Council.

Two devices developed in the Rutherford Laboratory were on show at the Annual Electronics, Instruments, Controls and Components Exhibition which took place in Manchester in September. These were an electronic analogue wattmeter to measure rapid power changes (such as occur in the Nimrod magnet power supply for which the instrument was originally developed), and a cryogenic liquid level sensor, based on a silicon diode, and used in liquid hydrogen targets and cryostats. Patent action has been taken in respect of both the above inventions.

Conferences, Meetings and Visits

Two conferences were organised during the year; technical sessions were held in the Lecture Theatre, with accommodation for visiting participants provided in Oxford Colleges. There were 130 participants in the Radiation Protection in Accelerator Environments Conference (March 27-28) and 200 at the annual pre-Christmas Theoretical Physics Meeting (December 15-17). The Laboratory also provided facilities for a nuclear physics community "Town Meeting" (June 13), a discussion with a group of staff from the Lawrence Radiation Laboratory USA (August 21-22) and a joint meeting with NINA users to discuss the HEP research programmes of the two Laboratories (December 12-13).

Selected parts of the Laboratory's work were shown to members of the Science Research Council on the afternoon of May 20, the monthly Council meeting being held in the Laboratory the following day. Conducted tours have also been organised for groups of students and members of professional and learned societies. The number of visitors during 1969 was 1652, a substantial increase on the 1968 figure of 1050.

Other Services

Many groups and sections throughout the Laboratory provide support services of a more or less conventional nature and, as might be expected, operate in much the same way from one year to the next. Some statistics are given below to place on record the scale of operations in fields where there are no innovations to report. 1968 figures are given in parentheses for comparison.

21,600 (23,800) invoices paid, total value £4·78M (£5·21M).
508 (366) short term overseas visits arranged.
9,350 (8,500) travel and subsistence claims paid.
650 (650) jobs completed in RHEL workshops.
1,000 (2,000) jobs executed by outside industry.
Value of work in hand by industry at any time £46K (£32K).
130,000 (125,000) dye-line prints produced internally.
70,000 (60,000) drawings on microfilm.
27 (34) University agreements in force.
7,500 (6,100) items borrowed from the Library.
Library stock includes 7,500 (6,800) books and 18,700 (14,700) reports.
325 (267) addresses on the world-wide literature exchange list.
16 (16) reports (RHEL/R) and 51 (53) preprints (RPP) issued.

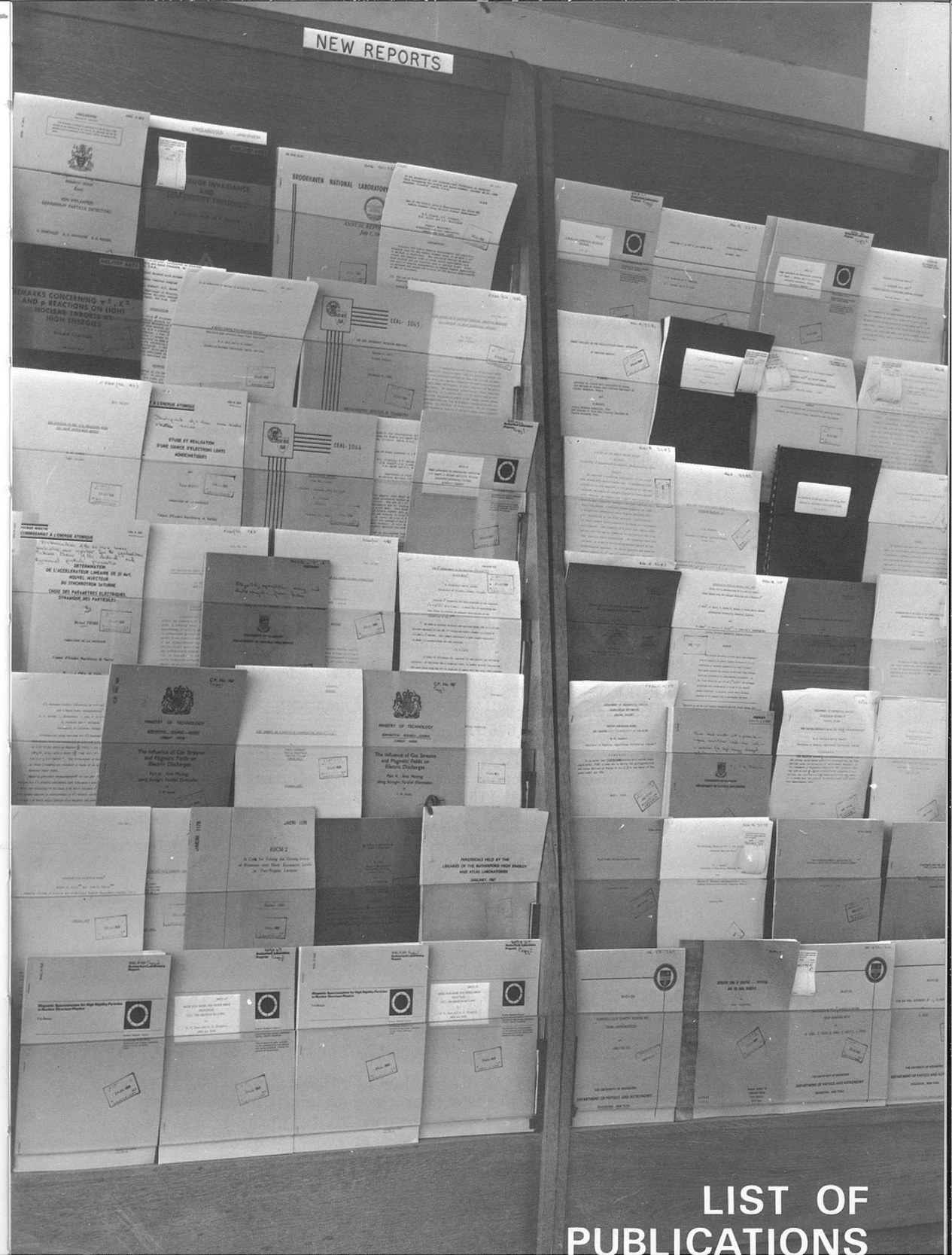
NEW REPORTS
LIST OF
PUBLICATIONS

List of Publications

JOURNAL ARTICLES

1 ARNISON G. T. J., WATKINS I. L., OLSEN R.
The fabrication and operation of remote ferrite core read-out wire spark chambers.
Nucl. Instrum. Meth., **76** (1) 177 (December 1969).

2 ASHKIN J., KABIR P. K.
Graphical representation of CP non-conservation parameters in K° decay.
Phys. Rev. (in the press).

3 ATKINSON D., DIETZ K.
Infinitely rising Regge trajectories and crossing symmetry.
Phys. Rev., 177 (5) 2579 (January 1969), preprinted as RPP/A42.

4 BARGER V., MICHAEL C.
Broken-duality model for pp → π^+d.
Phys. Rev. Lett., 22 (24) 1330 (June 1969).

5 BARGER V., MICHAEL C., PHILLIPS R. J. N.
Baryon exchanges from u-channel finite energy sum rules.
Phys. Rev., 185 (5) 1852 (September 1969).

6 BARGER V., PHILLIPS R. J. N.
Duality-preserving Regge cuts.
Phys. Lett., **29B** (10) 676 (August 1969).

7 BARGER V., PHILLIPS R. J. N.
Exploratory deductions at large t from new πN data.
Phys. Rev. Lett., 22 (3) 116 (January 1969).

8 BARGER V., PHILLIPS R. J. N.
Meson Regge exchanges from simultaneous analysis of πN scattering data and dispersion sum rules.
Phys. Rev., **187** (5) 2210 (November 1969).

9 BARGER V., PHILLIPS R. J. N.
Polarization and spin-rotation predictions from a new Regge fit to πN scattering.
Phys. Lett., **29B** (8) 503 (July 1969).

10 BATTY C. J., BONNER B. E., KILVINGTON A. I., TSCHALÄR C., WILLIAMS L. E., CLOUGH A. S.
Intermediate energy neutron sources.
Nucl. Instrum. Meth., **68** (2) 273 (February 1969), preprinted as RPP/P19.

11 BATTY C. J., FRIEDMAN E., GREENLEES G. W.
An analysis of quasi-elastic (p, n) reactions using a reformulated optical model.
Nucl. Phys., **A127** (2) 368 (April 1969), preprinted as RPP/P20.

12 BATTY C. J., GREENLEES G. W.
Proton and neutron distributions calculated using an effective single particle potential.
Nucl. Phys., **A133** (3) 673 (August 1969), preprinted as RPP/P21.

13 BATTY C. J., TSCHALÄR C.
The D-parameter for proton-nucleus scattering at 50 MeV.
Nucl. Phys., (in the press), preprinted as RPP/P26.

14 BLAIR I.M., TAYLOR A. E., CHAPMAN W. S., KALMUS P. I. P., LITT J., MILLER M. C., SHERMAN H. J., ASTBURY A., SCOTT D. B., WALKER T. G.
A study of nucleon isobar production in proton-proton collisions.
Nuovo Cim., 63A (2) 529 (September 1969), preprinted as RPP/H53.

15 BOWLER M. G., CASHMORE R. J.
Single pion production in π^+p interactions between 0·6 and 0·8 GeV/c.
Nucl. Phys., (in the press), preprinted as RPP/H59.

16 BRUNT D. C., CLAYTON M. J., WESTWOOD B. A.
Inelastic reactions in proton-deuteron scattering at 1·825 and 2·11 GeV/c.
Phys. Rev., **187** (5) 1856 (November 1969).

17 BUSZA W., DUFF B. G., GARBUTT D. A., HEYMANN F. F., NIMMON C. C., POTTER K. M., SWETMAN T. P., BELLAMY E. H., BUCKLEY T. F., DOBINSON R. W., MARCH P. V., STRONG J. A., WALKER R. N. F.
$\pi^{\pm}$p elastic scattering in the 2 GeV region.
Phys. Rev., **180** (5) 1339 (April 1969), preprinted as RPP/H49.

18 CARROLL A. S., CORBETT I. F., DAMERELL C. J. S., MIDDLEMAS N., NEWTON D., CLEGG A. B., WILLIAMS W. S. C.
Study of neutral final states produced in πp collisions at momenta of 1·71-2·46 GeV/c.
Phys. Rev., **177** (5) 2047 (January 1969).

19 CAVANAGH P. E., COLEMAN C. F., HARDACRE A. G., GARD G. A., TURNER J. F.
A study of the nuclear structure of the odd tin isotopes by means of the (p, d) reaction.
Nucl. Phys., **A141** (1) 97 (January 1970).

20 CLARKE N. M., BURGE E. J., SMITH D. A., DORE J. C.
Angle determination by sonic spark chamber in nuclear scattering experiments.
Nucl. Instrum. Meth., (in the press).

21 CLOUGH A. S., BATTY C. J., BONNER B. E., TSCHALÄR C., WILLIAMS L. E., FRIEDMAN E.
The isospin-dependent microscopic interaction.
Nucl. Phys., **A137** (1) 222 (November 1969), preprinted as RPP/P23.

22 CLOUGH A. S., BATTY C. J., BONNER B. E., WILLIAMS L. E.
A microscopic analysis of the (p, n) reaction on 1p shell nuclei.
Nucl. Phys., (in the press), preprinted as RPP/P25.

23 COLLEY D. C., EASTWOOD D., MACDONALD F., BLAIR W., GORDON J., HUGHES I. S., TURNBULL R. M., CHAUDHURI P., ESKREYS A., MILLER D. B., GOLDSACK S. J., BLUM W., DEHN G., DROSSELMEYER E., WOLF G., LOCKE D. H., LYONS L., WILKINSON K. I., FINNEY P., FISHER C. M.
Analysis of $\bar{K}N\pi\pi$ final states produced in K^-p interactions at 6 GeV/c.
Nuovo Cim., 59A (4) 519 (February 1969).

24 COUPLAND J. H.
Dipole, quadrupole and higher order fields from simple coils.
Nucl. Instrum., Meth., 78 (2) 181 (February 1970), preprinted as RPP/A68.

25 COX C. R., DUKE P. J., HEARD K. S., HILL R. E., HOLLEY W. R., JONES D. P., SHOEMAKER F. C., THRESHER J. J., WARREN J. B., SLEEMAN J. C.
Scattering of K^- mesons in the momentum range 1·08 to 1·37 GeV/c from a polarized proton target.
Phys. Rev., 184 (5) 1443 (August 1969), preprinted as RPP/H45.

26. COX C. R., DUKE P. J., HEARD K. S., HILL R. E., HOLLEY W. R., JONES D. P., SHOEMAKER F. C., THRESHER J. J., WARREN J. B., SLEEMAN J. C.
Scattering of π^- mesons in the momentum range 0·643 to 2·14 GeV/c from a polarized proton target.
Phys. Rev., 184 (5) 1453 (August 1969), preprinted as RPP/H46.

27 DANYSZ J. A., SPIRO M., VERGLAS A., BRUNET J. M., NARJOUX J. L., PENNEY B., THOMPSON G., LEWIS P. H., ALLEN J. E., MARCH P. V.
K^+p elastic scattering in the intermediate momentum range region (2·1-2·7 GeV/c).
Nucl. Phys., **B14** (1) 161 (November 1969).

28 DASS G. V., FROGGATT C. D.
Regge pole model for vector meson production — II: the reaction $KN \to K^*N$.
Nucl. Phys., **B10** (1) 151 (April 1969), preprinted as RPP/A47.

29 DASS G. V., KABIR P. K.
Possible charge asymmetry in radiative $\tau^\pm$ decays.
Phys. Rev. Lett., 22 (22) 1224 (June 1969), preprinted as RL/K/16.

30 DASS G. V., MICHAEL C., PHILLIPS R. J. N.
Regge pole models for kaon-nucleon scattering.
Nucl. Phys., B9 (4) 549 (March 1969).

31 DASS G. V., PAPAGEORGIOU S.
$A_1 \to 3\pi$ decay.
Nuovo Cim., 64A (1) 36 (November 1969), preprinted as CERN/TH/1036.

32 EDGINGTON J. A., HOWARD V. J., MILLER M. C., OTT R. J., DUKE P. J., HILL R. E., HOLLEY W. R., JONES D. P., THRESHER J. J., SLEEMAN J. C.
Polarization of Σ^- in the reactions $\pi^-p \to \Sigma^-K^+$ at 1130 MeV/c.
Phys. Rev., 177 (5) 2103 (January 1969), preprinted as RPP/H47.

33 EDWARDS V. R. W.
Some studies of realistic form factors for (d, p) and (p, d) reactions in the lead region.
Nucl. Phys., **A138** (3) 671 (December 1969).

34 EMMERSON J. McL., QUIRK T. W.
Branching ratio and possible CP non-conservation in radiative $K\pi 2$ decay.
Phys. Rev. Lett., 23 (7) 393 (August 1969), preprinted as RPP/H56.

35 FIELD J. H.
Effects of $\Delta S = -\Delta Q$ amplitudes on μ polarization in $K_L \to \pi\mu\nu$ decays.
Nuovo Cim., 64A (1) 184 (November 1969), preprinted as RPP/H55.

36 FIELD J. H.
Possible contributions of $\Delta S = -\Delta Q$ amplitudes to $K^\circ \ell 3$ decay rates.
Nuovo Cim., 61A (3) 532 (June 1969), preprinted as RPP/H51.

37 FROGGATT C. D., MORGAN D.
Non-evasive Chew-Low extrapolation for the study of $\pi\pi$ elastic scattering.
Phys. Rev., 187 (5) 2044 (November 1969), preprinted as RPP/A65.

38 GAILLARD J. M., GALBRAITH W., HUSSRI A., JANE M. R., LIPMAN N. H., MANNING G., RATCLIFFE T. J., FAISSNER H., REITHLER H.
The decay of long-lived neutral kaons into two neutral pions.
Nuovo Cim., 59A (4) 453 (February 1969), preprinted as RPP/H35.

39 GRIFFITHS R. J., HARBISON S. A.
Measurements of nuclear reaction cross-sections related to the anomalous composition of 3 Centauri A.
Astrophys. J., (in the press).

40 HARBISON S. A., GRIFFITHS R. J., KINGSTON F. G., JOHNSTON A. R., SQUIER G. T. A.
Nucleon-nucleon final state interactions in the reactions He^3 (p, d) 2p, He^4 (p, t)2p, He^4 (p, He^3)pn.
Nucl. Phys., **A130** (3) 513 (June 1969).

41 HERBST L. J.
Fast amplitude discriminators for nuclear instrumentation.
Nucl. Instrum. Meth., 70 (2) 189 (April 1969).

42 HERBST L. J.
Fast d.c. coupled analogue fan-in and fan-out modules.
Nucl. Instrum. Meth., 70 (2) 185 (April 1969).

43 HENZI R., KOTANKSI A., MORGAN D., VAN HOVE L.
$\bar{K}^-p$ and $\bar{p}p$ elastic scattering and the shadow of generalised anihilation processes.
Nucl. Phys., **B16** (1) 1 (January 1970), preprinted as CERN/TH/1086.

44 HEY A. J. G., KABIR P. K.
Nucleon polarization transfer in high-energy electron scattering.
Phys. Rev., 187 (5) 1990 (November 1969).

45 JACKSON D. F.
Effective nucleon number in high energy reactions.
Nuovo Cim., 63A (1) 343 (September 1969).

46 JACKSON D. F., KEMBHAVI V. K.
Scattering of medium energy alpha particles. II — Microscopic analysis of elastic scattering.
Phys. Rev., 178 (4) 1626 (February 1969).

47 KABIR P. K.
Can CP-invariance be saved?
Phys. Rev. Lett., 22 (19) 1018 (May 1969).

48 KABIR P. K.
η-asymmetry without C—non-conservation?
Phys. Rev., 178 (5) 2486 (February 1969).

49 KABIR P. K.
Questions raised by CP—non-conservation.
Springer Tracts in Modern Physics, 52.

50 KAMAL A. N.
Crossing symmetry, current algebra and the KSRF relation.
Phys. Rev., **180** (5) 1454 (April 1969).

51 KAMAL A. N.
Spectral function sum rules in a broken SU(3) symmetry.
Nucl. Phys., **B12** (1) 123 (August 1969), preprinted as RPP/A60.

52 KAMAL A. N., KENNY B. G.
Calculation of Re ϵ for the $K^\circ\overline{K}^\circ$ system.
Phys. Rev., **186** (5) 1473 (October 1969), preprinted as RPP/A66.

53 KAMAL A. N., SHYMKO R. M.
Pion form factors and phase shifts.
Ziet. Phys., **228** (2) 120 (October 1969).

54 KARBAN O., GREAVES P. D., HNIZDO V., LOWE J., BEROVIC N., WOJCIECHOWSKI H., GREENLEES G. W.
The elastic scattering of protons by O^{16} in the energy range 16 to 30 MeV.
Nucl. Phys., **A132** (3) 548 (August 1969).

55 KARBAN O., GREAVES P. D., LOWE J., HNIZDO V.
Polarization in B^{11} (p, p) and B^{11} (p, p′) at 30·3 MeV.
Nucl. Phys., **A133** (2) 255 (August 1969).

56 KENNY B. G.
A consequence of T violation in Kℓ3 decay.
Nuovo Cim. Lett., **1** (15) 746 (May 1969).

57 KENNY B. G.
Charge asymmetry in $K_2^\circ \to \pi^\pm \ell^\mp \nu$.
Phys. Rev., **179** (5) 1617 (March 1969).

58 KENNY B. G., OADES G. C.
The form factors for Kℓ3 decays.
Nucl. Phys., **B11** (1) 222 (June 1969), preprinted as RPP/A62.

59 KILVINGTON A. I., BAKER C. A., ILLINESI P.
Reflective coverings for scintillation counters.
Nucl. Instrum. Meth., (in the press).

60 LAWSON J. D.
The dynamics of high current electron ring beams in a time varying magnetic field with axial symmetry.
Phys. Lett., **29A** (6) 344 (June 1969).

61 LEA A. T., OADES G. C., WARD D. L., COWAN I. M., GIBSON W. M., GILMORE R. S., MALOS J., SMITH V. J., KEMP M. A. R.
Further evidence for $N^*_{1/2}$ nucleon resonances in the mass range 1800-2200 MeV.
Phys. Lett., **29B** (9) 584 (August 1969), preprinted as RPP/H57.

62 L'ECUYER J., GILL R. D., RAMAVATARAM K., CHANT N. S., MONTAGUE D. G.
The Ne^{20} (p, t) Ne^{18} reaction as a test of the Ne^{18} wave function.
Phys. Rev., (in the press), preprinted as RPP/P24.

63 LITCHFIELD P. J.
Inelastic π^+n interactions in the centre-of-mass energy range 1·40-1·65 GeV.
Phys. Rev., **183** (5) 1152 (July 1969), preprinted as RPP/H52. Erratum ibid., **188** (5) 2544 (December 1969).

64 LO S. Y.
Zeros in the droplet model.
Nuovo. Cim. Lett., 2 (4) 124 (August 1969), preprinted as RPP/A64.

65 MICHAEL C.
Double Regge-pole exchange and K^-p backward scattering.
Phys. Lett., **29B** (4) 230 (May 1969).

66 MICHAEL C.
Exchange degeneracy, duality and Regge cuts.
Nucl. Phys., **B13** (3) 644 (November 1969).

67 MICHAEL C.
Regge pole absorption model for πN charge exchange and cross-over.
Nucl. Phys., **B8** (2) 431 (December 1968), preprinted as RPP/A45.

68 MICHAEL C., WILKIN C.
Elastic pion-deuteron scattering at high energies.
Nucl. Phys., **B11** (1) 99 (June 1969).

69 MITRA A. N.
Form factors for hadronic decays in broken SU(6) × O(3).
Nuovo. Cim., **61A** (3) 344 (June 1969).

70 MORGAN C. G., JACKSON D. F.
Scattering of medium energy alpha particles. III — Analysis of elastic and inelastic scattering from Ca^{42} and Ti^{50}.
Phys. Rev., **188** (4) 1758 (December 1969).

71 MORGAN D., SHAW G.
Low energy pion-pion parameters from forward dispersion relations.
Nucl. Phys., **B10** (2) 261 (April 1969).

72 PAJAS P., WINTERNITZ P.
Representations of the Lorentz group: new integral relations between Legendre functions.
J. Math. Phys., (in the press), preprinted as RPP/A61.

73 PHILLIPS R. J. N., RINGLAND G. A.
Resonance recognition criteria in a Veneziano model.
Nucl. Phys., **B13** (2) 274 (October 1969).

74 PORTNER P. M., MOORE R. B.
An improved cryogenic target for nuclear experiments with He^3 and He^4.
Nucl. Instrum. Meth., (in the press).

75 RANFT G., TURNBULL R.
A double-Regge analysis of the reaction $K^-p \to K^-\omega p$.
Nuovo Cim., **61B** (2) 317 (June 1969), preprinted as RPP/H48.

76 SCOTT D. K., PORTNER P. N., NELSON J. M., SHOTTER A. C., MITCHELL A. J., CHANT N. S., MONTAGUE D. G., RAMAVATARAM K.
The reactions N^{14} (p, He^3) C^{12}, N^{14} (d, α) C^{12}, C^{13} (p, d) C^{12} and the 4+ level of C^{12}.
Nucl. Phys., **A141** (3) 497 (February 1970).

77 SHAW K. B., STEVENSON G. R., THOMAS R. H.
Evaluation of dose equivalent from neutron energy spectra.
Health Phys., **17** (3) 459 (September 1969), preprinted as RPP/R5.

77a SMITH P. F.
The technology of large superconducting magnets. Guide to Superconductivity (Fishlock D. ed.) MacDonald 1969.

77b SMITH P. F., BARBER A. C.
New three-component superconducting composites.
Cryogenics, 9 (6) 483 (December 1969).

78 SMITH W. A., ELLIOT C. T., CHATTERTON P. A., PULFREY D. L.
A photographic study of electrical breakdown at small gaps in vacuum.
Brit. J. Appl. Phys. (J. Phys. D) Ser. 2, 2 (7) 1005 (July 1969), preprinted as RPP/N14.

79 SQUIER G. T. A., JOHNSTON A. R., SPIERS E. W., HARBISON S. A., STEWART N. M.
Cross-section measurements for the reactions B^{10} (p, d) B^{9} and B^{10} (p, t) B^{8}.
Nucl. Phys., A141 (1) 158 (January 1970).

80 THOMAS G. L.
A comment on proton and neutron distributions in Ca^{40}.
Phys. Lett., 28B (7) 446 (January 1969).

81 THOMAS G. L., BURGE E. J.
Differences in optical model parameters between pairs of isotopes as found from difference functions of scattering data.
Nucl. Phys., A128 (3) 545 (May 1969).

82 TSCHALÄR C., BATTY C. J., KILVINGTON A. I.
A polarization analyser for 40 and 50 MeV protons.
Nucl. Instrum. Meth., 78 (1) 141 (February 1970).

83 TSCHALÄR C., MACCABEE H. D.
Energy straggling measurements of heavy charged particles in thick absorbers.
Phys. Rev., (in the press).

84 WILLIAMS L. E., BATTY C. J., BONNER B. E., TSCHALÄR C., BENÖHR H. C., CLOUGH A. S.
Evidence for broad resonances in the three nucleon system.
Phys. Rev. Lett., 23 (20) 1181 (November 1969).

85 WILSON M. N., WALTERS C. R., LEWIN J. D., SMITH P. F., SPURWAY A. H.
Experimental and theoretical studies of filamentary superconducting composites.
Brit. J. Appl. Phys. (J. Phys. D)., (in the press), preprinted as RPP/A73.

UNPUBLISHED PREPRINTS

86 BAKER C. A., BONNER B. E., BLAIR I. M., BRADY F. P., EDGINGTON J. A., HOWARD V. J.
A measurement of nuclear interactions in plastic scintillators.
RPP/P22.

87 BARGER V., PHILLIPS R. J. N.
Regge cuts, Pomeranchuk theorem and the Serpukhov total cross-section data.
Wisconsin preprint COO-260.

88 BERTHON A., RANGAN L. K., VRANA J., BUTTERWORTH I., LITCHFIELD P. J., SEGAR A. M., SMITH J. R., MEYER J., PAULI E., TALLINI B.
The reaction $K^{-}p \to \Lambda\pi^{\circ}$ in the c.m. energy range 1915 to 2168 MeV.
RPP/H60.

89 BOTTERILL D. R., BROWN R. M., CLEGG A. B., CORBETT I. F., CULLIGAN G., EMMERSON J. McL., FIELD R. C., GARVEY J., JONES P. B., MIDDLEMAS N., NEWTON D., QUIRK T. W., SALMON G. L., STEINBERG P. H., WILLIAMS W. S. C.
Form factors in the decay $K^{+} \to \pi^{\circ}\ell^{+}\nu$.
RPP/H62.

90 COX G. F., ISLAM G. S., COLLEY D. C., EASTWOOD D., FRY J. R., HEATHCOTE F. R., CANDLIN D. J., COLVINE J. G., COPLEY G., FANCEY N. E., MUIR J., ANGUS W., CAMPBELL J. R., MORTON W.T., NEGUS P. J., ALI S. S., BUTTERWORTH I., FUCHS F., GOYAL D. P., MILLER D. B., SCHWARZCHILD B.
A partial wave analysis of the reaction $K^{-}n \to \pi^{-}\Lambda$ in the cms energy region from 1900 to 2100 MeV.
RPP/H63.

91 DASS G. V., FROGGATT C. D.
Comments on the Regge-pole model for the reaction KN → K*(890)N.
RPP/T7.

92 DASS G. V., KAMAL A. N.
Magnetic radiation in $K^{\pm} \to \pi^{\pm}\pi^{\circ}\gamma$ decays.
Alberta preprint.

93 FAYYAZUDDIN, RIAZUDDIN.
Kℓ3 form factors, χ meson width and symmetry breaking.
RPP/T5.

94 JONES P. B.
Limits on derivative couplings in the weak leptonic current.
RPP/H54.

95 LO S. Y.
Chou-Yang model, current-current interaction and nucleon-nucleon scattering.
RPP/T2.

96. MONTGOMERY W., O'RAIFEARTAIGH L., WINTERNITZ P.
Two-variable expansions of relativistic amplitudes and the subgroups of the SU(2, 1) group.
RPP/A59.

97 MORGAN D., SHAW G.
Pion-pion scattering below 1 GeV: a unique solution.
Columbia preprint N70-1931 (2)-160.

98 MORGAN J. T., SHELDON R., STAPLETON G. B.
An exploratory study of radiation damage in polyethylene at liquid helium temperatures.
RPP/E13.

99 OADES G. C., RASCHE G.
Electromagnetic structure and Coulomb corrections to strong interactions.
RPP/T1.

100 PAJAS P., WINTERNITZ P.
Relativistic partial wave analysis in two variables and the crossing transformation.
RPP/T4.

101 RANFT J.
Monte Carlo calculation of energy deposition by the nucleon-meson cascade and total-absorption-nuclear cascade (TANC) counters.
RPP/N20.

102 REEVE P. A.
Differential matrices for beam transport systems.
RPP/H61.

103 SCHARENGVIVEL J., GUTAY L. J., MILLER D. H., MEIERE F. T., MORGAN D., JACOBS J. D., MARATECK S., FROGGATT C. D., HUWE D., MARQUIT E.
The forward structure of the single-pion production amplitude.
Purdue preprint.

104 VENTURI G.
Infinitely rising Regge trajectories and unitarity.
RPP/T6.

105 WINTERNITZ P.
The Poincaré group, its little groups and their applications in particle physics.
RPP/T3.

106 WINTERNITZ P.
Two-dimensional expansions of relativistic amplitudes in the Mandelstam triangle and crossing symmetric reactions.
RPP/A63.

CONFERENCE PAPERS

107 ARMSTRONG A. G. A. M., O'CONNELL M. J., EDWARDS V. W., MORGAN R. H. C., SHEEHAN M. J.
Energy-loss extraction system with thin-septum plunged magnet at Nimrod.
Particle Accelerator Conference, Washington, USA, 5-7 March 1969, (Proceedings: IEEE Trans. Nucl. Sci., NS-16 (3) 266 (June 1969)), preprinted as RPP/N15.

108 CARNE A., PLANNER C. W., RANFT J., WALSH T. R., WEST N. D., WROE H.
Some results of studies of proton beam production and transport for PLANIM.
Ibid., p. 148, preprinted as RPP/N16.

109 FOX J. A.
Static power supplies for pulsed loads.
Ibid., p. 677.

110 GILBERT F. S.
High stability high current programmed power supplies for Nimrod extraction systems.
Ibid., p. 706, preprinted as RPP/N17.

111 LEWIN J. D., SMITH P. F., SPURWAY A. H.
Recent work on superconducting synchrotrons.
Ibid., p. 715, preprinted as RPP/A67.

112 SHAW K. B., STEVENSON G. R.
Radiation studies around extracted proton beams at Nimrod.
Ibid., p. 570, preprinted as RPP/R6.

113 LAWSON J. D.
Studies at the Rutherford Laboratory on the problems of superconducting synchrotrons.
7th. International Accelerator Conference, Yerevan, USSR, September 1969, preprinted as RPP/A71.

114 LAWSON J. D.
How can we calculate the radiation loss in the electron ring accelerator.
Ibid., preprinted as RPP/A70.

115 LAWSON J. D.
Some physical limitations of linear and ring shaped relativistic particle beams.
Ibid., preprinted as RPP/A69.

116 LAWSON J. D.
Radiation from relativistic electron rings passing through cavities.
Ibid., preprinted as RPP/A72.

117 COLEMAN F. J., SHAW K. B., STEVENSON G. R.
Studies of the cascades induced by 4 GeV electrons in concrete.
2nd International Conference on Accelerator Radiation Dosimetry and Experience, Stanford, USA, 1969, preprinted as RPP/R7.

118 EVANS D., SHELDON R., STAPLETON G. B.
Properties of thermoplastics at low temperatures.
Cryogenic Engineering Conference, Los Angeles, USA, June 1969, preprinted as RPP/E12.

119 JONES P. F.
An interrupt handler with masking for the PDP8.
5th DECUS European Seminar, Stockholm, Sweden, 11-13 September 1969, preprinted as RPP/N19.

120 TAYLOR R.
Questions on the future of FORTRAN.
SEAS Conference, Grenoble, France, September 1969.

121 BURREN J. W.
Overall data flow in RHEL road guidance system.
HPD Conference, Amsterdam, Holland, September 1969.

122 BURREN J. W.
Data analysis from pictures in the new bubble chambers.
Ibid.

123 SCOTT D. B.
Summary of patch-up system.
Ibid.

124 HALLOWELL P.
Rutherford filter system.
Ibid.

125 OXLEY A. J.
RHEL results.
Ibid.

126 BRUETON T.
Recent improvements in RHEL HPD control program.
Ibid.

127 PERRY D. R., HARGREAVES D. M.
Accelerators, Physics and Health.
Conference on Radiation Protection in Accelerator Environments, Rutherford High Energy Laboratory, UK, March 1969, (Proceedings, (Stevenson G. R. ed.) p. 3).

128 STEVENSON G. R., SHAW K. B.
The external radiation field from proton synchrotrons.
Ibid., p. 19.

129 SHAW K. B., STEVENSON G. R.
Dose and dose equivalent estimation from broad neutron spectra.
Ibid., p. 69.

130 HACK R. C.
Personal fast neutron dosimetry around Nimrod.
Ibid., p. 91.

131 PERRY D. R., HACK R. C.
Health physics instrumentation for accelerators.
Ibid., p. 111.

132 HACK R. C.
Practical health physics around Nimrod.
Ibid., p. 153.

133 BOOTH N. H.
Polarization in pion-proton scattering.
International Conference on High Energy Physics, Chania, Crete, 1969, preprinted as RPP/H58.

134 CHOLLET J., GAILLARD J. M., JANE M. R., RATCLIFFE T. J., REPELLIN J. P., SCHUBERT K. R., WOLFF B.
A measurement of the phase and the modulus of η_{oo}.
Topical Conference on Weak Interactions, CERN, Switzerland, 14-17 January 1969. (Proceedings, CERN 69-7, p. 309).

135 KABIR P. K.
Discussion remark on TCP– and T– invariance.
Ibid., p. 307.

136 LIPMAN N. H.
Operational experience with a vidicon system.
International Seminar on Filmless Spark and Streamer Chambers, Dubna, USSR, 1969.

137 DEEN S. M.
A new determination of the Ξ^- decay parameters.
Conference on Elementary Particle Physics, Cambridge, UK, 1969.

138 HUTTON J., HART J.
An experiment to test the $\Delta S = \Delta Q$ rule for Ke3 decay.
Ibid.

139 ISLAM G. S.
Partial wave analysis of $K^-n \to \pi^-\Lambda$ between 1800 and 2200 MeV.
Ibid.

140 MILLER R. J.
Elastic scattering and K*(890) production in K^-p collisions between 1·26 and 1·84 GeV/c.
Ibid.

141 OTT R. J., PRITCHARD T. W.
Measurement of the K^+ lifetime.
Ibid.

142 SMITH J. R.
A study of the reactions $K^-p \to \bar{K}^\circ n$, $K^-p \to \Lambda\pi^\circ$, $K^-p \to \Lambda\eta$ in the centre-of-mass energy range from 1·9 to 2·2 GeV/c.
Ibid.

143 LIPMAN, N. H.
Work of the Rutherford Laboratory.
Summer School on Elementary Particle Physics, Herceg Novi, Yugoslavia, 1969.

144 LIPMAN N. H.
Present status of CP violation.
Ibid.

145 SAXON D. H., MULVEY J. H., CHINOWSKY W.
Information on I = J = 0 $\pi\pi$ phase shifts from π^-p interactions at low incident π^- momenta.
Conference on $\pi\pi$ and Kπ interactions, Argonne, USA, 14-16 May 1969, (Proceedings (Loeffler F., Malamud E. eds.) p. 316).

146 MORGAN D., SHAW G.
Low energy pion-pion parameters from forward dispersion relations.
Ibid., p. 726.

147 FROGGATT C. D., MORGAN D.
Non evasive Chew-Low extrapolation for the study of $\pi\pi$ elastic scattering.
Ibid., p. 740.

148 BAKER S. L., DORNAN P. J., GOPAL G. P., WEBSTER G. J., BULL V. A., MARCH P. V., TAYLER V., TOWNSEND D. W.
Positive pion-proton elastic scattering at 900, 950 and 1000 MeV/c.
International Conference on Elementary Particles, Lund, Sweden, 25 June-1 July, 1969.

149 BERTHON A., RANGAN K. L., BEANEY J. A., BUTTERWORTH I., DEEN S. M., FISHER C. M., LITCHFIELD P. J., SEGAR A. M., SMITH J. R., MEYER J., PAULI E., TALLINI B., VRANA J.
A study of the reaction $K^-p \to \Lambda\pi^\circ$ in the centre of mass energy range 1915-2168 MeV.
Ibid.

150 BERTHON A., RANGAN L. K., BEANEY J. A., BUTTERWORTH I., DEEN S. M., FISHER C. M., LITCHFIELD P. J., SEGAR A. M., SMITH J. R., MEYER J., PAULI E., TALLINI B., VRANA J.
Confirmation of the spin-parity assignment of the Σ (1915).
Ibid.

151 BIRMINGHAM / EDINBURGH / GLASGOW / IMPERIAL COLLEGE, LONDON.
Partial wave analysis of $K^-n \to \pi^-\Lambda$ between 1850 and 2150 MeV.
Ibid.

152 BOWLER M. G., CASHMORE R. J.
Inelastic reactions in π^+p collisions in the momentum range 600-800 MeV/c.
Ibid.

153 BRUNET J. M., NARJOUX J. L., DANYSZ J. A., SPIRO M., VERGLAS A., PENNEY B., STEWART B., THOMPSON G., ALLEN J. E., LEWIS P. H., MARCH P. V.
The reaction $K^+p \to NK\pi$ in the momentum range 2·1-2·7 GeV/c.
Ibid.

154 CASHMORE R. J., BOWLER M. G.
Single pion production in π^+p collisions in the momentum range 600-800 MeV/c.
Ibid.

155 COLLEGE DE FRANCE / RHEL / SACLAY / STRASBOURG.
A study of two-prong interactions in K^-p collisions in the momentum range 1·26-1·84 GeV/c.
Ibid.

156 DANYSZ J. A., SPIRO M., VERGLAS A., BRUNET J. M., NARJOUX J. L., BAKER S., PENNEY B., THOMPSON G., ALLEN J. E., LEWIS P. H., MARCH P. V.
K^+p elastic scattering in the intermediate momentum range 2·1 to 2·7 GeV/c.
Ibid.

157 DANYSZ J. A., SPIRO M., VERGLAS A., BRUNET J. M., NARJOUX J. L., GOLDSACK S., PENNEY B., THOMPSON G., ALLEN J. E., LEWIS P. H., MARCH P. V.
The reaction $K^+p \to NK\pi\pi$ in the momentum range 2·1 to 2·7 GeV/c.
Ibid.

158 IMPERIAL COLLEGE, LONDON / WESTFIELD COLLEGE, LONDON.
Single pion production in positive pion-proton interactions at 900, 950 and 1000 MeV/c.
Ibid.

159 KEMP M. A. R., MACKENZIE R., APLIN P. S., COWAN I. M., GIBSON W. M., GILMORE R. S., GREEN K., MALOS J., SMITH V. J., WARD D. L.
Differential cross-sections for π^-p elastic scattering in the momentum range 1206 to 2486 MeV/c.
Ibid.

160 LEA A. T.
What's new in πN phase shift analyses.
Ibid.

161 LEA A. T., OADES G. C., MARTIN B. R.
K^+p scattering below 2 GeV/c.
Ibid.

162 SAXON D. H., MULVEY J. H., CHINOWSKY W.
A study of single pion production in π^-p interactions at 456, 505 and 552 MeV/c.
Ibid.

163 BARRETT R. C.
Shapes of nuclei (invited paper).
International Conference on Properties of Nuclear States, Montreal, Canada, August 1969.

164 DAVIES W. G., McCLATCHIE W., KITCHING J. E., MONTAGUE D. G., RAMAVATARAM K., CHANT N. S.
The structure of the even nickel isotopes from the (p, t) reaction.
Ibid.

165 EDWARDS V. R. W., GANGULY N. K., MONTAGUE D. G., RAMAVATARAM K., ZUCKER A., PLUMMER D. J.
The structure of $Sm^{142, 143, 145, 146}$.
Ibid.

166 JACKSON D. F., MORGAN C. G.
Effective interaction for alpha-particle scattering.
Ibid.

167 KARBAN O., GREAVES P. D., HNIZDO V., LOWE J., BEROVIC N., WOJCIECHOWSKI H., GREENLEES G. W.
Resonance effects in proton – O^{16} elastic scattering between 16 and 30 MeV.
Ibid.

168 KARBAN O., LOWE J., GREAVES P. D., HNIZDO V.
Polarization in B^{11} (p, p′) at 30·3 MeV.
Ibid.

169 SQUIER G. T. A., JOHNSTON A. R.
Differential cross-sections for the reaction B^{10} (p, t) B^8 at 50 MeV.
Ibid.

170 THOMAS G. L.
The real part of the optical model potential at 30 and 50 MeV.
Ibid.

171 THOMAS G. L., BURGE E. J., SMITH D. A.
Proton elastic scattering from Cu^{63} and Cu^{65} at 30 and 50 MeV.
Ibid.

172 BATTY C. J., TSCHALÄR C.
Measurement of the depolarization parameter for proton-nucleus scattering at 50 MeV.
Symposium on Nuclear Reaction Mechanisms and Polarization Phenomena, Quebec, Canada, September 1969.

173 JACKSON D. F.
Can the nuclear matter distribution be studied through alpha-particle scattering?
Ibid.

174 JACKSON D. F., SHAH M. B.
The optical potential for C^{12} between 100 MeV and 1 GeV.
Ibid.

175 NELSON J. M., CHANT N. S., FISHER P. S.
A comparison of polarization analysing powers of two-nucleon transfer reactions leading to mirror final states.
Ibid.

176 BARRETT R. C., ELTON L. R. B., WEBB S. J.
Single particle wavefunctions in a non-local potential.
3rd International Conference on High Energy Physics and Nuclear Structure, New York, USA, September 1969.

177 JACKSON D. F.
Effective nucleon number in high energy reactions.
Ibid.

178 KEMBHAVI V. K., JACKSON D. F.
The optical potential for high energy pion-nucleus and nucleon-nucleus scattering.
Ibid.

179 JACKSON D. F.
Investigation of hole states in nuclei by means of pick-up, knock-out and related relations (invited paper).
Symposium on Pick-up and Quasi-free Knock-out of Particles and Clusters, Maryland, USA, April 1969.

180 ELTON L. R. B.
Nuclear radii (invited paper).
Gordon Conference on Nuclear Chemistry, USA, 1969.

181 CAVANAGH P. E., COLEMAN C. F.
A study of the nuclear structure of the even tin isotopes using (p, p′) and (p, t).
IPPS Conference on Nuclear and Elementary Particle Physics, Brighton, UK, 24-26 September 1969.

182 GREAVES P. D., KARBAN O., LOWE J., HNIZDO V.
Polarization in B^{11} (p, p′) at 30·3 MeV.
Ibid.

183 KARBAN O., HNIZDO V., LOWE J., GREAVES P. D.
Inelastic scattering of polarized protons from Fe^{56}, Ni^{58}, Sn^{120} and Pb^{208} at 30·3 MeV.
Ibid.

184 SINHA B. C.
Optical model analysis of Pb^{208} proton scattering with a surface peaked symmetry term.
Ibid.

185 BATTY C. J., BONNER B. E., TSCHALÄR C., WILLIAMS L. E., CLOUGH A. S., BENÖHR H. C.
Evidence for broad resonances in the three nucleon system.
IPPS Conference on the Three Body Problem in Nuclear and Particle Physics, Birmingham, UK, 8-10 July 1969.

186 STEWART N. M., GIBSON W. R., KINGSTON F. G., MEGAW J. H. P. C.
Triple scattering parameter measurements in 50 MeV proton-deuteron scattering.
Ibid.

DOCTORAL THESES

187 AHMED M. (University of Birmingham).
Nuclear reaction studies with 10 MeV protons.

188 BOTTERILL D. R. (University of Oxford).
Form factor measurements in K^+ leptonic decays. Reprinted as HEP/T/2

189 CASHMORE R. J. (University of Oxford).
A study of inelastic pion-proton interactions in the range 600-800 MeV/c.

190 CLARKE N. M. (King's College, University of London).
Backward angle scattering of 50 MeV protons.

191 DIX A. D. B. (University of Manchester).
Studies of elastic and inelastic scattering of 50 MeV protons by lithium isotopes.

192 EASTWOOD D. (University of Birmingham).
Resonance production and formation in 1·45 GeV/c and 1·65 GeV/c K^- – neutron interactions.

193 FLEMING-TOMPA E. (University College, University of London).
Eta meson decay and electron measurements in a heavy liquid bubble chamber.

194 GRACE J. M. (King's College, University of London).
Proton reaction cross-section for carbon between 20 and 50 MeV.

195 GREAVES P. D. (University of Birmingham).
(i) Polarization studies with 30 MeV protons.
(ii) A search for a state in Be^8.

196 HARBISON S. A. (Westfield College, University of London).
Few nucleon studies with polarized and unpolarized protons.

197 HEATHCOTE F. (University of Birmingham).
K^-d interactions at 1·45-1·65 GeV/c.

198 ISLAM G. (University of Birmingham).
A partial wave analysis of $K^- n \to \Lambda^\circ \pi^-$ at 1·9-2·2 GeV cms energy.

199 JACQUES D. (University of Manchester).
Inelastic proton scattering by P-shell nuclei $Ca^{42\ 44}$ and Sc^{45}.

200 JONES D. J. (University of Manchester).
Elastic and inelastic scattering of 50 MeV protons by zirconium isotopes.

201 KINGSTON F. G. (Westfield College, University of London).
A study of pick-up reactions at 50 MeV.

202 MGBENU E. N. (University College, University of London).
The development of a wire spark chamber system for studying elastic scattering of high energy particles.

203 MORGAN G. C. (University of Surrey).
Investigations of nuclear structure through the analysis of alpha-particle scattering.

204 ROSNER R. A. (University College, University of London).
The automatic acquisition and analysis of high energy elastic scattering data. Reprinted as HEP/T/5.

205 SAXON D. H. (University of Oxford).
A study of elementary particle interactions using the bubble chamber technique. Reprinted as HEP/T/6.

206 SHARROCK S. J. (University College, University of London).
A computer controlled kaon-proton scattering experiment. Reprinted as HEP/T/4.

207 SOPER P. J. R. (University of Surrey).
A 3-body model of deuteron-nucleus elastic scattering.

208 SQUIER G. T. A. (Queen's University, Belfast).
A study of the interaction of 50 MeV protons and 30 MeV He^3 particles with the B^{10} nucleus.

209 STEWART N. M. (Westfield College, University of London).
A measurement of proton-deuteron triple scattering parameters at 50 MeV.

210 THOMAS G. L. (King's College, University of London).
Differences in proton optical model parameters between pairs of nuclei.

211 WARD D. L. (University of Bristol).
A measurement of the differential cross-sections for π^-p elastic scattering at 31 momenta between 1·2 and 3·0 GeV/c. Reprinted as HEP/T/3.

212 WILKINSON E. M. (University of Oxford).
Coherent three-pion production in helium at 1·88 GeV/c.

REPORTS

213 BANFORD A. P., TELLING F. M. (eds.)
The work of the Rutherford Laboratory in 1968.
RHEL/R 180

214 BUTTERWORTH I., FISHER C. M. (eds.)
Proceedings of a seminar on future development of automatic bubble chamber film measurement, 13 October 1968.
RHEL/R 183.

215 DAVID D., JONES P. F.
An exercise in computer assisted control using an ion source.
RHEL/R 179.

216 DISERENS N. J.
Further development of the magnetostatic computer program TRIM at the Rutherford Laboratory.
RHEL/R 171.

217 ELLIOTT R. T.
Pulsed magnet command systems.
RHEL/R 177.

218 GIRARD P.
The rough digitizing 'Merge' program.
RHEL/R 189.

219 GRAY D. E. (ed.)
Nimrod operation and development quarterly report. July 1st to September 30th 1968.
RHEL/R 175.

220 GRAY D. E. (ed.)
Nimrod operation and development quarterly report. October 1st to December 31st 1968.
RHEL/R 178.

221 GRAY D. E. (ed.)
Nimrod operation and development quarterly report. January 1st to March 31st 1969.
RHEL/R 181.

222 GRAY D. E. (ed.)
Nimrod operation and development quarterly report. April 1st to June 30th 1969.
RHEL/R 188.

223 GRESHAM A. T., SHELDON R., STAPLETON, G. B.
A design proposal for a concrete insulated magnet for the European 300 GeV accelerator.
RHEL/R 184.

224 GRESHAM A. T., SHELDON R., STAPLETON G. B.
The construction of magnets for particle accelerator physics using cementatious aggregates.
RHEL/R 185.

225 RANFT J., STEVENS T. J.
Computer study of vertical beam blow-up during resonant ejection from Nimrod.
RHEL/R 174.

226 SACHARIDIS E. J.
Wide angle elastic proton-proton scattering at high energies (Diffraction or Regge poles?).
RHEL/R 186.

MEMORANDA

227 COLYER B.
The engineering problems of superconducting a.c. and synchrotron magnets.
RHEL/M 177.

228 COUPLAND J. H.
End effects in iron-free bending magnets.
RHEL/M 179.

229 CURTIS M. M.
Rutherford Laboratory central computer accounting programs.
RHEL/M 174.

230 EVANS W. R.
The application of electronic analogue wattmeters to the measurement of alternator power.
NIMROD (PS) 68-31.

231 GIBBINGS D.
Modular one remote terminal.
RHEL/M 182.

232 GILBY A. S.
CAMAC self-teach unit.
RHEL/M 181.

233 GREGORY E. J.
Computer aids to manufacturing progress systems.
RHEL/M 176.

234 HACK R. C.
Personal fast neutron dosimetry around Nimrod.
RHEL/M 168.

235 HACK R. C.
Radiation protection group (operations) progress report for 1968.
RHEL/M 171.

236 HYMAN J. T.
Accelerator controls embodying computers: a bibliography and review of achievements to date.
RHEL/M 167.

237 KNIGHT F.M., JACOB F. R.
The interfaces used to connect measuring machines on line to the IBM 1130 computer and to link the 1130 to the IBM 360/75 computer.
RHEL/M 166.

238 NORRIS W. T., WILSON M. N.
'MAGNA' – a program to calculate magnetic fields in three dimensions.
RHEL/M 172.

239 PORTER F. T.
Administration Division use of the Rutherford Laboratory IBM 360 computer. Part 1.
RHEL/M 178.

240 REEVE P. A.
A nuclear physics beam line for the VEC.
RHEL/M 170.

241 TROWBRIDGE P. S.
Design study for a cylindrical configuration electrostatic separator.
RHEL/M 165.

242 WEST N. D.
Acceleration of deuterons in Nimrod.
RHEL/M 173.

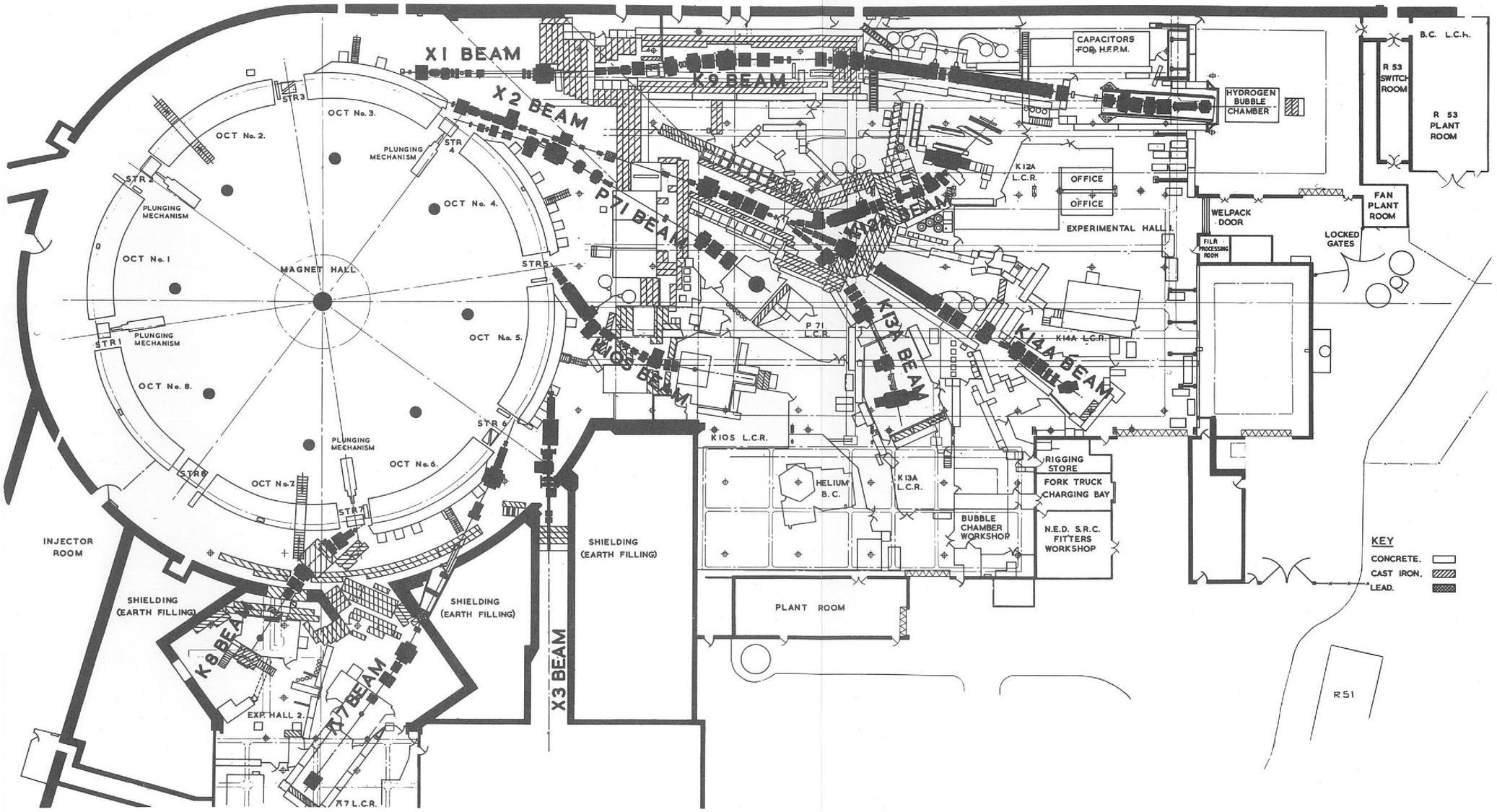

Nimrod Experimental Halls 1 and 2. Layout at December 1969.